Bistatic sonar and a novel form of variable depth sonar

Thesis

UNRESTRICTED

BISTATIC SONAR AND A NOVEL FORM OF VARIABLE DEPTH SONAR

(Sonar Systems Research Study)

Submitted by

W.K.Grimley OBE, MSc., C.ENG, F.I.E.E.

for the degree of Ph.D. of

The Open University

1996

Date of submission: 1 February 1996
Date of award: 17 April 1996

Contents.

Section 6.

Conclusions of System Research.

Recommendations.

Acknowledgements

The cooperation is acknowledged of the late M.D.Daintith of SACLANT ASW RESEARCH CENTRE,La Spezia. Italy. with the first formulations that gave support for the feasibility of my concept of using cardioid element units to resolved the port/starboard ambiguity of a towed line array.The advice, assistance and encouragement of Professor K Attenborough,The Open University, and of Professor R. Benjamin,Imperial College, during their period of supervising the project has been of great value.The School of Physics at the University of Bath afforded me the use of their facilities and Dr N Pace arranged the use of his acoustic laboratory to undertake the experiments on the cardioid network with twist compensation and Dr P Wingham the use of the Hydrodynamic Tow Tank for modelling the Towing Characteristics of the Wet End components of the towed line array. Professor H.O Berktay of the School of Physics gave time for many stimulating discussions on signal processing and M^{rs} C Dyer rendered invaluable assistance in converting my assembled data and rough sketches into acceptable figures and curves. Not least is my recognition of the part played by my wife Paule for her constant support and encouragement who over this intense period of activity at home, acted as secretary,general factotum and housewife in providing congenial conditions for the project.

Abstract

This thesis relates to the sonar system research undertaken for a Naval Requirement for proposals to improve the cost effectiveness of the defence of shipping against submarine attacks. Defence systems evolved as a function of the developing technology of the opposition which in this instance is the ability of a submarine to remain undetected below the sea surface while searching for,tracking and attacking its targets. An inherent problem for underwater detection with Escort Ships hull type sonars is its location on the air-sea interface with the need of a two-way propagation path to access the depth-range volume available to a submarine. As the power of an Escort's sonar is increased so is the size of ship, 5000 tons and more, to accommodate the optimum size of transducers required.Sonar system research at all times is a multi-discipline task and in this particular case was further broadened with a requirement to review the possibilities for sources of energy other than underwater acoustics.

The research confirms the dominance of sonar for underwater detection and establishes the feasibility of a Bistatic Sonar concept which replaces the two-way propagation path of a hull type sonar with a one-way path, source-target-receiver with a variable depth directive towed line receiver on a small ship as a distant receiver.A second objective which became feasible with the development of an adequate towed source was a variable depth sonar which has now been produced by British

Aerospace for a world market. A summary of the thesis is provided as an introduction to the subject matter of the different sections.

Summary of the Thesis.

The origin of this research was a request from NATO Naval Command, Norfolk, USA,for proposals that would attain an improved effectiveness in an Escort Ship's defence of shipping against submarine attacks without incurring a significant addition to the overall fleet costs. Countering the many ocean's threat posed by the increasing sophistication of the submarines of a major naval power through the traditional sonar approach of lowering the frequency and increasing the power, had led to a cost of weapon systems that small navies in NATO were finding difficult to fund, and hence could limit the effectiveness of their contribution to the Escort role. Included in the request was that advances in the technology of other associated sources of energy should be appraised to ascertain if the perceived limited value of their use in submarine detection remained valid. The author has analysed the range propagation losses of various energy forms as alternatives to sonar for the NATO requirement and confirms that there is a large shortfall. A more effective use of the high power sonar source of the large Escort ships is proposed through a bistatic geometry with a directive towed line array as a distant receiver on a small ship. Alongside the bistatic system research was an objective to add a towed source to the towed line receiver that would allow a bistatic receiving ship to have an independent active sonar role. The forms of active sonar sources then available were not suitable for small ship systems hence the emphasis on a bistatic solution. A

subsequent company funded project by British Aerospace,BAe, for a small ship Variable Depth Sonar provided the development of a low frequency source which, with the directive towed line array format of the Bistatic System, produced a small ship active sonar system with a performance equivalent to that of a medium power Escort Ship with a variable depth capability. The thesis is divided into sections along the lines of my research observing the interactive properties of the different subjects.

Section 1.

Introduction. Describes the purpose and scope of sonar system research and the diversity of the disciplines addressed. The concept of the Bistatic Sonar System is introduced together with the reasons for past failures so that the full system aspects had not previously been analysed. My own solution was to make more effective use of the source of the hull mounted sonars of the large and expensive Escort Ships then entering service with a distant directive towed line array on a small ship.
Appendix A. Outlines the reason for naval interest in other sources of energy and in particular displays of radar signals which gave rise to a belief that EM propagation in the sea was orders greater than presumed.
Appendix B. Reviews the basic physics that relate the underwater requirement to the major energy forms and confirms the continuing prominence of underwater acoustics. A plausible explanation for the radar underwater display observations is offered.

Section 2.

Hull Sonars. Analyses the capacity of hull sonars to detect targets within and below a surface duct as well as at a convergence zone, and the operational constraints that limit full advantage being taken of these additional propagation modes. It is shown that the traditional approach of increasing the surveillance volume by lowering the frequency and increasing the sonar power has certain benefits but at the price of decreasing cost effectiveness as well as on the optimum spacing of the Escort Ships.The large powers required to make use of seabed reflection paths to detect a submarine below a surface not only involves a high entry price, but also a splitting of observation time of a target free to decide on its depth tactics. The advantages of providing a small ship with a variable depth sonar are demonstrated and why developments of a flextensional configuration changed the prospects for such a sonar.

Section 3.

Directive Form of a Towed Line Array. Is an account of the considerations that led to the proposal for using an existing in-service hull sonar as the bench-mark for parameter formulation of a towed line with cardioid elements as a receiver for the Bistatic Sonar. The interactive nature in the choice of Wet-end components,line array,tow cable.telemetry bandwidth and deck handing equipment is analysed. An unresolved feature

was the level of flow noise which had to wait for trials with the private venture Variable Depth Sonar,VDS, for some real data.

Section 4.

Bistatic Performance Analysis. Lists the criteria chosen to obtain compatability of the receiver in a bistatic sonar role with that of the high powered Escort Ship sonar. Compared with a hull sonar, there are significant differences across the whole spectrum of functional outputs due to the separation of source and receiver and the elliptical geometry. An equivalence of detection probabilities includes an estimation model of detection against false alarm. Attention is drawn to the problem of accommodating the number of operators in a small ship for a match with the operator decision rate of a large Escort ship.

Section 5.

Commercial Variable Depth Sonar. The formulation of a small ship self contained variable depth sonar for a world market commenced with the background of the bistatic sonar research with the author as an active participant. The account of converting the results of sonar system research into cost-effective hardware demonstrates the value of the former in showing the interactive nature of different sections of the project, the significance of any unresolved grey areas, and the implications of parameter values on role value.These provided a measure of the possible effects throughout the system of proposed changes in parameters to improve engineering design features. A

modular arrangement allows a flexibility to match specific customer requirements. The system has now been supplied to a number of navies.

7 **Section 6.**

Conclusions of System Research. This presents the contribution which the system research of this thesis has made to the original NATO requests. In general the analysis has met all of the original objectives and although the immediacy of the original threat has now receded, the results of the research and the material outcome should continue to be a contribution for the future.

Section 1

Contents.

Section 1 FIGS.

Appendix A

Section 1

INTRODUCTION.

Sonar System Research.

1.1 The nature of System Research for Underwater Defence, as practised over many years by the author and as demonstrated in this thesis, is necessarily a many discipline task. The prime goal is to establish the feasibility and if positive, to derive the essential parameters for cost effective systems that will fulfil the operational roles as perceived by "Naval Requirements". Progressing a major new weapon system into naval service extends well beyond the provision of hardware and fig 1.11 illustrates the wide spread of understanding and facets of the problem areas that form part of the methodology. A first assignment is to be fully conversant with the role aspects and the place of the new requirement in terms of the balance of acceptable costs for the operational gains on offer and/or savings in present or future Force strengths. In this particular case, the goal of the research was to improve the active sonar control area around defended shipping through the addition of relatively lower cost small ships thereby achieving savings in the number of high value Escort ships. A first

Fig 1.11

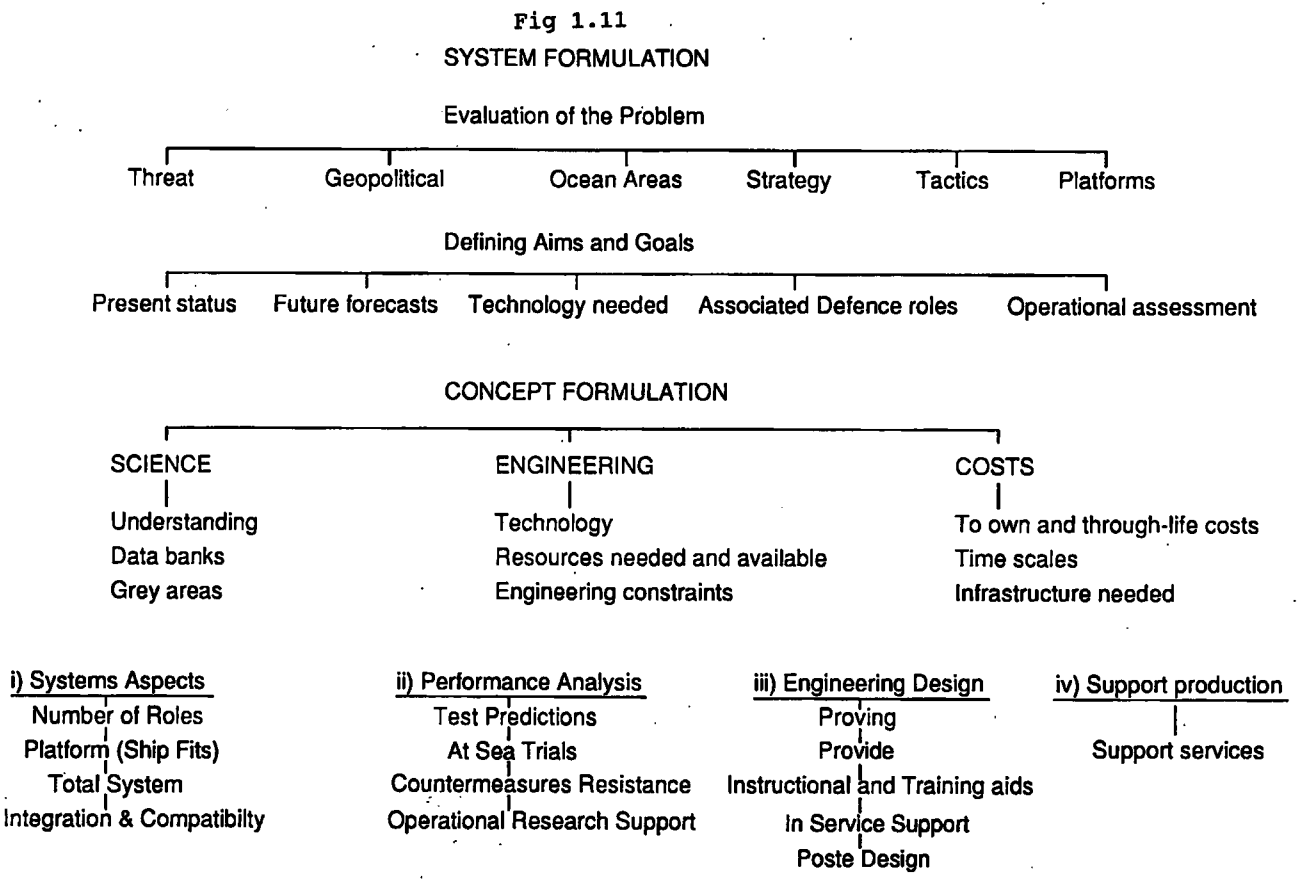
SYSTEM FORMULATION
Evaluation of the Problem
Threat
Geopolitical
Ocean Areas
Strategy
Tactics
Platforms
Defining Aims and Goals
Present status
Future forecasts
Technology needed
Associated Defence roles
Operational assessment
CONCEPT FORMULATION
SCIENCE
Understanding
Data banks
Grey areas
ENGINEERING
Technology
Resources needed and available
Engineering constraints
COSTS
To own and through-life costs
Time scales
Infrastructure needed
i) Systems Aspects
Number of Roles
Platform (Ship Fits)
Total System
Integration & Compatibilty
ii) Performance Analysis
Test Predictions
At Sea Trials
Countermeasures Resistance
Operational Research Support
iii) Engineering Design
Proving
Provide
Instructional and Training aids
In Service Support
Poste Design
iv) Support production
Support services

action is to assess the prospects for a match between the naval role requirement and the reality of the physics available. For a sonar system, fig 1.12, a synopsis of possible system formats is undertaken from which a notional integrated system is selected that offers the best prospects for an acceptable cost effective product. This establishes the case for a provisional listing in the defence budget. It is of note that the goal of any ensuing system research is the formulation of objectives and establishing feasible parameters that should satisfy the whole requirement: this forms the basis and acts as a guide for the subsequent detailed design and system development allowing freedom to make use of the latest technology; the latter is not an integral part of the research. In support of the above philosophy is past experience of the demise of many well publicised large scale projects abandoned at a late stage of the development programme after the expenditure of considerable public funds. The author at various times has been involved in rescue efforts for some such projects in both the U.K and USA. The gestation period for a major naval system is around a decade; or more if there are delays in the queue for funding. After acceptance trials it is also

Fig 1.12 Basic Sonar System.

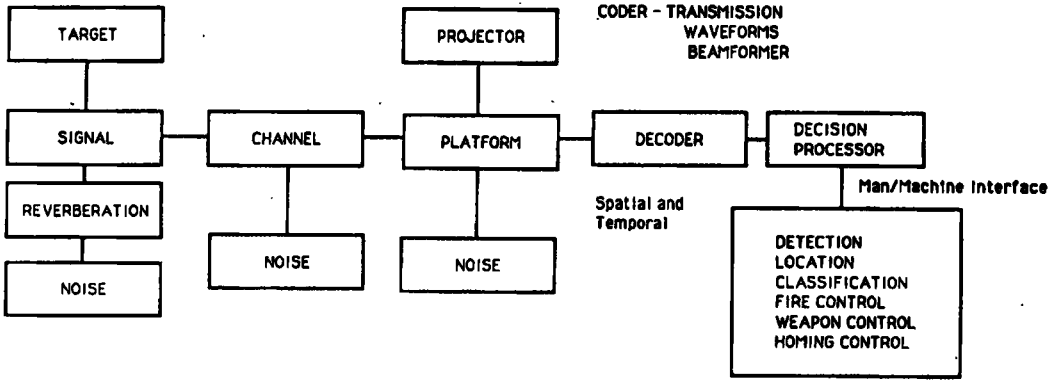

SIGNAL INFORMATION

PASSIVE (RADIATION)

Machinery
Cavitation
Hydrodynamic
Impulse

ACTIVE (PROJECTOR RETURNS)

Reflection
Scattering

NOISE (BACKGROUND)

Signal Interference
Platform Noise
Acoustic Interaction with boundaries
Shipping Noise
Biological Sounds
Wind/Sea Surface Returns

The problem is generally one of obtaining a quantitative measure for the degree of affinity between two measurements.

In all practical sonar situations only probability statements can be made at output of the decision processor.

of note that there is a substantial time lapse before a significant number of new major weapon systems are at sea since progress is tied to the timetable of ship refit periods: a missed date can mean a delay of several years before the ship again becomes available. Similarly, an expected in-service life of at least fifteen to twenty years can be much extended by such factors. A discernible pattern that was common to the troubled projects, and from which many of the ensuing problems followed, was the strong user pressure to minimize development time and optimism about programme dates before the system formulation and introduction into service costs had been fully researched: in particular, the totality of the overall role requirements, possible shifts in the defence roles over the lifetime of the system and delineation of the grey areas. These were compounded by assumptions that an early start could be made with the detailed design processes and hardware production as sufficient flexibility could be provided within the programmes to cater for any unforeseen parameter changes. In fact, late resolution of the grey areas generally resulted in some costly restructuring of key system functions with changes to programme schedules and inevitable delays and funding

increases. Over the years the total number of principal naval ships has continued to decline so that development costs for major weapon systems have become a significant part of the whole of the funds allocated for the capability. It is therefore not surprising that the impact of past failures on tightening budgets has been to afford priority to gradual system improvements with a low risk content. However where significant advances are needed, then the adage," a chasm cannot be crossed by a series of short hops," applies. A significant part of the system research task is to minimise the risk factors by clarifying the overall objectives and important grey areas that could affect the resources needed, programme schedules and costs before large scale funds are committed to the development of hardware.

1.2 The origins of the bistatic sonar system research in this thesis commenced near to the completion of the author's secondment in 1978 to NATO's S.A.C.L.A.N.T. Anti-Submarine Warfare Research Centre at La Spezia,Italy. It followed a request by N.A.T.O for proposals to effect an overall system improvement in the underwater submarine detection volume provided by a multinational group of naval Escort ships; specifically for active sonar roles. At this time the USN were bringing into service the latest high power active hull type sonars that followed the past trend of improving performance by lowering the operating frequency and increasing the source power to expand the capacity for duct, bottom bounce and convergence modes of propagation, fig 1.21. A problem with the above approach is that improvements in overall performance were becoming less cost effective in terms of the gains achieved for the ever rising cost and size of the Escort ships needed for the consequential large sonar systems. Also, as is brought out in the research, time spent on access to bottom bounce and convergence modes of detection is at the expense of less surveillance time in the above layer mode from where an attacker gains information and launches its weapons. A few

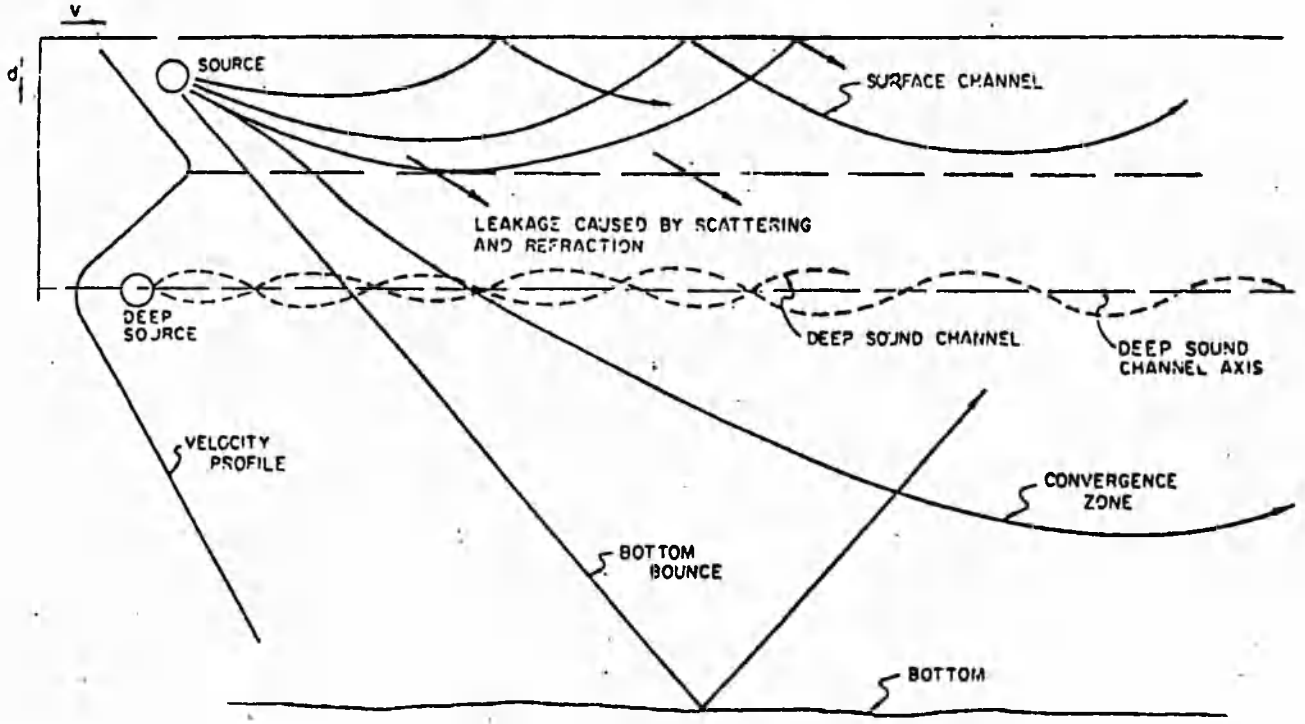

Fig 1.21 Modes of Sound Transmission

variable depth sonars were in service for the detection of below duct targets but their performance, size and cost limited their role value as an additional sonar system for most seas. Other navies of the Alliance had varying degrees of sonar surveillance and attack capabilities with a result that arranging an optimum protection force around the defended shipping presented difficulties. Implementing corresponding improvements in sonar capabilities following the above approach was beyond the budget of the smaller navies for the number of support Escorts required. Furthermore, even if afforded, an operational repercussion of more Escort sonars operating at the lower frequencies would be that with the smaller total bandwith available for separating the transmissions of the Escort sonars. When combined with the higher source levels, then optimum screening positions would also need to encompass the problem of minimising the mutual interference that could occur over greater ship separation ranges. Also of note is that the limited number of these high value Escorts made them of equal value as a target to an attacker as is the defended shipping.

1.3 At various times the author and others had examined the cost effectiveness of the Bistatic concept where a low cost satellite vessel is fitted with a hull mounted receiver to make use of the acoustic energy which is propagated beyond the monostatic sonar detection range. Such energy continues to reflect and scatter sound over a 360 degree arc. An obvious arrangement to utilize this extension of the propagation path is to place a receiver beyond the detection range of the monostatic sonar, fig 1.31. Transmission losses over the additional range from sonar source to target are compensated by the reduced distance from target to receiver. A previous major stumbling block for the bistatic concept was that the capacity of the source sonars as then fitted to Escort ships was limited to duct detection ranges and the size of the bistatic hull receivers needed for relatively small overall sonar area gains made the cost of the satellite platforms uneconomical compared with that of supplying another full sonar system. Such research was therefore terminated at an early cost effectiveness stage.

1.4 The arrival of the high power USN sonar allowed for a more adequate bistatic source with access to an increased number of propagation path modes. However, the bistatic

BISTATIC GEOMETRY

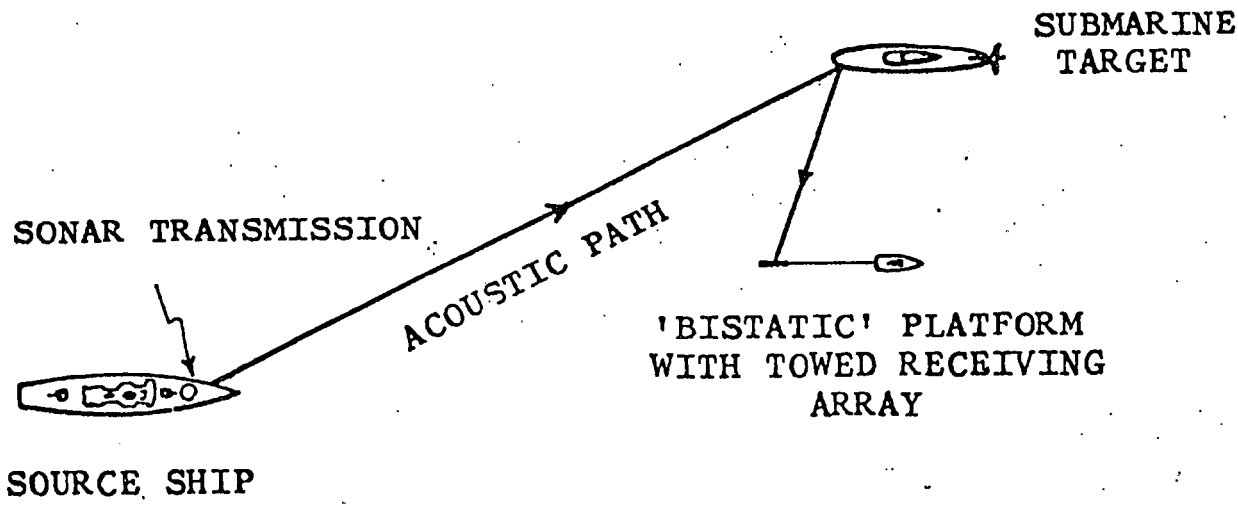

Fig 1.31 Bistatic Geometry.

hull receiver dimensions needed, particular for a small ship platform, presented even more difficulties for a bistatic role. The continuing development of the low frequency wide aperture passive sonar towed line arrays was viewed by the author as a possible way ahead but the lack of azimuth/port starboard discrimination, figs 1.41, made them unsuitable for an active sonar role. The relatively long ranges of passive sonar detections allows time for own platform manoeuvres to resolve the ambiguity, but was not an acceptable ploy for the shorter range and more rapid target manoeuvres that are often a feature of active sonar detections. After examining various ways in which the desired characteristics might be obtained, the author conceived the idea of a novel type of towed line receiver using cardioid sensing units having port\star-board discrimination in the place of the conventional omni-directional elements all within an acceptable hose volume that included the beamforming circuitry and means of compensating for cable twist.In view of the short time available to the author, a combined effort with a colleague, the late M.D Daintith, substantiated the basic

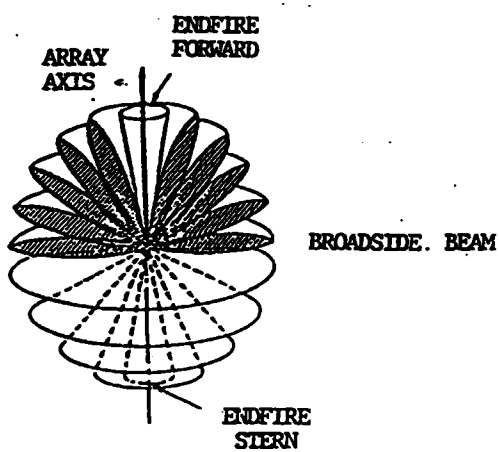

fig 1.41 Typical Beam Pattern for a Towed line Linear Array.

features of this key component. Continuance of the task of system research was not within the terms of SACLANTCENT's mission so that this initial work ended their involvement.

1.5 On retirement, a subsequent problem of confidence about the operational value of the bistatic sonar concept was recorded when two sets of ad hoc trials with a ship hull sonar as the source and an omnidirectional sonar buoy as a receiver failed to produce any worthwhile improvement in the active sonar detection control areas. The author was convinced that these trials were flawed. In early 1980 as a private enterprise, a start was made on the task of providing the case for a more innovative approach for the way ahead in underwater defence.Unfortunately, other unforeseen commitments arose with a higher priority so that this specific research was progressed in a piece meal fashion and thereby took an inordinately longer time span to complete than planned. First was an examination of the substance of the continuing claims made by experienced radar operators that advances in technology had increased underwater radar and optical detection ranges far beyond those previously predicted so that there was a strong case for development funding for an additional energy source system to sonar. The next objective was to present the

consequences in terms of cost and gains of continuing the trend for hull sonars of increased the power and lowering the frequency.This was followed by the system research for a bistatic sonar system and a commercial venture for a variable depth sonar based on great deal of the bistatic concepts and formulations.

1.6 Having confirmed (appendices A and B of this thesis) that none of the above alternative energy sources were candidates for the NATO requirement, a synopsis of the performance goals and essential features for a cost effective bistatic sonar system was completed. Potential advantages sought for the more innovative bistatic active sonar capability, the main system research subject, are listed below.

(i) Prospects for the detection of targets at ranges beyond those obtained by the conventional duct sonars. (Added range to the monostatic sonar source ship.)

(ii) Receiving array towed at an optimum depth from a relatively small and inexpensive ship.

(iii) Mutual interference between low frequency active sonars would not be increased since no additional active sonar source bandwith is involved.

(iv) The bistatic platform emits no sonar emissions and

hence submarines would be denied useful information to optimize their search and attack tactics such as varying operating depth and presenting the least target area to the searching sonars.

(v) Weapons fired from the bistatic platforms need less loss time to datum and so could be cheaper.

(vi) The concept combines the previous opposing philosophies of " small and many" with those of the "large and few."

Achieving a bistatic capability therefore offered the prospects of small navies contributing at relatively low cost to a significant improvement in the total sonar detection volume of an escort force. A substantial material time/cost advantage afforded by this particular bistatic concept is that there would only be relatively minor additions to the Escort ships so that an alongside fitting programme for both the Escorts and small ships could proceed without any disturbance to existing force strengths.

1.7 There was no evidence that any previous research had examined the system implications of the bistatic sonar geometry with an Escort/ small ship combination that in this case was further complicated by the inclusion of a

towed line array. From the start it was realized that the available data base for the concept was sparse and that questions of confidence in the perfomance predictions would arise if the usual modelling approach was followed.This was of particular significance for the author who was conducting the research from his own resources. The strategy adopted therefore was to link parameter formulations to the latest high power in-service sonar that would already be acquiring role experience in a large number of complex environments. This allowed the main array parameters to be set for an equivalence with those of the most suitable Escort sonars that would continue to operate in their monostatic sonar mode while at the same time providing a source for the bistatic receiver. Since a small ship fit as the satellite platform was a prime goal, the parameters of the towed array components, the so called "wet end", had to be aligned with the characteristics of a least size ship in terms of radiated noise, towing capacity, deck handling fixtures and not least manpower and costs.

1.8 For some years prior to secondment to S.A.C.L.A.N.T Centre the author had been Deputy Director of the Admiralty Underwater Weapons Establishment and was the

last of the line responsible for research and development of sonar systems for surface ships, submarines,mine hunting helicopter and underwater telephony; also fire control and intercept systems including towed torpedo decoys as well as Instructional and ASW tactical systems. On retirement from S.A.C.L.A.N.T the author became a Hon Research Fellow in The School of Physics, University of Bath and later, as the opportunity arose, was able to model and verify many of key system features of the directive towed line array, cardioid network image rejection parameters,error analyses, means for compensating for cable twist,order of tow forces and the constraints imposed to realise a small ship deck handling equipment.The total tow cable length to the array was arranged to reduce tow ship noise to an acceptable level while its mechanical specifications, structure, diameter and weight, were based on estimates of tow forces at Escort cruising speeds and on speed / depth profiles.The array hose volume, apart from the aperture length, was a compromise between sufficient separation between the cardioid elements, provision for circuit components, flow noise levels, a need to obtain a state of neutral buoyancy and of special import, winch weight and dimensions.The

size of the reels determined the bending radii's and the amount of cable storage. One other feature of the tow cable diameter was the telemetry bandwidth that could be provided since this determined at what point the processing of signal information could be transferred from within the hose volume to a more convenient location aboard ship. Attempts to obtain a measure of real flow noise values in the tow tank and wind tunnel of the University's hydrodynamic department were not successful. A consequence of the separation of the source and receiver was investigated where the quality of the target information at the receiver is very dependent on data supplied from a remote platform. Thus, timing of source transmissions, separation distance between the two ships, sum range, and bistatic angles are all important parameters for system performance. Other features of the bistatic geometry related to differences with its monostatic equivalent. Instead of obtaining range as in a monostatic sonar by the time taken by the transmitted pulse to travel to the target and back, resolving the target position and movement, Doppler for a bistatic situation, requires a great deal more information. On the space co-ordinates of the two platforms, time of transmission from source ship, a time of arrival of

target return, a measure of the base line separation distance, array distance astern of the tow ship, orientation of the array, and angle of target bearing all referenced to the receiving ship. Clarification of the relevant parameters on completion of this phase of the research enabled some of the key operational objectives to be tested and the reasons why the reported bistatic trials had failed to provide any worthwhile gains became very apparent. There was a positive naval reluctance to furnish a continuous radio link between source and receiver ships on the grounds of intercept information for the enemy and it was suggested that satellite navigation could be vulnerable in a major hostile situation: so provision for an underwater acoustic data channel was included in the system format. The intended approach for implementation of the signal processing chain was to follow that used in the source hull sonar. However, as my own research progressed, differences emerged which made it prudent to return to basic theory to explore what,if any, new parameter formulations were needed. The technology of the in-service sonars served as the basis for the task, with the assumption that implementation would embrace the more up-to-date high speed digital processes. To obtain a performance

parity between the two receivers the number of receiving beams of the bistatic system was increased and consequentially the larger number of decision cells per scan time meant changes in the false alarm thresholds; this also is investigated. The end point of the bistatic system research is the formulation of a system that offers cost effective gains in the extension of the sonar control areas of Escort ships at a price that small navies could afford.

1.9 The bistatic system research in this thesis has occupied the part time attention of the author at intervals over several years with a more continued application over the past three years to bring it all together in a coherent form. Events since the NATO requirement was issued have seen the removal of the specific many ocean threat by a major naval power and a wholesale decline in the forces arraigned to meet the particular challenge. Nevertheless it is considered that the results of the research remain an important contribution to the realization and way ahead of the bistatic sonar concept and provide a format for any future trials on the theme. One positive outcome is that the variable depth capability of the directive towed array could be an important adjunct to hull sonars by providing

a variable depth sensor at an optimum depth particularly in a bottom bounce mode. Throughout the period the author had a collateral goal of providing the bistatic ships with an own variable depth source since such an addition would improved the flexibility of the total defence force by allowing the hull sonars to give greater attention to in-duct detection with the bistatic ships having the dual capacity of either extending the in-layer detection ranges or as a variable depth monostatic sonar for below-layer target detection. As is presented later in this thesis, this aspiration eventually materialized with the commercial development of a new form of variable depth active sonar for small ships having value for a world market. This system is seen by the author as having potential as a secondary sonar fit for a hull system. The bistatic system research formed the basis and support for the commercial sonar project which during the succession of proving and demonstrator trials provided evidence for the validation of many of the intended key element of the bistatic concept.

Private Venture Variable Depth Sonar.

1.10 In early 1982 Sperry UK expressed interest in the author's progress with the system research for a bistatic capability and in particular the prospects for a small ship variable depth sonar that would attract a world wide market. A report prepared for the Sperry company in May 1982, introduced the main features of the research together with the grey areas to be resolved in the development of a relatively low cost variable depth active sonar that could be installed in a wide range of small ships, down to 250 to 500 tonnes displacement with a detection performance comparable with that of most hull mounted sonars. Shortly thereafter, Sperry U.K was taken over by British Aerospace and latter's Director of Underwater Engineering, Dr J Wood, continued this interest. Market Research was undertaken to test potential sales and showed that many navies could use the capability for a range of own defence needs with, as expected, a low priority for the bistatic sonar facility. In early 1983 a company funded aimed research programme was arranged that would support the development of a sufficiently engineered system capable of demonstrating performance to potential customers. This was given the acronym ATAS, (Active Towed

Array Sonar), the basis for which at the start made much use of the author's research results on the bistatic sonar and ideas for the VDS application. A list of the author's main reports in the references is an indication of the extent of his participation.

1.11 A key component shortfall was the acoustic source which together with the directive line array was required to be within the size, weight and tow forces of a small ship deck handling equipment. The search for compact low frequency acoustic sources has a long history with the restriction in the ATAS requirement being that only those having a true transfer function were of merit; where the acoustic output is related in some specific way to the input waveform.Thus seismic impulse sources were not suitable candidates; the basic problem is examined in the thesis, section 2. A promising development was the Class IV Flextensional transducer which BAe pursued and produced in a practical form that met the requirements of ATAS. At the commencement the company was short of ASW experience in ship sonar systems and as for the Bistatic Sonar parameter formulation, the available data bank had a large number of grey areas. The philosophy adopted for the system formulation therefore resembled that described for

the Bistatic Sonar. A significant difference was that the many navy market strategy meant that provision for a broad spectrum of possible operational scenarios had to be part of the ATAS demonstrator system capabilities and was kept under constant customer review.As research and system development progressed, trials results expanded the data base and progressively reduced the number of gray areas; thus trials were an important part of the programme of system development and also served to validate many of the formulations made in the bistatic system research. Private venture sonar projects in industry have the general problem of obtaining access to sea-going facilities for the least cost. To fill the gap, ships and crew were hired at appropriate intervals and the most effective employment planned for maximum benefit taking account of fitting out times and weather conditions. Maximum speeds available varied, the best being 14 knots at the demonstrator trials, and this experience with the trial ships was in accord with the type of platforms for which there was the most market place interest. The programme was subjected to continuous review procedures with the overall goal of obtaining equable cost effective solutions across the whole system. This led on occasions to changes or a shift

in emphasis as was the instance of a reduced receiving array performance for a number of advantages in other parts of the system, all of which had to be achieved under the pressure of fixed budgets and deadlines in programme dates. An important factor was a modular format which allowed the system to be tailored to customer's specific requirements and installed in ships alongside. Among additional system features investigated by the author was the inclusion of torpedo detection, and an intercept facility for the detection of high speed intruder craft. As the programme progressed into the design and hardware stages responsibility passed to the specialists in the different disciplines.The author's involvement ended in 1992 on completion of a series of successful customer demonstrator trials in a wide spectrum of acoustic operational environments the results of which met the predicted overall performance expectations.

References

Grimley .W. K . Small Ship ASW Sonar Systems. Sperry Report. May 1982.

Introduction to the Concept.

Grimley W.K. Small Ship ASW Sonar Systems BAe Report P5010 1982

Anti-Subarine Warfare: Small Navies:,The Active Sonar Problem:.

Propagation Modes:.Sonars for VDS: Ship Noise Platform Noise:

Line Arrays: Cardiod Element Line Array;

LF Acoustic Sources of Small Dimensions.

Grimley W.K ASW Acoustic Countermeasures BAe Report P5021 1982.

Purpose of Countermeasures .

Detection,Classification ,Tracking and Counter-action.

Channel Information Rates.

Information in Terms of Space, Bandwith and Signal-to-Noise Ratio.

The Intercept Problem and False Alarm Rate.

System Requirements.

Grimley W.K. System Aspects of Small Ship Towed Sonar. BAE (Dynamics Group) Report P5025 June 1983.

Small Ship Platform Movement: Array Perfomance: Tow Cable Factors:

Depth of Tow: Ship Noise Levels:

Cardioid Element Array Performance Estimates.

Comparisons With Hull and Towed Line Array.

Operational Roles:Search,Screening and Patrol, (includes Barrier type)

Grimley W.K. Applications of Non-Linear Acoustics. BAe Report 5035 1983.

Prospects for a LF Non Linear Acoustic Source.

Finite Amplitude Acoustics.

Parametric Sources Receiving Arrays.
Cavitation as a Source and Sub Harmonics.
Conclusions.

Grimley W.K. Small Ship Systems Project. BAe Report, 1984

Flexibility in Design to Meet Market Requirements.
Proposal for a Family of A.T.A.S Sonars.

Grimley W.K Underwater Acoustic Telemetry. BAe Report March 1984.

Listing of Coded Commands.
Pay-Offs Range vs Channel Capacity and System Hardware.

Grimley W.K. Bistatic Sonar Systems. BAe Report TR 5018 1985.

Bistatic Geometries and Ovals of Cassini.
Estimates of Increase In Active Sonar Range Volume Detection.
Operational Roles.

Grimley W.K. Torpedo Decoy System. BAE Report TR5034 1985.

Submarine Approach Zones.
Torpedo Sensing and Homing Systems.
Problem of Decoy Strategy.
Proposal For Improvements.

Grimley W.K Small Ship Development Programme. BAe Report P 5155 1986

Marketing Issues: Operational Features.
System Parameters.

Grimley W.K. Pro-Submarine Acoustic Intercept Receivers. BAe report TR5079 . 1986.

Sources of Underwater Radiated Noise.
Basic System Formats.
Typical Intercept Operations.

Grimley W.K. Submarine Radiated Noise. BAe Report TR 1989.

Mechanical Sources.

Grimley W.K. Operational Roles for ATAS. BAe Tech Note 1989.

Aspects of ASW: Active and Passive Sonar Detection.

Operator Role and Needs.

Grimley W.K. Low Frequency Active Sonar. BAE Tech Note 1989.

Review paper.

Note on Alternative Energy Sources.

The choice of an energy source for underwater detection is dependent on four factors:

(1) Useful propagation range in the medium.

(2) Ability to differentiate real targets from the background and other objects in the medium.

(3) Speed of propagation.

(4) Generation and reception of source energy.

If the range criterion is not met then the other three are irrelevant and so propagation loss was taken as a key element for choice.

There are many specialist technical books and much supporting literature relating to the different energy sources reviewed in the following two Appendices, those listed below provide a perspective of the basic physics used for the analyses.

1 Heat Sources.

Thermodynamics. Sixth Addition.

V.M.Faires and C.M Simman.

Macmillan Pub Co. 1978.

Thermodynamics. An Engineering Approach.

Y.A Cengel and A.Boles

MacGraw-Hill. 1989.

2 Magnetic Field Detection.

Prior to the research of Orsted(1820) and Faraday(1831) magnetism as a branch of physical science was developed without the background of electromagnetics and so the magnetic field was described in terms of bar magnets in

units which have a formal analogy with an electrostatic field. (See the first two references below.) In geophysics the concept of the Earth as a large magnet with disturbances of its field caused by the introduction of other magnetic objects continues to have value.

The Classical Theory of Electricity and Magnetism.

By M.Abraham, revised by R. Becker,translated by J.Douglas.

Blackie and Son. 1932.

A Textbook of Physics.

By E.Grimsehl,translated by L.A.Woodward.

Blackie and Son. 1933.

Physics, Parts 1 and 2.

D.Halliday and R.Resnick.

J.Wiley .1978.

Applied Electromagnetism.

P.Hammond.

Pergamon Press.1979.

Principles of Ocean Physics.

J.R.Apel.

Academic Press. 1987.

Electromagnetics.

J.A. Edminister.

Schaum's Outline Series.1993.

3 Electromagnetic Propagation in the Sea.

Physics of Waves.

W.C. Elmore and M.A.Heald.

Dover Publications. 1969.

Fields and Waves in Communication Electronics.

S.Ramo, J.R.Whinnery and T.H.Van Duzer.

J.Whiley.N.Y 1965.

Theories for the Interaction of Electromagnetic and Ocean Waves.

A review by G.R. Valenzuela.

Boundary Layer Met. Vol 13 p 61. 1978.

Radio Science and Oceanography.

E.D.R. Shearman.

Radio Sci.18(3) 1983.

Introduction to Radar Systems.

M.I. Skolnik.

McGraw-Hill.N.Y. 1985.

Introduction to Satellite Oceanography.

R.Reidel Pub Co. Netherlands.1985.

Opportunities and Problems in Satellite Measurements of the Sea.

Eds J.F.R Gower and J.R.Apel.

UNESCO Technical Papers in Marine Science.

46 UNESCO, 1986.

Radar Handbook.

Ed M.E. Skolnik

McGraw-Hill.N.Y 1990.

4 Visible Light

Optical Properties of the Sea.

J.Williams.

U.S.Naval Institute,Annapolis.Md.1970

Optical Aspects of Oceanography.

Ed N.G.Jerlov and E.S. Nielson.

Academic Press.U.K. 1974.

Marine Optics.

By N.G.,Jerlov.

Elsevier Scientific Pub Co. 1976.

Suspended Solids in Sea Water.

Ed R.J.Gibbs.

Marine Science Vol 4 Plenum Pub Co. 1974.

Optics.

by E. Hecht and A. Zajac.

Addison-Wesley Pub Co 1980.

Appendix A

OTHER ENERGY DETECTION PROSPECTS.

Naval Interest In Other Energy Sources.

A1.1 A renewed naval interest in the prospects for using other forms of energy to supplement the Escort Ship sonar roles had been stimulated in consequence of reported improvements across a whole gamut of sensor devices and observations of the ocean images obtained by aircraft radar and surveillance satellites.This led to the belief that there were new possibilities for these other sources of energy and that windows were available in the EM spectrum which had not been fully explored. Observed radar images appeared to show features of the sea bed beyond the limits of the accepted EM penetration depths.It was the author's opinion that in most instances the observed patterns could readily be explained in terms of sea surface features where ocean currents disturbed loose material from the tops of pronounced sea bed contours. Analogous phenomena had been observed many years previously by the author during minehunting trials off the East coast of the UK where the peaks of the seabed sand-waves were prominent at the sea surface as bands of displaced sand particles carried to the surface by the tidal velocity gradients.

This disturbed material reproduced an image of the sea floor contour which was superimposed on the normal surface wind wave patterns. In other personal at-sea experience, the presence of an internal wave structure was thought to be the underlying mechanism. A sharp density gradient between the mixed layer and the water below the thermocline can occur quite frequently in the top 200m or so of the ocean.This gives rise to gravity oscillations along the density discontinuity with typical wave speeds of around 0.3 knot and a length of 50m. Vertical oscillations of these waves can be induced by air pressure changes and fluctuating winds at the sea surface. A submarine traversing a volume of water with such conditions can cause layer oscillations that sweep organic matter to the surface to form streaks detected by microwave radars. However, to obtain detection, the right ocean environment is required for the formation of the internal waves and more importantly, numerous false streaks occur due to natural sea surface movement so that there is a high false alarm rate. But it was conceded that there were other unexplained random returns which naval operators suggested could be EM

returns from a submerged target. The difficulty was a lack of documented evidence as most of the affirmations were apocryphal reports and interpretation.

A1.2 A first goal with respect to the viability of any new energy source was to demonstrate that an adequate information channel could be attained along those paths that are commensurate with the location of possible targets. If this were shown to be feasible, then a next stage would be a more detailed investigation into the competing background and defining techniques for extracting information from the returned energy over useful ranges. The signal information flow at the man-machine interface should allow for search, location and classification of targets, together with track movement and fire control data for weapon delivery. Not least was the necessity of ensuing that any new system could be integrated into the whole of each individual ship's defence arrangements as well as that of the accompanying escort defence strategies with a plethora of naval environments. Paired with the above were the practical aspects of the suitability of the source and sensors for ship installation. Figs A1.21 lists some of the energy sources that have been investigated over past decades to varying degrees by Naval funded

Fig A1.21 Sources of Energy.

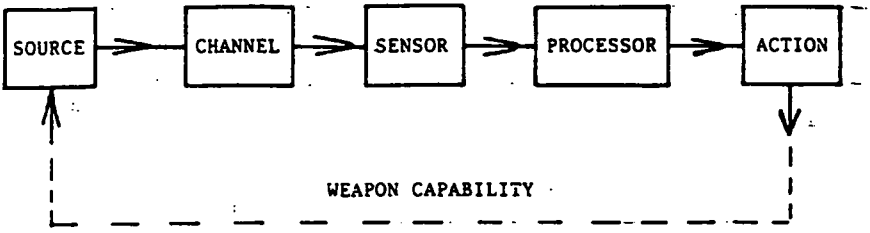

SOURCES OF ENERGY

HEAT	EM WAVES
LIGHT	ELECTRICAL POTENTIAL
SOUND	GRAVITY WAVES
MAGNETICS	SEISMIC WAVES
	COSMIC WAVES
	TRACER ELEMENTS

laboratories for underwater target detection. Fig A1.22 lists some of the main Above and Underwater Sensor Techniques.

A1.3 Evaluation of the prime system parameters may conveniently listed under the following headings.

(i) Those which relate to the characteristics of the appropriate propagation paths ; the transmission loss, information bandwidth and the coherence of the returned signals.

(ii) Those which describe the characteristics and values of the interfering background.

(iii) Those features which distinguish desired target signals from the unwanted background and provide the information input; signal waveform, time integration, spatial discrimination and target movement,etc.

(iv) Man-machine interaction factors which are particularly difficult to quantify for new systems because of the number of indeterminate variables involved. Thus, type and form of the background interference,number of possible targets, time availability of signals, methodology of output presentation, confidence of observations , alertness of operators, methods of reporting and operational value and not least in a naval environment,

TASKS	ABOVE WATER TECHNIQUES	UNDERWATER TECHNIQUES
NAVIGATION	OPTICS, RADIO, RADAR	ACOUSTICS
COMMUNICATION	RADIO, OPTICS, (ACOUSTICS)	ACOUSTICS, (ELF RADIO)
DETECTION AND LOCATION (ACTIVE)	RADAR	ACOUSTICS
DETECTION AND LOCATION (PASSIVE)	RADIO AND RADAR INTERCEPT, OPTICS	ACOUSTICS
CLASSIFICATION OR IDENTIFICATION	RADIO, OPTICS	ACOUSTICS
WEAPON GUIDANCE	RADAR AND RADIO	ELECTRIC (VIA WIRE), ACOUSTICS
WEAPON HOMING	INFRA RED, RADAR	ACOUSTICS

Fig A1.22 Sensor Techniques

the effect of ship movement. The overall system task then would be to attempt to meld together any possible positive physical features into a system format that would provide the most benefits over a wide spectrum of ill-defined roles and environments in a form, at a cost and within a time scale, that would be attractive to participating NATO navies, not all having similar operational priorities.

Comparisons with Acoustic Energy.

A1.4 In Appendix B2 the author reviews various range energy detection prospects as an addition to or as a substitute for sonar. Basic models are used with the acceptance that the listed results are necessarily first order approximations but nevertheless, provide substance for some general conclusions to be drawn about the viability to meet the NATO requirement. Thus, if the energy transmission over the path from the receiving platform to the target operating depth is shown to be insufficient for detection as opposed to communication, then its application is not a practical proposition and other real system features are irrelevant.The results of the basic energy models support informed opinion that although advances in techniques for the listed energy sources of fig A1.21 might produce some extra detection range for specific tasks, in the crucial

issue of ultimate range prospects the size of the attenuation losses are orders of magnitude above that needed to satisfy the specific N.A.T.O requirement. Acoustic energy over most of the frequency band in a seawater medium is attenuated orders of magnitude less than that for the optical,radar and radio spectra,ref fig A1.41. Green blue light may have a maximum viable range of a few hundred metres, radar waves less than a metre. A radio frequency of a less than a kilohertz is needed for a detectable signal communication range of the order of 100m. On the other hand at sonar frequencies of around 200 Hz, the passive detection range of ship noise signals can be several hundred kilometres while at the other end of the acoustic spectrum,frequencies of 1MHz, the range is about 10 metres or less. Surface ship active sonar frequencies are from around 2.5 kHz to say 10 kHz with average echo ranges from 8 to 30 km and more.As the EM frequency increases the sea penetration depth decreases, transmission loss large, and more of the energy is reflected at the sea surface. Observations of below surface features and in some instances of submarine targets, can therefore have their physics more closely tied to the increased discrimination of detailed sea

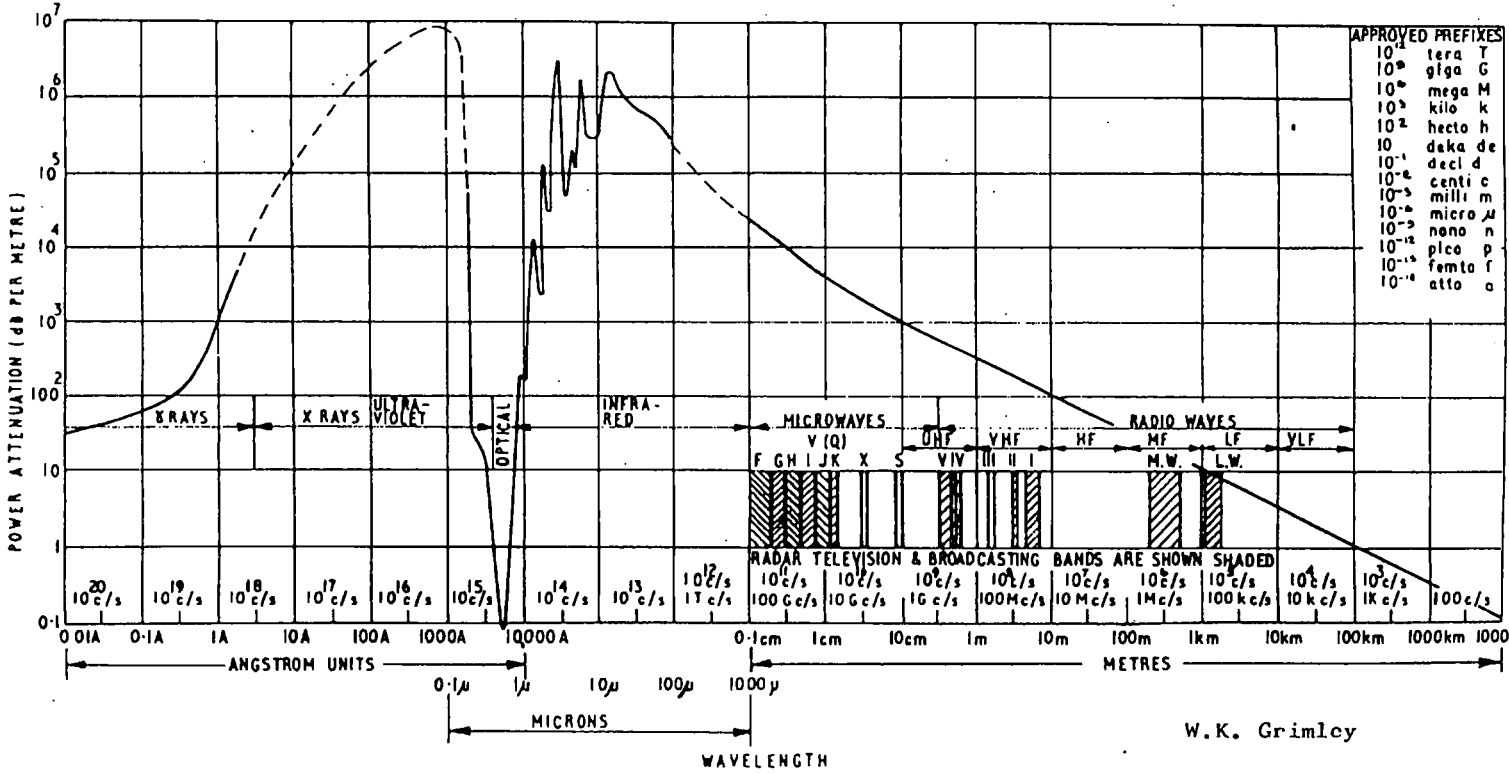

Fig A1.41 Attenuation of Electro-Magnetic Radiation in Sea-Water.

surface patterns afforded by the shorter EM wavelengths rather than as an indication of extraordinary below seawater range detection. This analysis has confirmed the viewpoint of previous expert opinion that the range limitations of energy sources other than sonar are orders less than those required for an Escort ship defence role. A conclusion is that a more profitable way-ahead to counter the known sonar operational constraints and rising costs of Escort sonars is to explore more innovative ways in making better use of the radiated sonar energy.

Appendix B.

Alternative Energy Sources.

Heat Sources.

B1.1 It might be assumed that the large power plants of a submerged submarine platform would leave a detectable heat footprint at the sea surface.

$$Q = cM\Delta t \qquad \text{B1.11}$$

Q = Energy flow, Joules.

M = mass.

ΔT = Temperature change, K.

K = Degrees Kelvin.

c = Specific heat capacity of substance. $J/kg.K$.

Water has an exceptionally high heat capacity = 4186 $Jkg^{-1}K^{-1}$

The high heat capacity of sea water when combined with the large volume flow of water due to target movement, means that in most ocean conditions the temperature changes at the surface have a high probability of being within the normal random temperature variations. Although a nuclear powered submarine may release as much as 188 million joules of heat per second into the ocean, at a speed of 5 knots the dissipated energy over large ocean areas increases the water temperature behind the submarine by less than 0.2 degree Celsius. Moreover, the temperature of this slightly warmer water decreases with target speed and takes time to arrive at the sea surface. Of course, the colder the ambient water the higher the discrimination factor available. EM thermal radiation is at the lower end of the spectral radiant emittance and the signature at the sea surface is also negligible under most circumstances.

The cost of providing ship towed and airborne sensors for the times that the heat signature is detectable has been previously investigated and not considered to be statistically cost effective.

Magnetic Field Detection.

B1.2 Submarine hulls are generally formed from steel plates which disturb the local earth's magnetic field and Magnetic Anomaly Detection,(MAD), uses the principle that the presence of a submarine disturbs the magnetic lines of force surrounding the earth.There are three components of a target's magnetic field that contribute to the observed anomaly in the Earth's field.

(1) The permanent magnetism induced during building.

(2) The induced field produced by the local values of the Earth's field.

(3) The induced field due to movement of conductors in the Earth's field.

There are two main classes of magnetometers, Vector and Scalar.The first types measures the component of magnetic field along their axis; examples are, Fluxgates, Hall Effect magnetometers, Coiled Rods and Rotating Coils. Scalar magnetometers measure the intensity of the magnetic field irrespective of its direction and most magnetic measurements at sea are of the total field type: examples are, Nuclear Precession Magnetometers,Alki Resonance magnetometers and Helium Magnetometers.The essential components are small bottle of some organic fluid rich in hydrogen with a polarizing field considerable stronger than that of the Earth's field, say 50 to 100 oersted obtained by passing a direct current through a solenoid wound round the bottle. When the solenoid current is abruptly cut off the proton's spin relaxes to the direction of the Earth's field and precesses around it

like a spinning top at an angular velocity known as the Larmor pression frequency which is proportional to the magnetic field strength F.

$$\omega = \gamma_p F \qquad \text{B1.21}$$

ω = The angular velocity.

γ = The gyromagnetic ratio of the proton,

= ratio of magnetic moment to spin angular momentum.

The detection is via a coil surrounding the source: the proton being a moving charge induces a voltage in the coil which varies at the precession frequency.

$$F = \frac{\omega}{\gamma_p} = \frac{2\pi f}{\gamma_p}$$

$\frac{2\pi}{\gamma_p}$ = 23.4874 ± 0.0018 in units of gamma/Hz.

Frequency is in the audio band = 2130 Hz for F = 0.5 oersted.

B 1.22

For a field sensitivity of 10γ a frequency difference of 0.4 Hz is to be measured.

B1.3 The magnetic field can be represented by lines of force and Coulomb's Inverse Square Law in CGS units is:,

$$\text{Force} = \frac{p_1 p_2}{\mu r^2}$$

μ is the medium magnetic permeability = unity for air and water in CGS units.

Magnetic field strength H, is force in dynes per unit magnetic pole.

$$H = F/p_1 = \frac{p}{\mu r^2}$$

Number of lines of magnetic force is the flux ϕ

and the number per m^2 is the flux density B.

Magnetic intensity is the number of force lines crossing one sq cm of area perpendicular to the field direction. Lines of force /sq cm.

$$\phi = B.A \text{ and } H = \frac{B}{\mu}.$$

Field strength at a point distant r cm from a pole of p units in air is,

$$H = \frac{p}{r^2} \quad [\mu = 1] \qquad \text{B1.31}$$

H is the magnetic field strength of the poles whilst B refers to the effect of the medium: if the pole strength is referenced to a sphere a factor of $4.\pi$ is included in the divisor. Two unit poles separated by a unit distance attract or repel each other with the unit magnetic field strength in oersted and magnetic induction or flux density in gauss and magnetic flux in units of maxwell. The force field at a distance from a magnet is the combined effects of north and south poles each decreasing as the inverse square law and a measure of this is the dipole moment. A magnet having poles of strength p units a distance 2L cm apart is said to have a magnetic moment of 2pL units.This term arises from the fact that, if a magnet were placed in a magnetic field of unit intensity it would be acted on by two forces each of p dynes. These forces form a couple

whose turning moment is 2pL dyne-cm the symbol M being used to express the magnetic moment.The intensity of magnetisation I, of a magnet is expressed by the ratio:

$$I = \frac{\text{pole strength}}{\text{cross sectional area sq cm}}$$

Thus $I = p/A$.

In the case of a bar magnet of uniform cross section A sq cm with the poles at the extreme ends the magnetic moment is 2pL and, the volume (V) of the magnet is 2L A cub cm, when.

Intensity I = p /A = 2pl / A 2L = M/Vol. B 1.32

Thus the intensity of magnetization may be expressed as the magnetic moment per unit volume. Magnetic potential V is defined in a similar manner to that used for electrostatic potential, as the work required to bring a unit positive pole from infinity to a point r. If Hx is the field strength at distance x cm from a pole of m units strength, then the potential in ergs is expressed by:

$$V = \int_{x}^{\infty} H_x . dx \text{ ergs}$$

$$\text{and } H_x = p/r^2$$

So that the potetial at a point r cm from a pole of strength p units is given by,

$$V = \int_{x}^{\infty} p/x^2 . dx = p/r$$

The dipole potential at a point r from a small bar magnet is the result of the two poles energies.

$$V_p = \frac{p}{r - L\cos\theta} - \frac{p}{r + L\cos\theta}$$

$$V = \frac{M}{r^2} \cos\theta . \text{ ergs.}$$

The magnet moment is a vector and the force equation is:

$$H = -\nabla V . \text{ when,}$$

$$H = \frac{M \cdot \bar{r}}{r^3} \qquad \text{B 1.33}$$

1

The magnetic behaviour of a dipole as above is related to magnets but a more fundamental approach is to regard the source of the magnetic field as due to a loop of circulating charges which produce a magnetic dipole. Experiments by Ampere and Weber demonstrated that a current loop is magnetically equivalent to a dipole with its centre at the midpoint of the loop circuit. Symbolically a current i

---

1 In the literature relating to geophysics both CGS and MKS (SI) units continue to be used consequence of the convenient size of the former and the amount of survey data referenced to the supporting theory. Units in the CGS electromagnetic system are derived by defining the unit magnetic pole as an extra dimension to mass, length and time and putting the proportional factor for space in the inverse square law as unity.

flowing in a small loop of area S is magnetically equivalent to a dipole of moment m, where:

$$m = \mu i S$$

Torque on dipole T is α to $2.pl.B.\sin\theta$.

α to $m.B.\sin\theta$.

Torque on current loop $i.S.B.\sin\theta$.

In MKS units B is defined to make the torque equal to

$$T = i.S.B.\sin\theta \quad \text{newton -metre.} \qquad \text{B 1.34}$$

One tesla is the strength of the magnetic field in which a unit test charge travelling perpendicular to the magnetic field experiences a force of one newton. Because a coulomb per sec is an ampere,(1 C /s = 1 A), the tesla in its more common form is then, 1 T = 1 N / A.m. The magnetic field strength of a small current loop is proportional to the current and the area of the loop while the strength of a dipole is proportional to the pole strength and length. The range of values for the Earth's magnetic field in the two systems is as below.

CGS units.

Magnetic intensity in oersteds 0.25 to 0.7.

Magnetic induction in gauss 0.25 to 0.70.

Magnetic induction in gamma 25,000 to 70,000.

One gamma = 1 / 100,000 oersted = 10^{-5} oersted.

MKS units.

The unit of B is a tesla or weber per m^2

The Gauss or lines per sq cm = 10^{-4} tesla.

In CGS units μ_0 for air is unity,

so either oersted or gauss may be used.

An EMU ampere = 1 / 10.

In SI units $\mu_0 = 4.\pi.10^{-7}$

Range of values for Earth's magnetic field.

newton / weber = 20 to 56

weber / sq m = tesla = 0.000025 to 0.000070

An oriented magnetometer measures the total field, i.e. Target Field + Earth's Field. In effect because the target field is much smaller than the Earth's field in CGS units it measures:

$$(H_x^2 + H_y^2)\cos\phi\cos\theta + H_z\sin\theta. \qquad \text{B1.35}$$

Where,

ϕ = Angle of dip.

θ = Angle of declination.

Limits of Magnetic Field Detection.

B1.4 The horizontal component of the earth's magnetic field in temperate latitudes is between 0.15 and 0.3 oersted. Assume the permeability of steel to be 300 then a submarine placed along the field would have a magnetic induction of no more than B = 300 x 0.3 or 90 gauss. Allow a 7.5 m diameter and a hull thickness of 2.5 cm,then the strength of its induced magnetic pole is $90x750\pi x2.5 = 53x10^4$ gauss cm^2. Its magnetic moment, M , is the sum of these vertical poles along its length and the

whole field has the characteristics of a dipole i.e. $\frac{M}{r^3}$.

Assume that the magnetic moment of the target is say

10^6 EMU/ Tonne.

For a submarine of 4000 tonnes displacement,

$M = 4.0\ 10^9$ EMU.

Field at 500 m = $(5.10^4 cm)$ is given by ;

$$H = \frac{M}{r^3} = \frac{4.10^9}{1.25\,10^{12}} = 3.2.10^{-5} \text{ orsted.}$$

$$= 3.2 \text{ nano tesla.}$$

Field at 1 km = 0.4 nano tesla. B 1.41

MAD can detect signal to about 1 nano tesla.

Note,

Specifications for MAD systems are often described in CGS units.

The degree of degaussing applied to the target could further reduce the above detection ranges and it is clear that airborne magnetometers need to be flown close to the sea surface. Local deviations of as much as 19% of the earth's field may be present due to deposits of magnetic type material with fluctuations of 0.3 gamma per minute plus other noise due to the motion of the magnetometer through spatial background variations. In general therefore, although advances in sensitivity based on higher temperature super-conductors and signal processing could be expected, the practical ranges with a propagation cube law clearly demonstrate that this form of detection system would remain orders less than that needed for the NATO requirement.

Blank

Blank

Electomagnetic Propagation in the Sea.

B1.5 Over the years a large amount of experimentation with undersea electromagnetic propagation has simply confirmed the principles known and inherent in Maxwell's equations. Some of the properties that have received attention are listed below.

(i) Propagation of EM energy.

(ii) Information extraction.

(iii) Radar reflection from the sea surface.

(iv) Emission of electromagnetic energy, infrared, from the sea surface.

(v) Propagation of radio, radar and light energy within the sea medium.

(vi) Induced voltages caused by the movement of sea water in the earth's magnetic field.

A comprehensive description of EM wave propagation in seawater would be very complicated as it would include attenuation, reflection, refraction and scattering both at the air / sea interface and within the medium itself over the whole frequency spectrum. However, the kernel of its utility for the specific NATO need is the range intensity loss so this analysis has concentrated on a comparison between range attenuation losses in free space (air) and seawater. Not fully discussed is the problem of what constitutes detection, location and classification of submerged targets over the frequency spectrum band.

B1.6 Maxwell's Equations are the essence of all electromagnetic field theory, **with no known exceptions**, and the developed technologies in radio, radar, and light are testimony to their validity and widespread variety. The general set of point form equations with a sinusoidal time dependence for both the B and H fields, noting that there is also a corresponding integral form, is given below.

$$(i)\quad \nabla x \overline{H} = (\sigma + j\omega\epsilon)\overline{E}$$

$$(ii)\quad \nabla x \overline{E} = -j\omega\mu\overline{H}$$

$$(iii)\quad \nabla . \overline{D} = \rho$$

$$(iv)\quad \nabla . \overline{B} = 0 \qquad \text{B 1.61}$$

E = electric field vector, volts/meter.

H = magnetic field vector, amps /meter.

D = electric flux density, coulombs/sq metre.

B = magnetic flux density, weber/sq meter = tesla.

Jc = conduction current, amps / sq metre

Jd = displacement current, C dV/dt. B 1.62

$\overline{D} = \epsilon\overline{E}$: D = Electric Flux Density. ϵ = permittivity

$\overline{B} = \mu\overline{H}$: H = Magnetic Field Intensity μ = permeability

$\overline{J}_c = \sigma\overline{E} = i/A$: σ = Conductivity

$$J_d = \frac{\partial \overline{D}}{\partial t} = \text{Displacement Current}$$

For free space, a perfect dielectric,

$$\epsilon = \epsilon_0 \text{ and } \sigma = 0$$

$$\text{velocity} = \frac{\omega}{\beta} = \frac{1}{\sqrt{\mu\epsilon}} \qquad \text{wavelength } \lambda = \frac{2\pi}{\beta} = \frac{2\pi}{\omega\sqrt{\mu\epsilon}}$$

while for seawater $\epsilon = \epsilon_r\epsilon_0$

$$\epsilon_r = \frac{\epsilon}{\epsilon_0} \text{ and } \sigma \text{ is not 0.} \qquad \text{B 1.63}$$

[2]

Most complicated wave forms can be approximated as a superposition of a number of plane waves so that the properties of a plane sinusoidal linearly polarized EM wave propagating in free space and seawater are taken as the basic model for analysis.

---

2 The treatment of Maxwell's equations has made use of " Fields and Waves in Communication Electronics." Simon Ramo et al,1965. The kernel of the propagation loss of EM waves in the sea is presented by L.N. Lieberman, " The Sea " Vol 1 ," Other Magnetic Radiation" Ed M.N.Hill,1962.

The vector wave equation is obtained by the operator curl curl and the Laplacian of the vector.

$$\nabla^2 \overline{H} = j\omega\mu\ (\sigma + j\omega\epsilon)\overline{H} = \gamma^2 \overline{H}$$

$$\nabla^2 \overline{E} = j\omega\mu\ (\sigma + j\omega\epsilon)\overline{E} = \gamma^2 \overline{E}.$$

$$\nabla^2 \overline{H} - \gamma^2 \overline{H} = 0$$

$$\nabla^2 \overline{E} - \gamma^2 \overline{E} = 0$$

$$\gamma^2 = \left[j\omega\mu\sigma\left(1 + \frac{j\omega\epsilon}{\sigma}\right)\right]$$

$$= (-\omega^2\mu\epsilon + j\omega\mu\sigma) \qquad \text{B 1.64}$$

γ = the propagation constant.

The real and imaginary parts of the complex propagation constant are:

$$\gamma = \alpha + j\beta = (\omega^2 \cdot \mu\epsilon + j\omega\mu\sigma)^{1/2}.$$

$$\overline{E}_x = E_0 . \exp -\alpha z . \exp j(\omega t - \beta z)$$

$$\overline{H}_y = H_0 . \exp -\alpha z . \exp j(\omega t - \beta z)$$

σ = conduction current, S/m

$$\alpha = \omega\left(\frac{\mu . \epsilon}{2}\right)^{1/2} \left[1 + \left(\frac{\sigma^2}{\omega^2 . \epsilon^2}\right)^{1/2} - 1 \right]^{1/2}$$

$$\beta = \omega\left(\frac{\mu . \epsilon}{2}\right)^{1/2} \left[1 + \left(\frac{\sigma^2}{\omega^2 . \epsilon^2}\right)^{1/2} + 1 \right]^{1/2} \qquad \text{B 1.65}$$

The above demonstrates that for a conducting medium a plane wave travels with a phase velocity of $v = \omega/\beta$. and has an exponential attenuation as well as a phase change. The ratio of **E / H** is the intrinsic impedance.

$$\eta = \frac{E_0}{H_0} = \left[\frac{\mu}{\epsilon(1 + (\sigma/j.\omega.\epsilon))} \right]^{1/2} = \frac{j\omega}{\gamma} \qquad \text{B1.66}$$

and for free space the σ term is zero.

For a perfect dielectric such as free space, air, a summary of main characteristics that relate to the propagation of EM waves is listed below.

The intrinsic impedance $Z\angle\phi$ is,

$$\frac{E_x}{H_y} \text{ and,}$$

$$\nabla x \overline{H} = (\sigma + j\omega\epsilon)\overline{E}$$

$$\nabla x \overline{E} = -j\omega\mu\overline{H} \text{ so with,}$$

$$\alpha = 0 \qquad \beta = \omega\sqrt{\mu\epsilon} \quad m^{-1}$$

$$\mu = \mu_0 = 4\pi x 10^{-7} H/m$$

$$Z\phi. = \sqrt{\frac{\mu}{\epsilon}} \angle 0^0$$

$$\epsilon = \epsilon_0 \approx \frac{10^{-9}}{36\pi} = 8.854x10^{-12} F/m \qquad \text{B 1.67}$$

$$Z \approx 120\pi \text{ ohms}$$

$$v = c = \frac{\omega}{\beta} = \frac{1}{\sqrt{\mu\epsilon}}$$

$$c \approx 3x10^8 \text{ m/s.}$$

The space directions of E and H are normal to each other and the Poynting vector , P = E x H, which is the instantaneous rate of flow of energy per unit area, is normal to the plane containing E and H and in the z or r direction..

Using complex notation the Poynting vector is expressed by,

$$\overline{P} = 1/2\overline{E}x\overline{H}^*$$

$$\overline{E} = E_0 \exp j\omega t.$$

$$\overline{H}^* = H_0 \exp -j(\omega t - \phi)$$

ϕ is the phase angle between $\overline{E}$ and $\overline{H}^*$

$\overline{H}^*$ is the complex conjugate of $\overline{H}$

where $\overline{H} = H_0 \exp +j(\omega t - \phi)$

$$\overline{P} \text{ average} = \text{Re P} = 1/2E_0\ H_0 \cos\phi \quad W/m^2 \qquad \text{B 1.68}$$

ϕ is the phase difference between $\overline{E}$ and $\overline{H}$,

which in free space = 0.

From the basic description of E and H in free space, it is observed that they are identical functions of z and t and although in time phase their magnitudes differ by the factor:

$$\overline{E}_x = E_0 \sin(\omega t - \beta z) \text{ N/m}$$

$$\overline{H}_y = H_0 \sqrt{\frac{\epsilon}{\mu}} \sin(\omega t - \beta z) \text{ A/m}$$

$$\eta = \frac{E_0}{H_0} = \frac{\text{volts /metre}}{\text{amps /metre}} = \text{ohms}$$

$$\eta = \sqrt{\left(\frac{\mu}{\epsilon}\right)}$$

$$= \sqrt{4\pi x 10^{-7} x 36\pi x 10^9} \sim\sim 376.7 \text{ ohms} = 120\pi \qquad \text{B 1.69}$$

When E and H are in time phase, η is a pure resistance.

With a perfect dielectric, no conduction current, and an isotropic medium the electric intensity component is dominant and with no attenuation in the E and H waves the range intensity loss would be that due geometric spreading and boundary losses.

B1.7 The sea, unlike space, is not a perfect dielectric and has a conductivity, Jc, which is the point form of Ohm's law. As might be expected,it is a complex function of frequency,temperature and salinity: however its intrinsic frequency dependence is small for frequencies extending to well over 100 GHx.

$$\bar{J}_c = \sigma \bar{E} = \text{amps / sq m}$$

$\bar{J}$ = conduction current density. amperes / sq m .

σ = conductivity of the medium. siemens /m,

$$= \frac{\text{amps/metre}}{\text{volts /metre}} = 1/\text{ohms} \qquad \text{B 1.71}$$

The permittivity parameter ϵ

= ϵ_0 of free space x ϵ_w the dielectric constant for sea water.

$$\epsilon_0 \sim \frac{1}{(36\pi x 10^9 F/m}$$

$$\epsilon_w \approx 81$$

$$\sigma = 4.3$$

μ is the permeability of free space and seawater,

$$= 4\pi x 10^{-7} H/m$$

B 1.72

When the conductance term is include the space equations are:

$$\overline{E}_x = \overline{E}_0 \exp(j\omega t - \gamma r)$$

$$\overline{H}_y = \overline{H}_0 \exp(j\omega t - \gamma r)$$

$\overline{E}$ and $\overline{H}$ are related by :

$$\frac{\partial \overline{E}_x}{\partial r} = -\mu \frac{\partial \overline{H}_y}{\partial t}$$

and if E and H vary sinusodally with time,

$$\frac{1}{\mu}\frac{\partial^2 \overline{E}}{\partial r^2} = j\omega(\sigma + \omega\epsilon)\overline{E} = \gamma^2 \overline{E}$$

γ is the propagation coefficient = $(\alpha + j\beta) = (-\omega^2\mu\epsilon + j\omega\mu\sigma)^{1/2}$

and $\overline{E} = E_0 \exp j\omega t \exp -\gamma$ in the range direction. B 173

The above is of the same form as the propagation of the wave in space,eqn B1.65, except for an exponential range loss of energy due to the conductivity of the medium which is no longer zero, eqn B1.66.

$$\eta = \frac{\overline{E}_x}{\overline{H}_y} = \frac{j\omega\mu}{\gamma}.$$

$$\eta = \sqrt{\frac{\mu}{\epsilon}} \times \sqrt{\frac{1}{1 - j(\sigma/\omega\epsilon)}} \qquad \text{B1.74}$$

The intrinsic impedance is now a complex quantity, so that the electric and magnetic fields are no longer in time phase.

The relative magnitude of the conduction current to displacement current is expressed by $\frac{\sigma}{\omega\epsilon}$. In passing through the sea surface the E component of an EM wave induces a current flow which produces a magnetic field at right angles which in turn will generate an induced Ei field in opposition to Eo.The result is an exponentially decaying E field as it penetrates into the sea. The Poynting field is

therefore losing energy due to resistance and the induced E field so that:

$$\overline{P} = \overline{E} x \overline{H} = \frac{E^2}{\eta}\cos^2(\omega t - \beta z)\ W/m^2 \qquad \text{B 1.75}$$

$$\overline{E}(z,t) = \overline{E}_0 \exp(-\alpha z)\exp(\omega t - \beta z) \text{ and,}$$

$$\overline{H}(z,t) = \frac{\overline{H}}{\eta}\exp(-\alpha z)\exp(\omega t - \beta z - \theta) \qquad \text{B 1.75}$$

The depth z to which the level has decreased to 1/e or 36.9 % of its value is δ known as "skin depth". Binomial expansions of the expressions for α and β provide estimates of the propagation parameters for two cases of relative magnitude of conductance current to displacement current:

case 1 $\frac{\sigma}{(\omega\epsilon)} \ll 1$ Medium is only slightly lossy

$$\alpha = \frac{1}{2}\sigma\left(\frac{\mu}{\epsilon}\right)^{1/2}\left[1 - \frac{1}{8}(\sigma/\omega\epsilon)^2 + \ldots\right] \sim\sim \frac{1}{2}\sigma\left(\frac{\mu}{\epsilon}\right)^{1/2}$$

$$\beta = \omega(\mu\epsilon)^{1/2}\left[1 + \frac{1}{8}(\sigma/\omega\epsilon)^{1/2} + \ldots\right] \sim\sim \omega(\mu\epsilon)^{1/2}$$

case 2. $\sigma/\omega\epsilon \gg 1$ The conduction current is dominant.

$$\alpha = \left(\frac{\omega\mu\sigma}{2}\right)^{1/2}\left[1 + \frac{\omega\epsilon}{2\sigma}\ldots\right] \sim\sim \left(\frac{\omega\mu\sigma}{2}\right)^{1/2}$$

$$\beta = \left(\frac{\omega\mu\sigma}{2}\right)^{1/2}\left[1 + 1 - \frac{\omega\epsilon}{2\sigma} + \ldots\right] \sim\sim \left(\frac{\omega\mu\sigma}{2}\right)^{1/2} \qquad \text{B 1.76}$$

In case 1 the attenuation constant to a first approximation is independent of frequency and the phase constant tends to be that of space. In case 2 the attenuation and phase constants are equal. In the frequency regions where the conductance to displacement current is a prominent feature the attenuation is an additional range loss term

added to the geometrical spreading loss.The phase constant β in a conducting media is different from that in space and increases with conductivity. Hence the wavelength for a given frequency becomes smaller and the velocity of propagation is reduced so that the sea medium is then dispersive: waves with different frequencies have different velocities.The velocity of propagation and the wavelength are given by:

$$v = \frac{\omega}{\beta} = \frac{1}{[\mu\epsilon/2\ (\sqrt{1+(\sigma/\omega\sigma)^2}+1)]^{1/2}}$$

$$\lambda = \frac{2\pi}{\beta} = \frac{2\pi}{\omega[\mu\epsilon/2\ (\sqrt{1+(\sigma/\omega\sigma)^2}+1)]^{1/2}} \qquad \text{B1.77}$$

The fields below the sea surface have the properties of rapid exponential decay with depth and a phase difference between **Ew** and **Hw** with the magnetic field being much larger than the electric field. The Debye formulation for the constants for sea water treat polarization in terms of relaxation theory similar to that for acoustics.The region up to f = 250 GHz is taken as a typical frequency for which a conductivity of 4.3 siemens per m at T = 15 degrees C and s = 35 psu is an acceptable value with a relative dielectric constant of 81.The index of refraction for electromagnetic radiation, n , is a function of the dielectric properties and conductivity and light is treated as a separate subject.

B1.8 The order of magnitude of the skin depth for the sea constants as given is:

$$\delta = 250/\sqrt{f} \qquad \text{B 1.81}$$

The order of magnitude of δ for typical marine radars, for f ~~ 10^{10} it is 0.025 m, while at 10^{3}it is 7.9 m.The velocity at the lower frequency is about 15 times that of sound.

Frequency Hz	Velocity km/s	Wavelength m	Attenuation Skin Depth m
20	6.82	341	54.3
100	15.3	153	24.3
1000	46.3	48	7.68
10,000	152,7	15	2.43
100,000	483.8	4.8	O.77

B1.9 Nearly all of electromagnetic radiation originating above the sea is reflected at the sea surface the reflectivity for a smooth surface depending on the conductivity and angle of incidence.

Incident:

$$E_1 \exp j(\omega t - k_0 z)$$

Reflected:

$$E_1^j \exp j(\omega t + k_0 z)$$

Transmitted:

$$E_2^j \exp(-z/\delta) \exp j(\omega t - z/\delta)$$

k_0/c = the vacuum wave number.

δ is the skin depth parameter.

The superscript j indicates that the amplitudes are complex quantities. 1.91

The order of the transmission loss is expressed by the power reflection coefficient for normal incidence.Since the incident and reflected waves are in the same medium;

$$R_a = |R_E|^2 = \frac{[1+(1-\omega\delta k_a/c)^2]}{[1+(1+\omega\delta k_a/c)^2]}$$

$$\approx 1 - \frac{2\omega\delta k_a}{c}$$

Conservation of energy requires that the fraction of power in the sea is:

$$T_s = [1 - R_a]$$

$$\approx 2\omega\delta k_a/c$$

For a good conductor, $\delta \to 0$, 192

when the wave is almost perfectly reflected.

Above shows that the wave amplitude attenuates by a factor of "e" in each skin depth and that the effective wavelength $\lambda = 2\pi\delta$ is reduced from its in-air value $\lambda_0 = 2\pi c/\omega$ by the large factor

$$\frac{\lambda_0}{\lambda} = \frac{c}{\omega\delta} \gg 1 \qquad 1.93$$

It follows that the wave speed in water is less than that in air by the same factor. The magnetic component B may be derived in a similar fashion when it is shown that the E and B fields are not in phase. In a good conductor the magnetic field lags the electric and, as expected, a large fraction of the energy is carried by the magnetic field.The returns from sea waves as observed at a distant point would be the sum of coherent,reflection, and random, scattering components each with its own angular dependency.Three regions of object recognition are distinguished:

(1) Where the object dimensions are greater than the intercepting wavelength. This is the optical region.

(2) Where object dimensions are about the same as wavelength. This is known as the resonance or Mie region with large fluctuations about the optical value.

(3) For target dimensions much less than the wavelength the scattering returns have a λ^{-4} dependency,the Rayleigh region.

It follows that distinguishing features of the sea waves will increase as the wavelength decreases: thus a 3MHz radio wave has a wavelength of 100 m while for frequencies from about 3 to 300 GHz the wavelengths are from 10cm to 1mm. Noting that the skin depth is:

$$\delta \approx (2/\mu_0\sigma_s\omega)^{1/2} \qquad 1.94$$

then it is clear that the potential for increased resolution is obtained with increasing attenuation of the transmitted wave in seawater.In remote sensing advantage is taken of Synthetic Aperture Radar with wave lengths of

the order of centimetres. At 3 GHz the wavelength is 0.1m and a focussed SAR array could have a spatial resolution of the order of metres. Range discrimination is obtained by transmitting a chirp pulse with pulse compression processing that should provide a resolution of centimetres when distinctive features of the patterns formed by scattering particles on the seawaves could be observed.In general the capacity for EM waves to propagate below the sea surface is a feature of the lowest frequencies and is evident in the very low frequencies needed for long range communications to submarines where the penetration depth is tens of meters. Although the below sea surface propagation losses are smaller the very long wavelengths, low EM wave velocity and narrow bandwidths rules out target detection possibilities.The use of EM radiation for below ground object location is another example of the range depth limitations.

Frequency	10 kH	100kHz	1MHz
Wet earth σ = 0.03 S/m	2.5 m	0.7 m	0.25 m
Dry earth. σ = .003 S/m	92 m	29 m	9.2 m

B1.10 In general a key feature for the capacity of electromagnetic radiation to propagated in the sea depends on the transmission loss, fig B1.101. The range to which this is attained is related to the frequency of the wave while the ability to provide target details will be allied to the

wavelength. The EM spectrum as used for defence purposes extends from ELf frequencies below 1000 Hz with wavelengths of the order of km to millimeters in the frequency band around 300 GHz. At 100hz, the attenuation in sea water is about 0.3 dB/m, at 1 kHz it is 1 dB/ and then increases to 30 dB/m up to the optical window frequencies. Because of the dispersive nature of the sea medium the transmission rate over the ELF, 30 to 300 Hz may be only about 1 bit\s so messages are slow.Also underwater communication at the lowest frequencies is characterized by very large aerials. Experiments in shallow water with submerged dipoles have shown that in situations where the seabed and above sea surface form part of the propagation path a limited communication range of around 100m was possible at 10 kHz. At the highest EM frequencies the penetration depth is insignificant but discrimination of sea surface features is high due to the small dimensions of the wavelength. The latter could explain the increase in recent years of presence of below sea material at the sea surface being attributed to below water detections.

Visible Light.

B1.11 The visible light range ,violet to red, spans wave length from 0.4 to 0.8 micron and the subject of light in the sea has a long history supported by a substantial number of papers particularly on solar radiance and its relevance to living organisms. Although optical radiation is electromagnetic in nature, it is usually described in the terminology of intensity, radiance, irradiance, and a wide variety of absorption, scattering and attenuation coefficients and only rarely in terms of the physical descriptions applicable to electric and magnetic fields. A great deal of the literature relates to incoherent, wideband sources and the use of lasers is still being explored.

B1.12 Three intrinsic optical properties of sea water are defined; light intensity, absorption, wave scattering and geometrical spreading. Absorption refers to the loss of energy due to dissipative mechanisms while scattering describes the loss of energy from the propagating wave by scattering due to the presence of particulate matter in the media; geometrical spreading as the name implies refers to beam spreading. Pure water is most transparent to blue light,0.48 um = 480 nm, and least so to red. Salts dissolved in sea water increase the absorption only to a minor extent a minimum being in the blue green, 460 nm: the effective limit of useful wavelengths is in the band between 300 and 1000 nm. On a local scale, the underwater light field is generally homogeneous on azimuth but changes rapidly with depth. Snell's law implies that a

light ray at grazing incidence on a smooth water surface will be refracted towards the normal to the surface. An average value for the optical refractive index is 1.34 which means that the speed of light in seawater is $2.24x10^8$ m /s and the wave length, n approx (4/3), is about three-quarters of that in air. The critical transmission angle is near 48 degrees so that the light illumination is constrained to a cone of 96 degrees full angle. When viewed from above, a consequence is to make targets appear to be closer,1/n ,larger and travel faster than is actually the case.The magnification factor M,is the ratio of the subtended incident angle to the subtended refractive angle:

$$M = \frac{\delta\theta_i}{\delta\theta_t}$$

$$= n\left[\frac{(1-\sin^2\theta_t)}{(1-n^2\sin^2\theta_t)}\right]$$

θ_t is the angle of refraction.

The largest value for M is near to the critical angle. 1.121

Beyond the global variability of solar illumination, the intensity is a function of diurnal and seasonal changes. In some specific areas submarines operating close to the sea surface have been sighted by aircraft and helicopters within this restricted cone area in conditions of strong sunlight and in calm sea states, but rarely when the surface was disturbed.The effect of wind and waves modifies the smooth surface with a variation of reflectivity that characterizes any EM radiation.

B1.13 In ref, Gazey has made a comparison of the range and resolution capabilities of short range acoustical and optical imaging systems in turbid waters. The material scattering will be higher for light than for acoustics because of the functional dependence on wave-number. As is observed with any energy source, an underwater object can only be differentiated from its background returns if a minimum signal to background level is realised. In the optical case the image contrast depends upon the intensity difference at the receiver between the radiance of the object and the interfering background as described by

$$Co = (Lo - Lb) / Lb \qquad \text{B1.131}$$

The inherent contrast Co is defined in terms of the brightness of the object, Lo, and the background intensity, Lb. The reduction of light intensity from the source to target over range r is subject to spherical spreading, attenuation and scattering,

$$I_r = I_o / r^2 \exp(-\gamma r) \qquad \text{B1.132}$$

I_o = Source intensity level

I_r = Received intensity level

γ = total attenuation coefficient

$1/\gamma$ = attenuation length of medium

r = *range*

For the simple case of a constrained horizontal optical path the contrast ratio is ,

$$C_r = C_o \exp(-\gamma r) \qquad \text{B1.133}$$

Detection of the object depends on coherent light rays that are returned directly to the receiver. With wide angle illumination and, like reverbertion, the background scattering is the limiting backgound and a great deal of the data on light in the sea is for such a situation.

B1.14 A table taken from ref Jerlov, of the ranges of dark objects in silhouette against their natural background with b measured at an optical wavelength of 0.5 u m and the eye as a detector for different water conditions is ,

Sea Water State	γ per m	Sighting Range m
Clear Oceanic	0.03	133
Normal Oceanic	0.117	34
Turbid Oceanic	0.174	23
Normal Coastal	0.342	11.7
Turbid Coastal	0.755	5.3

B1.15 The above sighting range values demonstrate that the already large medium attenuation scattering is increased even more when particulate matter within the sea is present.In general underwater sighting ranges are usually controlled by water clarity and the contrast between

object and background. Unlike the pulse systems of radar and sonar, light propagation data generally refers to continuous sources. Research on high power lasers, 500kW and more, with pulse duration of less than 0.01us in the visible spectrum offers the prospects of orders reduction in the competing background with a range improvement closer to the limits set by the attenuation parameter, say several hundred metres but still far short of the goal needed.

References.

Apel J.R. Principles of Ocean Physics. Academic Press 1987

Austin R.W and Petzold. Spectral Dependence of the Diffuse Attenuation Coefficient of Light in Ocean Waters. Optical Engr, Vol 25,1984.

Blizard M.A Ocean Optics. V11, Pro SPIE, Vol 208, 1980.

Born M. And Wolf E. Principles of Optics. 5th Ed Pergamon Press 1975.

Caimi F.M. Refractive Index Measurements in Seawater: Several Methods. Oceans '90 Conference, Proc IEEE, p 1594.

Duntly S.O. Ed Ocean Optics. V1 Proc SPIE, Vol 208, 1980

Duntly S.O Light in the Sea. Benchmark Papers in Optics. Ed Tyler J.E. Dowden ,Hutchinson And Ross Inc. 1977.

Elachi C. Spaceborne Radar Remote Sensing Applications And Techniques. I.E.E.E N.Y 1988.

Gazey B.K A. Comparison of Acoustical and Optical Imaging Systems in Turbid Water. I.R.E. Conference Proceedings. No 19 Sept 1970. Electronic Engineering in Ocean Technology.

Gower J.F.R. Ed. Oceanography from Space. Plenum Press .1981.

Hovart V. Underwater Radio Transmission. Handbook of Ocean and Underwater Engineering. McGraw-Hill NY 1969.

Jerlov N.G. Optical Oceanography. Elservier, 1968.

Jerlov N.G.and Nielson E.S. Optical Aspects of Oceanography. Academic Press 1974.

Klien L.A and Swift C.T. An Improve Model for the Dielectric Constant of Seawater at Microwave Frequencies. I.E.E.E. Trans Attennas and Proc Vol AP- 25 p 104.. 1977.

Lieberman L.N. Other Magnetic Radiation. The Sea. Ed, M.N.Hill Vol 1 J Wiley 1962.

Ramo R. Whinnery J.R and Van Duzer T. Fields and Waves in Communication Electronics. J Wiley 1965.

Saltzmann B. Ed. Satellite Oceanography. Advances in Geophysics. Vol 27 Academic Press 1985.

Valenzuela G.R. Theories for the Interaction of Electromagnetic and Ocean Waves. A Review. Boundary Layer Met. Vol 13, p 61.. 1978.

Tyler J.E and Preisendorfer. Light. The Sea. Ed, M.N.Hill Vol 1. J Wiley 1962.

Section 2

Contents.

Section 2.

Hull Sonars.

Section 2 Figs.

Fig 2.11 Construction of Regions of Approach.

Fig 2.12 Transmission Loss Curves.

Fig 2.31 Surface Duct Propagation.

Fig 2.32 Distribution Curves of Layer Depth in North Atlantic.

Fig 2.33 Distribution Curves of World Wide Layer Depths.

Fig 2.34 Surface Duct Transmission. 2.0 kHz.

Fig 2.35 Surface Duct Transmission. 8.0 kHz.

Fig 2.36 Target Range Plot. Hull Sonar and VDS at 100m Depth.

Fig 2.37 Target Range Plot. Hull Sonar and VDS at 100m Depth.

Fig 2.38 Target Range Plot. Hull Sonar and VDS at 200m Depth.

Fig 2.41 Depth Excess for Convergence Zone.

Fig 2.42 Depth Excess Contours for Feb and Aug.

Fig 2.51 Depressed Sound Channel Propagation.

Fig 2.52 Incidence of Depressed Sound Channels Throughout the World.

Fig 2.61 Ship Noise Sources.

Fig 2.91 Sea State and Acoustic Loss at the Sea Surface..

Fig 2.111 Curves of Reflection Loss vs Grazing Angle.

Fig 2.112 Bottom Loss for "Fast" and "Slow" Sediments.

Fig 2.141 Average Bottom Loss for Two Regions.

Fig 2.161 Two Way Propagation Loss.

Section 2.

Hull Sonars.

Operational Factors.

2.1 A particular defence problem for many in-service sonars in surface duct conditions is that of countering a submarine that makes its approach below the layer with brief excursions into the duct to obtain information on the location of the surface ships. At the start of the pursuit, the submarine's tactics are largely determined by the time available for the mission, distance to the target zone, and best estimates of the relative velocities of the submarine to that of the defended shipping. A simple situation is where the ultimate goal of the pursuer is to attain a favourable attack position against shipping which is proceeding at a fixed speed to reach a predetermined end point. Fig 2.11 illustrates the main parameters in the approach region. The velocity of the aggressor is 'u' and 'v' that of the shipping. Not shown is the disposition of the Escorts with their variable patrol areas which advance at about the same forward speed as the shipping. To obtain a favourable attack position for missiles or torpedoes at say Q, then the ratios of ut to that of vt determine the limiting angles of approach. For positive values of vt and observing how the moving circle varies about the centre point and the radius, it is seen to sweep out an angular region between two fixed tangents drawn from zero, point P. The angle $\sin^{-1} u/v$ is known as the limiting angle of approach.The angular space between the two tangents to the circle is the locus of all starting positions of the

attacker if it is to close the defended shipping, Three typical situations are:

(1) $u < v$

A submarine is limited to start points at geographical ahead positions of the shipping route and is required to reach the forward region of A by the time the shipping reaches the pursuers location.

(2) $u = v$

The submarine now has more flexibility in the angle of its ahead position of approach. An ultimate limit is where the tangents coalesce into a horizontal line tangent to regions A, as set by weapon range and firing angles.

(3) $u >> v$

The only limiting boundary is the time available. Endurance is included in the vt product, the greater the attacker's speed advantage the less the time needed to gain the target area. Limits on u are related to the submarine power plant as well as radiated and self noise levels: a nuclear powered submarine in a long range pursuit has the possibility of closing the location of the defended shipping from any quarter. At the approach stage, advantage would be taken of a below surface duct track at a speed set by an acceptable level of radiated noise and the time required to attain the defended location. As the range to the target area decreases, an enhanced information bandwidth is needed for classification, weapon firing and plotting a favourable escape route which requires entering the duct when speed would be adjusted for optimum self noise levels. An appreciation of the attacker's

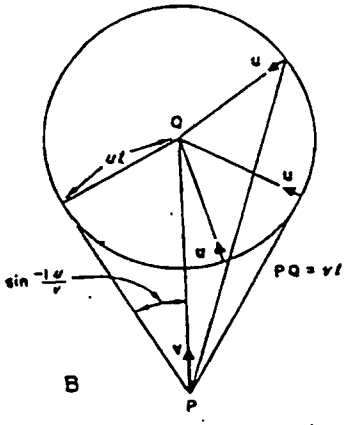

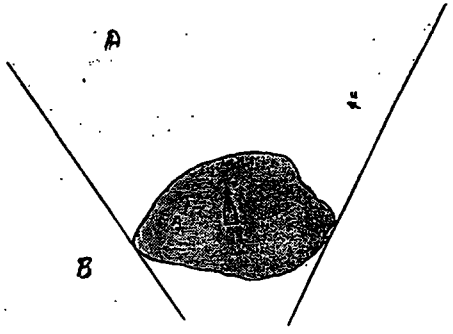

Fig 2.11 Construction of Regions of Approach.

problem is given by a rough guide to the passive sonar transmission loss at a range where spreading loss = range attenuation loss.

$$TL = 60 + 20 \log r + \alpha r$$

$$\frac{\Delta(TL)}{\Delta r} = \frac{8.7}{r} + \alpha$$

$$20 \log e = 8.67.$$

Spreading Loss = Absorption Loss at Range r_c.

$$r_c = \frac{8.76}{\alpha} \approx \frac{10}{\alpha} \qquad 2.41$$

r = range km.

α = absorption coefficient in dB/km.

kHz	a	r km
0.5	0.019	526
1.0	0.053	188
2.0	0.128	78

Fig 2.12 illustrates the effect of the increase of attenuation with frequency. For some underwater weapons the firing range distance from target could be as much as 10 to 20 km.

1

Above is intended to illustrate that Escort target detection opportunities within the duct may be limited to the intermittent intervals when the submarine is obtaining passive sonar information on the force location and ship disposition during the approach phase or for longer excursions during the weapon firing stage. The dilemma for

---

1 An extensive treatment of Naval Operations Analysis is in the book of that name.See ref.

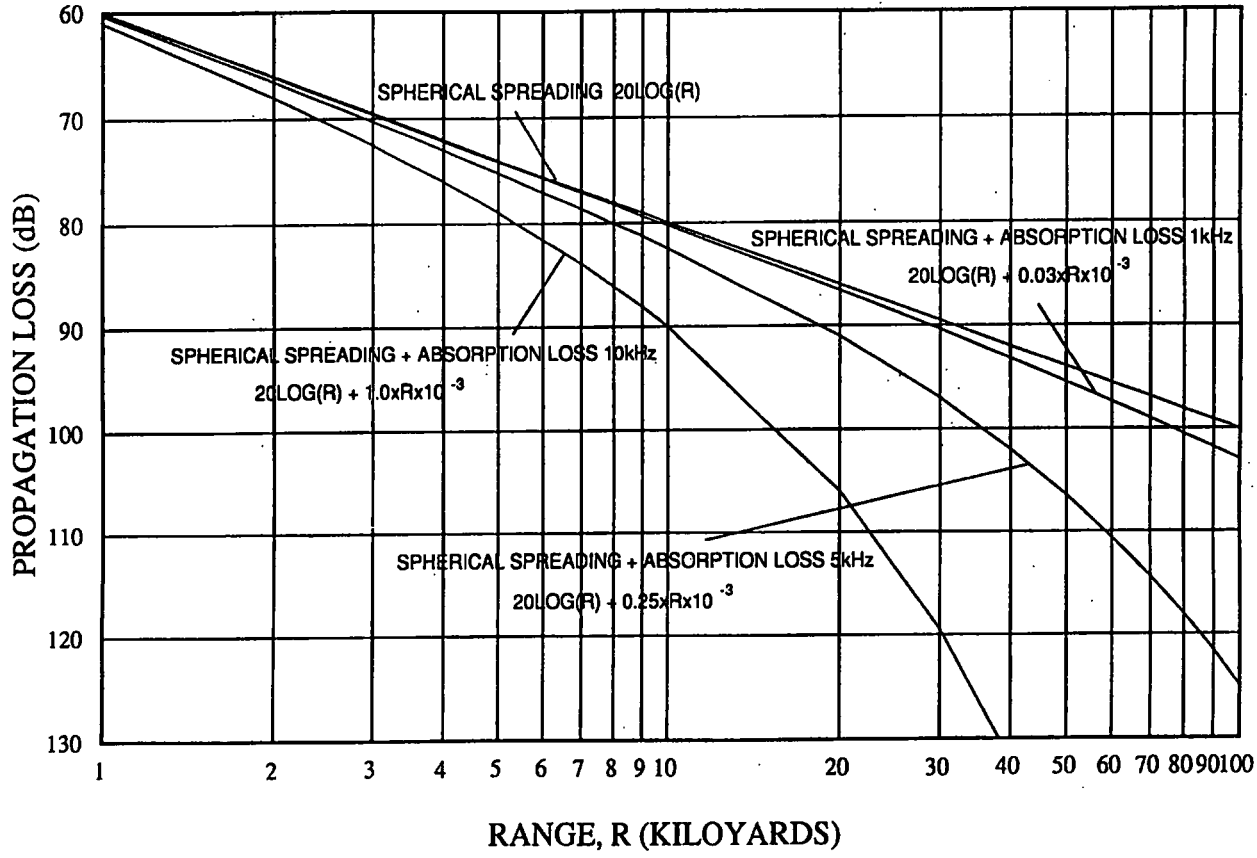

Fig 2.12 Transmission Loss Curves.

operators of multi-mode hull sonars, higher power lower frequency, is that only one mode can be accessed at any one time. Time spent in the different modes must be balanced against possible lost opportunities or fewer integrated returns in one of the other modes with in-duct detections generally having priority.

2.2 Almost all surface ship sonars use the same transducers for both transmission and reception, a so-called monostatic mode of operation. The combined transmit/received unit is contained within a keel dome at about 1/3rd hull length back from the bow, or in the case of the bigger deep draught ships, in a dome at the foot of the bow. One consequence of a hull sonar fit is that both the transmit and receive paths are at depths close to the air-sea interface. At the time of the NATO request large Escort ships were entering service fitted with a powerful bow mounted active sonar operating at a nominal 3kHz, a source level of 240 dB re u Pa at 1m and a directivity index of say 25dB. The higher power and lower operating frequency enhance the potential for longer detection ranges with access to additional propagation paths a representation of which is shown in fig 1.21; i.e., by a reflected path from the sea bed, to insonify targets below a surface duct, as well as for convergence zone detection.The propagation paths of sound in the oceans are mainly determined by the depth velocity profiles in the water column and the properties of any intercept boundaries.Three independent variables determine the velocity of sound; temperature,

salinity and pressure, temperature being the dominant term.

$$\frac{\Delta c}{\Delta T} \sim 3.0 \text{ m /s /}^{\circ}C.$$

$$\frac{\Delta c}{\Delta S} \sim 1.2 \text{ m /s/ppt.}$$

$$\frac{\Delta c}{\Delta d} \sim 0.017 \text{ m /s /m.}$$

T is the temperature in degrees $^{\circ}C$.

S is the salinity in parts per thousand.(35% is the norm.)

d is the depth in meters.

At the near surface is a diurnal layer influenced by the regular cycle of solar heating and surface wind action. On calm sunny days an "Afternoon Effect" can occur when the morning solar radiation heats up the top surface water and if combined with a slight wind stirring a near surface shallow duct ensues. From about mid-day this can limit hull sonars to the detection of targets that are within a surface channel depth of about 10m or so until night time cooling cancels the conditions. Below this near-surface level and extending down to a few hundred meters, is the seasonal thermocline which as its name implies is induced by seasonal heating and cooling combined with wave stirring and conduction: this accounts for most of the duct propagation of surface sonars. A more general description of this channel is the Mixed Layer Depth which is defined in terms of density which is a function of temperature, salinity and pressure, temperature being the most dominant factor. For a surface duct to exist the

negative temperature depth gradient effect on sound velocity must be less than the positive pressure gradient of sound, 0.017m/s/m.

2.3 Fig 2.31 is a ray diagram illustrating surface duct propagation for a sound source in a surface layer and Fig 2.32 is a distribution curve for layer depths in the North Atlantic over the seasons; Levitus (1982),fig 2.33, has derived global charts of mixed layer depths using a temperature criterion of a difference 0.5 degrees C between the surface and the layer depth. Such data demonstrates that sonar surveillance in the presence of duct conditions is an important role consideration. Figs 2.34 and 2.35 show surface duct transmission losses at 2kHz and 8 kHz for various combinations of mixed-layer depth,source depth and receiver depth.[2] Figs 2.36 to 2.38 are ray-trace propagation curves for different velocity profiles which are applicable for comparing hull sonar performance with that of a combined VDS source and directive line array receiver at depths of 100m and 200m. The model used inputs of the basic parameters of the ocean environment.e.g. depth and sound speed profiles. Rays are then projected from the sound source in equal intervals of time at an equal number of elevations. At the end of each time step, the propagation loss due to spreading, and absorption as well as contributions from back scattering

---

2 Figs 2.32, 2.34 and 2.35 are from Urick. Principles of Underwater Sound.(1983).
Fig 2.33 is from S.Levitus. Climatological Atlas of the World Ocean. National Oceanic and Atmospheric Administration,Washington.DC (1983).

Fig 2.31 Surface Duct Propagation.

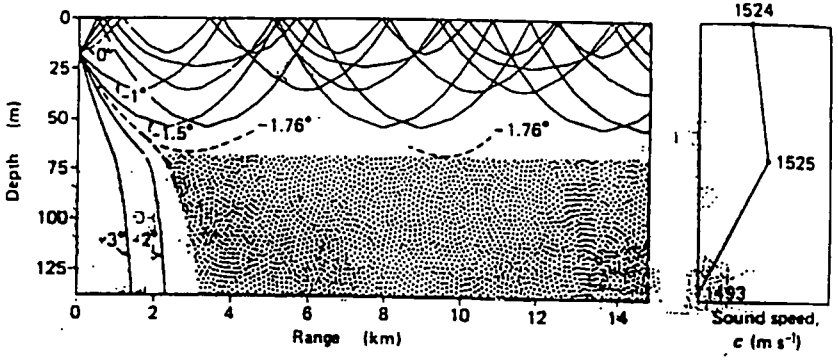

Ray diagram for a sound source located at a depth of 16 m, showing propagation and trapping of energy in the surface duct, with a shadow zone below 60 m, for the sound speed profile shown at the right (Urick, 1983; *Principles of Underwater Sound*, 3rd edn)

Fig 2.32 Distribution Curves of Layer Depth in North Atlantic.

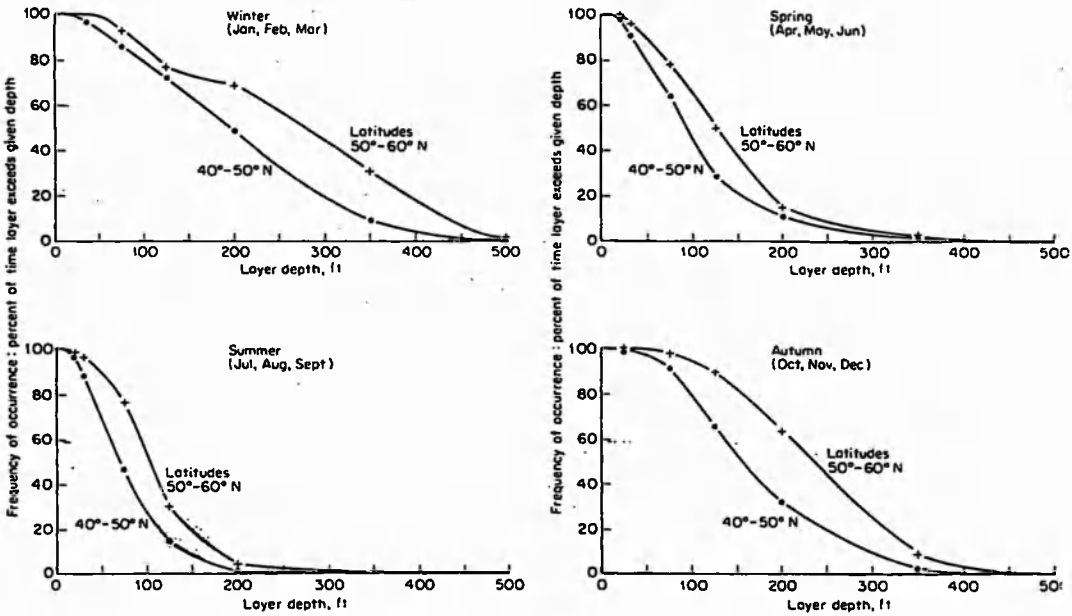

Distribution curves of layer depth in the North Atlantic. Ordinate is the percentage of occurrences of a layer depth greater than abscissa. Based on original data provided by the Navy Oceanographic Office.

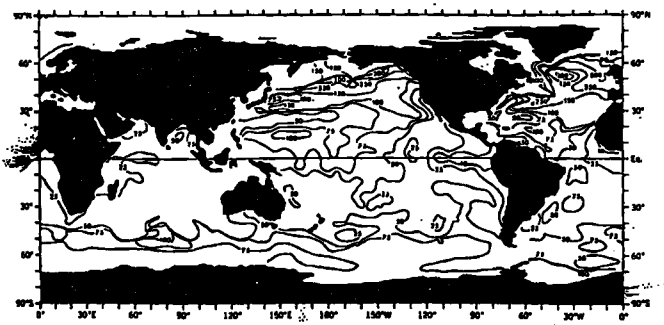

Mixed layer depths (in meters) for March based on a temperature criterion of 0·5°C

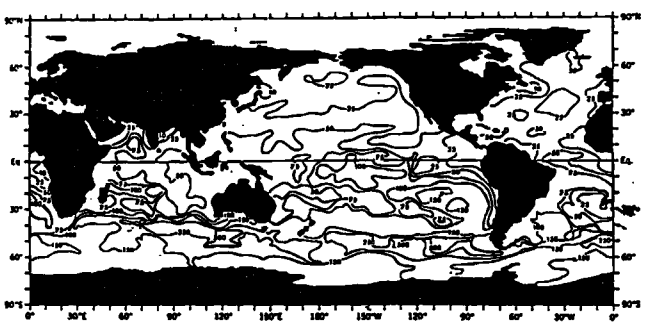

Mixed layer depths (in meters) for September based on temperature criterion of 0·5°C

Fig 2.33 Distribution Curves of World Wide Layer Depths.

Fig 2.34 Surface Duct Transmission. 2.0 kHz.

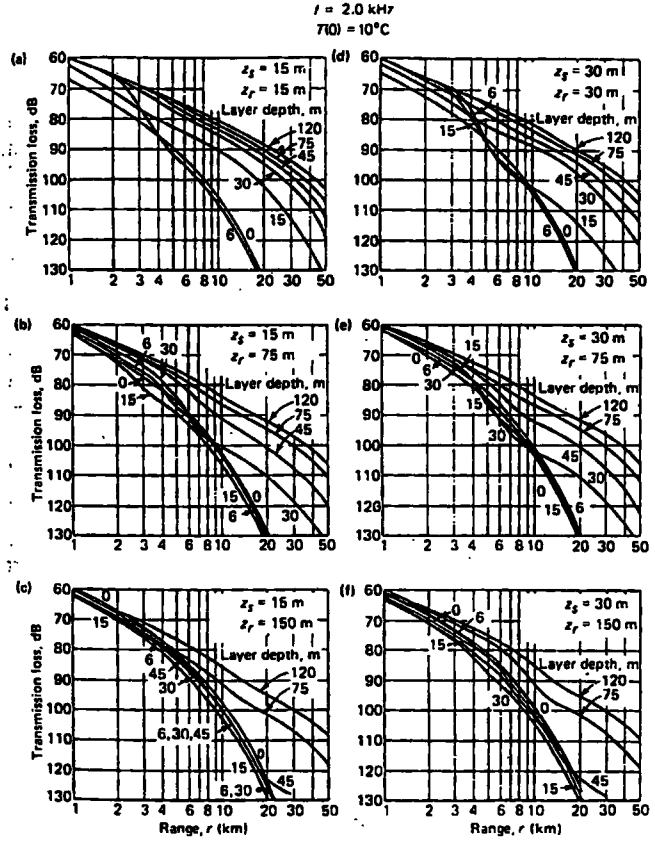

Surface duct transmission loss estimates generated from the AMOS empirical relationships at a frequency of 2 kHz for various combinations of mixed-layer depths, source depths (z_s) and receiver depths (z_r).

Fig 2.35 Surface Duct Transmission. 8.0 kHz.

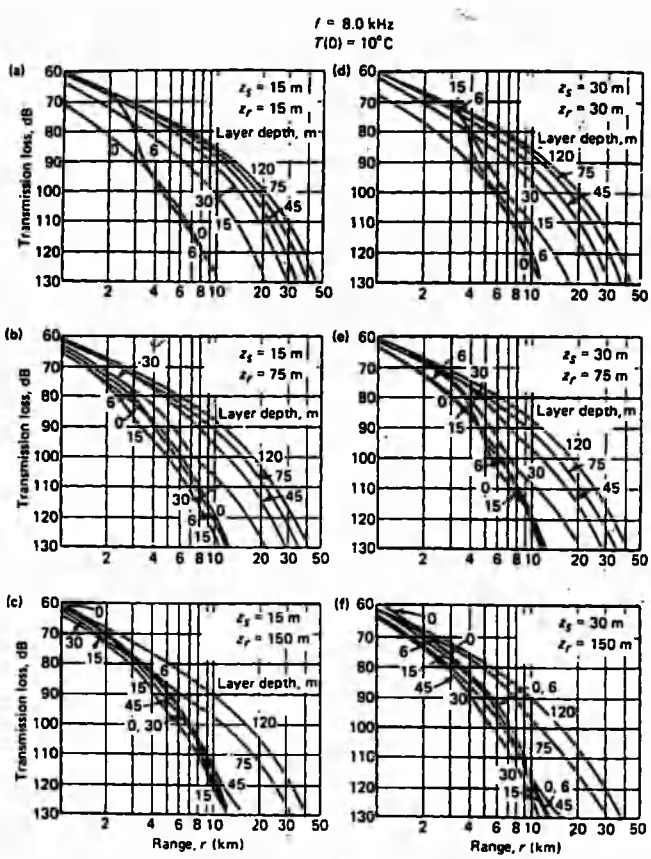

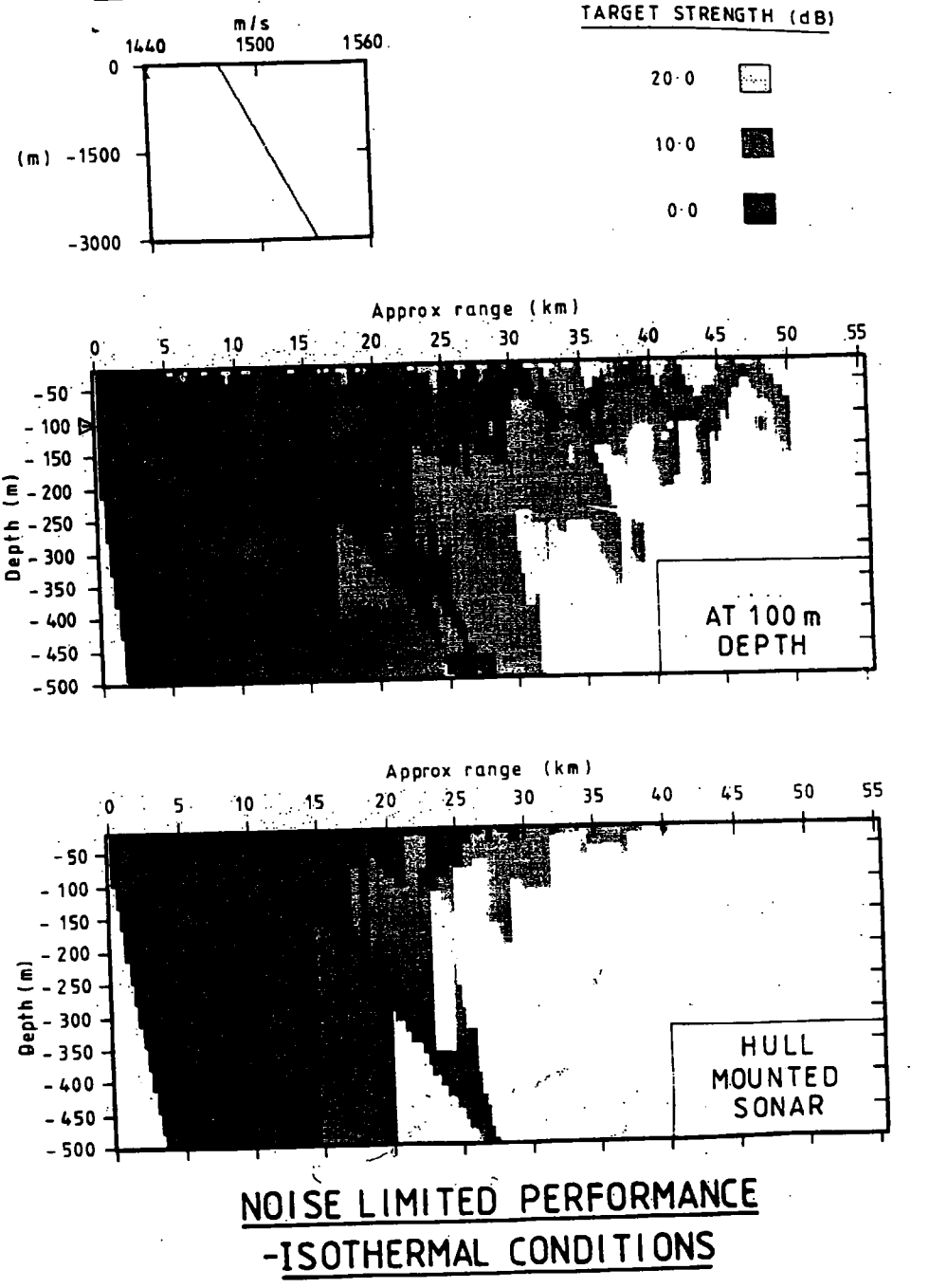

Fig 2.36 Target Range Plot. Hull Sonar and VDS at 100m Depth.

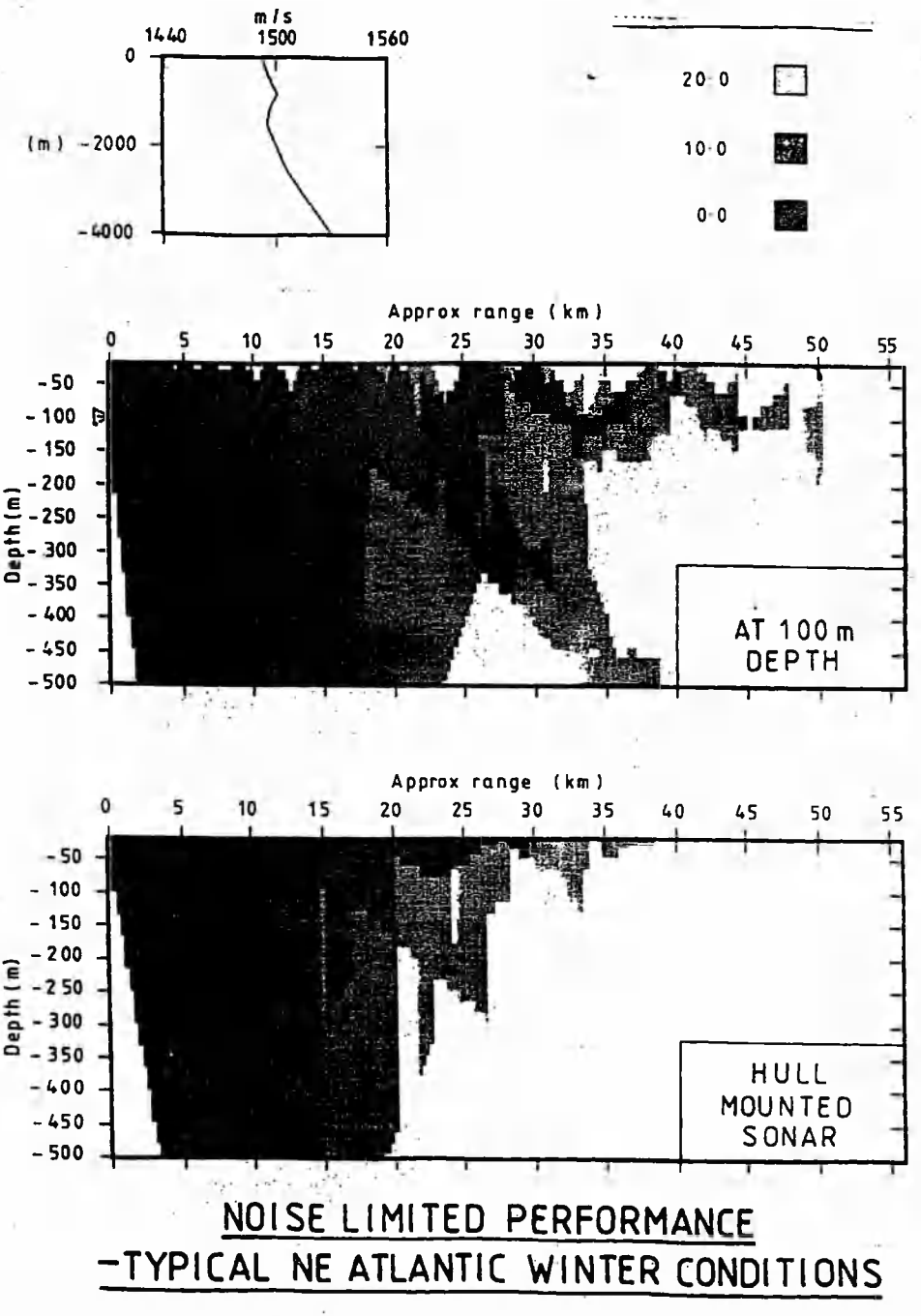

Fig 2.37 Target Range Plot. Hull Sonar and VDS at 100m Depth.

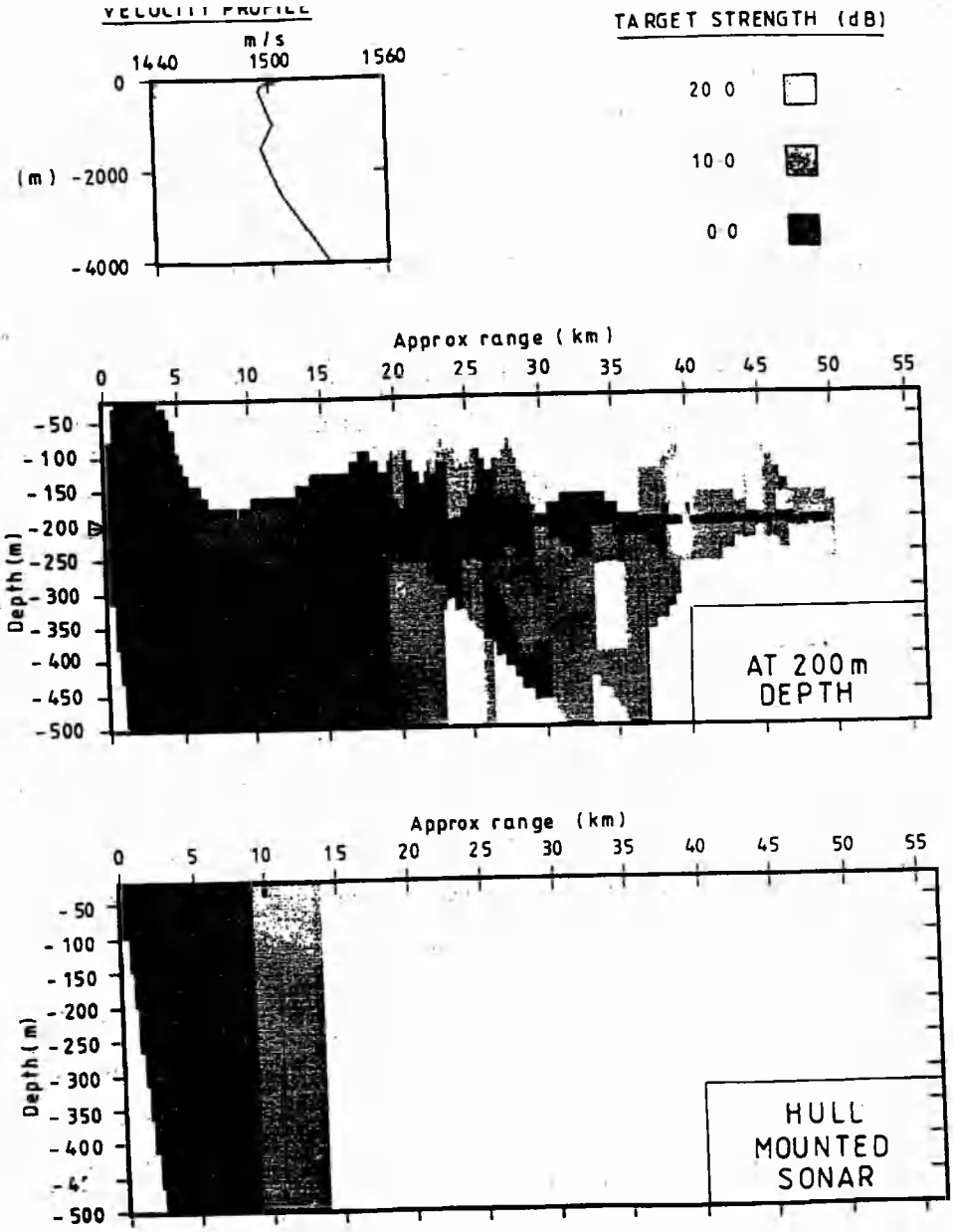

Fig 2.38 Target Range Plot. Hull Sonar and VDS at 200m Depth.

at the boundaries are added, calculated and stored. These contributions are finally summed over all elevations and plotted to give propagation loss, target range and reverberation levels as a function of range,time and depth. Values of false alarms are then added to obtain an indication of the target range for different target strengths which is shown by the shading.In the interests of simplicity and interpretation no time variance of the environmental features or target aspects are included, so that the statistical nature of sonar detection is not an output. Plots of CW processing may be obtained by incoherently summing all active sonar returns within given system parameter, range/depth intervals. FM processing is simulated by the maximum return from cells within the time pulse interval.The value of an active sonar VDS capability for small ships is clear.[3]

2.4 The main thermocline is a transitional region between the meteorological influences and the deeper water with a near constant temperature of 4 degrees C where the pressure gradient term becomes prominent. Rays that leave the source at a sufficient steep angle will escape being entrapped by any surface duct and at a depth of around 1200m a minimum in the sound velocity profile is reached where the temperature/ pressure effects equate thereby providing conditions for a deep sound channel,fig 1.21. Rays continuing beyond this depth, providing there is sufficient water depth, will eventually attain a vertex

---

3 Figs 2.36, 2.37 and 2.38 were obtained using the ray plotting programme of BAe.

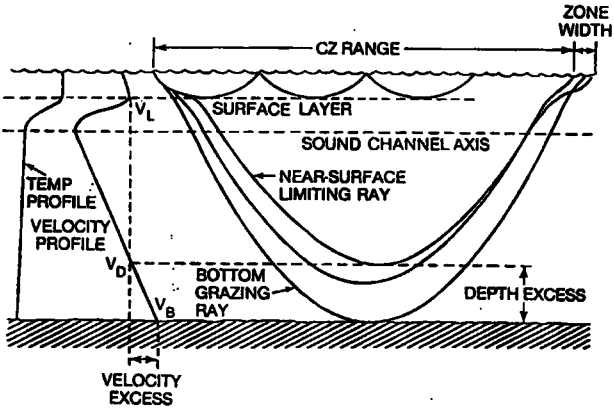

Fig 2.41 Depth Excess for Convergence Zone.

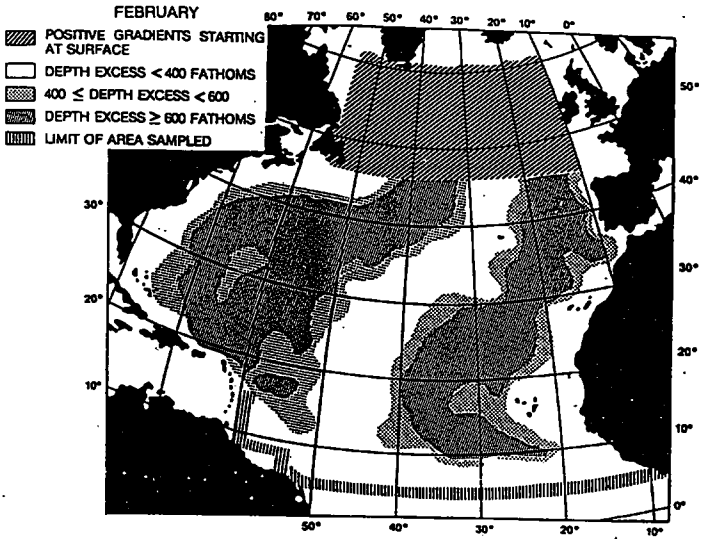

Areas where Depth Excess Exceeds 400 and 600 fathoms – February.

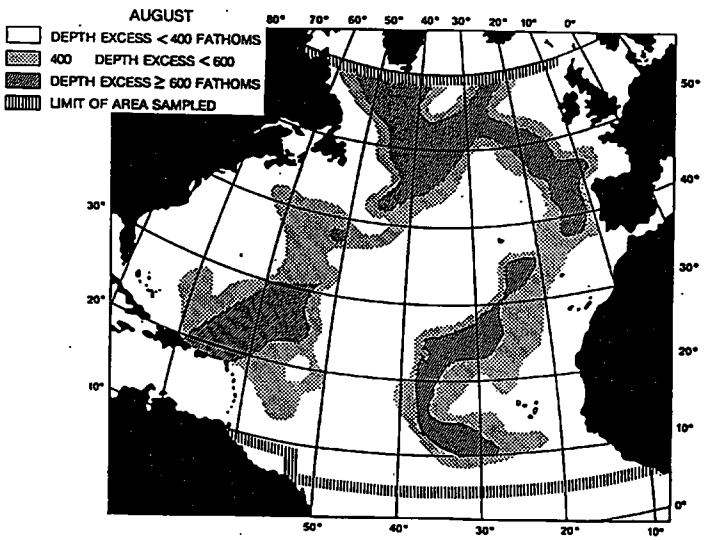

Areas where Depth Excess Exceeds 400 and 600 fathoms – August.

FIG 2.42 Depth Excess Contours for Feb and Aug.

velocity where the ray path is horizontal and will then follow a converging return path to the source depth. Figs 2.41 shows the geometry of the sound rays and the need for a depth excess sufficient to allow the increase in sound velocity due to pressure to cause the deep going acoustic ray paths to be reversed and returned to the surface. Fig 2.42 is typical for the Atlantic in February and August with depth excess contours in hundreds of fathoms; ref J.J. Hanrahan(1986).[4] Towards the poles the surface water is at a low temperature and so the seasonal thermoclines become less pronounced in these regions. In the N Atlantic the range is typically about 55 km and about 60 km at the equator to about 25 km at higher latitudes. By virtue of a focusing effect the one way spreading loss has a gain of between 6 and 15 db over spherical spreading and the ensuing detection region of say 5 to 9km is related to the magnitude of the focusing gain.It is observed that the velocity profiles in the near surface regions strongly influence the zone path. In the case of the bistatic towed array receiver this would be located at a favourable depth within the convergence zone azimuth paths. The target would reflect or scatter sound over 360 degrees so that the detection range while the target is in the CZ zone would be much greater than the focusing region thereby allowing for flexibility in the placement of the bistatic ships.

---

4 Figs 2.41 and 2.42 are ref J.J.Hanarahn (1986).

2.5 An ideal system would provide for continuous surveillance of all three of the possible propagation modes and to counter below layer tactics, a few ships are fitted with a separate variable depth active sonar, the key components of which are smaller versions of the hull transmit/receive sonar transducers. The latter are contained in a streamlined body connected to a tow cable directly below the ship at a predetermined depth, down to about 300 m. These additional sonars are expensive, difficult to handle and distinguished by the use of high frequencies, 10kHz and more, with a relatively short range. A specific application is where depressed sound channels exist at shallow water depths within which the location of source and receiver is at an optimum for range detection; Fig 2.51, and fig 2.52 shows the global incidence. In a total defence screen, helicopters with variable depth sonars and sono-buoys can provide additional mobile support with guard submarines patrolling in the deep field. As will be presented later, a towed line receiver in a bistatic configuration with a Hull type sonar source would allow for the prospects of a further increase in the range of duct detections, or improved detection in the bottom bounce mode or an increase in the incremental detection range annulus at the convergence range. Analysis of the properties of bottom bounce detection is treated separately.

2.6 A consequence of a hull type sonar system is that both the source and the receiver are close to the air-sea interface. Furthermore, the receiving array is closely

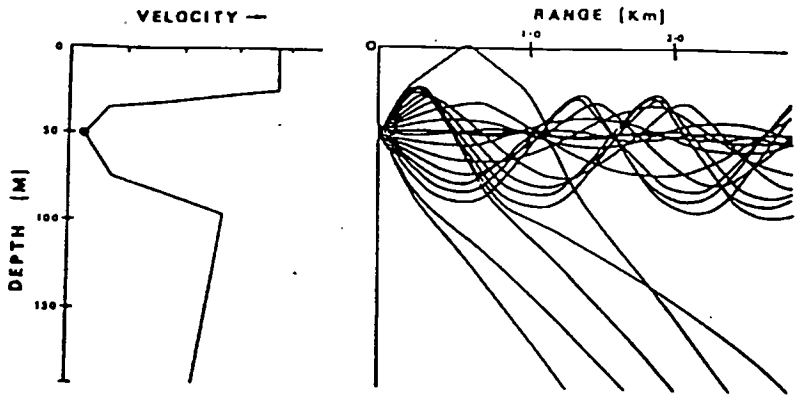

Fig 2.51 Depressed Sound Channel.

Fig 2.52 Incidence of Depressed Sound Channels Throughout The World.

coupled to the platform's self noise sources some of the prominent mechanisms being, propeller cavitation, machinery vibrations and turbulent water flow with entrapped air along the hull and around the dome. As the sonar operating frequency is lowered, the intrinsic self noise levels increase and to obtain full measure of a lower propagation loss remedial measures are necessary to maintain equivalent signal-to-self noise levels at the longer ranges. As is well known, self noise reduction is like peeling an onion, removal of one source reveals another at a slightly lower level and the lower the frequency the more difficult it is to obtain significant reductions, fig 2.61. Some of the possible measures for the medium frequency sonars, say around 7kHz, include improved hull shielding of the propellers and injecting air at the blade tips to minimize propeller cavitation noise. Against hull plate vibrations is improved balancing of rotary components, isolation mounts, installation of hull plate damping material, and a band of air bubbles around the hull at the machinery positions. All of these palliatives become more demanding or less effective the lower the frequency. In general therefore, prominent ship penalties for a lower frequency sonar at a higher source level is an increase in the size of the hull to accommodate the larger transmitter and receiver array with an increased degree of self noise reduction. Also, as the ships grow in size and value, so does the sophistication of the weapon systems needed for their own protection against above and below-water missile attacks, all of which in turn raises the cost of the

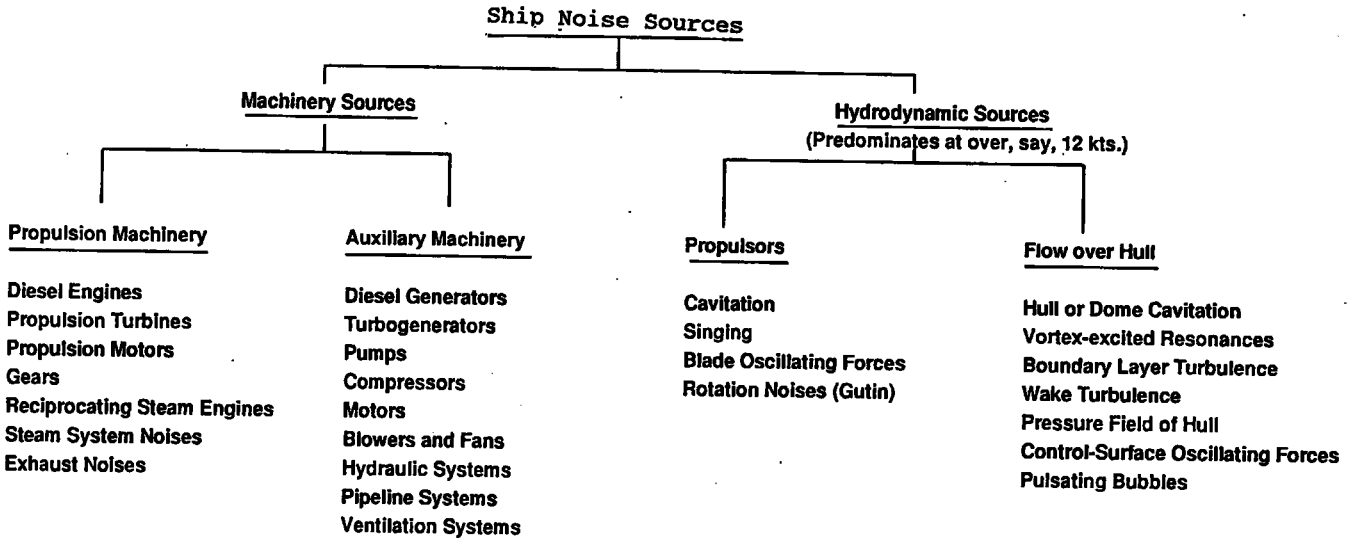

Fig 2.61 Ship Noise Sources,

Escort ships and has import for the manpower requirements. The goal set by the author was to obtain additional gains in the sonar surveillance volume through small ships in a bistatic configuration at a lower and more acceptable cost than could be obtained by further increases in the sonar power of the major Escort ships. Of import was that it would allow small navies to have an important role in the defence of shipping at a price they could afford. Such a capability would combine the so called contrary doctrines of the few large and high value compared with the small cheap and many.

Sonar Performance Models.

2.7 A salient issue when attempting to predict the at-sea performance of a sonar system using model formats is how the forecasts will compare with what will actually be achieved.In choosing means of estimating the gains on offer there are four interrelated research inputs in the field of Basic Sonar Acoustics: Propagation, Environmental Studies, Signal Processing and Sonar Performance Estimates. The latter is of particular significance for system research but the most difficult to formulate since by definition it is a compilation of the first three fields as well as many other additional functions. A first problem is a workable description of the underwater acoustic communication channels which are known to be extremely complex and imperfect. Inhomogenities in the volume of the sea, boundary conditions, roughness of the sea surface and bottom structure and multipath interactions all introduce various distortions so that even at an elementary level model forecasts of overall system performance needs to be treated with an awareness of errors. Three associated models can be distinguished: the scientific approach with the aim of explaining through theory and by experiment all of the physical processes involved; an empirical approach where very large area surveys are conducted with specialized equipment to measure key sonar parameters with the purpose of extracting some statistical rules; local estimates where system performance parameters are evaluated during trials and role operations. Over the past decade the explosion of

computer power has had a major impact on the number crunching capacity for modelling underwater environments and processes by allowing an ever increasing number of features to be included. Of importance to Systems Research is the significance of role parameters over a whole range of environments. In many instances the added sophistication now available aids understanding but is beyond the capacity of at-sea system measurements to authenticate. Even in well used trial areas with so called comparable environments and same targets, significant short and long term variations in system performance are commonplace for which no satisfactory explanations can be derived from the data available at the site. A practical problem for prediction is a listing of the variables to the detail needed. Thus the list would include not only the environmental and sonar parameters but also man/machine responses for different operational situations and altered sea states, i.e, self-noise variables, platform movement, target features and manoeuvres, operator task load and time allowed to the operator/command to counter specific types of threats and, not least, motion sickness. Over the years one approach to closing the gap between model predictions and actual sonar performance has been to assemble semi-empirical models formed from a combination of theory and acquired data relevant to sonar class types.This semi-empirical approach has particular value for ranking the key parameters of equivalent classes of sonar in terms of expected performance or some other figure of merit. As evidence becomes available of actual

performance a crude dB fudge factor can be applied to adjust the parameter values within the model. The more innovative the system the less viable is this approach unless means are found to relate to the established data bases. What is recognized is that all forms of model prediction for a broad spectrum of actual environments remains severely limited when compared with actual at-sea system performance.For the purposes of demonstrating propagation range gains through a lowerihg of the operating frequency, the band from 8kHz to 2kHz was chosen encompassing the upper band of medium power hull sonars and the present lowest frequency of 3kHz.

Hull Type Sonar Models.

2.8 Hull type sonars have well established, although incomplete, model formats which can be applied for a comparison of similar classes of sonars noting the prospects of an increasing shortfall in data support as the parameters are extended beyond experiment and at-sea experience. The basic sonar equations for active sonar can be expressed in dBs by:

Ambient sea noise-limited situation.

$$SL - 2TL + TS - NL + DI \gg DT$$

Reverberation-limited situation.

$$SL - 2TL + TS - RL \gg DT \qquad 2.81$$

SL = Sonar source level.

2TL = Two way transmission loss.

TS = Target strength.

DI = Receiver directivity index.

NL = Noise level.

RL = Reverberation level.

DT = Detection threshold.

The passive sonar equation can be similarly formulated in terms of signal and noise.

$$SL - TL - NL + DI \geq DT . \qquad 2.82$$

Noise source level of target minus propagation loss
minus the sum of interfering noises
plus improvements in spatial gain
must be equal to or greater than the detection threshold.
To be more inclusive, a separate processing gain term
should be included.

The effect of the signal processing is included in the DT parameter which is the signal to noise ratio in dBs required for an acceptable value of detection probability (PD) with an associated probability of false alarms (FA). Another functional measure of sonar capability is the figure of merit (FOM).

$$\text{Passive FOM} = SL - NL + DI - DT.$$

$$\text{Active FOM} = SL + TS - NL + DI - DT . \qquad 2.83$$

The FOM of a system is the maximum transmission loss that will allow the necessary detection probability as specified by DT to be attained.The FOM is improved by raising the source level, lowering the frequency, increasing the absolute value of the directivity index and decreasing the interference background level.The latter would improved,i.e. decrease, the DT value. A full expression would include a comprehensive description of each of the terms for a range of role environments. For comparison purposes allow that the parameters (SL+TS -NL+ DI- DT) = a constant and it is common to set TS to zero. Transmission loss describes the reduction in intensity I at some distant point referenced to that Io at a meter from the source,

$TL = 10 \log \frac{I_0}{I_r}$ dB. . For two sonars with equivalent system parameters except for operating frequency, the geometrical spreading factors are similar but the change-over point, where the incremental range absorption term becomes significant, are not the same, fig 2.12. At the lower frequency the spreading loss is a prime term to longer ranges so that the prominence of the incremental range

loss is delayed and so allows for additional range gain.

The absorption loss, ar, expressed in dB/ky, is:

$$a = \frac{0.036f^2}{f^2+3600} + 3.2x10^{-7}f^2$$

and for the frequency range 8 kHz to 2.0 kHz.

$$a \approx 0.01f^2 \qquad 2.84$$

f = frequency in kHz.

The correction for km is 0.914 kyd.

Taking the directivity index DI as a measure of the required transducer dimensions;

$$DI \approx 10 \log\left(\frac{4\pi A}{\lambda^2}\right) \qquad 2.85$$

" A " is the active transducer area and

λ is the wavelength, so that the price to pay in terms of the size of a hull fit at lower frequencies for equivalent DI values is an inverse function of frequency squared.

2.9 As previously stated, a key issue was what new advantages a bistatic system with a variable depth line array would bring to a low frequency hull sonar with emphasis on surface duct conditions in shallow and deep water environments. Over the years the complex field of acoustic propagation in the sea has been the subject of intensive study and with limited resources a choice had to be made on how much detail to include in the analysis and the availability of relevant data banks.The USN AMOS (Colossus) survey in the 1950's, the results of which continue to be appropriate, is the most comprehensive set of at-sea data that is openly published. Some 10,000 field measurements were made of transmission loss over the frequency range 100Hz to 10kHz from a spread of geographical areas and the measurements were first evaluated and fitted to semi-empirical ray type equations by Marsh-Schulkin, 1962, with further extensions by Schulkin and Mercer in 1985. Different models are derived with parameters of transmission loss as a function of frequency, depth of the positive gradient layer, sea state or wave height, water depth and bottom type. Three equations were developed to provide for the gradual transition from short to long range propagation. In shallow water or duct conditions it is assumed that the sound first propagates with spherical geometry to a range ro and then by cylindrical spreading as it fills the channel.

Spreading loss to range r.

$$SL = 20 \log r_0 + 10 \log r - 10 \log r_0.$$

r_0 is the spherical spreading range,

and above reduces to,

$$SL = 10 \log r_0 + 10 \log r \text{ dB}, \quad r > r_0$$

Including the attenuation due absorption and leakage,

$$TL = 10 \log r_0 + 10 \log r + [r_0 + r](\alpha_s + \alpha) x 10^{-3}. \qquad 2.91$$

α_s is the loss out of the duct, dB/km.

α is the absorption coefficient, dB/km.

An estimate of ro is obtained by assuming that all the rays remain in the duct up to the point of the start of cylindrical spreading.

Assuming a VDS midwater source all the rays are confined between angles $+\theta$ and $-\theta$, then,

$$r_0 = \frac{H}{2\sin\theta} \approx \frac{H}{2\theta}. \qquad 2.92$$

θ is the angle in radians with the horizontal at the source of the trapped rays.

H is the duct thickness.

At an intermediate range this AMOS(Colossus) model formulates an effective skip distance, Rs, based on the depth of the surface layer and water depth. This is used to define regions where wave-front spreading follows square, three-halves and first-power laws as a function of range r.

Short range (r < Rs).

$$TL = 20 \log r + ar + 60 - K_L$$

Intermediate range ($R_s < r , < 8R_s$)

$$TL = 15 \log r + a r + \alpha[r/R_s - 1] + 5\log R_s + 64.5 - K_L$$

Long range (r >> $8R_s$)

$$TL = 10 \log r + ar + \alpha[r/R_s - 1 + 10 \log R_s + 64.5 - K_L \quad 2.93$$

where;

$R_s = [(H + D)/3]^{1/2}$ = skip distance. km.

H = mixed-layer depth. m

D = water depth. m

r = range. km.

a = absorption coefficient. dB/km.

α effective sea surface loss,dB per bounce.

K_L near-field anomaly. f(freqency and range.)

Expressions for the leakage coefficient at the sea surface per bounce, α_b, have been deduced by Schulkin (1968) from the AMOS data.The dB loss per bounce in terms of the crest-to-trough wave height is a function of the product of mean wave height h(ft), and acoustic frequency f kHz, as shown in fig 2.91, which indicates an advantage for the lower frequency. Values of the recorded sea surface loss varied from about 1dB/bounce to 8 dB/bounce. The K(L) value is a function of frequency,sea state and bottom composition, and represents a gain due to multiple bottom and surface losses: this is a surprising term at the longer ranges since the mode stripping process is assumed to be complete at a range of about 8 times the layer depth. Figs 2.34 and 2.35 are characteristic plots of the

Fig 2.91 Sea State and Acoustic Loss at the Sea Surface..

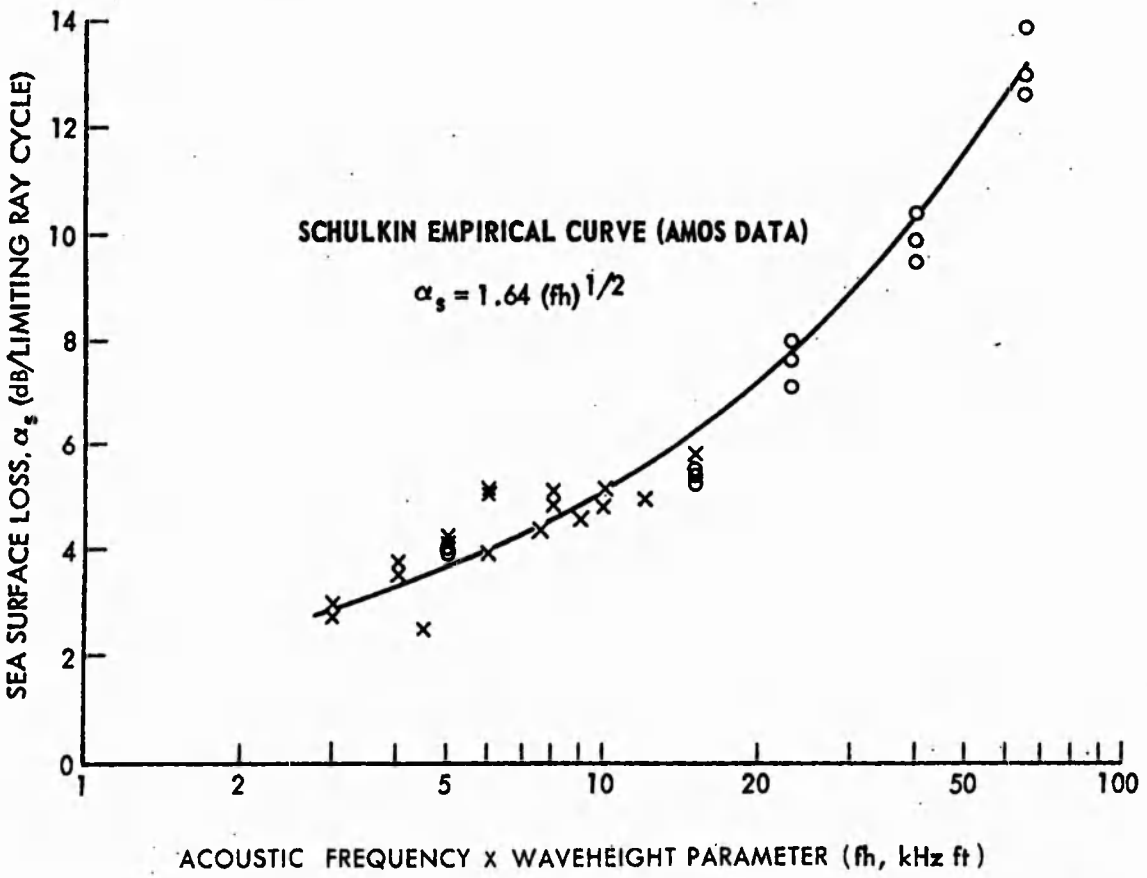

surface duct transmission loss at frequencies of 8kHz and 2 kHz for various combinations of mixed-layer depth, source depth and receiver depth computed from the AMOS measurements and demonstrate some of the main features. They apply for low sea states and for an average velocity gradient below the mixed layer.The lower frequency has the range advantage and as do the deeper combined source and receiver with the deeper layer depths,The trends shown in Figs 2.36 to 2.38 at the lower frequency were observed in trials with the commercial VDS at 3kHz where the source and receiver were at the same depth. Some recent data made available to the author of typical grossly smoothed mid ocean transmission curves are tabled below.

Depth - Source 10m - Receiver 50 m						
Range	7	11	15	18	27	km
10 kHz	80	89	97	102	119	TLdB
5 kHz	76	82	88	92	103	TLdB
2 kHz	70	74	78	80	86	TLdB

The receiver at 50m would correspond with the one-way propagation loss to a target at that range. At a frequency of 10khz the transmission loss of 89dB equates to a range of 11km to 15km at 5kHz and better than 27km at 2kHz. Probable errors are likely to be more than 6dB. In terms of system applications all of the above data indicates

trends rather than absolute predictions since, as observed in other similar surveys, there is a considerable spread in the smoothed raw data.

2.10 In the case of a hull sonar at a depth of 10m the transmit and receive transducers are close to the sea surface pressure-release effect which is a node point. Most acoustic transducers are sensitive to pressure and at the depth of a pressure antinode would be 3dB up on the mean. The mean square pressure, ref Weston 1971, varies as $r^{-5/2}$ and for both transducers as $r^{-7/2}$.A hull type sonar with a vertical beam width of 15 degrees would impinge on the sea surface at a range of 75 m when the presure-release effect will produce a phase reversal and hence generate doublet type sound sources in the water column with range. The closer the source to the sea surface the greater is the amount of energy flux that is redistributed within the sea column which is then no longer a simple geometrical term. A Rayleigh criterion is to assume specular reflection occurs if;

$$2h\sin\theta < \frac{\lambda}{4}. \qquad 2.92$$

θ is the grazing incidence of the sound ray with the surface.

h is the wave height.

The roughness factor increases as the grazing angle increases.

Depending on the velocity profile and depth of the layer,the lowest boundary is the turning point of the down-going rays with no loss. A more favourable location for the source and receiver is at the mid-depth of the

channel with the prospects of a 6dB enhancement and a 3dB for the receiver only. In environments where the seabed is part of the propagation path a description of the acoustic field now includes parameters of sea floor roughness and structure. This situation is analysed later for the bottom bounce mode. The author, a long time ago, was witness to a series of model tank experiments on shallow water propagation by A.B. Wood and was made very aware of the sensitivity of the water column intensity patterns to small changes in channel parameters. D.E Weston's reports on extensive experiments in shallow-water sound propagation in the Bristol Channel area has amply demonstrated this problem of prediction in real environments even with copious at-site supporting data. A common observation with hull sonars when operating in surface duct environments is the variability of target signals where successive returns can follow a sequence of one of high level followed by others of decreasing intensity. The indications are that there are significant intensity variations in the duct with range. Such situations have operational consequences in setting optimum observation times for a sequential search in each of the three modes; duct,bottom bounce and convergence zone.

Bottom Bounce Propagation Mode.

2.11 The purpose of the bottom bounce mode of propagation is to provide a detection path to targets which attempt to avoid detection by transiting the shadow zone below a surface duct. With bottom bounce target detection the forward and return paths include reflected energy at the sea bed a fraction of which may be lost by partial transmission into the sea floor sediments plus a signal coherence loss due to surface roughness scattering and multiple paths within the sea-floor sediment.The range propagation equation for a bottom bounce mode with a unit target may be expressed by :

$$I_{rf} = I_s \cdot K^2 \cdot \frac{1}{(2r)^2} \cdot \exp-(2\alpha r) \qquad 2.111$$

I_{rf} = Intensity of the returned source transmission,

I_s = Intensity of source.

K = Functional one way loss of intensity at the sea floor.

$\left[\frac{1}{(2r)^2}\right]$ = Transmission loss due to spherical spreading.

$\exp-(2r\alpha)$ = Attenuation factor, nepers /m.

Attenuation in units of dB/m =

α = a 20(log e) nepers /m) = a 8.6859(nepers/m.

r = Range to unit target.

Since

$$I_S = \frac{p_S^2}{\rho_1 . c_1} \text{ and } I_{rf} = \frac{p_{rf}^2}{\rho_1 . c_1}$$

p_S is the sound pressures of the source.

p_{rf} is the sound pressure of the return.

c_1 = velocity of sound in water.

ρ_1 = density of water.

Then

$$\frac{p_{rf}^2}{\rho_1 c_1} = \frac{p_S^2}{\rho_1 c_1} . K^2 . \frac{1}{(2r)^2} . \exp -2\alpha r. \qquad 2.112$$

The fractional loss of intensity in dBs is:

$$20 \log K = -20\log p_s + 20\log p_{rf} + 20\log 2r + 2r\alpha. \qquad 2.113$$

Measures of acoustic reflectivity can be expressed in terms of peak amplitude, rms amplitude and total energy of the returned waveform.

Integrating with respect to time,

$$\frac{1}{\rho_1 c_1} \int_T^{T+\tau} p_{rf}^2 dt = \frac{K^2}{\rho_1 c_1} . \frac{1}{(2r)^2} . \exp -2\alpha r . \int_0^{\tau} p_s^2 dt.$$

$$= \frac{K^2}{\rho_1 c_1} . \frac{1}{(2r)^2} . \exp -2\alpha r \ . p_s^2 . \tau.$$

K may be defined on a rms basis by,

$$K^2 = \frac{p_{rf}^2}{p_S^2} . (2r)^2 \frac{1}{\exp -2\alpha r} \qquad 2.114$$

If p_i is the source wave pressure at 1 meter from the sea floor boundary, and p_{ref} the reflected pressure at 1 m, then K may be referenced to the Rayleigh coefficient, a one way fractional intensity loss, by,

$$R_{rf}^2 = [\frac{p_{ref}^2}{\rho_1 c_1} / \frac{p_i^2}{\rho_1 c_1}] \text{ when } R_{rf} = p_{ref}/p_i \qquad 2.115$$

$\rho_1 c_1$ is the specific acoustic impedance of the medium.

The Rayleigh specular reflection coefficient, Rrf, refers to a plane wave incident on a smooth surface and is a function of the density, compressibility, rigidity, absorption, angle of incidence and layering of the bottom materials: important practical parameters are the sound speeds and density contrasts between the overlying ocean water and the materials that form the sea bed. Assume a plane wave incident on a level sea floor surface without absorption then:

An incident wave in medium sub (1) is ,

$$p_i, \text{ of phase } \omega t + k_1 z \cos\theta_i - k_1 y \sin\theta_i.$$

Medium sub 1 is the sea and angle θ_i is the angle to the normal.

Above divides into two components.

A reflected wave , p_r of phase $\omega t - k_1 z \cos\theta_i - k_1 y \sin\theta_i$

sited on the other side of the normal,

and another transmitted into the sea floor, medium sub(2),

p_t of phase $\omega t + k_2 \cos\theta_t - k_2 \sin\theta_t$, 2.116

noting that,

$$k_1 \sin\theta_i = k_2 \sin\theta_i \text{ and } \frac{\sin\theta_i}{\sin\theta_t} = n = \frac{k_2}{k_1} = \frac{c_1}{c_2} = \text{refraction index.}$$

Let the x z plane, z the depth = 0 , be the incident plane and the amplitude of the incident wave be unity. Using the concept of the wave impedance:

$$Z = \frac{\rho c}{\cos\theta}$$

and with $m = \frac{\rho_1}{\rho_2}$ the reflection cefficient is:

$$\frac{p_r}{p_i} = R_{rf} = \frac{m\cos\theta_i - n\cos\theta_t}{m\cos\theta_i + n\cos\theta_t}$$

$$\text{or} = \frac{m\cos\theta_i - \sqrt{n^2 - \sin^2\theta_i}}{m\cos\theta_i + \sqrt{n^2 - \sin^2\theta_i}} \qquad 2.117$$

The sea bed transmission coefficient is expressed by:

$$p_t / p_i = \frac{2Z_2\cos\theta_i}{Z_2\cos\theta_i + Z_1\cos\theta_t}$$

$$= \frac{2m\cos\theta_i}{m\cos\theta_i + \sqrt{n^2 - \sin^2\theta_i}} \qquad 2.118$$

Seabeds may be categorised as high or low velocity ,in both cases the density of the sediments is greater than that of the overlying sea water. A fast velocity seabed corresponds to $m < 1$, and $n < 1$, i.e ,$\rho_1/\rho_2 < 1$ and $c_1/c_2 < 1$. and is a common situation in the deep ocean, notably on the abyssal plains where the sediments are very fine silty-sand. From Snell's law $k_1 \sin\theta_i = k_2 \sin\theta_t$ and as $k_1 \sin\theta_i$ is real, so is the product $k_2 \sin\theta_t$.This means that $k_2 \cos\theta_t$ is imaginary.

$$k_2\cos\theta_t = jk_2\sqrt{(\sin^2\theta_i - 1)} = (j/n)k_2\sqrt{(\sin^2\theta_i - n^2)} \qquad 2.119$$

[5] An angle of intromission, no reflection, would correspond to:

---

5 Fig 2.111 is reference, Sound Propagation in the Sea, Urick(1982).
Fig 2.112 is reference Basic Acoustic Oceanography, USN Department of Navy.

$$R_{ref} = 0, \text{ when,}$$

$$m\cos\theta_i - \sqrt{(n^2 - \sin^2\theta_i)} = 0.$$

For an angle of intromission;

$$\sin\theta_i = \sqrt{\frac{(m^2 - n^2)}{\sqrt{(m^2 - 1)}}} \qquad 2.110$$

Since $\sin\theta_i \leq 1$, and omitting attenuation, then the angle of intromission should exist when,

$$c_1/c_2 < 1$$

Beyond the critical angle, and again no attenuation, $\theta_i \geq \theta_c$ the reflection coefficient is:

$$R_{rf} = \frac{m\cos\theta_i - j\sqrt{(\sin^2\theta_i - n^2)}}{m\cos\theta_i + j\sqrt{(\sin^2 - n^2)}} = |R|\exp(j\phi)$$

This has the form $\frac{a - jb}{a + jb}$. $\tan\phi = \frac{-2ab}{a^2 - b^2}$

$$\text{when } \phi = -2\tan^{-1} \frac{\sqrt{(\sin^2\theta_i - n^2)}}{m\cos\theta_i} \qquad 2.111$$

The transmitted wave propagates in the x direction only, the amplitude in the z direction decreasing exponentially with depth. The transmitted wave may be written as:

$$p_t = A_t\exp(-k\sqrt{(\sin^2\theta_i - n^2)}z.\exp(-jk\sin\theta_i.x)$$

The amplitude of the surface wave at depth z has decayed by 1\ e when:

$$k[\sqrt{(\sin^2\theta_i - n^2)}]z = 1$$

This can be expressed in terms of wavelength penetration depth by:

$$(z/\lambda) = [2\pi\sqrt{(\sin^2\theta_i - n^2)}]^{-1} \qquad 2.1112$$

The average energy flux in the x direction is returned to the upper medium at an angle θ_i and velocity c_2 to the upper medium. Figs 2.111 and 2.112 illustrate the Rayleigh model reflection loss characteristics for various combinations of m and n with grazing angle as the ordinate. In the usual derivations of reflection coefficients, reflected and transmission angles are referred to the normal to the boundary but in underwater acoustics it is more convenient, particularly in regard to acoustic survey data, to reference the incident grazing angle when the sin and cos functions are interchanged.

2.12 To achieve the bottom bounce mode of detection there are various penalties to be paid in terms of the required system parameters one of which to obtain significant surveillance ranges is an increase in the effective vertical source/receiver beamwidths with a reduction in the directivity index values. Employing a source and receiver depression angle of 45 degrees an approximate sonar range to the shadow zone is::

$$r\,(b) \sim 2z/\sin 45^\circ = 2.83z.$$

and the insonified range is:

$$= 2.83z\ \theta_z. \qquad 2.121$$

where θ_z is the effective vertical beamwidth in radians.

For average ocean depths, 3.8 km, the propagation spreading range loss to the shadow region is 10.78.km and 7.2 secs travel time. Assume a common effective vertical beamwidth of say 20 degrees, the azimuth range in the shadow zone is only about a 1.9 km : increasing the

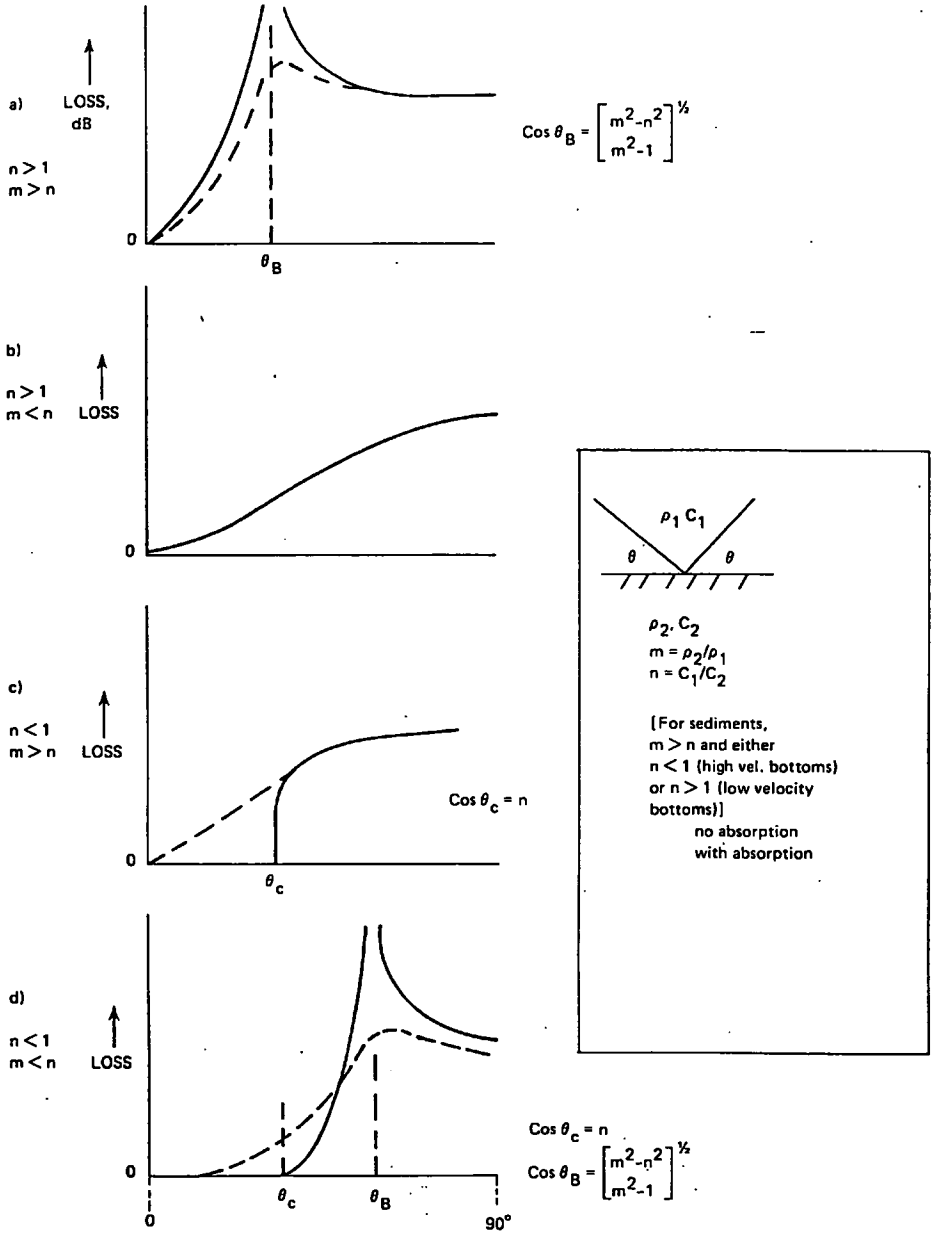

Curves of reflection loss vs. grazing angle for two fluids separated by a plane boundary. For most real bottoms only cases a) and c) apply. The dashed curves show the effect of attenuation in the bottom.

Fig 2.111

Fig 2.112 BOTTOM LOSS FOR "FAST" AND "SLOW" SEDIMENTS—RAYLEIGH MODEL (ACOUSTIC FREQUENCY = 1 kHz).

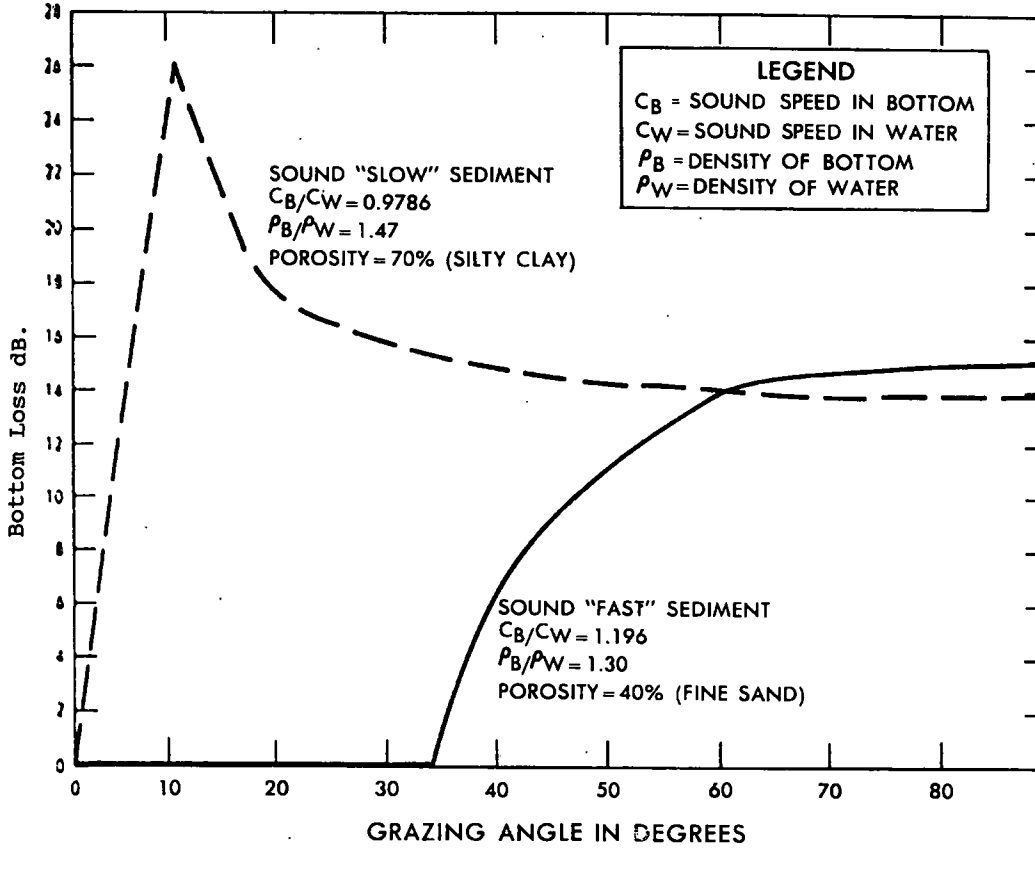

vertical beamwidths to 90 degrees centred around the depression angle would provide for an insonification range of say 8.5 km roughly equivalent to a medium power sonar in a duct mode. In deep water it is of note that the hull sonar depression angle is not the incident angle at the sea floor being a function of water temperature at the source and the velocity pressure term at the sea bed. Lowering the depression angle increases the range at the expense of a loss in near range detection but not all of the source energy may be utilised since some could be lost to the surface duct and with sufficient depth of water some of the energy could access the convergence mode of propagation with a negative bottom loss. There is also the possibility of interference from common range reverberation, i.e, returns of direct paths to and from a rough seabed via the sidelobe response. At shallow water depths the available below shadow zone range by the above route is obviously reduced. As the source level is raised and frequency reduced there are environments where multiple returns occur due reflections from sediment layering within the sea floor. Consider a two layer return of an incident signal f(t) differing by a time τ, and in amplitude by a ratio A , then:

$S(f) = f(t) + A.(f(t)+\tau)$ and the Fourier transform is,

$$g(\omega) + A.\ g(\omega).\ \exp j\omega\tau.$$

$g(\omega)$ is the FT of f(t) when the power spectrum is,

$$P(\omega) = [\ g(\omega).g^*(\omega).(1 + A.\exp j\omega\tau).(1 + A^*.\exp -j\omega\tau)\ ]$$

$$= [|g|^2.\{1 + A^*A + (A.\exp j\omega\tau + A^*\exp -j\omega\tau)\}]$$

and if A is real,

$$P(\omega) = |g|^2\ (1 + A.^2 + 2A.\cos\ \omega\tau) \qquad 2.122$$

The osillating term is $2A\ \cos\ \omega\tau$

and the coefficient of $|g|^2$ varies between

$(1+A)^2$ and $(1-A)^2$

in the radial frequency interval π/τ.

If the duration of the return is less than $2d/c_2$, where d is the depth of the second layer, then there will be mutual interference with a loss of coherence. If the second layer is greater than $2z/c_2$ then there would be two separated returns. To reproduce the same pulse waveform the relative phase change for each frequency along the time axis should be the same for all frequencies,when, $\Delta t = \epsilon\tau$, where ϵ is the phase change.

2.13 In modelling the characteristics of the target returns in a bottom bounce mode, the reflection coefficient as derived above is for plane waves incident on flat surface, with no absorption in the sediment layer and no non-specular scattering from roughness features.The existence of attenuation in sediment layers and surface undulations tends to smooth out some of the above prominent model predictions of the bottom bounce returns. E L Hamilton 1972 demonstrated that the absorption of sound within

marine sediments is approximately dependent on the first power of frequency, $\alpha = aF$ where α, is in dB/m , F is in kHz: a typical value for α is 0.25F dB/m which is orders higher than the absorption value for seawater. In the absence of attenuation using the adiabatic law:

with a fractional change in density σ and acoustic pressure p in phase.

$$p = \beta\sigma.$$

β is the bulk modulus.

The velocity of sound in the medium is,

$$c = \sqrt{\frac{\beta}{\rho_0}} \qquad 2.131$$

ρ_0 = equilibrium density.

Real elastic- constant values correspond to a media without absorption while complex values imply exponential absorption with a decrease in amplitude with distance.

$$A_2 = A_1 \exp -\eta x \qquad 2.132$$

A and A_0 are values of the amplitude of the wave front at two points distance x apart.

η is the absorption coefficient.

With volume absorption there is a delay between application of pressure change and the state of condensation stability when the phase speed is no longer a constant c.

Amplitude decays with depth as, $A_0 \exp(-\eta z)$

$$A = A_0 . \exp -\eta z . \exp j(\omega t - kz).$$

$$= A_0 . \exp[j\omega t . -(k + j\eta)z]$$

$$= A_0 . \exp[j\omega\{z(1/(c + j\eta/\omega)) - t]$$

The velocity c_2 has the form a + jb

$$c_t = \frac{\omega}{k + j\eta} = \frac{\omega/k}{1 - j(\eta\lambda/2\pi)} = \frac{c_2}{1 - j(\eta\lambda/2\pi)}$$

$$= \frac{c_2}{1 - j(\alpha/2\pi . 8.7)} \qquad 2.133$$

where α is the attenuation in dB per wavelength and,

c_2 is the sound speed in the absence of attenuation.

A consequence of attenuation in the second medium is that there is no angle of intromission since c is complex. The other mechanism which is the cause of significant departures from the plane surface model is the presence of roughness. The ratio of the intensity of the returned sound from a rough sediment surface is expressed by:

$$I_b = I_R \exp\left(\frac{-4\pi h \sin\theta_g}{\lambda}\right)^2 = I_R \exp(-R^2) \qquad 2.134$$

I_b is the reflected intensity.

I_R is the reflection from a plane surface.

θ_g is the grazing angle.

$-R^2$ is the Rayleigh roughness parameter.

Assume a plane wave incident on a surface with undulations of height h , then the path difference on reflection is:

$$2\Delta r = 2h\sin\theta_g.$$

The phase difference is:

$$\Delta\phi = \frac{4\pi h\sin\theta_g}{\lambda}.$$

At $\Delta\phi = \pi$ the sediments being the same then, reflected and incident waves will tend to cancel. But, by conservation of energy principles the energy must be redistributed in other directions ie, scattered. 2.135

In many cases the bottom roughness is assumed to have a Gaussian probability distribution function h(x,y) of amplitude heights.

$$p(h)dh = \frac{1}{(2\pi\sigma_h^2)^{1/2}}\exp(-h^2/2\sigma_h^2)\,dh \qquad 2.136$$

σ is the rms heights of the undulation, assumed statistically the same throughout the region. The bottom roughness may then act as a spatial filter analyzer, thus for small degrees of roughness the scattering could be confined to small departures from the geometrical angle of reflection. As the roughness heights increase for surface dimensions less than a wavelength then the trend would be towards omni-directional scattering.

2.14 Ocean areas may be categorized into regions of Continental Shelves, Terrace Plateaus, Continental Slopes, Continental Rises and Basins with Abyssal Plains, Ridges, Seamounts and Knolls. In shallow water, sediment types may vary greatly over short distances while in deep water regions such as the Abyssal Plains occupy vast areas. The

bulk acoustic properties of a sedimentary type sea floor that influence the reflection and attenuation of compressional waves are functions of the material components which are generally an aggregate of mineral deposits whose interstices are filled with seawater. In natural sediments the compressibility of sea water is between one and two orders of magnitude greater than that of the mineral grain components so that its bulk compressibility may be described in terms of porosity, the volume fraction of sediment occupied by sea water. The reflection of acoustic energy from the sea floor and the importance of sound velocity as a marine sediment index has received considerable attention over the years, L Hamilton 1974, I Tolstoy and CS Clay 1984, and empirical relationships have been established between the acoustic reflectivity and the constituents of the sediment and their porosity values. Differences in the elastic constants mean that shear waves have lower velocities and an order higher attenuation than those for compressional waves. The porosity of sediments ranges from zero to as much as 75%. Mud and silts have a high porosity and a low density with a compressional wave velocity a few percent less than the overlying sea water. Hard sands have a low porosity and a higher density with compressional wave speeds as much as 10 to 20 % greater than seawater. As the depth of the sediment layer increases the rise in pressure squeezes out the water and the wave speed increases with associated refractive effects. Abyssal plains consist of a mixture of sand,silt and clay with a series of lower layers grading into finer

silt and clay known as graded bedding. For sediments with porosities greater than 65 percent, sound speed in the sea bottom is slower than that in overlying deep water.For such sediments there is an angle of intromission at about 10 degrees grazing angle with large losses of the order of 26db.The losses then decrease to about 14 dB from 40 to 90 degrees grazing angles.On the other hand with sound speeds greater than the water, there is a critical grazing angle at about 30 degrees with only small reflection losses from 0 to 30 degrees grazing angle, followed by a sharp rise to about 15 dB from 60 to 90 degrees. Scattering of sound from the sea bed and reflections from within the sediment would be expected to produce waveform distortions: as roughness is measured in units of wavelength this would decrease at the lower frequencies but as attenuation within the sediments is lower the amplitude of multiple paths from within the layer may increase. Propagation velocity in an absorbing medium is complex and so therefore is the wave number and hence the phase velocity. From the above it is clear that the bottom bounce mode is not a universal panacea for all role operations of below layer detection. At all times the signal return from seabed reflections and scattering is an order more complex than that from the sea surface. A practical problem for system research is prediction in regions for which there is no actual sonar data. Sedimentary nomenclature is commonly based on sand-silt- clay ratios. Since clay is more porous than silts, and both silts and clays are more porous than sands there is a general relationship between

class names and porosities , albeit poorly defined. Reflection loss increases according to the following sequence allowing that the range of class names overlap: sand, silty-sand ,silt , sandy-silt clay , clay- silt , silt, silty-clay and clay . The surface loss increases as porosity increases,ie approaches matched impedance when the addition of sublayer returns can produce waveform distortion or multiple returns. Fig 2.141 shows the average bottom loss in two North Atlantic regions and is typical of the AMOS data and other unpublished bottom bounce surveys which show a loss rising with angle at low angles. A representative bottom loss at 3 kHz for grazing angles $20^0 < \theta_g < 50^0$ in deep water is between about 8 to 15 dB.[6] Possible regions for reasonable bottom bounce applications are the Abyssal Plains where bottom tidal currents can generate roughness waves some one to two meters in height. Rayleigh's criterion of surface roughness considers a surface to be smooth if the phase difference between the top and bottom of the surface irregularity is less than $\lambda/4$ or $h\sin\theta < \lambda/8$. For one and two metres rms ripple height at 3 kHz this would correspond to grazing angles of less than 3.5 to 1.6 degrees of grazing angle below which the surface would be considered smooth.

2.15 Estimating system sonar performance in the real world of bottom bounce detections is fraught with uncertainty by the number of variables involved and in particular a lack

---

6 Fig 2.141 reference Urick.Sound Propagationn in the Sea.(1982).

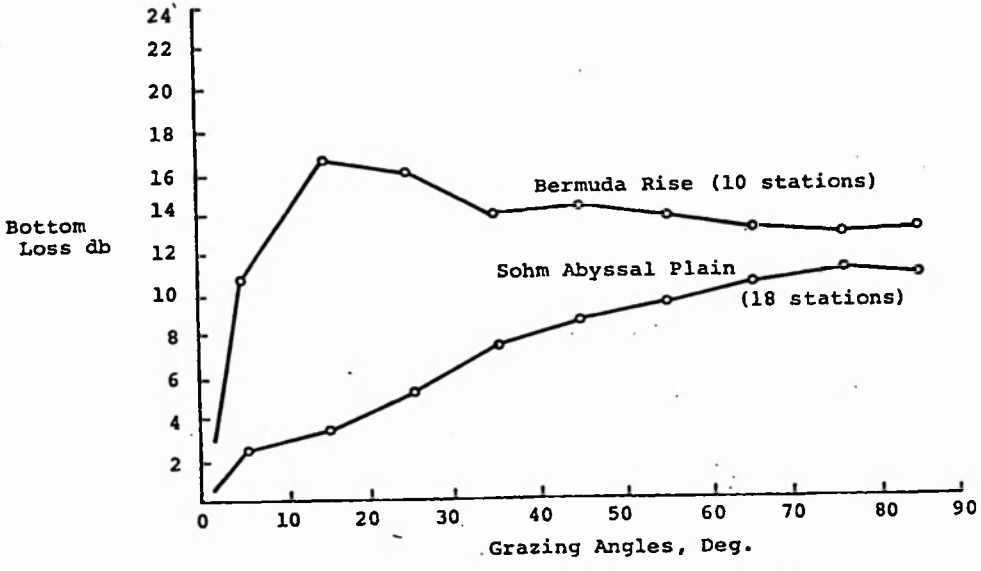

Average Bottom Loss in Two Physiographic Provinces of the North Atlantic Ocean in the Frequency Band 0.5-8.0 kHz. Based on Marine Geophysical Survey data.

Fig 2.141 Average Bottom Loss in N Atlantic.

of substantive sonar system data in a sufficient number of representative operational areas. Most of the data banks refer to propagation loss with little reference to the coherence factors needed to assess signal processing gains and losses. Author experience on the Abyssal Plain regions is that a bandwidth of about 200 Hz is available. In general, practical bottom bounce sonar performance should be available, at a cost, for regions such as the Abyssal plain environments, with areas like the Mid-Atlantic Ridge areas having excessive signal loss. Ranges below the duct are related to water depth and the combined vertical beamwidth with a minimum source level to compensate for the bottom losses. System performance, as demonstrated above, can only be described in very broad terms with the possibility of large errors.

A Bistatic Sonar Role .

2.16 It is seen that lowering the frequency and increasing the power of hull sonars has certain benefits and penalties.For two equivalent sonars except for frequency and higher power,the geometrical spreading losses, excluding any surface reflection losses, would be similar for both sonars with improved range gains at the lower absorption value.This would be at the cost of a larger transducer fit if the same bearing discrimination is to be obtained. Fig 2.161 is illustrative of the two-way propagation losses for the three modes of transmission available to surface ship sonars.For low sea states,SS1, and a target located in the surface duct, modest increases in acoustic power at 5 kHz produce cost effective increases in the probable detection range of hull sonars over a range 10 to 15 Kyds. This frequency is lower than the more usual 7 to 8 kHz and above that of the high power sonars at 3kHz. At higher sea states ,SS6, the relative cost per additional range interval rises more steeply due to higher propagation losses within the duct. The additional acoustic power or the size of the transducer arrays needed becomes expensive in terms of range gain. For targets below the duct, in the shadow zone, the range for "duct only" sonars is limited to the point of the limiting ray where the intensity flux becomes trapped by the surface duct. The ray paths at the near ranges depends less on the velocity profile and more on the combined transmit and receive vertical beamwidths; that for below duct layer detection is usually under 2000yds. These "duct

Fig 2.161 Two Way Propagation Loss.

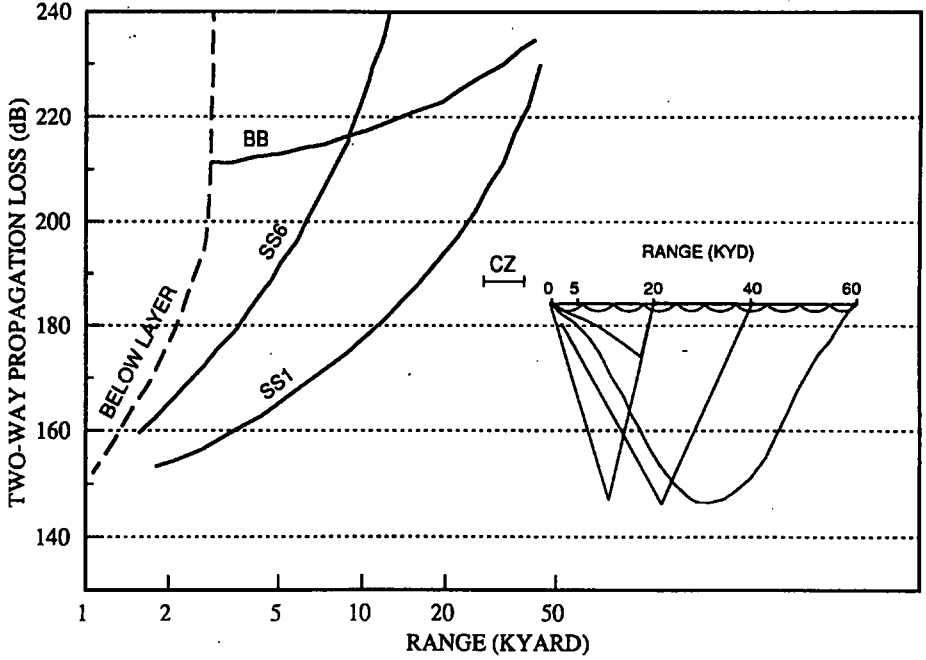

DUCT
LAYER DEPTH = 150 FT
FREQUENCY = 5kHz

WATER DEPTH	2500 FTH
FREQUENCY	3.5kHz
BOTTOM LOSS	20dB
D/E ANGLE	20/40 5/10

only" limitations were, and still are, typical of many in-service small navy sonars.In the bottom bounce mode of operation the lower frequency higher power makes more areas available for shadow zone detection but the entry price for this mode is the large initial loss for the two-way go and return sea bed propagation path to the shortest azimuth range target plus a reflection and coherence loss at the sea bed. In areas with roughness features the sidelobe control on the transmit-receive beams must more than equal the difference between the two-way bottom loss and the two-way direct path loss to minimize the competing scattering returns from direct path reverberation.

2.17 With a bistatic operation it is assumed that the monostatic sonar would continue with its normal sonar surveillance roles with the bistatic ship adding to the information input. What a bistatic operation should achieve is a significant improvement in the detection range in **Duct** operations where the one-way path at double the range has the same interval observation time as the monostatic sonar at half the range. This postulates that the bistatic sonar has returns over the total range. In the **Bottom Bounce Mode**, a horizontal path is insonified over the range of the source vertical beamwidth thereby forming a distributed source. The usual first wait time is that of the two-way travel time with a transmission interval thereafter set to correspond to returns corresponding to the source azimuth range, a minimum being the point where the returns overlap. With a bistatic array

below the duct the distributed source azimuth range is the same but the seabed losses are reduced to a one-way path and so better use can be made of the available power. Allow a target with omni-directional scattering then, with a directional receiver and the same distributed source range, the surveillance range now equates to sources with a one-way target path to the line receiver at the target depth; this range would be greater than the monostatic horizontal source beam dimension. Matching the transmission periods to the increased ranges slows down the data rate but the overall advantage of the additional bistatic input is to improve the detection opportunities which would increase the effectiveness of the bottom bounce surveillance mode. It is clear that a more satisfactory below layer detection system would be an independent variable depth sonar at a cost less than that of the traditional V.D.S systems that could access these vulnerable zones. A similar situation to the bottom bounce mode applies to Convergence Zone operations where the power over the focussed region forms a distributed source over the path where the rays are converging. Increasing the depth of the receiver at the focus zone increases the convergence range interval at a reduced equivalent source level which is compensated by the array gain.The transmission interval in a normal convergence zone interval is set by the need to avoid multiple returns within the focussed range so that a gain in range would affect the monostatic transmission time periods, but as before, with improvements in the total surveillance

performance. From the commencement of the bistatic research programme it had been recognized that the combination of a directive towed line array with a towed transmitter would allow small ships the capacity for many other independent sonar roles beyond that of a bistatic capability. Desirable features were a low frequency towed source of small dimensions in units of wavelength with a source level around 200dB ref 1 uPá at 1m and a Q of 2 to allow for some flexibility in choice of operating frequency for each Escort ship, an omni-directional beamwidth in azimuth and a near 25 degrees in the vertical. Choice of frequency could allow for system compatability with the Escort ship sonars for a bistatic role, noting that this would preclude their use for independent roles in the vicinity of Escort Ships in the same frequency band.

Appendix C

Small Dimensional Sources

C1. A further goal throughout the bistatic system research was to provide the bistatic sonar receiver ships with an own low frequency source of sufficient power to allow for additional active sonar roles. Handling arrangements for the wet end assembly of towed line array and source were to have the capacity for launch and recover up to say sea state 4 and towing down to a depth of about 200m or more, all within the limits of a small ship deck space: the conventional Variable Depth Sonar assemble with an integral transmitter/receiver using Tonpiltz-type piston elements was not an acceptable format on the grounds of weight, space and cost. A tentative objective was for a 3kHz source with an output of around 200 dB to 210 dB vs 1μ Pa at 1 m over a bandwidth of around 1 kHz with a projector beam pattern near omni-directional in azimuth and 25 degrees in the vertical. The practical problems in obtaining such relatively high power sources within small dimensions is demonstrated by the control parameters of the most elementary source; this is a pulsating spherical sphere of radius 'r' where the acoustic source strength Q is defined in terms of the peak of the volumetric displacement. For a surface of area A with a uniform radial displacement,then:

$$S d\hat{\epsilon}/dt = S\hat{u} = Q. \qquad \text{C 1.1}$$

where

$\hat{\epsilon}$ = peak radial displacement.

$\hat{u}$ = peak particle velocity normal to the surface,

S = active suface area.

For a sphere of radius r,

$$Q = 4\pi r^2 \hat{u}.$$

Pressure and particle velocity are related through the Force equation.

$$\delta p/\delta r = - \rho_0 \delta u/\delta t.$$

and for a harmonic motion,

$$p = \frac{j\omega_0 \rho Q}{4\pi r} \exp\{-j(\omega_0 t - kr)\} \qquad \text{C1.2}$$

The acoustic intensity Ir at range r in terms of the total radiated acoustic power W is,

$$I_r = W/4\Pi r^2$$

and in terms of peak pressure ,

$$I_r = \hat{p}^2/2\rho_0 c_0.$$

so that the power radiated by a monopole is given by,

$$W = \frac{\omega^2 \rho_0 Q^2}{8\pi c_0} = \frac{k^2 \rho_0 c_0 Q^2}{8\pi}$$

$Q = S\hat{u}$ and $\hat{u} = \omega\hat{\epsilon}$

When ,

$$W = \frac{\omega^4 S^2 \hat{\epsilon}^2}{c_0 8\pi} \qquad \text{C1.3}$$

Thus the power radiated is proportional to the square of the peak displacement and the surface area and as the fourth power of the radial frequency. For harmonic

vibrations the particle velocity and pressure may be derived from the velocity potential :

$$\phi = 1/r\ f(r-ct)$$

$$u = -\partial\phi/\partial r \text{ and } p = \rho\partial\phi/\partial t.$$

$$p = \hat{P}\cos(\omega t - kr)$$

$$\text{Far-field} = u_{far} = \frac{\hat{p}}{r\rho c}\cos(\omega t - kr) \text{ and,}$$

$$\text{Near-field} = u_{near} = \frac{\hat{p}}{\omega\rho r^2}\sin(\omega t - kr)$$

The amplitude ratio of near-field to far-field is,

$$\frac{u_{near}}{u_{far}} = \frac{\rho c r}{\omega\rho c r^2} = \frac{1}{kr} = \frac{1}{2\pi}\frac{\lambda}{r} \qquad \text{C1.4}$$

Radiation efficiency is defined as the ratio of acoustic power to the total source power supplied for radiation and hydrodynamic fluid motion, a reactive component.

$$\eta_{rad} = \frac{W_{ac}}{W_{ac} + W_x}$$

$$= \frac{R_r}{\sqrt{R_r^2 + X_r^2}}$$

$$Z_r = R_r + jX_r. \qquad \text{C1.5}$$

$W_{(ac)}$ the acoustic power, is proportional to the radiation resistance, R_r

W_x is proportional to the reactance or wattless component, jX_r

Z_r = pressure / particle velocity.

The acoustic power output is given by u^2R_r where u is the vibration velocity, and again from the velocity potential it is shown that both components of the wave impedance are functions of the wave number k and the radius r of the source.

$$R_{sp} = \frac{\rho c (kr)^2}{(1+(ka)^2)} =$$

Radiation resistance per unit area and.

$$jX_{sp} = + \frac{j\omega\rho r}{(1+(kr)^2)} =$$

Reactance per unit area .

Latter represents an added mass per unit area of,

$$M_{sp} = \frac{\rho r}{(1+(kr)^2)} \qquad \text{C1.6}$$

When kr is large compared with 1,i.e when $2\pi r$ is large compared with the wavelength , Rsp approaches the far-field plane wave impedance of pc per unit area while M tends to zero.

At low frequencies where $(kr)^2 \ll 1$ the resistive term,

$$r_{sp} \text{ -- } \rho c (kr)^2,$$

and the reactive term = $jXsp$ - $j\omega\rho r$.

The radiation resistance increases with the square of the frequency up to .$(kr) = 1/2$, $2r \sim \lambda/6$ and attains 80% of its maximum value at,

$$(kr) = 2r \sim 2\lambda/3 \qquad \text{C 1.7}$$

Whereas the effective mass remains fairly constant.

The ratio of near field to far field amplitude is,eqn C 1.4,

$$\frac{u_{near}}{u_{far}} = \frac{\rho c a}{\omega \rho r^2} = \frac{1}{2\pi} \frac{\lambda}{a}$$

The ratio of near to far-field amplitudes decreases rapidly for small r/λ values but relatively slowly as r continues to increase and is unity when kr = 1 or $2\pi r = \lambda$. At frequencies where the sphere dimensions R are small in units of a wavelength,then,

a small pulsating source of any shape ,σ, may be approximated to a sphere of radius R if its equivalent diameter is < $1/3\lambda$.

$$\sigma = 4\pi R^2 \text{ or } R = \sqrt{\frac{\sigma}{4\pi}}$$

Its radiation resistance is $r_r = \rho c k^2 R^2 = \rho c k^2 \frac{\sigma}{4\pi}$ C 1.18

Above is a consequence of sources that produce equal volume flow will at sufficiently large distances generate the same sound pressure and the same sound energy. In contrast to the radiation resistance, the effective mass depends greatly on the shape of the pulsating surface.

The frequency dependent mass per unit area has magnitude,

$$m_r = \frac{\rho r}{1+k^2r^2} \text{ is } \approx(\rho r) \text{ if } k^2r^2 \ll 1 \text{ and } \approx \frac{\rho r}{k^2r^r} \text{ if } k^2r^2 \gg 1)$$

$$\text{At low frequencies } k^2r^2 = \frac{4\pi^2r^2}{\lambda^2}$$

$$X_{sp} = \omega M_{sp} = \omega(4\pi r^2 \rho r)$$

where the term in the brackets M_{sp} = the added mass.

$$M_{sp} = 3\left(\frac{4\pi r^3}{3}\rho\right)$$

and is three times that displaced by the sphere.

In contrast, that for a piston in a baffle is,

$$M_p \text{ is } \left(\frac{8a^3}{3}\rho\right) = \left(\frac{4\pi a^3}{3}\rho\right)\frac{2}{\pi} \qquad \text{C 1.9}$$

or $\frac{2}{\pi}$ times the mass of the circumscribed sphere.

For a body of complexed shape the mass of a circumscribed sphere is an upper limit and that of an inscribed sphere a lower limit. In general, extended surfaces having dimensions that are comparable with a wavelength do not have the spherical radiation field of the simple source.

As the source dimensions are increased the radiation resistance increases as the square of the frequency to a maximum of pc while the reactance reaches a maximum and then decreases eventually to zero. When the diameter exceeds a wavelength the acoustic impedance approaches that of a plane wave with a more directive radiation field. This basic monopole source clearly demonstrates the problems which apply to the generation of high power low frequency sound from compact sources.

C2. A monopole radiator has a volume expander surface with a compressible interior and for operation at depth one of the many design problems is providing an interior low acoustic impedance with a highly-compliant vibrating surface. As the ambient pressure increases with source depth the air compression mode of compliance, as used in near-surface applications, becomes less effective. At the beginning of the research, reviews of the various types of available developed sources disclosed no acceptable unit of the required performance within the allowed weight and dimensions for small ship use. The common Tonpliz piston type transducer was not a candidate since the high stiffness of the direct drive piezoelectric ceramic elements generates only small strains. A possible way ahead arose in early 1980 with reported progress in the development of experimental Flextensional transducers, (Royster 1970). Instead of using piezoelectric ceramic elements with high stress/low strain in a direct thickness piston mode the stack is affixed to an elliptical shell at the two major axis points when the small piezoelectic

strain is by lever action transformed to a larger displacement of the shell walls. The Class IV flextensional type was a preferred choice for the form and size of the towed body and results by Oswin and Turner 1984, with elliptical shells made of aluminium provided some preliminary data on the relationship between resonance frequency, bandwidth and shell thickness for a given ratio of major/minor axis. At 3kHz with a shell eccentricity ratio of 2.0 the semi-major axis was estimated as 10 cm and hence omni-directional and by stacking a number of elements in the vertical plane the vertical beamwidth could be achieved.The area needed of a Class 1V flextensional source at 3 kHz, was:

Perimeter of Ellipse (semi-axes a,b.) = $2\pi\sqrt{1/2(a^2+b^2)}$

a = 0.1 m, b = 0.05 m when P = $0.51m$

The directional pattern of the shell in the height dimension is:

$$D(\theta) = \frac{\sin(\pi h \sin\theta/\lambda)}{\pi h \sin\theta/\lambda} \qquad \text{C 2.1}$$

θ is the incident angle, half beam spread.

Above is the familar sin x / x form.

A beamwidth of about 25 degrees was required.

When $\sin\theta = \pm 0.5\lambda/h$ then

$D(\theta) = 2/\pi = 0.637 = -3.92$ dB below broadside response.

$\Delta\theta = 2 \arcsin(0.5\lambda/h) \approx \lambda/h$. for $h \gg \lambda$.

$D(\theta) = -3$ dB when $\sin\theta = \pm 0.443\ \lambda/h$.

First major side lobe is - 13.26 dB at,

$$\theta = \arcsin\ 1.43\ \lambda/h. \qquad \text{C2.2}$$

A tentative specification for the flextensional source was therefore:

Perimeter = 0.5 m.

Height = 1.3 m.

Area = 650 cm^2

DI = 7 dB.

SL = 210 dB re 1μP at 1 m

say, 1.7 kW. C2.3

Loading per surface area = 1700/650 = 2.6 W/cm^2

Cavitation threshold =

$$I_c = 0.3(1.8+z/10)^2 W/cm^2$$

z = water depth, when for $I_c = 2.6 W/cm^2$

z = 11 m C2.4

This would be a minimum depth and in particular if there is the possibility of higher intensity hot spots. The radiation efficiency was related to the ratio of reactive to radiated energy; a large eactive component would mean that the efficiency of the source would be poor. The latter would increase the size of the relatively large excursions in shell displacement since, as required by linear theory, the radiated power is proportional to the square of the velocity amplitude. Another feature is that the drive power amplifiers would also have a low efficiency. Making extensive use of finite element modelling J Oswin et Al developed an efficient 3kHz towed source that met the requirements of source level and bandwidth with a maximum operating depth of 200m. Increasing the depth limit involved an even more sophisticated unit with compliant elements within the shell space.

References

Ainslie M.A. And C.H. Harrison. Diagnostic Tools for the Ocean Acoustic Modeller. IMACS Symposium on Computational Acoustics. Princetown. March 1989.

Allen. J.R.L. Physical Processes of Sedimentation. G Allen and Unwin. 1979.

Apel.J.R. Principles of Ocean Acoustics. Int Geophysics Series, Vol 38. Academic Press. USA 1987.

Baker.W.F. New Formula for Calculating Acoustic Propagation Loss in a Surface Duct. Jo Ac Sc Am 57, 1198. 1975.

Berktay H.O. Non-Linear Acoustics. Proc of N.A.T.O. Advance Study on Signal Processing. Academic Press, 1973.

Berktay H.O. Some Proposals for Underwater Transmitting Applications of Non-Linear Acoustics. J.Sound and Vibration 6(2), 1967.

Brekhovskikh.L.M. Waves in a Layered Medium. Academic Press.1960.

Clay S.C. and Medwin H. Acoustical Oceanography. J Wiley.1977.

Dinapoli.F.R. and R.L. Devanport. Numerical Models of Underwater Acoustic Propagation in Ocean Acoustics. Ed J.A.DeSanto. Springer-Verlag. 1979

Etter.P.C. A Survey of Underwater Acoustic Models and Environmental Acoustic Banks. ASWSPO Report. 84-001. April 1984.

Fisher.F.H. and V.P Simonds. Sound Absorption in the Ocean .JASA 63, 558, 1977.

Fortuin.L. The Sea Surface as a Random Filter for Underwater Sound Waves. SACLANTCEN Report SR-7 June 1974.

Grimley W.K. Status of Underwater Acoustics. M.Sc Thesis.Unv of Bath.1972

Hamilton.E.L. Compressional-wave Attenuation in Marine Sediments. Geophysics,v.37, pp 266-288.1972.

Hamilton.E.L. Geoacoustic Modelling of the Seafloor. J. Ac Soc.Am. 86. 1103-17. 1980.

Hamilton.E.L (Edit). Physics of Sound in Marine Sediments. Plenum Press 1974

Hanrahan.J.J. Predicting Convergence Zone Formation in the Deep Ocean. Progress in Underwater Acoustics. Plenum Press 1986.

Harrison.C.H. From Advanced to Simple Propagation Models. Inst. of Ac. Con. Proc. Vol 12 Pt 2, July 1990.

Harrison.C.H. Ocean Propagation Models. Applied Acoustics. 27 .1989.

Hill. M.N. (Editor). The Sea. Interscience Pub. Vols 1-4 J.Wiley & Sons. 1962.

Levitus.S. Climatological Atlas of the World Oceans. NOAA Professional Paper 1982.

March.H.W. and Schulkin.M. Report on the Status of Project AMOS. Underwater Sound Laboratory Research Report 255, 1955.

Marsh.H.W. and Schulkin.M. Shallow Water Transmission. J. Ac Soc Am 34 1962.

Medwin.H. Speed of Sound in the Water; a Simple Equation for Realistic Parameters. J Acoustic Soc Am.58. 1318-1319. 1975.

Naval Operations Analysis. Naval Institute Press, Annapolis,Maryland.USA.1979.

Novik B.K.,and O.V.Rudenko and V.I.Timoshenko. Nonlinear Underwater Acoustics. Ac Soc Am .1987.

Officer.C.B. Sound Transmission. McGraw-Hill 1958.

Oswin. J.R. and Turner.A. Design Limitations of Aluminium Shell,Clas !V Flextensional Transducers. Proc Inst Ac V6 Pt 3 1984.

Pace.N.G and Langhorne.D.N.(Ed). Acoustic Classification of the Seabed. Vol 15 Pt 2. Conference Proceedings 1993.Inst of Acoustics.

Physics of Sound in the Sea.Pt 1. U.S National Research Council. 1946.

Rayleigh.J.W.S. The Theory of Sound. 1877. Reprint, Vols 1 and 2. Dover Publications 1945.

Robinson.A.R and Lee.D.(Ed) Prediction and Propagation Models. A.I.P NY 1994,

Royster.L.H. The Flextensional Concept : A New Approach to the Design of Underwater Acoustic Transducers. Applied Acoustics 3,117-126. 1970.

Schulkin.M. and Thorp.W.H. Transmission by Way of the Bottom. Study D. Project Amos,Unclassified Report .U.S.N. Underwater Sound Lab. May 1967.

Schulkin.M. Surface Coupled Losses in Surface Sound Channels. J. Ac Soc of Am.44,1152,1968.

Schulkin.M. Basic Acoustic Oceanography. US Naval Oceanographic Office Reference, Publication 1,(1975). Department of the Navy, Washington.DC.

Schulkin.M.and Mercer.J.A. Colossus revisted:A review and extension of the Marsh-Schulkin shallow water Trasmission loss model. Appl.Res.Lab.Univ. Washington. APL.UW8508. 1985.

Stansfield.J Underwater Electroacoustic Transducers. Bath Univ Press 1990.

Tolstoy.Ivan and C.S.Clay. Ocean Acoustics. Ac Soc Am. 1987.

Underwater Acoustic Propagation. A Tutorial Meeting. Proc of Inst of Acoustics. Vol 12 Pt 2 0.

Urick.R.J. Principles of Underwater Sound. McGraw Hill 1975 (and later editions.)

Urick.R.J. Sound Propagation in the Sea_.Pensinsula Publishing.1982.

Vernberg. F.J. and Diemer.F.P. Processes in Marine Remote Sensing. Unv of South Carolina Press. 1982.

Weston.D.E. Acoustic Flux Formulas for Range-Dependent Ocean Ducts. J.Ac. Soc. AM. 68. 1980.

Weston.D.E. Intensity-Range Relations in Oceanographic Acoustics. J.of Sound And Vibration. 1971.18(2)

Weston.D.E. Problems in Ocean Sound Propagation. Journal of R.N Scientific Service. Vol 14 No 3.1988.

Weston.D.E. Propagation of Sound in Shallow Water. J.Brit I.R.E. 26, 1963.

Weston.D E. and P.B.Rowlands. Guided Acoustic Waves in the Ocean. Rep Pro Phys.42. 1979.

Wood.A.B. Scale Model Study of Propagation In Shallow Water. Underwater Acoustics. Ed V.M. Albers. Plenum Press.NY. 1963.

UNRESTRICTED

BISTATIC SONAR AND A NOVEL FORM OF VARIABLE DEPTH SONAR

(Sonar Systems Research Study)

Submitted by

W.K.Grimley OBE, MSc., C.ENG, F.I.E.E.

for the degree of Ph.D. of

The Open University

1996

Author number: M7096449
Date of submission: 1 February 1996
Date of award: 17 April 1996

Section 3

Contents.

Section 3.

Directive Form of a Towed Line Array.

FIGS.

Section 3.

A DIRECTIVE FORM OF A TOWED LINE ARRAY.

Towed Sonar Line Arrays.

3.1 The usual role of towed sonar line arrays in naval service is for the long range passive detection of targets that radiate very low frequency noise in a band from a few Hz to around 1 kHz. To achieve a sufficient angular space resolution of the received signals at these low frequencies, a sensor aperture of several hundred metres in length is needed. This dimension is obtained by towing a line of connected omni-directional hydrophone sensors contained within a neutrally buoyant hose at a distance astern of the tow platforms, surface escort ships and submarines, the length of the connecting tow cable being set by the required array depth and the level of the tow platform radiated noise at the sensor positions. Fig 3.11 shows a typical array deployment, and fig 1.41 a typical beam pattern. The great advantage of these low frequency line arrays over the hull planar shapes is this capacity for an extended aperture at depth with lower self noise levels but with the disadvantage of a one dimensional response pattern and hence a loss of vertical directivity and no port /starboard discrimination of signal inputs and noise. Also, being a long flexible line, it may be distorted in a number of ways: with changes in ship's heading the towed line will track the new path so deviating from its straight line shape and at the same time the loss of forward speed reduces the drag forces on the tow cable thereby initiating a shift in depth of the array.

Fig 3.11 Surface Vessel Towed Array Deployment.

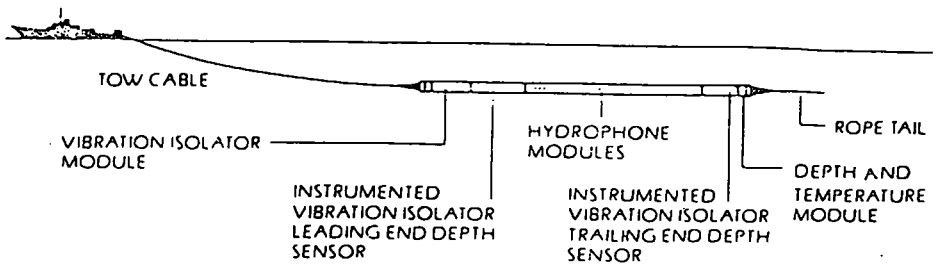

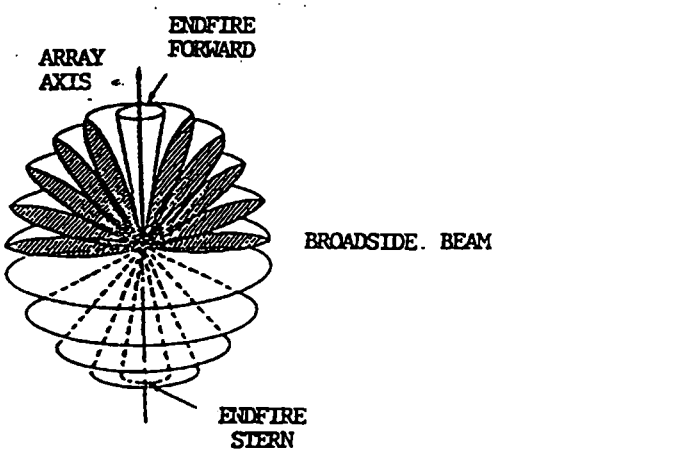

Fig 1.41 Typical Beampattern for Towed Line Linear Array.

These effects are very significant with large helm changes and to a lesser extent may be evident following small corrections to a ship's helm for a steady course. A consequence is that under real at-sea conditions these perturbations may be responsible for a loss in array gain performance, particularly during the transitory stage of sprint and drift manoeuvres.

Port-Starboard Ambiguity.

3.2 One of the common procedures to resolve the port-starboard ambiguity in passive sonar towed array operations following a first detection at a low search speed, low self-noise condition, is for the platform to make a 90 degree change of course and sprint a known distance to a cross target bearing location where another set of target bearing inputs is obtained, also at low speed. Moving to a new location involves bringing the array to short stay during the high speed sprint,then re-streaming with a lapsed period to obtain a stable tow state.These so-called high-low speed manoeuvres are necessary where platform self-radiated noise and low frequency array flow noise are the limiting backgrounds and so constrain the ship search speeds. The available passive sonar listening time can be of the order of tens of minutes to several hours and in the latter case loss of contact on a continuous noise source during the sprint and drift manoeuvre is an acceptable tactic since the sequence involves only a small part of the total detection time. Active sonar operations occur at much shorter ranges with a possible intermittent target return during the pulsed transmission interval and many

more uncertain false echo returns; so there is a greater urgency for an action response once a target is located. In active sonar, two positive target returns out of three is often considered sufficient for a full detection alert. It followed that acceptance of a line receiver for a small ship system in any active sonar role was critically dependent on a resolution of the ambiguity in the port starboard target location.The author's approach for a Bistatic receiver was based on the root technology of the passive towed line arrays but with a port-starboard discrimination in a package suitable for small ship operations. Since the source was to be a high power hull sonar the operating frequency was set in a band around 3kHz. For bistatic sonar applications it was accepted that the source sonar would at all times continue to operate in its normal monostatic sonar role, hence the bistatic line receiver could be viewed as a range displacement of a second source receiver.

The Directive Towed Line Array Concept.

3.3 Descriptions of towed line sonar systems may be separated into two parts, commonly termed "wet and dry ends." The wet end includes the hose containing the spatial array of hydrophones with associated electronics and the transmission arrangements for the array output signals and power links via the tow cable to the tow platform and embraces the deck handling gear. The in-board dry-end includes the array signal processing, displays, operator functions, data analysis and command-decision formats, the whole forming part of the total platform weapon system.

This system division, although there is a great deal of overlap, appeared to be a convenient split in the progress of the research and design stages. The overall detection goal for the bistatic system was an additional range gain equivalent to double that of the monostatic sonar. This required that the receiver performance of the Bistatic array be equivalent to that of the source sonar. Section 4 shows that area gain is a function of S/N range gain and the two ship separation distances.

3.4 To obtain a port/starboard discrimination for active sonar operations required additional orthogonal sensing elements at each hydrophone position of the intended towed array, figs 3.41. The maximum element separation distance and volume was constrained by the allowed hose dimensions and the tow cable which in turn was determined by the size and weight of acceptable small ship winches that could cope with the cable stowage, drag forces and the deck handling processes for launch and recovery; latter ruled out any prospects for a coupled multiple towed line solution. What was needed was some compact arrangement of sensor elements that would produce single steered azimuth beams in the port and starboard directions. A first solution considered was the use of velocity or pressure gradient hydrophone units: unlike pressure, gradient outputs are vector quantities and with a doublet sensor arrangement an output can be obtained with a $\cos\theta$ response in azimuth. A pressure gradient unit would consist of two closely spaced omni-directional hydrophones aligned

orthogonal to the array x axis when the pressure gradient of an incoming wave is given by:

$$\frac{\partial p}{\partial y}\cos\theta.$$

If S is the size of the hydrophone area,

θ the angle that the incoming wave

referenced to the normal to the hydrophone surface,

Δl the separation between the hydrophones.

The complex rms force is,

$$f_d = -S\frac{\partial p}{\partial y}\,\Delta l\,\cos\theta.$$

For a steady state sinusoidal wave,

$$f_d = \frac{j\omega_0 p_0 S\Delta l\cos\theta}{c}\,\exp -jkr. \qquad 3.41$$

where $k = \frac{\omega}{c}$ and p_0 = rms pressure at y = 0 = $\pm\Delta l/2$.

In its doublet form the two hydrophone elements would have a separation distance small compared with the signal wavelength in water. The steady state pressure gradient is proportional to $j\omega\rho$ times the component of particle velocity,u, in the direction of the gradient:ρ is the density of sea water when:

$$|f_d| = |u|\,\omega\rho_0\Delta l\cos\theta. \qquad 3.42$$

The rms force acting on the hydrophones of a pressure gradient unit is proportional to the frequency, effective area of the hydrophones, the density of the medium and is a function of the angle to the direction of the incoming waves.The sensitivity of the unit when expressed in units of pressure differs from the sensitivity expressed in

terms of velocity by the constant factor,

p/u = ρc = the characteristic impedance.. The doublet arrangement is sensitive to acoustic particle velocity with a maximum in the positive direction of propagation as well as in the reverse direction.The two lobes of the figure of eight pattern have opposite phases and if the output from the doublet is added to the scalar pressure output from one of the omni-directional hydrophones arranged for equal response,the resultant is a single beam response. Such a pattern is known as a "cardioid" being uni-directional as compared with the ambiguity of the dipole response. Figs 3.41,3.42, with 3.43 show the pattern multiplication principle for such a cardioid pattern and fig 3.51 the cardioid network.

If the output voltage of the omnidirectional pressure element is,

$$e_0 = Ap. \text{ and}$$

that for the presure gradient unit is,

$$e_g = Cp\cos\theta.$$

Letting C/A = B

$$e_s = Ap(1+B\cos\theta) \qquad 3.43$$

which is the equation for a cardiod.

B will only be a real number if e_0 and e_g are in phase.

There are several inherent difficulties for a towed line array with the pressure gradient format, one being that the assembly must be small to avoid distortion of the wave field and so the output is also small. A more serious problem is that to obtain the differential output,the signals from the two gradient sensors must be differenced which requires a high degree of matching with a low

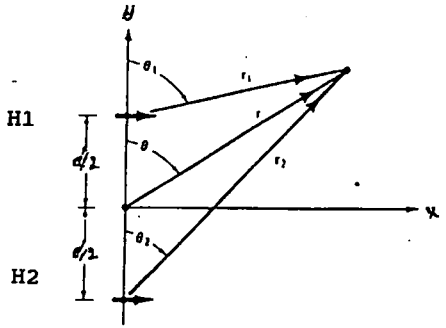

(a) Two Omni-directional hydrophones. Near field.

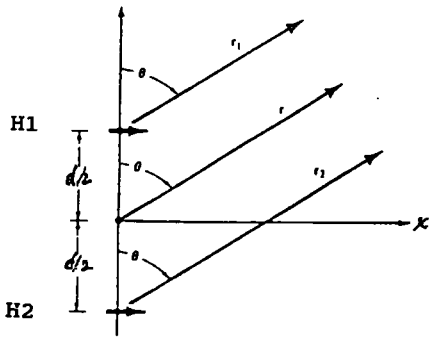

(b) Two Omni-directional hydrophones. Far Field.

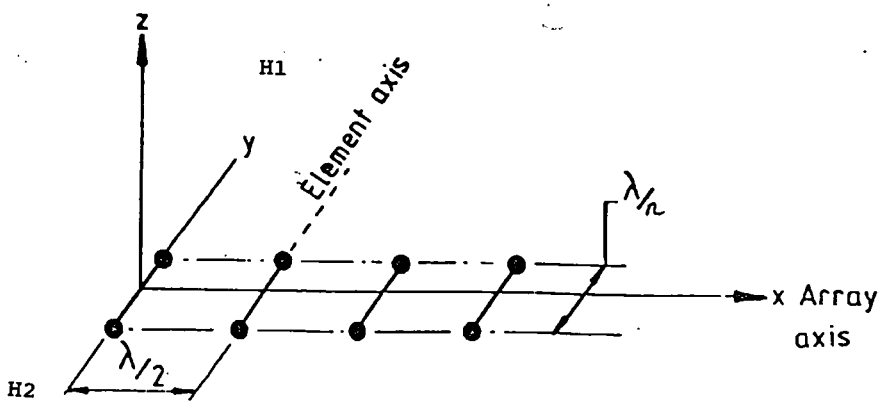

Fig 3.41 Geometry of Bipolar Elements.

ARRAY FORM

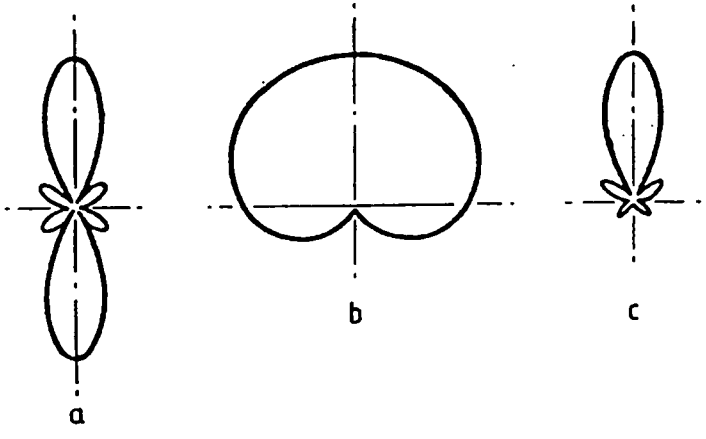

PRINCIPLE OF PATTERN MULTIPLICATION

Pattern c = Pattern a × Pattern b

Fig 3.42 Cardioid Element Response Pattern.

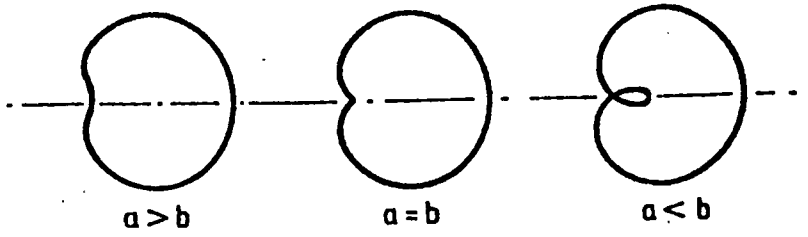

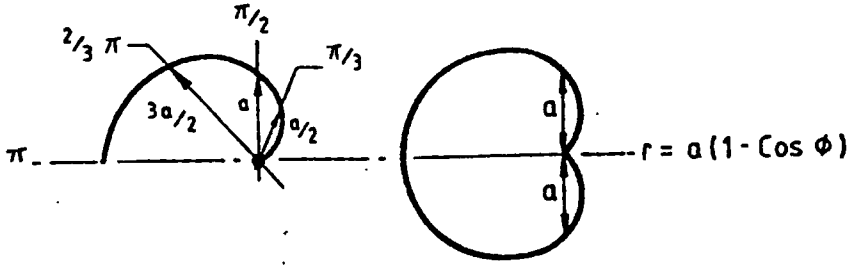

GENERAL EQUATIONS

$r = a + b \sin\phi$ $\qquad$ $r = a - b \sin\phi$

$r = a + b \cos\phi$ $\qquad$ $r = a - b \cos\theta$

ϕ	0	$\pi/3$	$\pi/2$	$2\pi/3$	π
$r = a(1-\cos\phi)$	0	$a/2$	a	$3a/2$	$2a$

Fig 3.43 Cardioid Polar Beam Pattern.

sensitivity. Furthermore,the background noise of the omni-directional hydrophone responds to the total noise field and will be more sensitive to any unrelated very near noise sources in the vicinity of each of the gradient hydrophones. Another unknown effect is that of vibration within the array hose which could add to the background of an already low signal ouput.There are a number of other analogous arrangements of the gradient form that produce a figure-of-eight response but all had similar problems.The author therefore decided to pursue a more attractive technique of using a doublet of pressure units in a sum and difference configuration on the grounds of offering a more acceptable performance, a robustness in design and at an acceptable cost.

Cardioid Format.

3.5 Two point ceramic hydrophones orthogonal to the axis of the array replace the single sensor at each element position as fig 3.41. A time delay is inserted at the output of the first element matched to the wave propagation travel time in the azimuth direction to the second element when the two hydrophone outputs sum in phase. Wave inputs from the reverse azimuth direction are set to have outputs with an opposite time delay so that they sum to zero, figs 3.51 and 3.61. Advantages over the pressure/velocity gradient formats include a better response sensitivity as signals are summed with a higher signal-to-background ratio and the addition of omni-directional noise to a differenced signal input is no longer a necessary part of the cardioid response pattern. The

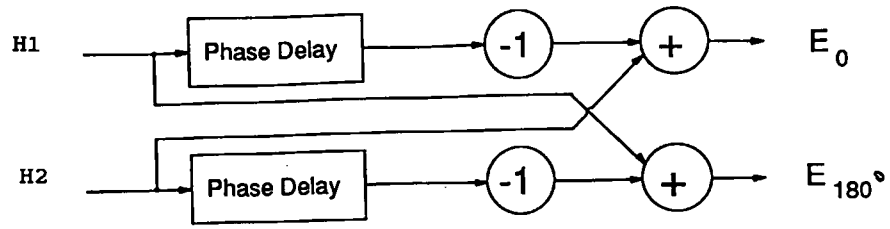

Fig 3.51 Cardioid Network.

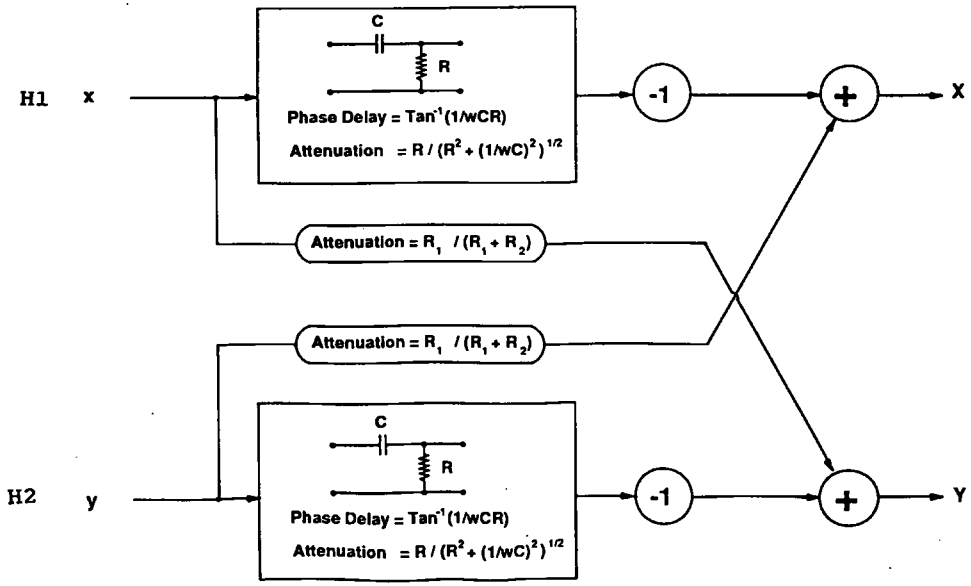

Fig 3.61 RC Carioid Network.

selection of parameters was set by three objectives.

(i) That a single array should provide an acceptable operational performance over the band of the active sonar frequencies of the powerful low frequency ship source sonars.

(ii) That the array hose diameter and hence available element volume for the sensing and any processing units should be compatible with the tow ship handling equipment. Also, a state of neutral buoyancy was a requirement.

(iii) That a minimum port starboard rejection ratio of 10 dB over the reception arc should be the objective.

Cardioid Processing.

3.6 Consider a sinusoidal plane wave incident at an azimuth angle Θ to the line joining two point hydrophones equally spaced a distance d/2, orthogonal to the array axis which is taken as a reference point,see fig 3.41. The outputs of the two sensors, H_1 and H_2, are connected to a cardioid network as in fig 3.51. Assume a wave direction at angle Θ from H_1 to H_2 then the hydrophone outputs reference to the mid point are:

$$V_1 = V exp j[\omega(t-\tau/2)+\psi] \text{ and,}$$

$$V_2 = V \exp j[\omega(t+\tau/2)+\psi] \qquad 3.61$$

V_1 = Output voltage of hydrophone H_1.

V_2 = Output voltage of hydrophone H_2.

ψ = Intial phase of incident signal.

τ = Time delay : reference mid point arrival time at array axis line, direct distance d/2.

$\tau/2 = \frac{d}{2c}\cos\theta$.

c = speed of sound.

θ = azimuth angle relative to array axis.

Assume a wave travelling in a direction H_1 to H_2 then after applying the output voltages to the cardioid network, at the point of summation the time/phase differences are:

$$H_1 \rightarrow \quad -\exp j\omega\left(-\frac{\tau}{2}+\beta\right)$$

$$H_2 \rightarrow \quad \exp j\omega\left(+\frac{\tau}{2}\right)$$

$E_0 = (H_2 - H_1)$ via Cardioid Network and phase reversal.)

β is the inserted time delay.

After summation, unit output.

$$= \left[\exp j\omega\left(+\frac{\tau}{2}\right) - \exp j\omega\left(-\frac{\tau}{2}+\beta\right)\right]$$

$$= \left[\exp j\omega\left(\frac{\tau}{2}-\beta/2\right) - \exp j\omega-\left(\frac{\tau}{2}-\beta/2\right)\right]\exp j\omega\beta/2, \text{ when,}$$

$$E_0(\text{ Array Factor}) = 2\left[\sin\omega\left(\frac{\tau}{2}-\beta/2\right)\right] \qquad 3.62$$

Setting $\tau/2 = \beta/2$ then the output at Eo is zero for an input wave in this direction.

A wave propagating in the reverse direction, H_2 to H_1. will generate hydrophone outputs:

$$H_1 \rightarrow \quad -V \exp j\left[\omega\left(+\frac{\tau}{2} + \beta\right)\right] \text{ and,}$$

$$H_2 \rightarrow V \exp j\left[\omega\left(-\frac{\tau}{2}\right)\right]$$

After summing, $(H_2 - H_1)$, unit inputs,

$$= \left[\exp j\omega\left(-\frac{\tau}{2}\right) - \exp j\omega\left(\frac{\tau}{2} + \beta\right)\right]$$

$$= -\left[\exp j\omega\left(\frac{\tau}{2} + \beta/2\right) - \exp j\omega - \left(\frac{\tau}{2} + \beta/2\right)\right]\exp\left(j\omega\,\frac{\beta}{2}\right)$$

$$Eo(AF) = -2\sin\left[\omega\left(\frac{\tau}{2} + \beta/2\right)\right] \qquad 3.63$$

A maximum response would be twice that of a single array, but compromises are necessary to allow for an element separation within a limited array hose diameter and the azimuth wave direction term of $\cos\theta$, so that the practical maximum gain is less than twice that of a single element. The network is symmetrical so that corresponding summations will apply at the E (180°) terminal output.

A port to starboard amplitude discrimination ratio may be defined by:

$$D_r = \frac{|[\sin\omega(\alpha + \beta/2)]|}{|[\sin\omega(\alpha - \beta/2)]|} \qquad 3.64$$

and $\frac{\omega}{c} = k$ = wave number. $= 2\pi/\lambda$

$$\alpha = kd\cos\theta\backslash 2$$

Maximum image rejection is when β in units of λ is,

$\beta = \ = 2\alpha$ at frequency ω.

It is observed that for any given hydrophone separation,d, it is always feasible to obtain a delay network that will reduce the denominator to zero but at the cost of a lowering the sensitivity in the signal direction. As the frequency is varied from a nominal 3kHz over a possible frequency range of 2.kHz to 4 kHz ,then:

for fixed values of d ,β and travel time,τ,

$$\beta = \tau = \frac{d\cos\theta}{c}$$

Over the frequency band,D_r, would retain the rejection ratio so long as β is a real time delay.

However if phase correction is applied,

$$\beta = [\sin(kd\cos\theta)] \qquad 3.65$$

which is an inverse function of wavelength.

For either of the delay arrangements set for broadside reception the port-starboard discrimination would be reduced by the $\cos\theta$ term.For a wave travelling along the array axis there is no separation between elements so;

$$\tau = \frac{d\cos\theta}{c} = 0$$

$$D_r = \frac{[\sin\omega(+\beta/2)]}{[\sin\omega(-\beta/2)]} = |1| \qquad 3.66$$

when as might be expected there is no image rejection.

. One or more further sets of displaced elements and networks would be needed to obtain directivity as the received angle approached end-fire. Fig 3.61 shows the RC cardioid network that was used for the VDS version of the array in Section 5.

Basic Towed Line Array.

3.7 With an acceptable image rejection technique established, the next system task was to determine the main parameters of the primary towed array that would form the basis for the azimuth directional array. The format was a line of N omni-directional hydrophones, which in an ideal operation would be towed through the water at a uniform speed and at a predetermined depth in a direction parallel to the line axis. Most practical engineered arrays have equally spaced elements that allows for a lower cost implementation of beam steering networks and side lobe control through amplitude weighting. A well known technique for designing linear line arrays, ref Steinberg 1975, makes use of the theorem that every linear array with commensurable separations between the elements can be represented by a polynomial and every polynomial can be interpreted as linear array. The total length of the array is the product of the separation between elements and the degree of the polynomial is one less than the number of elements .

$$F(z) = a_0 + a_1 z + a_2 z^2 \ldots\ldots a_{N-1} z^{N-1} \qquad 3.71$$

The weighting coefficient a_i expresses the amplitude and phase of the ith element reference to some specific element.

The unnormalized power beam pattern $AF(\theta)$ can be written as,

$$AF(\theta) = |F(z)|^2 \qquad 3.72$$

The independent variable z is a complex number with an associated angle ψ on the circumference of a unit circle.

Each term of the polynomial represents the response of an element of the array.

Variable ψ maps beam pattern to points on the circle and is defined by,

$$\psi = 2\pi(d/\lambda)\sin\theta - \alpha$$

d is the element spacing.

θ is the direction from broadside.

α is a progressive phase delay.

as ψ decreases, z moves in a clockwise direction.

Range of ψ as θ changes from $\frac{\pi}{2}$ to $-\frac{\pi}{2}$ is $R = 4\pi\frac{d}{\lambda}$,

When $d = \frac{\lambda}{2}$ the range of R of ψ is 2π 3.73

The array beam pattern may be synthesised in terms of the roots on the unit circle, ϕ or θ.

$$\text{If } d < \frac{\lambda}{2}$$

z will traverse less than one complete turn on the unit circle.

$$\text{If however } d > \frac{\lambda}{2} \text{ then z will traverse}$$

more than one complete turn and some lobes will be repeated.

$$\text{If } d = \lambda$$

two complete patterns including two main beams will occur for one complete cycle of z. 3.74

Setting values of "a" to unity then for an N element array,

$$E_a = \sin\left[\omega t + (N-1)\frac{\psi}{2}\right]\frac{\sin(N\psi/2)}{\sin(\psi/2)} \qquad 3.75$$

The first factor is the incident wave with a phase shift of $\omega t + (N-1)\psi/2$. while the second is the array factor, AF.

If the spacing between array elements is half wavelength, the half-power beamwidth at broadside is approximately,

$$\theta_{-3dB} = \frac{101.8^{\circ}}{N} \qquad 3.76$$

The space pattern response, $b(\theta)$, for a line of omni-directional hydrophones is obtained by summing the output voltages with the common sinusoidal term suppressed. If the phase factor is taken at the centre of the array then the normalized broadside beam pattern for an unscanned array is given by

$$b(\theta) = \left\{ \frac{(\sin Nu)}{N \sin u} \right\} \qquad 3.77$$

$$u = \left(\frac{\pi d \sin\theta}{\lambda} \right)$$

This expression is valid for equal response elements summed in phase.

When a uniform progressive phase at the array elements' outputs is introduced to position the main beam in space then;

$$u = \left[\left(\frac{\pi d \sin\theta}{\lambda} \right) - \frac{\alpha}{2} \right] \qquad 3.78$$

α is the phase/time shift factor.

If α is varied, the beam will scan to a new angle.

Expressions have been developed which give the half-power or -3dB beamwidth of a line array as a function of length L, wavelength λ, and the scan position, θ_s,

$$BW_{-3} = 1.77\left(\frac{\lambda}{L}\right)\sec\theta, \text{ in radians at or near broaside.}$$

$$BW_{-3} = 4\sqrt{\left(0.886\frac{\lambda}{L}\right)} \text{ at endfire, in radians} \qquad 3.79$$

Actually when, $L > 5\lambda$,

the above approximation for the first BW is in error by less than 4 % when the beam is scanned to within 5 beamwidths of end-fire.

The second BW is in error by less than 1%.

In the ref Steinberg,1975, it is also demonstrated that the far-field response pattern of the modified array is equal to the product of the response pattern of the cardioid element at each sensor position times the response of the line array with omni-directional elements. Fig 3.42, i.e:

$$F(\theta,\phi) = F_L(\theta,\phi)F_C(\theta,\phi) \qquad 3.710$$

Bistatic Line Array Parameters.

3.8 An equivalence between the hull and bistatic receiver parameters was set by postulating a simple degradation ratio factor, L , for two active sonar limiting detection states, reverberation and noise.In the case of the active sonar mode, the source level is the same for both systems, monostatic, S, and bistatic, B. With the assumption of parity for other system parameters, and in particular, spatial and signal processing, detection thresholds, displays and operator reactions, then the following relationship would apply for a noise background,

$$Ln = [\ TS(B) - TS(S)\ ] + [\ NL(S) - NL(B)] + [\ DI(B) - DI(S)] \quad 3.81$$

Ln = Degradation ratio factor for noise.

SL = Source Level .

TS = Target Level .

NL = Noise Level .

DI = Directivity Index of Receiver .

DT = Detection Threshold .

S = Monostatic .

B = Bistatic .

For equality Ln = 0

The parameters for a reverberation limiting environment, Lr, were defined by,

$$Lr = \frac{(\theta B)}{(\theta S)} x \frac{(TS)}{(TB)} x \frac{(RB)}{(RS)} \qquad 3.82$$

θ = horizontal beamwidth .

TS = Target Strength .

R = reverberation scattering level.

S denotes Monostatic Receiver .

B denotes Bistatic Receiver .

Note, ratios are in natural not dB units.

In terms of the so called figure of merit, FOM, the degradation factor for a noise limiting background was defined by,

$$10 \log Ln = FOM(S) - FOM(B)$$

where,

FOM = figure of merit for active sonars. (dBs)

$$= SL + TS - NL + DI - DT \qquad 3.83$$

NL = noise level.

Di = Directivity Index.

DT = Detection Threshold.

Array parameters are included in terms NL and DI.

With L = 0, then to a first order the range detection probabilities were assumed to equate.

A typical DI(S) for the 3kHz hull sonars is about 25 db. Some interim at-sea measurements suggested a value of TSm - TSb of 4 dB which was adopted: in natural units TSm / TSbs represented a loss in target strength of 10 log 2.5. (TSm = Target Strength Monostatic and TSb = Target

Strength Bistatic). In a private communication the author was informed that the largest number of measurements were for an incident bow angle of 60 degrees and, as is usual, there was a very large spread in the returns even between successive echoes. A later detailed analysis by the author of bistatic reverberation levels demonstrates that this latter parameter is more complex than was originally envisaged, being a function of the transmit/ receive intercept beam angle, bistatic angle, and the transmit pulse length; the evidence for this was not very evident in the spread of the sparse trials data. For a noise-limiting background, comparison of the detection performance of the hull sonar with the bistatic system involved estimates of the line array outputs for tow ship radiated noise at the role tow lengths, the reduction properties of the array to this source, and flow noise.

3.9 With a line of equally spaced units and a uniform progressive phase the broadside beam pattern is:

$$B(\theta) = \left[\frac{\sin Nu}{N \sin u}\right]^2$$

$$u = (d/\lambda)\pi \sin\theta. \qquad 3.91$$

θ is the angle from the array broad side.

d is the element spacing.

λ is the wavelength.

N is the number of elements.

Introducing a uniform progressive delay α to the array elements.

$$u = [(d/\lambda\ \pi\sin\theta) - \alpha/2]$$

α is the phase shift factor to position the array beam in space.

The width of the main beam is determined by Nxd which is approximately that of the length of the array. In order to avoid diffraction lobes as the array is steered towards end-fire the element spacing is set to slightly less than half a wavelength. The beam patterns are symmetrical about the axis of the array, fig 1.41 and the directivity index is approximately 10 log N for all steering angles. For continuity in sonar cover the scanned beams are required to over-lap over the scanned arc at 10 log B(u) = -3dB in directions $\sin\theta_s$.

$$u = \left(\frac{\pi d}{\lambda}\right)(\sin\theta - \sin\theta_s) \qquad 3.92$$

The first or broadside beam is not steered so from the expression fo u,we get;

$$u_0 = (d/\lambda)\pi\sin\theta_0$$

$$\text{or,} \quad \theta_0 = \sin^{-1} u_0(\lambda/\pi d)$$

The broadside and the first steered beam, θ_1, are required to cross/over at their 3dB points.

$$u_1 = \pi d/\lambda(\sin\theta_1 - \sin\theta_0) = u_0 = \pi d/\lambda\sin\theta_0$$

Above expression reduces to $\sin\theta_1 = 2\sin\theta_0$, when,

$$\theta_1 = \sin^{-1}(2\sin\theta_0). \qquad 3.93$$

The first steering angle.

The above procedure may be generalised so that:

$$\theta_n = \sin^{-1}[(2n+1)\sin\theta_0]$$

for the n crossover angles and,

$$\theta_n = \sin^{-1}[2n\sin\theta_0]$$

for the n beam steering angles where,

$$\sin\theta_o = \lambda u_0/\pi d. \qquad 3.94$$

The near broadside half-power,- 3db, of an N half wavelength element array is approximately :

$$BW\ 3 = 1.772\ /\ N-\ 1 \text{ radians.} \qquad 3.95$$

The operational limit to the scan beam angle is set at a point where the image rejection of the cardioid elements is less than 10 dB which is around ±60°. A further increasing of scan angle would be at a reduced image rejection or would require a further set of cardioid elements at an angle to the array axis. As the beam scan angle is increased from broadside the beam width increases.

$$BW_3 = 1.772(\lambda/L)\sec\theta \text{ radians, at or near broadside.}$$

$$BW_3 = 2[1.772(\lambda/L)]^{1/2} \text{ radians at end fire.} \qquad 3.96$$

To a first approximation the side lobes of the shifted beam remain in the same ratio and to maintain a constant over-lap the phase shift should be graduated. To keep down cost a single mean value was selected.

3.10 A typical hull type transmit/ receive unit was expected to have a DI of say 25 dB with an azimuth beamwidth of 10 to 15 degrees: the upper limit of a practical line array for a small ship bistatic system was a length of 30m, 60 wavelengths. The DI at 3kHz of the latter would be 18 dB and allowing a nominal - 1dB side lobe shading factor and an additional + 4 dB for the cardioid elements a total of 21 dB was close to the desired goal of equating the two sonar receivers. A significant difference is that the Dirictivity Index (DI) of the towed line is gained by the aperture length with little vertical directivity so there was the question of multipath interference from surface

and bottom ray paths. In fact,trials with the VDS version, Section 5, having source parameters similar to a hull sonar demonstrated that this was not a problem.The intended lowest passive sensing frequency was 500 Hz where the broadside beamwidth is six times that at 3kHz with a corresponding increase in beamwidth and reduction in array gain. A bonus of using a time delay beam scanning method would be that it is independent of frequency but the available inter-element spacing in units of wavelength is also reduced by a factor of six. Noting that ,

$$b(u)=\left\{\frac{\sin Nu}{N\sin u}\right\} \text{ and}$$

$$u_0=(\pi d/\lambda)(\sin\theta-\sin\theta_s) \qquad 3.101$$

The element spacing at the lowest listening frequencies approaches that of a continuous line of 30 m. Some consideration was given to the prospects of attaining super-directivity at the lower frequencies but the author's experience was that although an attractive goal, for sonar applications it is difficult to attain since the narrower major lobes are sensitive to out-of-phase and other misalignments that lead to unacceptable increases in sidelobe response. This would be exacerbated with the bistatic array taking into account the possible changes in the line geometry when towing from a small ship. As the prime role of the array at this time was to be for active bistatic sonar operations, any low frequency passive capability was a bonus. A tentative decision was therefore taken to retain the summed network outputs over the total bandwidth but not to make any special arrangements for low

frequency passive listening beyond frequency filtering until further evidence was available on cost effectiveness.

Cable Twist.

3.11 Previous experience by the author with towed body cables for similar conditions to the above was that significant twisting could be expected even after the best torque balancing techniques were applied. This meant that the two orthogonal cardioid sensors could be turned out of their azimuth plane thereby reducing the effectiveness of the image rejection. The cardioid element array may be represented as two sub-arrays placed symmetrically about the x axis in the xy plane. Fig 3.111 shows the modified form of spherical co-ordinates used for analysis; angle θ is the azimuth angle and angle ϕ is the twist in the yz plane. These two angles provide a natural partition between the effects of beam scan angle and twist and the product rule allows the effects on the dual element array to be parameters of the cardioid network, figs 3.41, 3.51, and 3.61.[1] Path differences between the dual elements at a mid-point x along the array are:

---

1 The co-ordinate system at Fig 3.111 was suggested by M.D.Daintith of SACLANT ASW Research Centre.

CO-ORDINATE SYSTEM

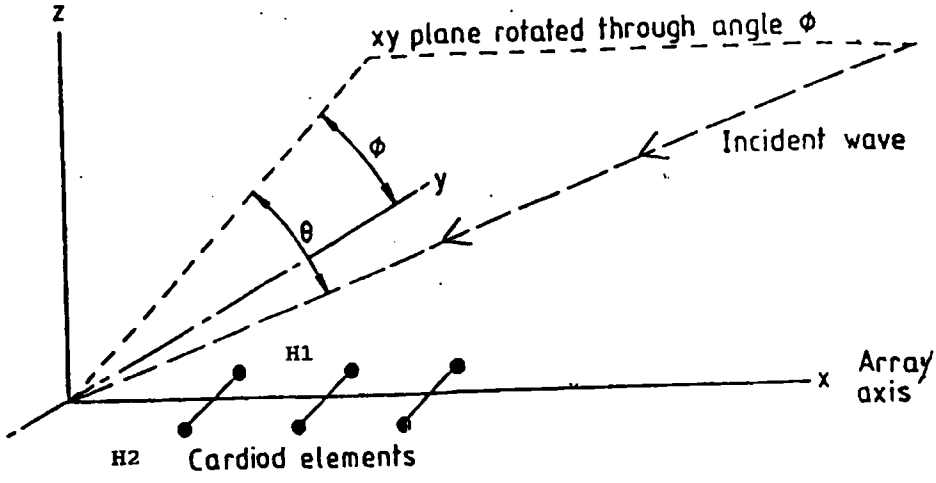

Fig 3.111 Co-ordinate System.

$$x\sin\theta \pm d/2\cos\theta\cos\phi.$$

The consequential phase changes are,

$$k[x(\sin\theta - \sin\theta_0)] \pm [(d/2\cos\theta\cos\phi + \beta]$$

$\sin\theta_0$ is the scan angle

β is the appropriate time delay.

Integrating over - L/2 and + L/2 after normalization yields the usual expression for a continous line array times the cardioid factor.

$$\exp\pm(j.k/2)(d\cos\theta\cos\phi + \beta) \qquad 3.111$$

For both the main beam scan angles and the cable twist with a fixed cardioid element separation distance d, the image rejection circuitry produces a maximum at some specific θ and ϕ. and lower elsewhere. Array hose constraints and cost effective solutions featured large in the consideration of setting some appropriate mean value for the networks and accepting that the receiving patterns would not meet the ideal elsewhere. More serious was the roll angle since this would be indeterminate over 2π as compared with a plus and minus 60 azimuth degree scan angle. The author's remedy to compensate for the cable twist was to distribute a number of cardioid elements around the circumference of a circle using small mercury tube gravity type switches to select an appropriate pair in the azimuth plane. The question was how many array pairs were the optimum and Fig 3.112 illustrates triple and quadruple array sets. Assume a plane wave incident on the 3 array geometry, then the condition for no-twist would be the full azimuth element separation. Clockwise

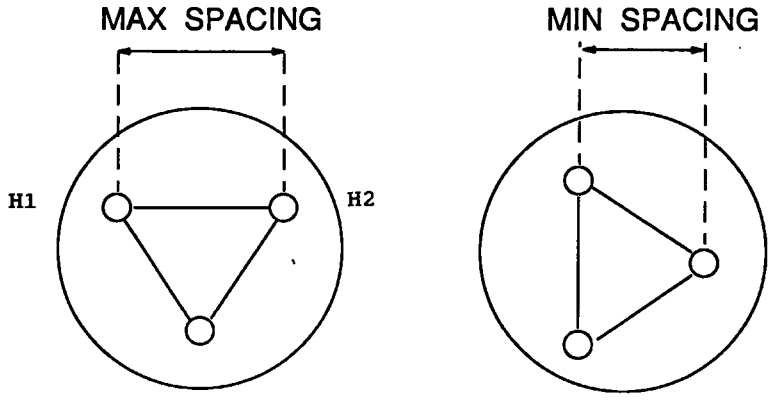

(a) TRIPLE ELEMENTS

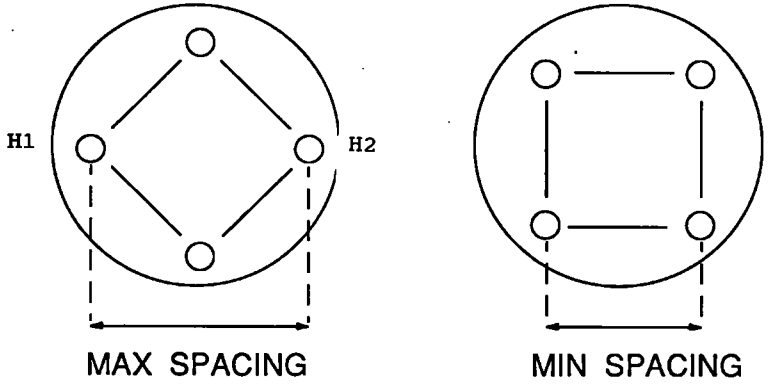

(b) QUADRUPLE ELEMENTS

Fig 3.112

EFFECTIVE SPACING OF MULTIPLE ELEMENTS

and anti-clockwise rotations would reduce the element separation distances by $\cos 30^0 = 0.866$ which corresponds to a variation of ±7% about the no-twist condition. On the other hand the ratios for 4 dual arrays is, $\cos 45^0 = 0.707$ i.e. ±17% which is two and a half times as great. In general for an odd number of arrays the ratio is, $\cos^{-1}(\pi/2n)$ and for an even number, $\cos^{-1}(\pi/n)$ The table below shows the effect on the discrimination factor for the two arrangements and is for a broadside direction with the dual element spacing set for $\lambda/5$, $\lambda/10$ and $\lambda/20$.

Spacing	Triple Cardioids	Quadruple Cardioids
	dB	dB
$\lambda/5$	20.8	13.8
$\lambda/10$	22.3	14.7
$\lambda/20$	23.6	15.0

It is evident that the triple form has a 7 dB advantage over the quadruple pattern and with fewer hydrophones and an effective utilization of 66 2/3 % as compared with 50 %. The more compact triple cardioid matrix also meant that there would be fewer switching operations, 6 double pole shifts per revolution compared with 8 and for a given mean spacing an additional prospect of some 10% less in the array hose diameter.

3.12 A comparison of the worst case reduction in array sensitivity in the broadside sensing direction compared with that of 2 x single element array output within the same hose diameter is as below.

SPACING	TRIPLE CARDIOIDS	QUADRUPLE CARDIOIDS
	dB	dB
λ/5	-0.7	-1.0
λ/10	-5.0	-5.8
λ/20	-10.0	-11.7

Thus contrary to expectations, increasing the number of dual elements does not necessarily improve performance.

3.13 As demonstrated above the port-starboard discrimination factor is given by:

$$D_r = \frac{[\sin\omega(\tau/2+\beta/2)]}{[\sin\omega(\tau/2-\beta/2)]}$$

Maximum discrimination is for,

$$\beta = \tau = \frac{d\cos\theta\cos\phi}{c}$$

and $\frac{\omega}{c}$ = k , wave number, when the numerator is,

$$= [\sin(kd\cos\theta.\cos\phi)] \text{ radians.}$$

d = cardioid element separation. 3.131

ϕ is the angle of cable twist.

The normalised amplitude in the unwanted direction of each cardioid element pair is,

$$E'_0 = \sin\left(\beta/2 - \frac{kd}{2}(\cos\theta\cos\phi)\right) \qquad 3.132$$

and this minimum value will vary over the range of the variables $\cos\theta$ and $\cos\phi$., the scan and twist angles. On space and cost grounds it was policy to minimize the number of delay /phase units and so an optimum value for β was needed. With a system of triple cardioid elements, the value of $\cos\phi$ varies between 1 and cos 30 degrees and that for the scan angle between 1 and cos 60 degrees so the strategy adopted was to selected the mean of the extremes with the possibility that the scan angle might be better slightly biased "off centre". That for the cable twist was:

$$\pm 1/2(1+\cos 30^\circ) \text{ or } \phi = 21.1^\circ$$

The above mean values of θ and ϕ determine the value of the fixed term, β.

The deviation between the new means of ϕ are the limits,

$$\pm (d/2)(1+\cos 30^\circ).$$

The effective spacing of the dual elements with twist correction is now,

$$d' = (d/2)(1+\cos 30^\circ)$$

The variation of $\cos\phi$ will be,

$$\cos\phi = (1+\eta) \text{ where } \eta \text{ varies between}$$

$$\pm[(1-\cos 30^\circ)/(1+\cos 30^\circ)] = \pm 0.072 \qquad 3.133$$

With this median value the deviation from the mean varies between the limits of,

$$\pm(a/2)(1-\cos 30^0),\ \cos\phi \text{ is always positive .}$$

$$\text{So } \cos\phi = \bar{a}(1+u) \text{ where}$$

u varies between the limits of,

$$\pm\frac{(1-\cos 30^0)}{(1+\cos 30^0)} = \pm 0.072 \qquad 3.134$$

So this recipe for the twist offset delay contribution was adopted. With a triple array the centres lie on a 4.0 cm diameter circle and allowing 1 cm annulus to accommodate the finite element size plus spacing to the hose boundary, an overall hose diameter of 7 cm was within the winch requirements.The size of suitable small gravity operated mercury switches presented no problem of containment within the hose volume. The following table lists the rejection ratio for these conditions over the 60 degree scan angle .

Back-to-Front Ratio in dB		
Frequency	Average over 60 Deg	Worst Case
kHz	dB	dB
1.5	-14.8	-9.5
2.0	-16.3	-10.8
3.0	-17.9	-12.1
4.0	-18.7	-12.6
5.0	-19.1	-12.9

The worst case values include a spacing error of 2 mm. Other probable errors that could occur could be in the time delay setting due to sampling rate errors and in the twist location due to the finite dual array switching. A comparison of the worst case reduction in array sensitivity in the forward sensing direction compared with that of 2 x single element array within the same hose diameter is as below.

Spacing	Triple Cardioids	Quadruple Cardioids
	dB	dB
λ/5	20.8	13.8
λ/10	22.3	14.7
λ/20	23.6	15.0

Element Sensitivity.

3.14 Each of the doublet positions makes its own individual contribution to the total array azimuth discrimination factor so it is required that the sum of the errors be within the allowed parameter deviations. This raised the question of a measure of the possible spread of differences in sensitivity between pairs of hydrophone outputs and the need to avoid the costly procedure of having to preselect N hydrophone pairs from a large manufacture's batch. An overall element sensitivity difference of 0.5 dB was the aim observing that this value would be more

variable than that of individual pairs. Suppose that two arrays of N single element hydrophones are made up from hydrophones chosen from a batch with sensitivities varying about a mean with a standard deviation $\sigma(dB)$.Then the expected difference for a single pair chosen at random would be $\sigma\sqrt{2}$ and an expected difference between the dual arrays of $[\sigma\sqrt{(2/N)}]$. Given the calibration of a batch of hydrophones, then by ranking in order of increasing sensitivity and selecting pairs with the least differences, the overall arrays errors should be further reduced. A sample of 20 hydrophones taken at random from a typical element batch were arranged to form 10 different dual element pairs and the array performance was computed using the pressure output levels which were summed and converted to dBs. For 10 different random selections the maximum difference was 0.53dB as shown below.

ARRAY OUTPUT	
(dB)	(dB)
(1) 25.94	(2) 26.17
(3) 26.43	(4) 26.14
(5) 25.95	(6) 25.94
(7) 26.26	(8) 26.47
(9) 26.30	(10) 25.96

It was therefore concluded that the problem of variations in hydrophone sensitivities was not likely to involve laborious selection of hydrophones and that at the worst a ranking procedure would be the most that was needed.

Tow Ship Noise.

3.15 The sum of the intensities of the locally generated noise fields relative to that of a distant target return, is a key parameter for both active and passive sonar detection. Masking self-noise sources may be generated by local vibrations or by flow noise at the line array boundaries while the surrounding noise field can originate from within the ocean or from the radiated noise of the tow ship. Increasing the DI of hull type sonars reduces the level of the ambient sea noise but not necessarily from sources such as propeller cavitation,flow noise and machinery. Typical self noise levels for Escort Ships at 20 knts is deep sea state 6 as is listed in the table below, observing that naval vessels are subject to continuous updates for remedial action.

FREQUENCY kHz	1.5	2	3	4	5
NOISE LEVEL dB(uPa/Hz)	67	63	60	58	56

For tow ship radiated noise, an expression due to Urick (1975) was used ,

$$SL = 60 \log K + 9 \log T - 20 \log F - 20 \log D + 35 \quad 3.151$$

In this empirical formula,

K = the forward speed in knots .

T = tonnage .

F = frequency in kHz .

D = distance of tow ship in metres .

Taking

K = 20 knots .

T = 500 tons .

D = 2000 m

The surrounding noise field values are as per the table below and are about the same as for the self noise of the hull sonar.

FREQUENCY kHz	1.5	2	3	4	5
NOISE LEVEL dB(uPa /Hz)	67	65	62	60	57

With regard to the above tow ship radiated noise values, a gain advantage of - 20 dB bistatic receiver side lobe reductions would apply. This represents the advantage of separating the receiver from the hull structure so that the internal platform noise sources are no longer an issue. In the computations of the array factor the common practice of plane wave inputs was assumed.The limit of the Fresnel distance regularly quoted is,

$$R_f = L^2/\lambda$$

At this range signals at the end elements are shifted 45^0 with respect to the centre element.

In general for a plane wave assumption ,

$$R > 4R_f = 4L^2/\lambda. \qquad 3.152$$

For the 30 wavelength array at 3 kHz the near field range extends to 1800 m. At lesser tow ship separation distances, within the near field, the spatial response discrimination and side lobe gains could be reduced but it was decided that there was a sufficient design margin to cope with any such degradation factors.Sea-noise limiting conditions with Escort Ships are a feature of low ship speeds.The DI for the hull-mounted sonar is say 24 dB, while that for the 30 wavelength line array with cardioid elements is 22 dB ,i.e, a 2dB disadvantage. A general conclusion was that the proposed line array would have real gains for tow ship radiated noise vs ship platform noise sources and be near equal for ambient noise backgrounds.

Flow Noise.

3.16 The receive-transmit transducers of a hull sonar are contained within a dome and every effort is made to obtain a smooth flow over its surface with more spacing to the boundary surface than is possible for a towed line array. A prominent source of self noise in the lower frequency towed arrays is that generated by fluctuating forces in the water flowing past the array hose and by vortex shedding from surface roughness features. Other local noise sources may be due to mechanically induced vibrations that can generate resonances in the hose wall and hydrophone mounts. At low tow speeds the flow pattern close to the hose surface is uniform and laminar, but as the speed increases the flow becomes unstable and shearing occurs causing eddies to form with local short time span

accelerations and de-accelerations that produce pressure fluctuations in accordance with Bernoulli's Law. The perceived frequency response of a hydrophone to these pressure variations is proportional to the corresponding Fourier component but, since it is not dependent on the compressibility of the medium, it does not propagate as sound into the far field, being described as "pseudo sound". Experimentally, it has been found that the flow phenomena can be described in terms of the Reynold's parameter where the viscosity term in a transition region gives rise to a velocity gradient normal to the boundary, the so called "boundary layer",within which the velocity declines from a maximum value of the tow ship speed to zero at the array surface. The critical Reynold's number is > 10^5 when the noise characteristics of the inner region are controlled by the local water flow near to the hose boundary while the outer region is dominated by eddies generated upstream. Dimensional analysis with a combination of dimensionless terms having well known names such as Strouhal,Reynolds,and Mach numbers provide tools for parameter formulation of flow noise. The pressure fluctuations radiate as quadrupole sources with a radiation efficiency which can be expressed as a function of the Mach number:

$$M = \text{Mach number} = \frac{U}{c}$$

defined as the ratio of

$$\frac{\text{Pertinent flow speed}}{\text{Acoustic sound speed.}}$$

Acoustic conversion efficiency =

$$\eta_{ac} = \frac{\text{Acoustic Power}}{\text{Mechanical Power}}$$

and,

$$\eta_{ac} \approx M^n$$

$$\eta_{ac} = \eta_{vib} \quad \eta_{rad} \qquad 3.161$$

= product of the Source and Radiation efficiencies.

The three prime forms of M^N acoustic sources are :

(1) Monopole = Volume expanders. n = 1

(2) Dipole = Vibrating body. n = 3

(3) Quadrupole = Free turbulence n = 5

A fleet speed of 20 knots was the aim.

At 20 knots = 10 m/s $M = 0.0067$

$$M^3 = 3\ 10^{-7}$$

$$M^5 = 1.3\ 10^{-11}$$

As a result of the low radiation efficiency only the very near flow noise sources would contribute to the hydrophone output noise. Low frequencies are generated by large eddies moving at a speed approaching that of the free stream velocity while the higher frequencies are generated by turbulence close to the hose boundary so that the consequential spread of velocities means that a given

pressure pattern will lose its coherence within a much shorter time interval than the individual disturbances. Below are some of the general flow noise attributes used to appraise the order of the flow noise levels since at this stage no real values applicable to the bistatic array were available.

(a) A flat flow noise spectrum was assumed up to a frequency of

$\omega = \omega_0$ and a decrease of - 9 dB/ octave for $\omega > \omega_0$.The transition frequency between the flat and sloping portion of the flow noise spectrum is given by fo = U / 5 d*. Here, U is the tow speed and d* is a so called displacement thickness of the boundary layer obtained from empirical data. The actual thickness is about 5 times this value.

(b) Neglecting the change in boundary layer thickness with velocity below $\omega = \omega_0$, the power spectrum noise dependence on tow speed would increase as the cube of the tow speed, a 9 dB increase in sound pressure level for a doubling of speed. For frequencies greater than fo ,the power spectrum level would increase as the sixth power of the tow speed.i.e for speeds greater than about 10 Knots: an increase in flow noise sound pressure level of about 1.8dB/knot.

While it was possible to establish trends there was sparse data on actual spectrum levels so these were referenced to low tow speed Seismic arrays with frequencies up to about a maximum of 1kHz. A suggested representative flow noise level for seismic arrays was 116 dB at 70 Hz and at 300 Hz it was 106 dB both ref ($\mu P_a/Hz$) as extrapolated to 15

knots. Adjusting for 20 knots and 3kHz gives a spectrum level of 78 dB which estimate was a matter of some concern since the 3kHz value compares with 60 dB for escort ship self noise. Other supplied data when extrapolated to 3000 Hz at 20 knots suggested a spectrum level of 65 dB, the general import being that the towed array active sonar signal-to-noise ratios at escort cruising speed could be dominated by flow noise and about equal to that of the hull sonars, para 3.15. It is also observed that peak values of the flow noise could register as active sonar false targets whereas the longer integration times for passive sonar smooth out such peak values. It was manifest that if the estimated values were real then a comprehensive restructuring of the array and deck handling gear would be needed for remedial action.i.e.:

(i) Increase the distance of the hydrophones from the hose boundary to take advantage of the fourth law decay of quadrupole sources.

(ii) Increase the size of hydrophones to several times the largest fluctuating wavelength at the flow noise frequencies. As the element dimensions in units of spatial wavelength become significant in terms of turbulent cell space the sensitivity to flow noise would be expected to decrease as a consequence of the integration process. It was also thought that the summed output of the array could further attenuate flow noise but attempts to allocate realistic values based on theory were not successful. Cognizance was taken that the estimated values had considerable scope for error as no provision had been made

for significant differences between the seismic and bistatic towed arrays namely:

(iii) Radiation efficiency and the fourth-power law decay of quadrupole sources in the extrapolation of the low operating frequencies to 3kHz with a different hose-hydrophone configuration. Also setting the value of the transition frequency was subject to arbitrary judgement.

(iv) If the hydrophones are uniformly sensitive to pressure around the surface of the hose, the instantaneous response will be the surface-average pressure,i.e. a function of the hose diameter.

General background data on the transition frequency point and spectrum levels refers to experiments with flat plates, hydrophones in rotating cylinders, and torpedo shaped bodies released from the bottom of a deep lake rising with increasing speed due to own buoyancy forces. Experiments by the author at the hydrodynamic facilities at Bath University to test the values were inconclusive due to the level of the system background noise. Some cause for optimism was subsequently provided by the author in an experiment in a canal with a towed single hydrophone in a hose type tube and later by more comprehensive sea trials during the development of the variable depth sonar version of the array. None of the sea trials vessels were capable of more than 14 knots so that the 20 knt estimates remained unresolved but the measured flow noise values at the lower speeds were below that from sea state 2 to 3 conditions. Extrapolation to 20knots of these real at-sea

measured values indicated an order less than the original estimated values.

The permissible roughness height before becoming significant as a noise source is approximately ,

$$h = 0.15 / V(k) \qquad 3.162$$

where h = roughness height in cm .

$V(k)$ = velocity in knots .

As the hose skin should be relatively smooth it would seem that noise due to hose surface roughness would be of a second order if the perturbations are contained in the laminar sublayer of the turbulent boundary layer. Attention was drawn to the need to avoid abrupt changes in the cross-sectional shape or area of the hose that could be significant sources of noise.

Coherence Factors.

3.17 The formulation of the bistatic line array relationships refers to plane-wave free field conditions with correlated signal wave fronts across the receiver elements. In real ocean environments the sampled acoustic field may be variable in both space and time as a consequence of refraction, reflection and multipaths along the propagation paths, It was thought that the longer dimension of the bistatic line array might be more responsive to these shifts in wavefront coherence than the hull planar receivers. Coherence here means the degree of similarity of the hydrophone outputs at any of two positions in the line array.The correlation coefficient ρ is a function averaging time T and delay time τ of all pairs elements

and is defined as equal to the normalised time average of the product of $s_1(t)$ and $s_2(t+\tau.)$

$$\rho(T.\tau) = \left[1/T \int_0^T s_1^2(t)dt . 1/T \int_0^T s_2^2(t)dt \right]^{1/2}$$

Array gain is related to the cross-correlation coefficients of the signal and noise taken between all elements of the array in pairs.

$$AG = 10 \log \left[\sum_{j=1}^{N} \sum_{i=1}^{N} s_i s_{j(\theta_s)ij} \right] / \left[\sum_{j=1}^{N} \sum_{i=1}^{N} n_i n_{j\theta_n)ij} \right] \qquad 3.171$$

The above equation represents 10 times the log of the ratio of the sum of the coherence matrix for input signal to the corresponding sum of the matrix for background noise. If both signal and noise are random, then there is no array gain.If the signal is completely coherent and the noise is random then the array gain is a maximum. In the absence of real data for line arrays of a length similar to the proposed bistatic receiver in a number of representative environments, analysis of this feature was a best guess guided by theory. An exponential form is generally assumed and with N large the array gain approaches a value of,

$$AG = \frac{(1+C)}{(1-C)}$$

where

$$C = Cs(\omega) = \exp\left(-\alpha\omega\frac{d}{\lambda}\right) \qquad 3.172$$

d = spacing between elements.

ω = radial frequency .

and $0 \leq Cs(\omega) \leq 1$

α is an adjustable parameter.

As an example of the order of possible correlation losses, an array of 100 elements at 1 kHz with Cs = 0.95 had an array gain of 15 dB which is 5 dB less than that with perfect correlation.This value would be further reduced if the noise had a coherent component. Two reference papers,by B.Scholt and R.Thiele, provided some background material about the measured time-space dependent properties of a typical far field shallow water transmission channel in the frequency range under consideration. The data exhibits a range, frequency and depth dependence with only a small influence of the rough sea surface on the spatial coherence. Much stronger factors were the sea bed structure and the spatially varying sound speed field. As the range increased,the cross-correlation index improved as is to be expected where the number of contributing modes is reduced. It was understood that the measurements were a worst case scenario and the 0.95 value at the long ranges would be a pessimistic value allowing for the relatively shorter

towed line array and the type operational environments envisaged for a bistatic operation ; this being the case, it was taken that deviations from the straight line geometry would form the largest contribution to any significant correlation losses. Here again deviations from a straight line in terms of length/ wavelength should be much less with the very much shorter bistatic array than that of the longer low frequency arrays, even allowing for differences in wavelength. Subsequent sea trials with the variable depth sonar line array in a number of different environments appeared to support this view.

Tow Cable Telemetry.

3.18 A preliminary specification for the active role of the towed line array was for operations with centre frequencies within the band of 2 kHz to 4 kHz, noting that this would be subject to review when the design stage had been progressed. The source wave forms would also be finalized when the types of hull sonars were known but it was expected that a high profile transmission could be a chirp signal with a frequency sweep of between 100 and 200Hz for 1- 2 s. Scan angles for each side of the array would be plus and minus 60 degrees and a total of some 96 beams would be formed, one set of 48 beams port and starboard with spatial widths varying from 1.8 degrees broadside to 3.6 degrees. Some thought had been given to extending the total scan angle to 160 degrees but was held in abeyance pending a closer examination of the cost effectiveness. A goal for the side lobes was -25 dB lower than the main lobe response. The original intention was

that after filtering and signal conditioning, including dynamic range compensation, each of the two-element outputs at each sensor position would be transmitted via the tow cable link to the surface ship. Within the array hose three switched hydrophone discs are required at each of the N hydrophone positions with a separation of 4.0 cm. Two cardioid networks form the image rejection process and the outputs are summed with the appropriate delays to obtain the port and starboard beams, Figs 3.51 and 3.61. The two cardioid base signals would require the insertion of two delays, two polarity reversals, two summations, followed by 2N weighting. Each of the port-starboard dual element cardioids networks has time delays of:

$$\Delta t = x_i(t + \tau_{i,\theta,\phi}) \qquad 3.181$$

$x_i(t)$ = Signal at ith element.

$\tau_{i,\theta,\phi}$ = Time delay at ith element in θ direction and with a ϕ roll angle.

The signal delay time between the cardioid elements is:

$$\tau_c = \frac{d\cos\theta\ \cos\phi}{c}$$

$$c = 1500 m/s.$$

$$d = 4cm.$$

$$\tau = 4\ 10^{-2}\ \cos\theta\ \cos\phi\ /c\ s$$

$\cos\phi$ is the roll contribution set to a mean of 21 degrees.

and $\cos\theta$ is here set to a mean of 40 degrees.

For a $\pm 60^0$ scan angle $\tau = 1.88\ 10^{-5}$ s .

At 3 kHz = 0.056 cycles.

For a $\pm 80^0$ scan angle $\tau = 10^{-5}$ secs.

At 3 kHz = 0.044 cycles. 3.182

The mean angles are arranged to even out the errors to allow for a single cardioid network to be used over the scanned arc. It has been observed earlier that error values in the signal time delays between cardioid pairs degrade the image rejection ratio with the appearance of a back lobe response in the cardioid pattern. The discrimination ratio is :

$$\eta_r = \frac{|[\sin\omega(\alpha+\beta/2)]|}{|[\sin\omega(\alpha-\beta/2)]|}$$

Relative to the array axis the two orthogonal elements at d/2 will have phase differences of $\alpha = \pm kd/2\ \cos\theta\ \cos\phi$.

β is the inserted time or phase delay network.

Max image rejection is when $\alpha = \beta/2$

The two conditions for error are:

$$\alpha > \beta/2 \quad \text{and} \quad \alpha < \beta/2.$$

The above related to errors in the time delay $\tau/2$. 3.183

Expanding the discrimination expression in terms of sin and cos terms then equating and converting to tan functions:

(i) $6\alpha > \beta/2$: $\beta/2$ less than optimum.

$$\text{Tan}\,\alpha = (\eta+1)/(\eta-1)\ \text{Tan}\beta/2$$

(ii) $\alpha < \beta/2$: $\beta/2$ greater than optimum.

$$\text{Tan}\,\alpha = (\eta-1)/(\eta+1)\ \text{Tan}\beta/2. \qquad 3.184$$

For a fixed mean scan and cable twist correction value of $\beta/2$, $D_r = \eta$ is the image rejection ratio.

Variations in the image rejection ratio relate to the shift in $\text{Tan}(\alpha_0 \pm \Delta\alpha)$.

Allow a worst case of a mean scan angle of 41 degrees for an extension of the scan angle to 160 degrees with a mean twist angle of 21 degrees, the cardioid element spacing delay time is:

$$\tau = 1.88.10^{-5} = 0.056 \text{ cycles} = 20.6 \text{ degrees.}$$

Above is when $\alpha = \beta/2$.

With $\beta/2 < \alpha$ and a - 10 db image rejection, the total shift is 9.6 degrees and at - 6dB it is 13.4 degrees, a difference of 3.8 degrees.

When $\beta/2 > \alpha/2$, the total shift for - 10 dB is 6.2 degrees and for - 6dB it is 36 degrees. 3.185

The total time delay corresponds to 126 degrees and for $\alpha < \beta/2$ a -10dB image rejection gives a difference of 9.7 degrees while that for - 6dB is 13.6 degrees, a difference of 3.8 degrees accounting for a -4dB degradation in the

port- starboard discrimination. With $\alpha > \beta/2$ a -10 dB image rejection the shift is 6.3 degrees while for -6dB it is 36.6 degrees a much less sensitivity to error.

3.19 There are three variable divisions that separate the array sensor processing chain; the portion within the hose volume, the tow cable telemetry bandwidth which limits the rate of information transfer, and the remainder contained aboard the tow ship. A simple beam-forming network is the time-domain-delay-sum beamformer where to form a beam in any azimuth direction the output from the cardioid networks is delayed by an integral multiple of the sensor position spacing over (N(b) -1) intervals, where N(b) is the number of beams. Associated with each beam direction is a set of integers, ki = 1.....M. After the delay operation, the sensor signals are multiplied by real weights, Ai,and summed.The essence of this type of beam former is:

$$S_0 = \sum_{0}^{N-1} x_k(t + \tau_{k,\theta,\phi}) \qquad 3.191$$

x_k is the signal received out of the kth network.

$\tau_{k,\theta,\phi}$ is the time delay inserted in the kth output to form a directional beam at angle θ_n.

N beams require N^2 delays.

Once the beams are formed then a simple addition shows that an analogue type of amplitude modulation information transfer would be within the tow cable bandwidth. Lumped constant LC delay lines were at one time a common technique but have been mostly replaced by analogue systems based on bucket brigade and other various charge

transfer devices. Modern digital beamformers would provide a considerably more flexible technique but at the price of an increase in telemetry bandwidth.To obtain a measure of the system arrangement assume the following:

Number of element positions in the array = 60

Mid acoustic frequency = 3 kHz.

Angle of steer ± 60 degrees.

Dynamic range = 60 dB

The dynamic range requires at least 10 bits to hold the amplitude of the signal in binary form. At 3kHz the wavelength is 0.5 meter and the array element spacing would be slightly less than 1/2 this value.

Minimum spacing for a steer angle θ is,

$$\tau = \text{spacing} \cdot \frac{\sin\theta}{c}$$

$$= 0.25.0.87/1.5.10^3 = 144\mu\ s$$

Sampling at the Nyquist rate, f_s = 13.9 kHz.

i.e say 4.6 times that of the signal frequency. 3.192

For sonar waveforms with frequencies confined to; $(\omega_0 \pm \pi\omega)$, the information content of the signals is contained in the complex envelope and need only be sampled at the bandwidth frequency. By demodulating the waveform to base band and then sampling the sin and cos components,i.e. quadrature sampling, a worthwhile reduction in the sampling rate is obtained. Another technique which produces an approximation to samples of the complex envelope is termed delay sampling. A phased array may also be realised by using the Fast Fourier Transform where again both the in-phase and quadrature

signals are needed in order that all N beams can be formed independently. Thus when a plane wave of frequency $\omega_0/2\pi$ is incident upon an array of elements spaced (2 a) apart along the line, the output from the nth element is:

$$x_n = V_0 \exp[j\omega_0 t + jnk2a\sin\theta]$$

θ is the incident angle , and k the wave number.

To produce co-phasal signals a phase shift of β_n must be inserted between elements.

$$V_s = V_0 \sum_{n=0}^{N-1} [\exp\{j\omega t + jn(k2a\sin\theta - \beta_n)\}]$$

For equally spaced beams $\beta_n = 2\pi n/N$. hence,

$$V_s = V_0 \sum_{n=0}^{N-1} [\exp(j\omega t + jnk\sin\theta][\exp -j2\pi n/N]$$

$$= \sum_{n=0}^{N-1} x_n \exp -j2\pi n/N \qquad 3.193$$

The latter of course, is the Discrete Fourier Transform (DFT) and can be realised by using Fast Transform algorithms. What the above is intended to demonstrate is that there are a number of ways in which sampling and beam forming can be achieved and the pace at which the integated-circuit technology is proceeding with ever-increasing through-put rates, reduction in sizes, improved reliability, and at reduced costs, means that there is considerable scope for design ingenuity in partitioning the required processing between the hose volume and aboard ship for a match with an expected telemetry bandwidth of 7M bauds. In the case of the VDS development, after beamforming, the more versatile digital data transmission was used with a sampling frequency of 12 kHz with beams as

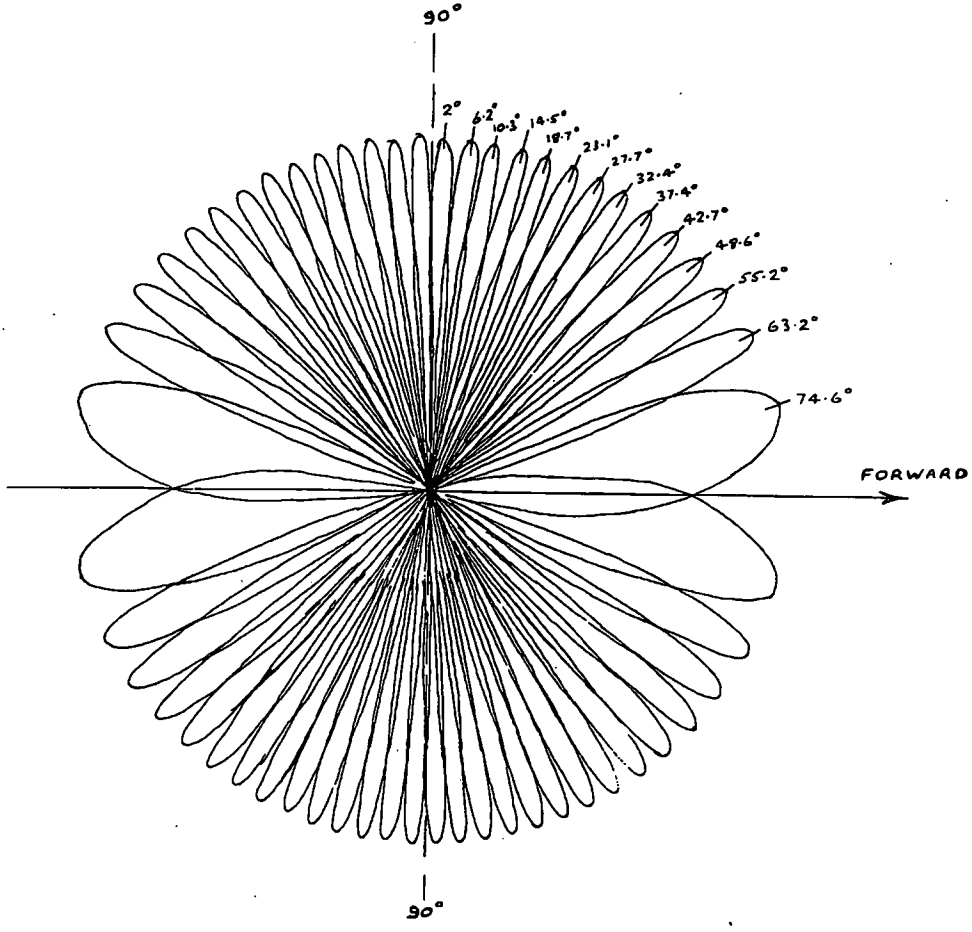

Fig 3.191 VDS Receiver Beam Pattern.

in fig 3.191.In order to preserve the beam forming information in digital form for telemetry, the number of cardioid elements was halved with an array length of 7.0 meters and to compensate for the increased beam width, interpolation was included to improve the spatial discrimination.

Comment.

3.20 A summary of the conclusions reached at this stage of the system research was that a more effective use of the high power acoustic source of the large Escort sonars could be achieved by the addition of a relatively small satellite ship supplied with a towed line receiver in a bistatic configuration, fig 1.31 Section 1 and fig 3.11.The escort sonar would maintain its normal surveillance role. A shortfall at this stage of the system research for an additional concept of a Variable Depth Sonar for small ships was the lack of an adequate acoustic source.The developed technology for the towed receiving arrays in being for seismic exploration and naval uses, did not have the capacity to discriminate between the port/starboard reception of signals, false targets and interference sources. Resolving the image ambiguity with the naval long range low frequency towed arrays requires a ship manoeuvre which is not acceptable for the shorter range active sonar reception roles.To obtain the essential image rejection capability,it is necessary to add additional orthogonal elements in the port/starboard azimuth direction. Analysis of the basic parameters for a towed line array with an equivalence to the source ship

sonar receiver, led to a linear line array 30 wavelengths long,15 meters at 3 kHz, the medium frequency band of the intended source sonars, with equally spaced elements at 0.48λ and Dolph-Chebyshev shading for a designed -30 dB with an expected -25 dB side lobe level. Continuous sensing over a 120 arc centred at broadside on each side of the array is arranged by overlapping beams at a minimum 3dB point. Use of closely coupled separate line arrays was not a practical answer for a small ship operations and replacing each line element with a velocity or pressure gradient hydrophone combination to form a cardioid space response pattern was examined and not deemed to be a satisfactory solution. The proposed approach is to use two pressure sensitive elements coupled to a cardioid network with the intent of attaining a minimum image rejection ratio of 10 dB over the scanned arcs, port and starboard, figs 3.41 and 3.51. The separation distance of the orthogonal elements determines the forward sensitivity of the two-element array and this distance is controlled by the maximum array hose volume and amount of tow cable that a small ship handling system could accept.To offset any cable twist, triple cardioids are arranged in a 4 cm circle within a 7 cm diameter hose and one set of cardioid elements is always maintained in azimuth within a ± rotation of 30 degrees by gravity activated mercury switches at an off-set of 21.1 degrees, fig 3.112. Estimates and sample measurements in the spread of element sensitivities predict that the selection of hydrophones for the cardioid networks was not likely to be a problem.

Over a frequency range 2 to 4 kHz with real fixed time delays the target value of 10 dB image rejection should be achieved over the whole of the frequency band. The combined Directivity Index for the cardioid element array was 22 dB which compares with say 24/25 dB for the planar array of the hull monostatic sonar.The hose diameter and tow cable lengths would be within the allowed capacity of the deck handling equipment for a small ship. The length of the tow cable is determined by the critical tow depth, down to 200m, over the operational speeds and/or the distance at which tow-ship radiated noise is reduced to an acceptable level. At the highest cruise speed this length is a nominal 2000m; at the lowest speeds the tow distance would be shorter with some loss in ship-noise rejection. The array itself would be neutrally buoyant with a 100m rope tail to maintain a constant drag force along the line and depth and temperature sensors would be provided. The ambient noise background of the proposed array is some 18 dB better than that of the bench-mark monostatic sonar and should this form the major contributor to the signal background noise then there are prospects for substantial gains in a passive listening band from say 500 Hz to 3 kHz as compared with a hull sonar. Not resolved was the level of the near field phenomenon of flow noise which, based on estimates made from sketchy data, suggested that it might be a dominant array background at a common Escort Ship cruising speed of 18 knots. Flow noise is usually considered as a prominent low frequency phenomenon, where theory predicts that hydrophone sensitivity to flow noise

decreases with increasing element size and the separation distance from the hose boundary. What has not been determined is the space wavelength relationship between the long low wave numbers and those at the active sonar frequency where the extrapolation process takes no account of any element size filtering effect.Theory also shows that the turbulence creates a distribution of quadrupole sources which are poor radiators of sound and this suggests a fourth law decay with distance. What was needed to resolve the issue was some experimental evidence which was not forthcoming at this stage. Considered but not pursued, was the possibility of using the unconnected dipoles to provide discrimination against vertical ray arrival angles and array gain against noise: the directive properties of the source sonar in the vertical plane, say 10 to 15 degrees, would of course limit the number of possible multipath returns.There is a strong case for digital beam forming on the grounds of design flexibility and the inclusion of adaptive processing but although feasible within the developed technology, the apportionment of processing units between the array hose volume and in-board of the ship involves detailed studies of possible system architectures that would satisfy the maximum tow cable data channel capacity. To positively complete this research required that an experimental array be produced including the features described above with measurements of performance in real acoustic environments and data on the unresolved values for flow noise. A model of the cardioid element arrangement was tested in the acoustic

facilities at Bath University and the measurements substantiated the doublet element performance forecasts. With the development of the commercial Variable Depth Sonar by British Aerospace,the system design of which was based on the bistatic sonar research with a suitable towed acoustic source developed by the company, at-sea tests of the proposed tow line array parameters with checks on the error analysis became possible, Sections 5 and 6.The Variable Depth Sonar is now a world-market product.

REFERENCES.

LINE ARRAYS.

Anderson V.C. Digital Array Phasing. J.Acoust Soc Am. 32, pp 867 -870.1960.

Andrew R.N. and Bull P.W. Hydrodynamic Behaviour Of Towed Array Sonars. Jour of Naval Science. U.K. Vol 14 No3 pp188-198.

Antenna Engineering Handbook. (Ed, R.J Johnson And H.Jasik) McGraw-Hill Sec Edition.

Aupperle. F.A and Lambert. R.F. Acoustic Radiation From Plates Excited By Flow Noise. Jour Sound and Vibration 26, pp223-245 .1975.

Burdic. W.S. Underwater Acoustic System Analysis. Prentice-Hall N.Y.1984.

Butler D. Beamforming with a Distorted Array. Adaptive Methods In Underwater Acoustics.(Ed H.G Urban) pp 469-475D. Reidel Pub Co 1985.

Conference Proceedings. Array Signal Processing.. Unv of Technology Loughborough.UK. Inst Ac 16 and 17 May 1985. (Papers on Array Signal Processing.)

Conference Proceedings. Signal Processing In Underwater Acoustics. Inst Ac 21 and 22 May 1980. (Papers on Beamforming.)

Conference Proceedings. Transducer Arrays And Array Processing. Inst Ac 13 and 14 Dec 1978. Unv Birmingham.U.K.

Curtis T.E and Ward R.J. Digital Beamforming For Sonar Systems. Proc I.E.E. Vol 127. Pt F, No 4 pp 257-265.1980.

Eliseevnin V.A. Operation of a Horizontal Line Array in a Water Layer in the Field of Narrowband Noise Signal. Sov.Phy. Acoust. 30(2). March-April 1984. Transl Am.Inst of Phy.1984.

Ferla C.M and Porter M.B Tow-Depth Selection For Horizontal Arrays. SACLANTCEN CP-38 NATO UNCLASSIFIED.

Griffiths. J.W.R. and Stocklin.P.L. (Eds) Signal Processing. Proc of the NATO Advanced Study Inston Signal Processing. Academic Press .London. 1973.

Haddle G.P. and Skudrzyk E.J. The Physics of Flow Noise. J.Acoust. Soc.A.46 130-157 . 1969.

Hansen R.C. Aperture Array Theory. Vol 1 Microwave Scanning Antennas (Ed R.C Hansen,) , N.Y Academic. 1966.

Harris F.J, On The Use Of Windows For Harmonic Analysis With The DFT. Proc I.E.E.E Vol 66 No1 pp 51-83

Johnson M.A. Phased-Array Beam Steering By Multiplex Sampling. Proc I.E.E.E. Vol 56 No 11 pp 1801-1811,1968

Kaye. G.W.C.and Laby. T.H. Tables of Physical And Chemical Constants. 14th Ed Longman. London, 1973

Kerr A.J. and Curtis T.E. A Fast 32-Bit Complex Vector Processing Engine. Pro Int of Ac Vol 11 Pt 8 1989.

Kinsler. E.L , Frey. R.F , Coppens A.B, Saunders. J.V. Fundamentals of Acoustics. J.Wiley. 1982.

Knight W.C, Pridham R.G and Kay S.M. Digital Signal Processing For Sonar. Proc of I.E.E.E. Vol 69 No 11 pp 1451-1506 Nov 1981.

Krauss J.D. Antennas. McGraw-Hill 1950.

Lamb.H.B. Hydrodynamics. Cambridge University Press. Sixth Edition. 1932.

Lighthill M.J. On Souund Generated Aerodynamically: General Theory.Proc.Roy. Soc. (london) A221, 564-587 (1952) and A221, 1-32 (1954).

Ma M.T. Theory and Application of Antenna Arrays. Wiley ,N Y 1974.

Maranda B. Efficient Digital Beamforming In The Frequency Domain. Jour,Ac,Soc,Am 85(5) pp 1813-1819. Nov 1989

Morgan D.R. Two Dimensional Normalization Techniques. I.E.E.E Jour of Ocean Engineering .OE-12 No1 pp130-142. Jan 1987.

Morse.P.M. Vibration And Sound. Am Inst Of Physics. !976.

Nielson R.O. Sonar Signal Processing. Artech House London. 1991.

Owsley N.L. Overview of Adaptive Array Processing. Adaptive Methods In Underwater Acoustics (Ed H.G.Urban) pp 355-374 D. Reidel Pub Co. 1985

Pridham.R.G. and Mucci. R.A. Digital Interpolation Beamforming For Low-Pass And Band-Pass Signals. Proc I.E.E.E Vol 67 6 June 1979 pp 904-919.

Rabiner.L.R ,McClellan J.H, and Parks.T.W. FIR Digital Filter Design Techniques Using Weighted Chebyshev Approximation. Proc I.E.E.E Vol 63. 4 APR 1975.

Ross. D. Mechanics Of Underwater Sound. Chp 6.6 Pergamon Press.1976

Scholz B. Horizontal Spatial Coherence Measurements With Explosives And CW-Sources In Shallow Water. Nato Advanced Study Institute On Signal Processing, With Emphasis On Underwater Acoustics. (SACLANT) Pt 3 Aug/ Sept 1976

Schwartz. M.B. Information Transmission, Modulation,and Noise. McGraw-Hill.NY.1959.

Skolnik M.I. Introduction To Radar Systems. McGraw-Hill.N.Y 1962.

Skudrzyk.E.J and Haddle. G.P. Noise Prediction In A Turbulent Boundary Layer By Smooth and Rough Surfaces. J Acoust Soc Am 32 pp 19- 34,1960.

Steinberg B.D. Principles Of Aperture And Array System Design. John Wiley & Sons 1975.

Strasberg M. Nonacoustic Noise Interference in Measurements of Infrasonic Ambient Noise. J.A.S.A Am. 66(5) Nov 1975.

Thiel R. Measurement Of The Weighting Function Of The Time-Variant Shallow Water Channel. Nato Advanced Study Institute On Signal Processing, With Emphasis On Underwater Acoustics. (SACLANT) Pt 3 Aug/ Sept 1976.

Urick. R.J. Principles Of Underwater Sound. McGraw-Hill.1975.

Urick.R.J. The Coherence Of Signals, Noise And Reverberation In The Sea. Report NOLTR 72-279 U.S. Naval Ordnance Laboratory. Maryland Nov 1972.

Van Trees H.L. Detection,Estimation,and Modulation Theory.Parts I,II,III .John Wiley & Sons. 1971.

Weston D.E. On The Problem Of Maximum Array Directivity. Proc of Inst Ac Vol 7 Pt 4 1985.

Winder A.A. Sonar Systems Technology. I.E.E.E Trans Sonics And Ultrasonics Vol su-22 No 5 pp 291-332 Sept 1975.

Section 4

Contents.

Section.4

BISTATIC PERFORMANCE ANALYSIS.

Section 4 FIGS.

Section 4.

BISTATIC PERFORMANCE ANALYSIS.

Basis for Analysis.

4.1 A salient issue of the analysis for the performance of the two receivers was testing for an equivalence in target detection and functional outputs, monostatic and bistatic, observing that the projector beam pattern and choice of waveform is set by the source sonar. Deriving the relevant criteria involved examining the influence of the factors listed below.

(a) Description of the bistatic geometry.

(b) Means of acquiring information at the bistatic receiver on transmission start time and platform separation distances.

(c) Comparison of mono/bistatic target strengths for different target orientations.

(d) Equivalence in propagation losses.

(e) Features of the additional sonar range detection region.

(f) Doppler shifts over the paths, Source/Target/Receiver.

(g) Ratio of mono/bistatic resolution cells.

(h) Variation of reverberation scattering coefficients with different source /receive scattering angles.

(i) Waveforms differences at the bistatic receiver.

(j) Implications for matched filtering.

(k) Interference from external source emissions.

(l) Role functional outputs .

(m) Man/Machine features.

Of these, the target strength variation has already been discussed and it is observed that for passive reception the system reverts to a monostatic configuration.

4.2 In essence, the maximum possible information transmission through an ideal channel is expressed by Shannon's equation:

$$I = 2BT \log_2 (1 + S / N) \text{ bits.} \qquad (4.21)$$

where S /N is the signal power to noise ratio ,T is the interrogation time, B is the bandwidth.

For a sonar array of n elements each forming a separate independent channel, again in an ideal medium,

$$I = 2BT\, n \log (1 + S / N) \text{ bits.} \qquad (4.22)$$

The BT product and waveform is set by the monostatic source sonar transmissions while the S/N ratio at the receiver is a function of the target returns and the ensuing spatial and time signal processing with a bistatic geometry. A comprehensive performance model at the receiving ship would have three prime stages:

(c) An assessment of the acoustic channel information at the input and output of the sensors arranged in terms of an assigned signal excess for detection.

(d) Computation of the competing background together with the processing gains for an allowed false alarm rate and a measure of the features that should provide an optimum cost effective operational performance.

(e) A sea test of the key parameters to validate and allow for corrections to the system performance estimates.

Excluded is a final stage which arranges the format of the

exchange of information for integration into an Escort's total weapon capability.

The substance of the above interrelated features may be expressed by:

$$I - N > DT \quad dB$$

I = Signal information content.

N = Unwanted background.

DT = Detection threshold i.e. that required at the operator man-machine output as compared to the Recognition Differential (RD) which is the end of the processing chain.

The left hand side of 4.23 refers to the diverse fields of physics that describe ocean acoustics as applied to functional values in space and time and referenced to the benchmark sonar. The right hand side relates to the conditions necessary to make effective use of the processed information, particularly for detection, with an operational value assigned to the cost of accepting alternative choices of target or false alarm.

4.3 A prominent consideration in the analysis was the pertinence of the assumed ocean acoustic environments since real measurements would only be obtained at a demonstrator stage. As previously stressed in section 2, considerable resources have been, and are being devoted to sonar environmental predictions directed mainly at monostatic sonar systems: mathematical modelling, physical ocean measurements, assembly of semi-empirical formula and at-sea system trials. The validity of this data bank for bistatic sonar applications depends first, on the degree

of relevance of the knowledge for the specific functions, and second, on how to affirm the role of different mechanisms from the crude parameters available for the major ocean areas. A major difference with bistatic propagation is that the source-target-receiver paths are dissimilar as are the projector-receive beam patterns and the incident and scattering/ reflection angles, figs 4.31 and figs 4.32. A plausible solution for the important transmission loss parameters was obtained by postulating a continuance of the source propagation conditions to an additional forward distance equal to the one-way monostatic range. Gains and losses in the bench mark sonar performance would be reflected by comparable variations in the assessed performance of the bistatic sonar.In a bistatic geometry there is a grey area between the angles where the dominant forward energy is the direct path propagation to those angles where the received energy is due to scattering. This point is discussed later.

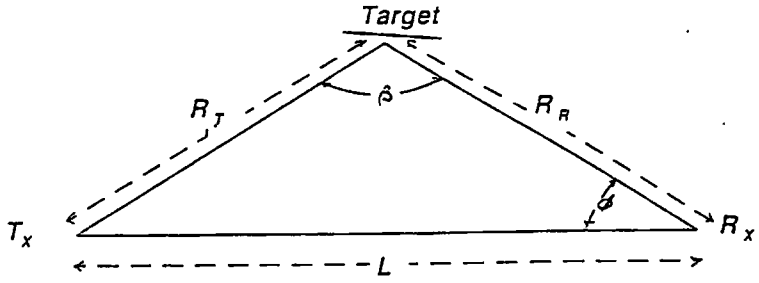

Fig 4.31 Bistatic Geometry

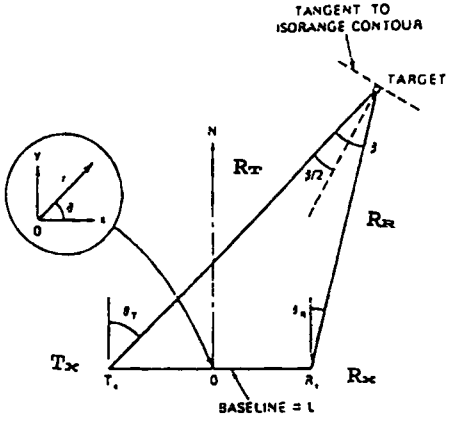

Bistatic Sonar.North coordinate system.

Fig 4.32

Sonar Equations.

4.4 The basis for setting the equivalence between parameter values for the two receiver systems was an assembly of the relevant Sonar Equations, the rationale for which is well described by Urick in his several editions of Principles of Underwater Sound. Simple forms of sonar parameters in units of dB can be arranged to express an equality between a desired signal input and interference backgrounds, noise or reverberation. The principle adopted was to employ wherever possible the most robust environmental models available, taking note of possible alternatives: random fluctuations are included in the assessment of the rate of false alarms. As a prime measure of transmission loss the ubiquitous spherical spreading law was used at the expected source mid frequency of 3 kHz. The basic active sonar equation for monostatic sonars in dB is,

$$SE = EL - BL - RD \qquad (4.41)$$

where

SE = signal excess .

EL = target echo level .

BL = background level , noise or reverberation.

RD = recognition differential at the processor output.

Echo levels are referenced to processing through a matched filter with a bandwidth B = 1/T, T = effective pulse duration, and the background spectral level,BSL, is the power sum of reverberation and noise spectral levels in the receiver beamwidth averaged over the same T s. Expanding the individual terms.

(i) Echo Level

$$EL = SL + TS - 2TL \qquad (4.42)$$

where,

SL = axial source level (dB ref 1 μ Pa at 1m).

TS = target strength (dB).

2TL = two way transmission loss (dB).

and,

$$SL = 171 + 10 \log W + DI \qquad (4.43)$$

W = acoustic power of projector in watts.

DI = transmit directivity index. (10 log DIR).

To allow for the different types of transmit waveforms and signal processing available to the source sonars it is often useful to develop the sonar equations in terms of energy flux. The intensity of a time varying plane wave is expressed by,

$$I = 1/T \int_0^T \frac{p^2(t)}{\rho c} dt. \qquad 4.44$$

when over the pulse interval T the intensity I is,

$$I = \frac{E}{T}.$$

The energy source level in Joules , ESL,

and the source level SL are related by,

$$SL = 10 \log E - 10 \log T. \qquad 4.45$$

Energy Spectral Density Level is ,

$$E = \int_0^\infty E(f) df. \qquad 4.46$$

With a spectral flat bandwidth B ,

$$E = E(f_0).B$$

f_0 is the energy spectral density at the centre of the signal band .

As above, the echo level is usually referenced to a matched filter output of bandwidth = (1 /T), the reciprocal of a pulse length of T seconds.

(ii) The transmission loss has three geometrical spreading components:

Spreading Loss.

$$TL = 10 \log \frac{I_0}{I_r} = 10 \log r_r^n$$

r^0 = no loss: propagation in a tube.

r^{-1} = 10 log r: propagation between parallel planes.

r^{-2} = 20 log r: free field. 4.47

At long distances the curvature of expanding wave fronts is negligible so that over a limited area the waves are essentially planar.

Absorption Term.

$$p = p_0(r)\exp(-\alpha r)\exp[j(\omega t - kr)]$$

α is the Absorption Coefficient in nepers/m.

In units of acoustic intensity = $\exp(-2\alpha r)$.

The reduction expressed in dB is:

$$10\log[\exp(-2\alpha r] = 20\alpha r.\log e = 8.7\alpha r = \alpha r \text{ dB/m}.$$

An aproximate value for "a" in dB/m, over the frequencies of interest is:

$$0.01 f^2 r.10^{-3} \qquad 4.48$$

f is in kHz , r is in yds. or 0.9144 a in m

[1] Other intensity loss terms could include:

Boundary Loss .

---

1 Absorption coefficient is as given in Urick 1975.

Absorption at the Sea Floor.

Scattering Loss.

Discontinuities in the Medium and Roughness Features.

(iii) Noise Limiting Background.

$$BL = BN + 10 \log Bo. \qquad (4.49)$$

BL = noise background level. (dB ref μ Pa.)

BN = noise spectrum level in the receiver beam. (dB ref μ Pa/ Hz)

Bo = noise bandwidth at the processor output. Equal to 1/T the inverse pulse duration, for a matched filter processing.

Depending on the local environment, noise within the medium may be described in terms of equal density over space,the usually description of ambient noise, or with a variable density in space and time that may include a plethora of ship and other man-made sources. Ambient noise at the higher frequencies generally originates from wind-generated sea-surface sources while at low frequencies in open seas it is commonly due to radiations from distant surface shipping. Self noise is associated with sources within the platform, machinery noise, propeller cavitation and flow noise which are speed dependent ; these components add incoherently. In multiple beam sonars the signal-to-noise ratio refers to the levels within the same beam.In general ,

$$BN = 10\log\{10^{ambient/10} + 10^{self/10}\} \qquad 4.410$$

Both components ref $1\mu Pa$ in a $1Hz$ band.

and are generally referred to as " Equivalent Plane Wave " levels.

In a line array the in-beam ambient noise rejection is ,

Omni-directional noise level in the surrounding water - Array Gain .

Array Gain = 10 log [(S/N Power in Single Beam) / (S/N Power in a Single Element)] (4.411)

If the noise is incoherent between elements then ,

AG = 10 log n where,

n = the number of array elements. (4.412)

An alternative omni-directional noise rejection measure is the Directivity Index ,DI, particularly for planar arrays having two dimensional discrimination where the vertical beam width is around 10 to 20 degrees. With an isotropic noise field , and an array of directivity DI , BN = the Isotropic Noise Level - DI, the level after beam forming for a noise bandwidth of 1 Hz. With ship sonars, self noise is a major background noise and it is common practice to add the directivity index, DI, to the measured level to obtain an Equivalent Isotropic Noise for compatability with Ambient Noise Levels. Ambient noise levels in the ocean are summarized by G Wenz(1961) and Urick (1984).

Bistatic Geometry.

4.5 Target input data with a monostatic active sonar is obtained from comparable two-way travel times so that the target location and movement direction relative to the platform may be derived directly at the source platform using the delayed time, receiver pointing angle and measurements of the Doppler shift. Data extraction is straightforward since it is referenced to a single platform polar co-ordinate system. Bistatic operations on the other hand have separated source and receiver platforms at different locations with their own range and Doppler shifts that are added to any target movement. At a first inspection, the elliptical geometry of a bistatic system appears to be straightforward, but combinations of the formulae lead to complex relationships which are best expressed by shifts in the elliptical parameters. The precision to which measurements of the required data inputs is obtained at the receiving platform is a key feature for an equivalence with the monostatic sonar parameters. A co-ordinate base line is the separation distance between the source and receiver, L, figs 4.31,4.32, and information on target position is the sum travel time from source-to-target-to-receiver with an azimuth reception angle. Knowing the start time "t_o", a measure of L, is the time difference between transmission start time and the direct path travel time from source to receiver. One solution to obtain the time "t_o" at the receiver was to activate the transmission start times and intervals by a clock aboard the source ship synchronised

with a clock aboard the receiving ship, but it was realized that this scheme would remove a great deal of the flexibility of the Escort Ship in the transmit sequences for duct, bottom bounce and convergence zone propagation modes, and when shifting patrol areas and in manoeuvres when tracking a detected target.It might be acceptable to broadcast mode changes by radio coded clock messages. A more complete solution is to provide a dedicated acoustic communication link, a simple version of the underwater telephone, using a higher frequency source as a transmitter within the hull sonar dome and one of the hydrophones as a receiver within the towed array .This would allow for a continuous data link in some form of pulsed code mode format to the receiver platform for updating signalling start times and changes in waveform modes, ship speed and Doppler data etc. Similarly, one of the hydrophones in the array would be used to measure the direct path propagation loss which would allow the two ship separation distance to be adjusted. The common source sonar transmissions would normally insonify a wide forward arc hence, knowing the transmission start time "t_o", and the delay interval, L/c, the separation distance L is available. This range with adjustments to allow for changes in acoustic propagation conditions would be maintained as near constant as ship positioning allowed. It is observed that the range errors would be greater than those of the monostatic sonar and part of a trials programme would be to obtain data for an assessment of target range accuracies and Doppler data. Three parameters

are needed to describe the azimuth source-target-receiver triangle instead of the two, L = 0, in the polar geometry of a monostatic sonar.

(1) The distance measured by a bistatic sonar is:

$$S = R_T + R_R$$

$$\text{Bistatic Travel Time} = [R_T + R_R]/c$$

(2) The two ship separation distance, L.

Equals the direct path time x c.

(3) The receiving ship target look angle is ϕ relative to the base line, L.

Applying the law of cosines to the geometry.

$$R_R = \frac{[S^2 - L^2]}{[2(S - L\cos\phi)]}$$

and,

$$R_T = \frac{[S^2 + L^2 - 2SL\cos\phi]}{[2(S - L\cos\phi]}. \qquad 4.51$$

The intersection of R_R and R_T locate the target on the surface of an ellipsoid of revolution which degenerates into an ellipse when confined to the azimuth plane, figs 4.31 and 4.32. Unknown at this time were the possible combined effects of the various alternative paths from the source to the receiver.Thus the strongest arrival would be the direct path from source to the receiver followed by the target path with routes that could include reflections from the sea surface and seabed. The shifts in path frequencies, Doppler, will be functions of the platform transmit and receive velocities in the direction of the

propagation paths together with that of the target and scatterers.

$$f_T = 1/\lambda[d/dt(R_T + R_R + \text{Target shift})]. \qquad 4.52$$

Allowing that the platform separation distance between the two receivers is maintained constant, or varies slowly between transmission sequences, and that there is parity between the active sonar parameters, then for equal transmission loss it was considered plausible to use these conditions as a basis for the analysis of bistatic range detection prospects.

4.6 The goal was for a bistatic range equal to twice the monostatic range with equivalent transmission losses.

(1) TL(m) = TL(T) +TL(T) (dB ref 1 m)

TL(m) = 40 log R(Tm) + 2 aR(Tm)

(2) TL(B) = TL(T) + TL(R)

TL(T) = 20 log R(T) + a R(T)

TL(R) = 20 log R(R) + a R(R) (4.61)

TL(m) = monostatic transmission loss to 50% probability detection range .

TL(T) = source- to-target range loss , bistatic.

TL(R) = target-to-receiver range loss, bistatic .

In a comparison of parameter values between the monostatic and bistatic systems it is the differences and not the absolute levels that matter bearing in mind that the real performance of the Escort Ship sonar would have been already established at-sea. For equality.

$$TL(T) + TL(R) = TL(m).$$

$$[20\log R(T) + \alpha R(T)] + [20\log R(R) + \alpha r(R)]$$

$$= 40\log R(m). + 2\alpha R(m) \qquad 4.62$$

In equating propagation losses out to equal distances the geometrical spreading loss is a dominant term to a point where the attenuation, which is a constant times range, commences to be the more prominent loss function. Of two sonars with the same frequency, but with different spreading losses for similar propagation conditions, then the one with the lesser geometrical spreading, 20 log R, would have an increased intensity at a similar range and so may be taken as a first order combination for parity. The monostatic sonar provides detection out to the range R (m) hence of specific interest is the condition $R_R < R_T > R_m$.

Ratio of Spreading loss power ratios

$$\frac{(R_m)^4}{(R_T^2 R_R^2)} = k \qquad 4.63$$

When the total bistatic range = the two way monostatic range, the attenuation losses are equal.

So the sum of the spreading losses, R_T, R_R,

is a measure of equality.

Difference relationships for reverberation and noise at a range where the bistatic range to target is equally divided are:

$$\Delta_1 = \left(TL_T - \frac{1}{2}TL_m\right) + \left(TL_s - \frac{1}{2}TL_m\right) \qquad 4.64$$

and

$$\Delta_2 = (RL_b - RL_m)$$

where Δ_2 = reverberation level differences .

Also

$$\Delta_3 = (N_b - N_m) = \text{noise level differences .} \qquad 4.65$$

(1) Noise Limiting

$$\begin{aligned} &SE(m) - SE(B) \\ &= [\ TS(m) - BL(m) - RD(m)] \\ &- [\ TS(B) - BL(B) - RD(B)] \end{aligned} \qquad (4.66)$$

TS = target signal at the receiver.

SE = signal excess.

BL(m) = hull sonar background noise level.

BL(B) = bistatic sonar background noise level.

(ii) Reverberation Limiting Background.

$$\begin{aligned} &SE(m) - SE(B) \\ &= [\ TS(m) - RL(m) - RD(m)] \\ &- [\ TS(B) - RL(B) - RD(B)] \end{aligned} \qquad (4.67)$$

RL = Reverberation Level.

A typical RD, Recognition Differential,for a monostatic sonar is 12 dB.

The target and reverberation range of the bistatic sonar can be at a greater source range than that of a corresponding monostatic sonar and hence the difference between the footprints of the two receiver beams is a key parameter for the azimuth intercept area.

The proposed parameters for the bistatic system are:

Monostatic Range = 22 km (20.11 kyd).

Bistatic Sum Range = 44 km (40.22 kyd).

Platform Separation. = 33 km (30.16 kyd).

Ellipse Eccentricity,= 0.75

Max Broadside Range = 14.6 km (13.16 kyd).[2]

(4.68)

Possible Man/ Machine differences for the two systems are treated separately so in the first instance the outputs of signal and noise are referenced to the input to the display.

4.7 FIG 4.71 shows the transmission range contours for the above parameters where the source ship and receiver are the two co-ordinates of an ellipse.

The equation of an ellipse in rectangular co-ordinates is :

$$\frac{x^2}{a^2}+\frac{y^2}{b^2} = 1$$

The shape of the ellipse is expressed by.

$$y = \pm b\sqrt{1-\frac{x^2}{a^2}}$$

$$x = \pm a\sqrt{1-\frac{y^2}{b^2}} \qquad 4.71$$

2a is the major axis and 2b the minor axis.

The equation for a circle.

$$= x^2+y^2 = a^2 \qquad 4.72$$

---

2 In the NATO navies it is common for ranges to be in Kyds.

BISTATIC TRANSMISSION CONTOUR

Fig 4.7 I

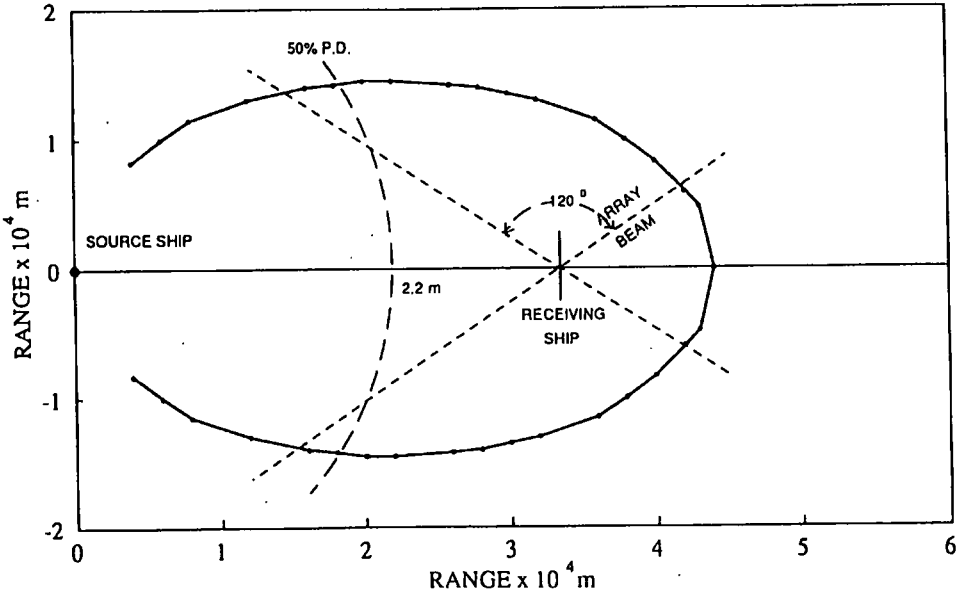

MONOSTATIC DETECTION RANGE = 2.2×10^4 m

SEPARATION DISTANCE BETWEEN PLATFORM = $2.2 \times 3/2 = 3.3 \times 10^4$ m

ARRAY RECEIVER BEAM = $\pm 60^0$ BROADSIDE

MONOSTATIC SHIP TRANSMIT/RECEIVE ~ 300^0

The ratio of the distance between the foci, L, to the length of the major axis of the ellipse 2a = S, is the eccentricity e, which is a measure of its shape.

Denoting the foci separation range by 2c = L.

and 2a = sum bistatic range = S, then by definition:

$$e = c/a = L/S$$

$$c < a \,, \quad e < 1 \,.$$

$$c^2 = a^2 - b^2 .$$

When,

$$e^2 = \frac{a^2 - b^2}{a^2} = 1 - \frac{b^2}{a^2}$$

Hence

$$e = \sqrt{(1 - b^2/a^2)} \text{ and } b/a = \sqrt{(1 - e^2)} \qquad 4.73$$

As eccentricity e approaches zero, L decreases and the sonar surveillance area approximates to a circle: as L increases, the ratio b/a decreases, and the broadside sonar area tends to zero.The setting for L is a compromise between range and area gains.It is required that:

$$\frac{R^4}{R_T^2 R_R^2} = 1 \qquad 4.74$$

The bistatic range equation is related to the corresponding monostatic range equation by,

$R_T + R_R = 2R_m$ and $R_T^2 R_R^2 = R_m^4$

By letting the product of the sonar terms in the full sonar equation, source level,receiver gain, target strength, noise and system losses be a constant, then the received signal power is:

$$S/N = \frac{k}{R_T^2 R_R^2}$$

The term k is the bistatic sonar constant.

S / N = signal-to-noise power at ranges R_T and R_R. 4.75

When R_T and R_R are changed to polar co-ordinates,

(r, θ) fig 4.32

$\sin\theta = y/r$: $\cos\theta = x/r$.

when $y = r \sin\theta$ and $x = r.\cos\theta$.

$$\theta = \tan^{-1} y/x \; : \; r = \pm.\sqrt{x^2 + y^2} \qquad 4.76$$

$$R_T^2 R_R^2 = [r^2 + L^2/4]^2 - r^2 L^2 \cos^2\theta \qquad 4.77$$

In a bistatic geometry constant S/N contours are not collinear with constant range sum contours, as for the monostatic sonar, but are instead described by Ovals of Cassini. Cassinian ovals are defined as the loci of all points P for which the product of R_T and R_R have a constant value α^2. For a fixed source level, as S/N decreases or L increases the ovals shrink, finally contracting to two locations around the source and receiver positions. The point at which the oval splits into two parts at some specific value of S/N,is the lemniscate. When L = 0, this is the monostatic sonar case where the ovals become circles. The curves,Fig 4.72 for different levels of required S/N ratios, show that the region between the transmitter and receiver accounts for most of the useful surveillance area, with the stern section in the direct source transmission path. Allowing a medium range for the monostatic sonar of 22 km , the attenuation constant, a, at 3kHZ is 0.17 so that TL(m) = 174 + 0.17 (2 R) x 10-3

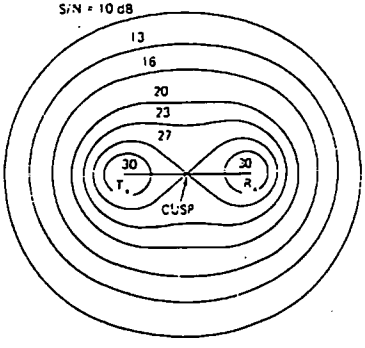

Contours Of Signal-To-Noise Ratio.

Fig 4.72

= 174 + 7.48 = 181.5 dB, when for equality,

$$TL(T) + TL(R) = 181.5 \text{ dB}. \qquad (4.78)$$

Choosing a Tx-Rx separation distance of 1.5Rm = 33 km then, $\sqrt{2}L/2 = 23.3km$ and S/2 = 22 km and so the contour approximates to an ellipse and the propagation losses would be similar to the 12dB contour of fig 4.72. Allowing a further 4dB loss for the display then on the model assumptions a proposed platform separation distance of 1.5 Rm appears to be a reasonable compromise for both broadside sonar area and S/N ratios.The source ship would continue with its normal wide angle active sonar search role with the satellite ship at an ahead position. Emphasis is given to an optimum broad side area detection vs range noting the 120 degree cardioid limits and the blanking out from the direct source path in the stern directions: the source ship forward detection arc would be effective in this region. Adding extra bistatic platforms was not fully explored beyond observing that an effective placing appeared to be on the port and starboard quarters of the monostatic ship at a range within the monostatic sonar 50% probability of detection range contour. The major axis of the ellipse describing the transmission contour is then rotated by 90 degrees from the forward geometry so that the direct source pulse arrival instead of being in the stern arc of the array is now in the broadside beam direction. This orientation suggested that increasing the scanned arc from 120 to 160 degrees might be cost effective. Part of the blanking range on the port-side arc would again be under partial surveillance by

the hull sonar.In setting up the equality relationships it is reiterated that the source levels are equal and the summed bistatic propagation loss is equated to the monostatic two way loss. The features of consequence are the dependence of surveillance area on signal to noise ratio, the platform separation distance, and constant S/N contours are not collinear with constant range sum contours.The conditions for equality assumed a constant noise limiting background but for a reverberation background the scattering cell size also varies with its position on the range contours. [3]

3 The formulations of the sonar bistatic geometries were adapted from those for Radar. A useful summary of the latter is provided by M.C. Jackson (1986).

Signal Processing.

4.8 The types of transmitted waveforms used by a typical hull sonar, are variants of Pulsed CW and Pulsed Frequency Modulation, set to provide

Range Resolution → 1 / Bandwidth.

or Doppler Resolution → Bandwidth.

In some role environments,it is the procedure for hull sonars to transmit a sequence of the two waveforms.

(i) Echo Length = $\frac{2L\sin\theta}{c}$ ↔ Broadband Pulse

(ii) Echo Doppler = $\frac{2f_0\dot{R}}{c}$, ↔ Long CW Pulse.

(iii) Doppler Spread = $\frac{2f_0\dot{\phi}\sin\theta}{c}$ ↔ CW Pulse.

(iv) Echo Stretch = $\frac{\Delta(L\sin\theta)}{L\sin\theta}$ ↔ Two Broadband Pulses. 4.81

(v) Echo Shift = ΔR and $\Delta\theta$ ↔ Target movement in range and azimuth bearing.

where ;

θ = Incident angle to plane wave front.

$L\sin\theta$ = Resolved length of target.

$\dot{R}$ = Range Rate.

ϕ = Relative aspect of incident sound on line target.

$\dot{\phi}$ = Bearing Rate .

The Required information potentials of the source waveforms are:

(i) Detection of Target.

(ii) Measurement Accuracy.

(iii) Ambiguity, Position and Movement.

(iv) Resolution Between Adjacent Targets.

Detection of the target is a function of the S/N ratio and the characteristics of the competing background.It is

independent of the waveform and depends only on the ratio of total energy to noise power.Shape of the waveform,assuming an adequate signal to noise ratio is available, is important for purposes of accuracy, ambiguity and resolution. Significant measures for comparison of operational parameters between the monostatic and bistatic receiver systems are any differences in the matched filter outputs for the two transmitted waveforms, CW pulse and Linear FM (Chirp pulse). Target range relative to the bistatic receiving ship is computed from the differences in the time arrivals of two source paths, the direct path and a bistatic sum path. A spatial position is obtained directly from the target bearing.

Signal processors may be formed in the time or frequency domains:

$$s(t) = a(t)\cos\omega_o t.$$

By definition the Fourier Transforms are:-

$$F|a(t)| \leftrightarrow A(f) = \int_{-\infty}^{\infty} a(t)\exp(-j2\pi ft)dt.$$

$$F^{-1}|A(f)| \leftrightarrow a(t) = \int_{-\infty}^{\infty} A(f)\exp(j2\pi ft)df.$$

and by Parsaval's Theorem

$$\text{Energy , } E = \int_{-\infty}^{\infty} |a(t)|^2 dt = \int_{-\infty}^{\infty} |A(f)|^2 df \qquad 4.82$$

All modern sonars make use of either time or spectral analysis for matched filter processing where the time delay and Doppler measurements are obtained by cross

correlating segments of the incoming signal with a set of stored references each of which is a replica of the transmitted wave. Replica correlation is an optimum provided that the background is equivalent to uniform additive Gaussian noise and so is related to the nature of the background inputs and the effectiveness of the normalisation process. Sufficient references are needed to allow for the total range time delay intervals and the spread of target Doppler. When a detection is obtained the elapsed time is an estimate of target range R which together with a match with one of the target Doppler filters provides a target information cell. Signal input bandwidth is set to B Hz and the ratio of input/noise to output signal/noise is B to 1/To or BTo. An FM processor would have a gain of 10 log BT while that for a CW Doppler processor is 0 db. The FM waveform gives better range discrimination, (1/B), while the potential for a CW pulse is for improved Doppler discrimination with slow moving targets. Errors in determining the Doppler contributions from the two moving platforms and the blanking overlap of target-direct transmission are two of the several differences that arise with the two ship bistatic geometry.

4.9 The output from the beamformer for the FM Chirp waveform would be processed through a comb of matched filters with pulse compression followed by detector, averager and threshold units for some predetermined RD output level.

Signal pressure is p(t) with duration To.

Energy source level, ESL , = 10 log E.

$$E = 1/\rho c \int_0^T p^2(t)dt$$

Intensity source level SL = 10 log I = 10 log E/ To.

ESL = SL + 10 log To.

Spectral density of E(f) is.

$$E = \int_0^\infty E(f)df.$$

$= E(f_0)B$ for white noise.

Energy spectral density at centre of signal band B = $E(f_0)$. 4.91

The transmitted waveform for the linear FM compressed pulse signal can be expressed as:

$$f(t) = A(t)\cos[\omega_0 t + 1/2.\mu t^2] \quad -To/2 \leq t \leq To/2.$$

$$= 0 \text{ elsewhere.}$$

μ = rate of radian frequency sweep.

μt = swept spectrum bandwidth, radians per sec.

A matched filter is the time reverse of the signal input with an input response of h(t).

$$h(t) = \sqrt{(2\mu/\pi)}\cos[\omega_0 - 1/2.\mu t^2] \quad -To/2 \leq t \leq To/2$$

$\sqrt{(2\mu/\pi)}$ is a factor for unity gain.

Filter output is obtained by convolving f(t) and h(t).

$$g(\tau) = f(t)h(\tau - t) \qquad 4.92$$

The output of the matched filter with pulse compression is required to produce a single target return that will enable near equal range targets to be resolved, the ultimate being an impulse function. Matched filter

detection of the linear FM chirp pulse is a sin x/x amplitude response, with corresponding side lobes. Use of appropriate weighting of the spectral response, as for arrays, can reduce time-side lobe levels at a cost of increasing the spread of the main lobe. It is observed that any additional measurement errors associated with the bistatic system,in both range and Doppler, would be added to those of the ambiguity function. The magnitude of the ambiguity function, ref Woodward (1953), is given by:

$$|X(\Delta t, f_d)| = (T_0 - |\Delta t|)\ \frac{\sin M}{M}\ \cos\left[\left(\omega_0 + \frac{\omega_d}{2}\right)\Delta t\right]$$

$$\text{where } M = (T_0 - |\Delta t|)\ (\omega_d - \mu\delta t)/2 \qquad 4.93$$

In general it refers to the combined correlation functions between a signal input and a replica of the transmitted waveform with the addition of time and frequency shifts based on best information of target returns. When normalized by $|X(0,0)|^2$, the volume is equal to unity and the effective area is a measure of the combined resolution properties of the input signal.The function may be represented as a series of surface areas containing time-frequency plots with a peak value, Dt = 0 , fd = 0. i.e coincidence values. When two targets at different ranges and moving at different velocities have the same value for their ambiguity functions then the positional features of the targets cannot be resolved; the higher the resolution errors the greater the uncertainty.The cosine function is the carrier term the phase of which changes rapidly with Dt. The remainder of the expression is the ambiguity function. Figs 4.91 and 4.92 show a typical

rectangular CW pulse frequency spectrum and its ambiguity diagram and fig 4.93 is the ambiguity diagram for a FM waveform as below.

For $\omega_d = 0$ the function reduces

to the auto- correlation of the signal, s(t).

By symmetry $X(f_d, \Delta t) = X(-f_d, -\Delta t)$

$$X(f_d, \Delta t) = \int_0^T f_{.d}(t)\ f_{.d}(t+\Delta T)dt. \text{ and,}$$

$$X(f_d, 0) = \int_0^T f(t)^2 \cos\omega_d t\ dt$$

For a maximum $\Delta t = 0$, $f_d = 0$ = signal energy. 4.94

Clearly for conditions where fd is known accurately, the time resolution is controlled by 1/B independent of pulse duration,To. Similarly when the target delay t_d at $\Delta t = 0$ the Doppler shift can be resolved to 1/To. A common arrangement for a monostatic sonar is to connect each receiver beam output to a number of tuned correlators, the other functional input being a range of replicas of the expected target signals. In operational roles both platforms will have similar forward velocities, but the angles on the bow of the directed transmission to the target which is required for extracting target Doppler, will vary with the bistatic angle: the combined platform frequency shifts should however be about the same as that of a related hull sonar.In practice it is possible that a number of the individual correlators could be replaced by a single unit operating on a time compression basis by sampling the signal and its replica at the Nyquist

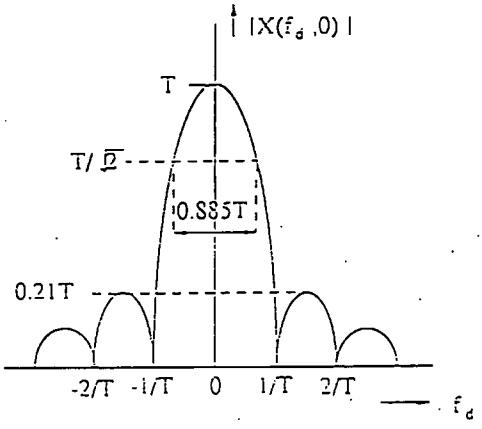

Fig 4.91 CW Pulse. Ambiguity Envelope Function.

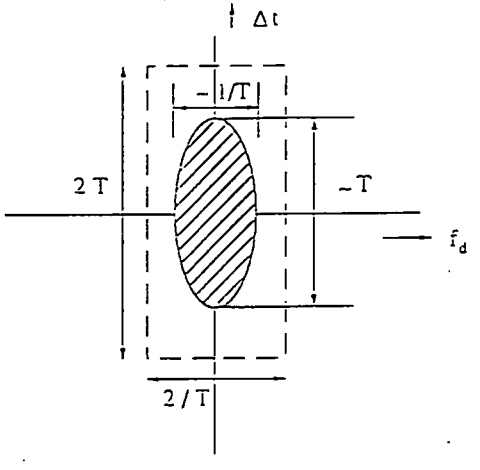

Fig 4.92 CW Pulse Ambiguity Contour Function

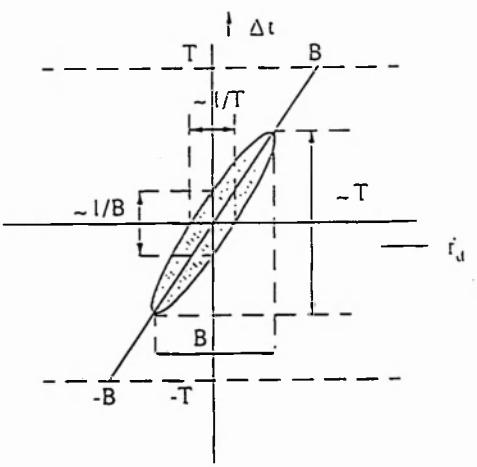

Fig 4.93 Ambiguity Function, Chirp signal.

sampling rate. Each output is fed to a threshold limiter; when the threshold is exceeded this is recorded as a best estimate of the true range velocity and course of a target. An FM compressed pulse has the potential advantage of better range discrimination.

4.10 In the forward arcs the source beam is near omni-directional and all waves over time intervals where R(T) + R(R) is a constant will arrive at the receiver at the same instant of time. These points are on the surface of a ellipsoid for volume returns or an ellipse for surface scattering and progression of the wavefront across the receiver beam intercept area is set by the intercept angles of R(T) and R(R), fig 4.101.There are two significant variations as compared with the monostatic geometry both due to the angle of the path of the transmitted pulse across the receiving beam.The leading edge of a pulse of duration To will arrive at the edge of the receiving beam at t_1 and leave the far edge of the receiving beam at t_2. If the crossing time is greater than $t_1 + T_0 < t_2$ then the full energy of the pulse is available for integration at the receiver. If however the leading edge of the pulse crosses the far edge of the receiving beam before the full pulse width has entered the beam then there will be loss of signal/noise ratio.The characteristics of the return may be summarized as below.

A rise in level at the pulse arrival time, t_1 with
full energy level at $t_1 + To$ at the end of the pulse.
Full value over the beam for travel time $t_2 - To$.
The level commences to decrease at a time
where the pulse leaves the far edge of the receiving beam, $t_2 - To$.
and ceases at t_2.
If however the pulse travel time across the beam is less than To,
then the amount of the pulse length that contributes
to the target energy and scattering return is set
by the beam dimension travel time. 4.101

With a monostatic sonar the transmitted pulse traverses the same path as the returned signals so that there is a progressive insonification of the information cells with the same range increments. From fig 4.101 it is observed that the time-insonification of the receiving beam depends on its mean angle relative to the transmission wavefront. As an example, at the mid point where R(T) = R(R) = R the volume of expansion along the ellipse b axis is:

$$v_b = \partial b / \partial t.$$

At the mid point $R^2 = b^2 + (L/2)^2$.

$$v_b = \partial b / \partial t = \frac{R}{2b.\partial(2R)/\partial t}$$

$$= R\frac{c}{2b} = \frac{c}{2\sin(\theta_R/2)} \qquad 4.102$$

θ_R is the beamwidth of the receiver.

Let Hb be the broadside height of the contour of the common source/receive surface then:

Fig 4.101 Bistatic Pulse Geometry.

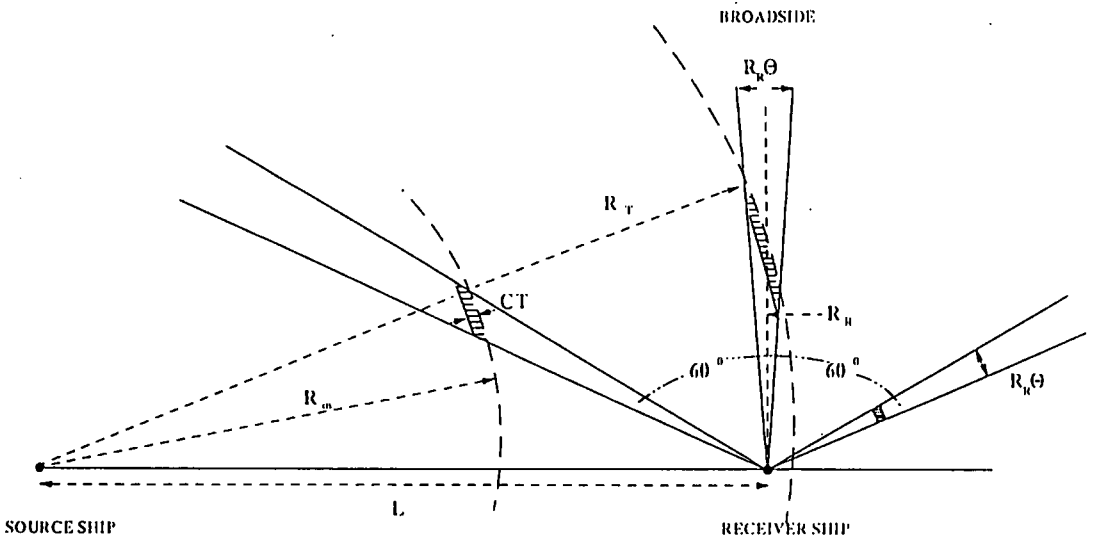

L = Separation Range

R_m = Monostatic Detection Range

R_T = Transmission Range

R_R = Receiver Range

$R_R\Theta$ = Across Beam Range at Broadside

Θ = Beamwidth, radians

CT = Transmission Pulse Length

T_o = Pulse Interval

S = Two way Monostatic Transmission Loss

$= R_T + R_R$

C = Velocity of Sound

Rise time for $To > t_2 - t_1 = H_b / v_b$.

$$v_b \sim c/2.\mathrm{Sin}(\theta_2/2)$$

The frequency band Δf for the rise time is.

$$\Delta f \sim 1/(t_2 - t_1) \sim \frac{c}{H_b 2\sin(\theta_2/2)} \qquad 4.103$$

If Δf is much greater than the frequency band of the transmitted pulse then there is no distortion of the wave form. With $To < t_2 - t_1$. $\Delta f < 1/To$ then, depending on the shape of the common area, there could be scope for considerable distortion.The differences are range and angle dependent with the forward scan angles approaching the monostatic geometry while at broadside the time rate of the insonification of the receiving beam, short range to the longer range,is a function of the bistatic angle. A shortfall with a line array is the lack of vertical directivity so that the receiver is open to multiple paths in various receiver beams, fig 4.102 What this demonstrates is that the attributes of the received energy with a bistatic sonar are functions of the receiver beamwidth, pulse length and orientation of the propagation and receive paths. The target processing would be constrained to a cell size 1/B but the differences in propagation paths could mean that the normalisation arrangements need to be tailored to the scan angles to allow for the more variable conditions.

4.11 At transmission, a conventional hull sonar mutes the receiver to a minimum close range of more than $\frac{1}{2}cT_o$ m in order to protect the receiver against the immediate intense field around the source ship. With the bistatic

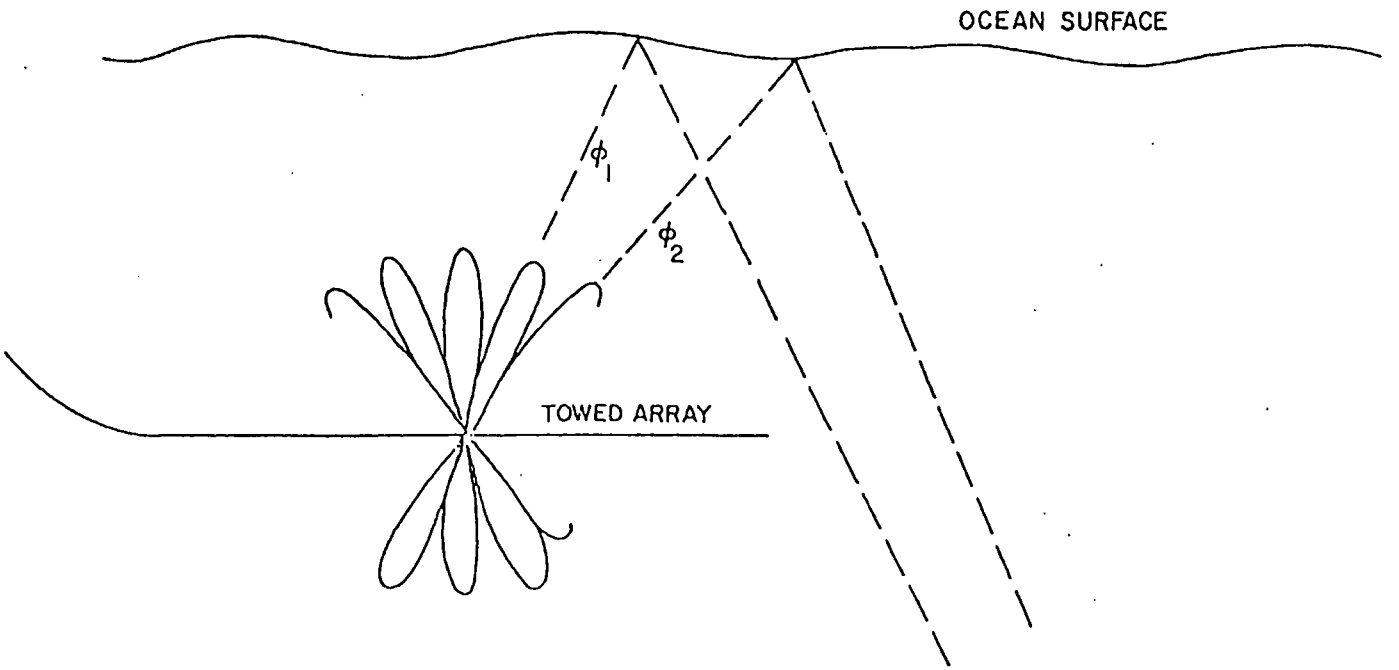

Fig 4.102 Multipath Reception.

geometry and an omni-directional source this is not needed, Fig 4.31, but a new situation is a range time overlap at the receiver between the direct path and a near range bistatic target return. The longer the effective pulse length the more drawn-out is the range at which a target return would compete with the direct path input. Assume all ray paths are straight lines, no changes in sound velocity in either the vertical or horizontal directions,then the propagation path at plane boundaries would continue forward at an angle equal to that at incidence.The sequence of arrivals at the receiver would be a direct path followed by a succession of boundary paths.

Time of arrival of direct path distance X is.

$$T_d = \frac{X}{c}$$

Time of arrival of first reflection is.

$$T_{b1} = \frac{2[(X/2)^2 + Z^2]^{1/2}}{c} = \frac{[X^2 + (2Z)^2]^{1/2}}{c}$$

and in general.

$$T_{bn} = \frac{[X^2 + (2nZ)^2]^{1/2}}{c} \qquad 4.111$$

Z = boundary depth , c = velocity of sound.

The equations for the times of arrival at the bistatic receiver as a function of distance X may be expressed as:

$$T_d - \frac{X}{c} = 0$$

$$T_{b1}^2 - \frac{X^2}{c^2} = \left(\frac{2Z}{c}\right)^2$$

and in general:

$$T_{bn}^2 - \frac{X^2}{c^2} = \left(\frac{2nZ}{c}\right)^2 \qquad 4.112$$

Arrival times as a function of distance, range and depth are equations of hyperbolae and a full expression would include additional terms for the propagation losses, reflection at angles of incidence greater than the critical angle and scattering losses. Boundary reflected arrivals would be at steeper angles than the direct path as shown in fig 4.102, and so with a line array could be intercepted by different azimuth beams. The direct path would be the first to arrive and continue to be an input to the receiver over the transmission pulse period so that a bistatic target return within any part of the same time interval will be subject to blanking: the extent of the blanking range interval is a minimum in the forward travel direction, a monostatic geometry, increases as the stern arc is approached, and worst if pointing at the source which fortunately is of least operational interest.

Equating ellipse receiver range time with the direct path.

$$(R_T + R_R)/c = S/c = [R_d/c + To]$$

$\frac{R_d}{c}$ = direct path time of arrival at the receiver.

A target return in the range interval,

$$R_d + cT_0. \qquad 4.113$$

would compete with direct path return.

Assuming situations where R_T is small compared with Rd then an approximation to the geometry is:

$$R_T \sim\sim [R_d - R_R \cos\theta]$$

This expresses the range difference.

and..

$$[R_R + R_T] = [R_d + cT_0]$$

This places the bistatic target range within the direct pulse interval.

when

$$R_R = cT_0/(1+\cos\theta) = cT_0/2 \sec^2\theta/2 \qquad 4.114$$

θ is the receiver pointing angle reference base line.

The table below shows how the ratio $R_R/(cT_0)/2$ varies with scan angle.

Θ	0	45	60	90	120	135
$R_R/cT_0/2$	1.0	1.2	1.3	2.0	4.0	6.83

A typical FM waveform is of one sec with a 200 Hz bandwidth which corresponds to a pulse length of 1/B, say, 5 m. The blanking range at 0 degrees from baseline is 2.5 m, 5 m at 90 degrees and 10 m at 120 degrees which represents the limit of the scanned range. More serious would be the use of a one second,1500m, CW pulse for better Doppler resolution: the void range spread varies from 750 m at 0 degrees,975 m at 90 degrees and 3000 at 120 degrees. Assuming spherical spreading the bistatic path propagation loss is TL(b) and assuming a target

strength of 10 dB the target would not be visible until this transmission path has been reduced to:

$$TL_b + TS < TL_d + 20\log cT_0. \qquad 4.115$$

With a 120 degree retricted scan angle the direct path arrival could be within the side-lobe response of several of the receiver beam patterns with an expected reduction of 20 dB relative to the main lobe.

The direct transmission assuming a spherical transmission loss is:

$$20\log R_d \text{ dB}$$

Its sidelobe contribution to the echo return will be.

$$[20\log R_d - 20]dB$$

A target strength of 10 dB would make the difference.

$$[20\log R_d - 30]dB \qquad 4.116$$

Over the common period the time variable gain and local automatic gain control will determine the output level so that the effect in the case of FM transmissions could resemble false target returns at known times. A foreseen advantage in using the hull sonar source is that the vertical beam angle of about 20 degrees or less should in many situations reduce the energy at the boundaries. Trials in a number of sample environments with the Variable Depth Sonar, the source of which has a vertical beam angle about equal to that of hull sonars,showed that any contributions by multipaths, if present,were obscured by other variables, Section 5. Control of the vertical beamwith of the receiving array is not available but it

may be feasible to provide range-dependent nulls on the affected beams,if any, should conditions be worse than predicted.

Doppler Frequency.

4.12 Doppler frequency shift provides a means for discriminating stationary objects from a slow moving target and on target movement, and so information is required of the Doppler frequencies of the two platforms. Target Doppler extraction at the bistatic ship is a function of the positions and velocity vectors of the source ship and the receiving ship referenced to a common set of co-ordinates at the base line L. A minimum of six measurements are needed to resolve the target Doppler,

(i) Transmission start time.

(ii) Time of direct arrival at receiver.

(iii) Velocity vector of source direction.

(iv) Time of target echo at receiver.

(V) Velocity vector of receiver.

(vi) Bearing of target echo at receiver.

There are three possible Doppler components in a target return at a bistatic receiver input instead of the two with a monostatic system:

(i) A Doppler shift of fs which is a function of the source ship velocity and angle on the bow relative to the target position.

(ii) A target Doppler shift f(T), which is a function of incidence and reflection angles at the target, its velocity and the bistatic angle.

(iii) A receiver component fr, which is similar to the monostatic case: a function of the receiver velocity and angle of look referred to the ships' bow. The above may be

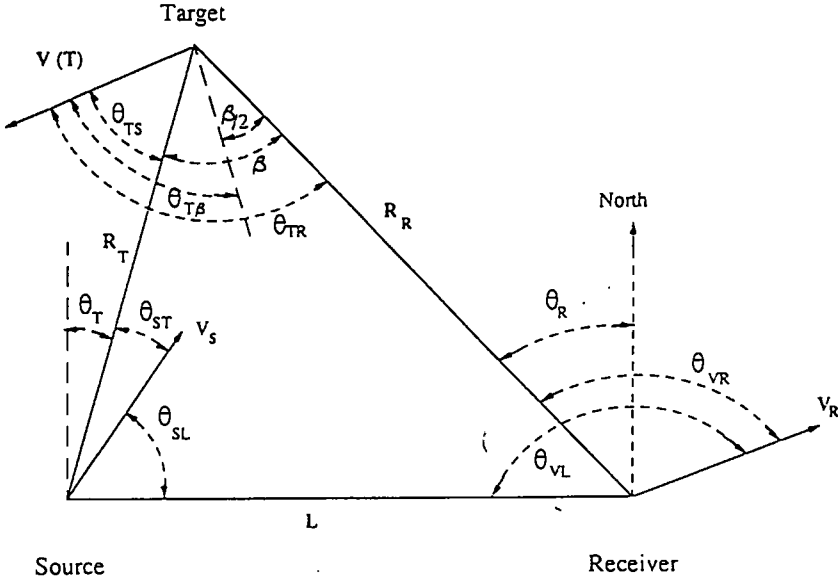

Fig 4.121 Bistatic Doppler Geometry.

expressed in terms of resolved direction vectors along the two platform paths to the target position.

$$f_t = \frac{1}{\lambda}\left[(\dot{r}_T \cdot V_T + \dot{r}_R \cdot V_R) - \dot{r}_t \cdot (V_T + V_R)\right] \text{ Hz} \qquad 4.121$$

$\dot{r}_T$ and $\dot{r}_r$ are unit direction vectors

along the source-target, target-receiver paths.

V_T and V_R are the ship velocities

along the directed paths.

$\dot{r}_t$ is the target direction vector

resolved in the direction of the ship velocities.

A listing of the reference angles, Fig 4.121, is given below.

(i) At the Source point S.

V_s is velocity vector of source.

θ_{ST} Angle between R_T and V_S

θ_{SL} Angle between V_S and L

θ_T Angle between R_T and broadside to L.

L is baseline distance between source and receiver.

R_T is the range vector from source to target.

R_R is the range vector from target to receiver. 4.122

(ii) At the Target point T.

V(T) is the velocity of the target.

β = The bistatic angle R_T to R_R.

θ_{TS} Angle between $V(T)$ and R_T.

θ_{TR} Angle between $V(T)$ and R_R

$\theta_{TS} - \theta_{TR} = \beta$

$\frac{\theta_{TS} + \theta_{TR}}{2}$ = angle $\theta_{T\beta}$.

$\theta_{T\beta}$ is the angle between V(T) and $\beta/2$. 4.123

Latter is equivalent to the target aspect angle.

(iii) At the Receiver point.

V_R is the velocity of the receiver.

θ_{VR} Angle between V_R and R_R

θ_{VL} Angle between V_R and L.

Θ_R Angle between R_R and broadside to L.

ϕ Angle between R_R and L

Bistatic angle is $\theta_T - \theta_R$ 4.124

There are variety of ways in which the above parameters may be assembled to obtain the required Doppler components.Those used below have made use of the static radar bistatic formulations with the addition of terms to provide for the contributions of the two mobile platforms.

(i) Source Doppler.

$$f_1 = f_s = f_o \left[\frac{1}{(1-(V_s/c)\cos\theta_{sT})}\right]$$

(ii) Addition of Target Doppler.

$$f_2 = f_1 \left[\frac{1+(V(T)/c)\cos\theta_{TS}}{(1-(V(T)/c)\cos\theta_{TR})}\right]$$

(*ii*) Target Doppler

$$f_T \approx [1+(2V(T)/c)\left(\frac{\cos\theta_{TS}+\cos\theta_{TR}}{2}\right]$$

Right hand term is of the form $\cos(A+B)\cos(A-B)$ when :

Target Doppler = $[1+(2V(T)/c)\cos_{T\beta}\cos\beta/2$ 4.125

$\theta_{T\beta}$ is the angle between $V(T)$ and $\beta/2$

Finally a last Doppler component is that due to the receiving platform.

(iii) Receiving Ship Doppler

$$f_d = f_1 f_2[(1+(V_R/c)\cos\theta_{VR}] \qquad 4.126$$

When the transmitter and receiver are stationary,

$$V_s = V_R = 0$$

The bistatic target Doppler at the reciver is then.

$$f_R[=(2V_T/\lambda)\cos\theta_{T\beta}\cos(\beta/2).$$

When $\beta = 0$, above reduces to the monostatic case.

and $\theta_{T\beta}$ now becomes the angle on the bow.

For a given $\theta_{T\beta}$, with a target sited within the bistatic angle, the bistatic Doppler never exceeds the monostatic Doppler. 4.127

Other relationships are:

For all β when $-90^0 < \theta_{T\beta}$

a closing Doppler generates a positive or closing Doppler.

For all $\beta \backslash 180^0$ the magnitude of the Doppler

is a maximum when the target velocity is collinear

with the bistatic bisector angle.

A significant target Doppler difference is the bistatic angle term cos b/2,and hence frequency shifts are functions of the ship separation distance and broadside range so that the filter arrangements with Doppler corrections will not be the same as for a monostatic sonar.

$$f = f_0\,[1+(2Vr/c)\cos\theta]$$

Vr is velocity of platform

θ is the angle on the bow.

To centre the reverberation frequency for all beam directions, fc is set as a function of each of the beam look angles.

$$f_0 = \frac{f_c}{[1+((2Vr)/c)\cos\theta]} \qquad 4.128$$

An assumption is that the ship separation distance remains constant over the interval of measurements.

The locus of the target position for constant Doppler frequency lies on a hyperbola and, ignoring S/N changes, location errors increase as the broadside range is reduced. Maximum Doppler paths for a monostatic sonar are along the radius vector, while for a bistatic target Doppler signal equivalent paths are hyperbolae orthogonal to the ellipses which means that the Doppler of a target on a hyperbolic trajectory corresponds to a radial path in the monostatic system.It is observed that the latter does not represent the speed towards the receiver but that

towards the baseline. Iso-range contours are the ellipses of constant range sums and not the radii of circles.The bisector of the bistatic angle is normal to the iso-range contours and a target traversing such a path would make no contribution to the Doppler shifts. At large distances relative to the baseline, the bistatic angle approaches zero when the monostatic and bistatic geometries merge.The foregoing again emphasizes that target velocity estimates based on subtracting platform inputs and then resolving target movement will be both more complicated and subject to larger errors than for the monostatic sonar. Pending sea trial data, some of which with regard to the performance of the directive line array became available during the development of the Variable Depth Sonar, it was not possible to proceed further with forecasts of other possible differences between the monostatic and bistatic equivalents .

Resolution Cells.

4.13 To evaluate the area of the resolution cell with respect to reverberation, the near range boundary is the ellipse sum range contour R(T) and R(R) with an incremental range determined by the effective transmit pulse length across equal range contours, fig 4.101. Inner and outer ellipses are then related by:

The semi-major axis lengths, a, of the inner and outer range ellipses are:

$$a_1 = \frac{1}{2}(R_T + R_R)$$

$$a_2 = a_1 + \frac{c}{2B}$$

Separation of ellipse contours is referred to pulse bandwidth, (B).

c is the speed of sound.

The corresponding eccentricities of the two ellipses are,

$$e_1 = \frac{l}{2a_1} \text{ and}$$

$$e_2 = \frac{l}{2a_2} \qquad 4.131$$

θ is the receiver pointing angle ref base line.

$\theta_2 - \theta_1$ is the receiver beamwidth.

In polar form:

$$y = r \sin\theta \text{ and } x = r \cos\theta.$$

$$r^2 = x^2 + y^2.$$

$$\theta = \tan^{-1}\frac{x}{y}$$

A closed form expression for cell area in the above co-ordinates has been derived by Moyer et al, in terms of the receiver pointing angle reference to the base line, beamwidth and eccentricity.

$$r_1(\theta) = \frac{a_1(1-e_1^2)}{(1-e_1\cos\theta)} = \frac{k_1}{(1-e_1\cos\theta)}$$

$$r_2(\theta) = \frac{a_2(1-e_2^2)}{(1-e_2\cos\theta)} = \frac{k_2}{(1-e_2\cos\theta)}$$

The azimuth beam intersects the elliptical contour over the angular range,

$$\theta_1 < \theta < \theta_2$$

at a receiver beam pointing angle,

$$\theta_p = (\theta_1+\theta_2)/2$$

The beam width is, $|\theta_2-\theta_1|$ 4.132

$$A_B = \int_{\phi_1}^{\phi_2} d\phi \int_{r_1(\phi)}^{r_2(\phi)} r\,dr. \qquad 4.133$$

$$A_B = k_2^2\{f_{e_2}(\phi_2)-f_{e_2}(\phi_1)\}-k_1^2\{f_{e_1}(\phi_2)-f_{e_1}(\phi_1)\} \qquad 4.134$$

where

$$f_e(\phi) = (1-e^2)^{-3/2}\{\tan^{-1}[\sqrt{\left(\frac{1+e}{(1-e)}\right)}\tan(\phi/2)]$$

$$+\frac{e\sqrt{1-e^2}\tan(\phi/2)}{(1-e)+(1+e)\tan^2(\phi/2)}\}$$

To gain insight into the variation of the bistatic footprint with different e value footprints, Moyer et Al computed the bistatic footprint for five eccentricity values (e = 0.10 , 0.25 , 0.5 , 0.75 , and 0.95.). With an assumed transmit-receive separation of 25km, a receiver beamwidth of 7.5 degrees and a transmit pulse bandwidth 3 MHz,(a pulse length of 150m) , so except for pulse length, the parameters are of the same order as the bistatic sonar system. In the same reference this exact expression is compared with a more commonly used radar approximation:

$$A_B \approx \frac{cR_R\theta_{AZ}}{2B\cos^2(\beta/2)} \qquad 4.135$$

R_R is the range from receiver to centre of resolution cell.

B = bandwidth.

β = the bistatic angle.

Azimuth receiver beam intersects the elliptical anulus over the range,

$$\phi_1 < \phi < \phi_2$$

Pointing angle $\phi_p = \frac{(\phi_1 + \phi_2)}{2}$ and,

$$\theta_{AZ} = |\phi_2 - \phi_1|$$

Comparison between the closed form and the more simple approximation showed a close agreement,the error being significant only when the receiver pointing angle is small and e is large, fig 4.131. This validation of the more simple expression supported some previous bistatic plots made by the author. It was evident that the effort required for the computations of the exact expressions for resolution cell areas did not merit the effort involved vis-a-vis the radar approximation in the light of the margins of error in the assumed parameters; so the latter was used. Bistatic sonar ellipse eccentricity values of 0.75 , 0.9 and 0.95 were chosen with a constant base line distance of 33 km. The pointing angle $\phi = 0°$ is defined as a receive beam directed at the source when the broadside zero scan angle would correspond to $\phi = 90°$. The range sums S were, 44km, 36.7km and 34.7 km respectively and the target receiver range contours were computed using the ellipse equations in the polar form with ranges, $R_1(\phi)$ and $R_2(\phi)$, denoting the respective distances from the receiver to the inner and outer range ellipses. A value

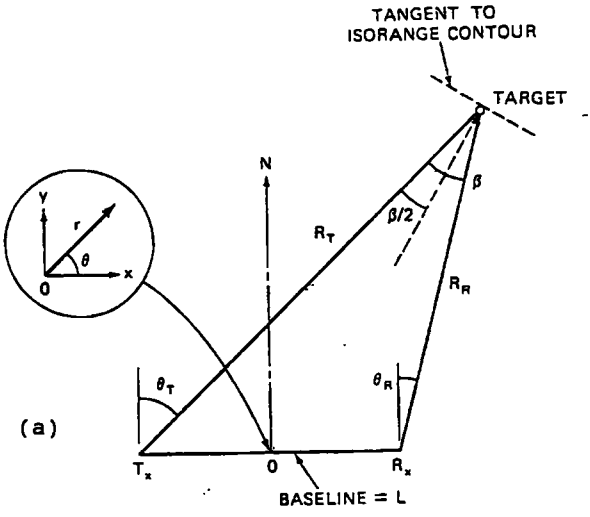

BISTATIC COORDINATE SYSTEM IN A PLANE

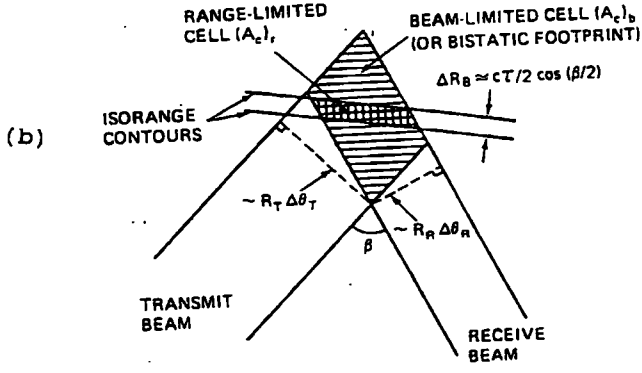

Fig 4.131 GEOMETRY FOR REVERBERATION SCATTERING AREA

for the source to target range was then obtained from $S-R_R$ and half bistatic angle, $\cos\beta/2$, using the sides of the range triangle.The reference monostatic sonar was assumed to have the combination of near omni-directional transmissions transmitter in azimuth and a vertical receiving beam angle of 12 degrees at 3dB down points. From the well-known optical law, with R(R) and R(T) as foci, the angles of incidence and reflection for an ellipse are equal = 2 (bistatic angle / 2).The towed line receiver beam after allowing for shading increases was 1.8 degrees at broadside and 3.6 degrees at scan angles of, $\pm 60°$, $\phi = 30°$ and $\phi = 150°$. Ratios of the bistatic to monostatic azimuth scattering areas were then tabulated.

For the bistatic.A_B ;

$$A_B \approx \frac{cR_R\theta_R}{2B\cos^2(\beta/2)} \qquad 4.136$$

c = Velocity of sound.

R_R = Receiver range to centre of bistatic resolution cell.

$\theta_R = |\phi_2 - \phi_1|$ = Receiver beamwidth .

B = Bandwidth .

β = Bistatic angle.

For monostatic sonar A(m);

$$A_m = \frac{c}{2B}.(\theta_R.R_R) \text{ when.} \qquad 4.137$$

$$\frac{A_B}{A_m} = \left(\frac{\theta_B}{\theta_m}\right).\frac{1}{[\cos^2\beta/2]} \qquad 4.138$$

Table A_1

e = 0.75 : S = 44.4 km : L = 33 km : R = km : b in degrees				
ϕ	R(T)	R(R)	cos b/2	β
30	16.6	27.4	0.68	94
60	28.6	15.4	0.72	87.9
90	34.4	9.6	0.8	73.7
120	37.0	7.0	0.9	25.8
150	38.0	5.8	0.978	12

Table A_2

e = 0.75 : θ and β in degrees. : A_β/A_m in sq km.				
ϕ	R(R)	θ_β/θ_m	$\cos^2\beta/2$	A_β/A_m
30	3.6	0.3	0.46	0.65
60	2.1	0.18	0.52	0.35
90	1.8	0.15	0.64	0.23
120	2.1	0 .18	0.81	0.22
150	3.6	0. 3	0.96	0.35

Table B_1

e= 0.9 : S = 33.67 km : L = 33 km:				
ϕ	R(R)	R(T)	$\cos\beta/2$	β
30	15.9	20.8	0.46	125.5
60	6.4	30.3	0.58	109.1
90	3.5	33.2	0.75	82.8
120	2.4	34.3	0.89	55.5
150	2.0	34.7	0.964	30.8

Table B_2

e = 0.9 : S = 36.7 km: L = 33 km : A_s/A_m in sq km.				
ϕ	R(R)	θ_s/θ_m	$\cos^2\beta/2$	A_s/A_m
30	3.6	0.3	0.21	1.43
60	2.1	0.18	0.34	0.53
90	1.8	0.15	0.56	0.27
120	2.1	0 .18	0.78	0.23
150	3.6	0. 3	0.93	0.32

Table C_1

e= 0.95 : S = 33.47 km : L = 33 km:				
ϕ	R(R)	R(T)	$\cos\beta/2$	β
30	9.6	25.1	0.34	140.2
60	3.6	31.5	0.50	120.0
90	1.7	33.0	0.72	82.8
120	1.3	33.5	0.85	63.7
150	2.0	33.8	0.973	26.7

Table C_2

e = 0.95 : S = 34.7 km: L = 33 km : A_s/A_m in sq km.				
ϕ	R(R)	θ_s/θ_m	$\cos^2\beta/2$	A_s/A_m
30	3.6	0.3	0.124	2.5
60	2.1	0.18	0.25	0.72
90	1.8	0.15	0.52	0.29
120	2.1	0 .18	0.72	0.25
150	3.6	0. 3	0.95	0.32

4.14 The sec b/2 factor is a measure of the obliqueness of the transmit-receiver-beam intercepts which modifies the range dimension from the usual c /(2 B) value for a monostatic sonar to $c/(2B \cos^2\beta/2)$. The scattering area decreases as the receiver beamwidth is reduced and as the signal bandwidth increases. Above demonstrates that,except for e = 0.9 and 0.95 at the 30 degree angle, 60 degree scan angle, the bistatic foot-print for the proposed receiver beamwidths is less than that for the monostatic sonar. I these largest foot-print directions the monostatic sonar would have its own detection capability. Over the remaining receiver beam scan angles the bistatic resolution cell more than satisfies the criteria of equality with the benchmark sonar although the progress of the pulsed wave form across cell area can be different,fig 4.101.

Reverberation Background.

4.15 For a monostatic sonar the reverberation level is the common source insonified / receiver intercept areas times a scattering coefficient.

As an example, for boundary reverberation, RL_b.

$$RL_b = SL - TL + 10\log[\sigma_b \int \{b_i(\theta,\phi)dA_i\} \int \{(b_s(\theta,\phi)dA_o\}]$$

σ_b is the scatterering coefficient for the cell.

$b_i(\theta,\phi)dA_i$ refers to the source insonified area.

$b_s(\theta,\phi)dA_o$ refers to the receiver intercept scattering area.

The monostatic area for the two integrals is approximately.

$$A = (cT_o/2)rd\theta. \qquad 4.151$$

In the stern arc of the line array the direct path source energy will be dominant while in the forward arc it is equivalent to the monostatic situation. There appears to have been no methodical system study of bistatic reverberation: the scant evidence to hand with two sonar beams trained for a series of intercept angles suggests that the scattering is isotropic from angles outside the source beam. Observations at-sea also follow this pattern in which case the monostatic scattering indices would apply to the bistatic geometry.In a bistatic configuration the transmission loss parameters are elliptical co-ordinates and the incident energy and bistatic receiver beam intercepts are functions of the bistatic angle.

$$RL_b = SL - TL_{s.A} - TL_{A.R} + S_s + 10\log A \qquad 4.152$$

RL_b is the reverberation level.

SL is the source level.

$TL_{s.A}$ is the transmission loss to the reverberation cell, and

$TL_{A.R}$ is the transmission loss of the scattered energy to the receiver

S is the scattering coefficient in dB.

Below is a repeat of Eqn 4.135 for the bistatic scattering area.

$$A_s \approx \frac{cR_R\theta_{AZ}}{2B\cos^2(\beta/2)} \qquad 4.135$$

R_R is the range from receiver to centre of resolution cell.

B = bandwidth.

β = the bistatic angle.

Azimuth receiver beam intersects the elliptical anulus over the range,

$$\phi_1 < \phi < \phi_2$$

Pointing angle $\phi_p = \frac{(\phi_1 + \phi_2)}{2}$ and,

$$\theta_{AZ} = |\phi_2 - \phi_1|$$

Multiplying the beamformer output by, 1/B = To, the input to the matched filter is then in the form of energy.

$$RL_R = ESL - TL_{s.A} - TL_{A.R} + S_s + 10\log A_\beta \qquad 4.153$$

RL_R = reverberation level at the receiver.

ESL = energy source level,

= intensity x pulse time (To).

$TL_{s.A}$ transmission loss from source

to reverberation area.

$TL_{A.R}$ transmission loss from

reverberation area to receiver.

S_s = reverberation scattering coefficient.

$10\log A$ = effective scattering area.

The energy spectral density. E(f),is:

$$E = \frac{1}{\rho c}\int_0^T p^2(t)dt.$$

$$= \int_E^\infty (f)df. \qquad 4.154$$

ρ = density.

p(t) = pressure signal for duration T.

E = signal energy flux.

I = signal intensity flux measured at 1 m.

The above equations show that the reverberation level is a function of both the receiver beam intercept direction with respect to the source path as well as the pulse crossing time. For a uniformly distributed scattering area,the intercept of the receiving beam and pulse length with the insonified transmission area will define the effective reverberation area and hence the scattering level.The parameters used for the tables in para 4.13 show that,except for scan angles of 60 degrees in the source direction at eccentricities of 0.9 and 0.95, the ratio of bistatic to monostatic for the chosen array parameters are less than those of the benchmark sonar. For a comparison analysis, the signal-to-reverberation after matched filtering does not depend on the source level but on the differences in the reverberation strength to target strength and any differences in propagation losses.

$$\Delta\,(\,S\,/RL\,) = [TL_{s.A} + TL_{A.R} - 2TL_{m.A}] + [TS_b - TS_m]$$

$$= \Delta[RD_m - RD_m\ \Delta\ Ls \qquad 4.155$$

Δ RD = differences in Recognition Differentials.

Δ Ls = differences in system losses.

Incident angles and scattering conditions are set equal.

The full expression would include effective reverberation areas.

Scattering coeffients are the same for both.

The simple model assumes that the sonar reverberation levels in a stationary situation with a uniform scattering coefficient would increase in direct proportion to the combined source/receiver pulse length-beamwidth parameters.

For surface reverberation.

$$TS_{R.s.b} = 10.\log I_o\ \sigma_v + 10\log A$$

For volume reverberation.

$$TS_v = 10.\log I_o\sigma_v + 10\log V \qquad 4.156$$

I_0 is the intensity of the incident wave.

I subs θ, (v,s,b) is the intensity of the back-scattered wave at 1m.

σ is a scattering coefficient.

In geometrial terms the Echo level varies as $\frac{1}{R^4}$

Volume reverberation as $\frac{1}{R^2}$

Surface and Bottom reverberation as $\frac{1}{R^3}$

A Target excess signal level at a near range would decrease at a rate of $\frac{1}{R^4}$

Reverberation would decrease a rate of $1/R^3$

At some range $R_E = R_R$

$$(TS - 40\log R) - (RL - 30\log R) = RD \qquad 4.157$$

Beyond this range, the reverberation returns would be the limiting background. At the longest ranges, noise,self or ambient, would be dominant.

4.16 If the filters are implemented by digital means, a flexible reference waveform with a variable clock rate is essential for the bistatic receiver.To cater for the diverse ship speeds and dispositions, different transmission waveforms, Doppler shifts and associated variables it is mandatory that each receiving beam has provision for;

(i) Computational facilities to provide input parameter values.

(ii) Normalisation of reverberation with range.

(iii) Pre-whitening of the noise input spectrum.

Combinations of:

(iv) Matched CW pulsed filtering.

(v) Matched Filtering for Chirp inputs.

(vi) Replica waveform generation.

(vii) Pulse compression.

(iix) Envelope detection.

(ix) Computation of parallax error; array-ship positions.

The detection index in classical terms provides probabilities for false alarm and target signal but in reality at the man-machine interface there are varying degrees of detection thresholds aligned to the nature of the naval operation, the form of the threat and its consequences together with any past knowledge of events. At the stage prior to envelope detection it is usual to model the background noise by a Gaussian distribution with zero mean and a variance noise power N .If a square law detector is used, the output of which is proportional to I^2+Q^2 processing is focussed on the Rayleigh distributed voltage envelope and it is common practice to provide a detection threshold selector at the output of the receiver passing to the display only those output signals that exceed a some predetermined recognition differential detection level, RD. Obtaining equivalent RD levels gives parity for the two systems at the input to the display but is not necessarily the case for the levels required by the operator for equal probabilities of detection. The background input within the bandwidth of the received signal waveform spectra is taken as incoherent while that for a discrete target with the addition of Doppler shifts return is coherent. Input waveforms are defined as narrow band,i.e. B/fo <<i, B is bandwidth and fo the carrier

frequency when the envelope statistics are described by a Rayleigh distribution.In some pulsed CW transmissions B/fo can no longer be classed as narrow band. When sufficient independent samples are available to allow the central limit theorem to apply, envelope detection is modelled as a multiplication, linear detection or square law with a correction for differences from a perfect time averaging,T. Successful detection or localization can only be accomplished if the properties of the signal are sufficiently different from those of the background returns.

4.17 Comparison of reverberation levels is on the basis of similar models for both receivers and hence referenced to the expected performance of an in-service sonar. On testing model predictions with real system performance in reverberation backgrounds, own experience is of a poor track record with large discrepancies that could not be resolved from the sparse environmental parameters to hand. As a typical example, Fig 4.171 shows some typical echo and reverberation levels taken during routine trials in the relatively shallow water areas around Portland and it is observed that the slopes of both target and reverberation with range are near equal: the implication being that, in such environments, unless a sufficient signal to reverberation background level is established then, as confirmed in the trials with real targets, detection at any range is improbable. Fig 4.172 shows a comparison of averaged reverberation levels for analogous sonars in the Portland area, Pacific Ocean and the Caribbean Sea with

the slopes for the first two regions very similar to Portland but differences in the latter case probable due to changes in the layering conditions as the range increased. Fig 4.173 shows the variation of volume reverberation in the Mediterranean Sea arising from the scattering volume of phytoplankton organisms which are sensitive to light moving upward at sunset and thereby entering the directional sonar transmit receive beams.This data was obtained with sonar frequencies of 7.5 kHz. It was these sort of variables that led the author over many years to support model studies with a system development policy of sampling actual reverberation in selected areas before finalising parameter values for new sonars, ref Grimley (1972) , a strategy not available for the bistatic sonar. Unlike radar,thermal noise in sonar acoustics only becomes a problem above about 50 kHz. The above data shortfall together with a lack of any previous experience in bistatic sonar systems was recognized from the start as one of the critical areas. At no time were resources available to the author to examine more than a fraction of the whole gamut of possible conditions except in a general sense, hence the strategy of using as far as possible comparisons with in-service monostatic sonar as benchmark for evaluation of parameters.

Echo and Reverberation Measurements.

Portland Area.

Fig 1.71

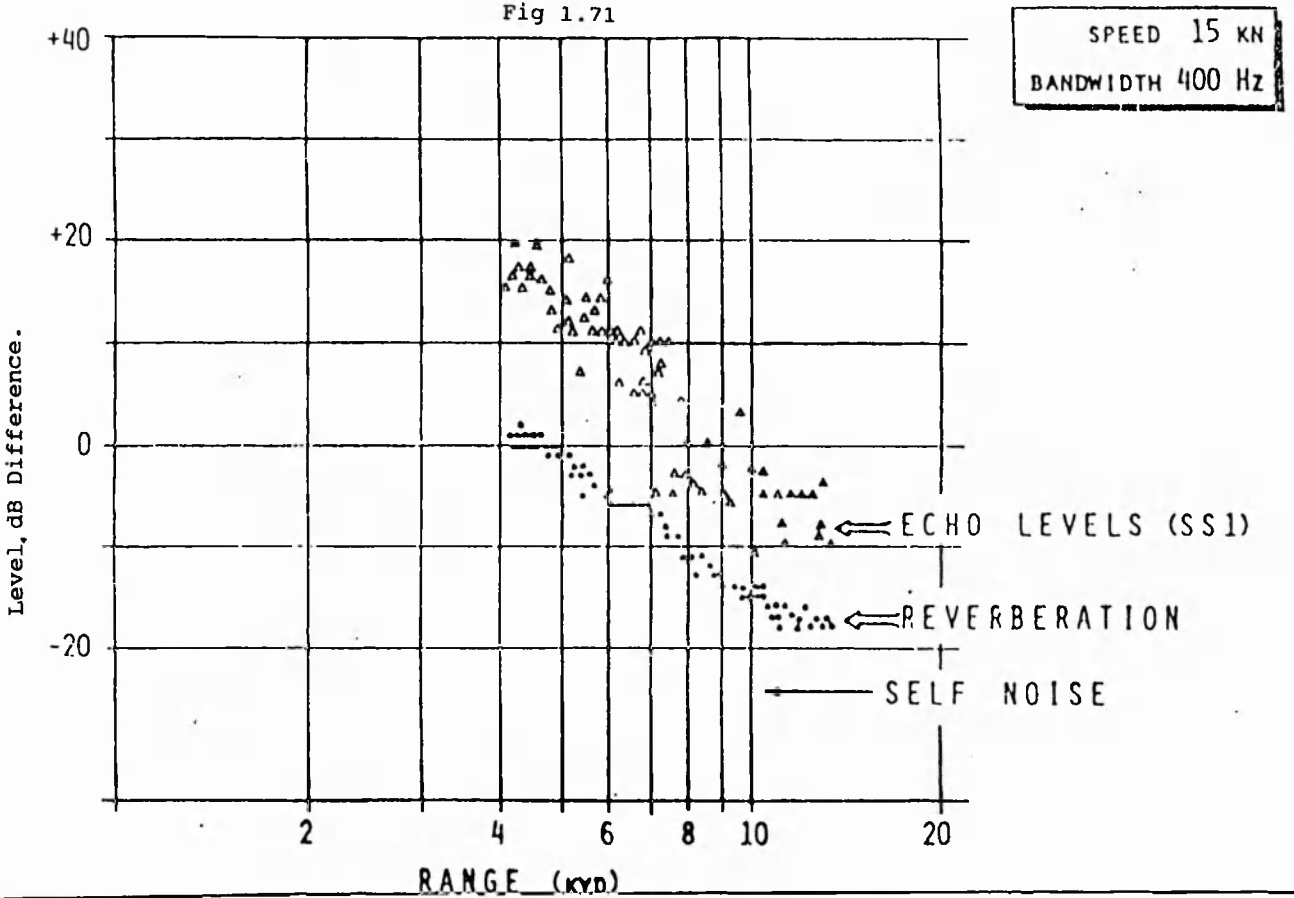

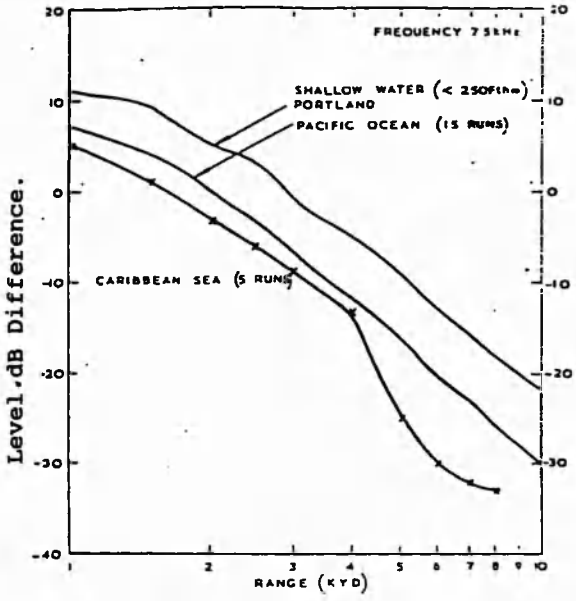

Fig 4.172 Comparison of Reverberation Levels.

Portland, Carribean Sea and the Pacific Ocean.

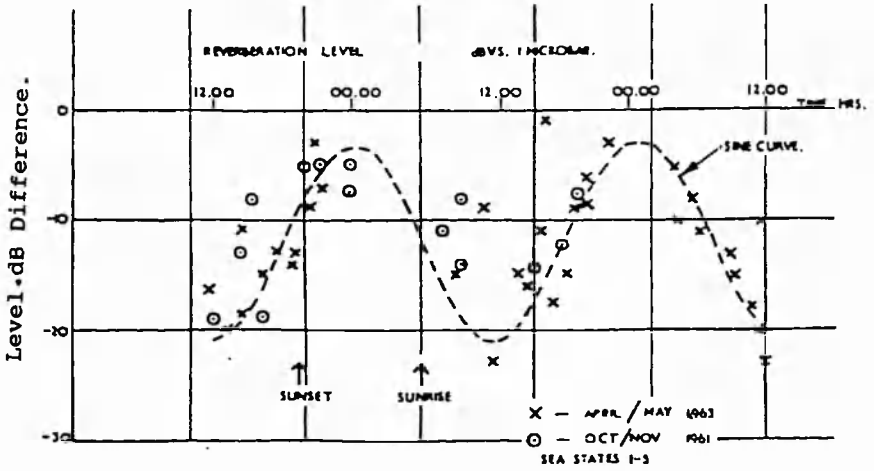

Fig 4.173 Variation of Reverberation Level

with Time of Day.

Normalisation of Array Outputs.

4.18 The general form of the active sonar equation for target signal excess includes a background that is the sum of all the unwanted sources in each of the receiving beams, but for simplicity it is usual to separate out and relate the contributing components, reverberation, ambient noise and self-noise to ranges at which each would be a signal limiting condition. Environmental considerations and experience show that reverberation, volume or boundary, for an active sonar is a first limiting background with either ambient noise or self noise as a far range situation.To maintain the input within the dynamic range of the sonar receiver, range compensation and normalisation is required so that at any range and bearing the smallest signal will be detected and the largest will not be distorted due to input overload. It is common to have two stages of normalisation, one being a time variable gain to compensate for the gross decay of input level with range and a local area control to allow target returns to rise above the immediate background. At the output of the beamformer and prior to AGC and matched filtering , normalisation or pre-whitening of the background is applied with a filter having a transform function of the form,

$$H(f) = 1 \; / \; \{ \; R(f) + N(f) \; \} \qquad 4.181$$

where R(f) and N(f) are the power spectra of the reverberation and noise respectively. The major part of the power spectrum of the received reverberation is assumed to be formed by densely distributed incoherent

frequency components characterized by a Rayleigh distributed envelope with a decreasing strength as time elapses, as much as 50 to 70 dB in 10 s, but the precise law cannot be accurately predicted. A constant temporal variance combined with a fixed threshold level would give a constant false alarm probability and for a constant bandwidth this implies a constant false alarm rate. The occurrence of false alarms depends on the total number of resolution cells, the information observation time and the characteristics of the background returns. At the operator's display the goal is that distinctive changes in input levels should produce the best contrast and an optimum for target detection would be one with a constant and uniform background in both the temporal and spatial dimensions: such a condition would allow a reference threshold level to be set independent of range and bearing. A problem is to arrange the background fluctuations and signals for a best fit with the operator's dynamic range of noticeable differences.The rate of change of the gain correction is a compromise between the need to highlight the S+N response increases while maintaining a near constant N level background. A fast gain recovery time will distort the target echo and cause an increased number of background patterns to add to the false alarm rate; a long time constant avoids echo distortion but suppresses weak signals as well as lowering tracking sensitivity. For short CW pulse, say 20 ms, the reverberation tends to have an impulse shape with a higher number of false alarms per transmission than longer pulse lengths

,say over half a second, where the increase number of samples appears to effect a smoother contour; a great deal of course depends on the nature of the acoustic environment. A general setting is to make the error control time interval about three to four times the transmitted pulse length. Defining an equivalence in the response between the two receivers, bistatic and monostatic,for a reverberation limiting background is bound to be more complex consequence of the increased number of variables. Thus the number of beams is increased which decreases the receiver cell size and the inclusion of the bistatic angle means that both the effective scattering area and the propagation path across the array varies with both scan angle and range so that the prospects of a grouping of beams for normalisation processing is likely to be more limited, particularly as Doppler shifts are sensitive to errors in the platform data inputs. Other means of normalisation include the use of log amplifiers and clipper amplifiers or zero crossing detectors which would ease the material requirement.In a clipped system the absolute amplitude information is lost and the only retained information is in the zero crossing times; there is however a relationship between the (S/N)in and (S/N)out and further processing makes use of this and obtains the phase of the information.The advantages of the clipped input type of normalisation is that dynamic ranges better than 80 dB may be obtained from a single comparator coupled to simplicity in implementation and its relevance to digital techniques. Its main disadvantage in active sonar is the removal of

absolute amplitude information with a 2 dB loss at low signal to noise ratios. Own experience is that sonar operators often make use of distinctive features of the boundary scattering as an aid to eliminating false targets and loss of amplitude information is not favoured as large scale scattering features can produce returns classified as false alarms.In a bistatic system both the form of the reverberation and the noise is not so well described as for the monostatic sonar and it would appear to confirm the need for flexibility in the arrangements for automatic gain control, AGC, and associated matched filters. When the reverberation input decays to the ambient or self noise values then the process becomes more like that for a monostatic sonar. Many of the interacting features in the practical application of dynamic range correction and automatic gain control that embrace the man-machine interface are usually excluded in detection and estimation theory.

Threshold Levels.

4.19 Target signal detection is always against a background of noise or reverberation and decisions on target present or absent is very dependent on the ratios of signal-to-noise in terms of their probability-density functions. Various sonar models are available for a matched filter receiver with detection, averaging, and threshold level circuits that allow the decision process to be expressed in terms of maximum peak signal to average noise power ratio.The purpose of the normalisation process is to maintain the

background at an appropriate level so that only a prescribed number of fluctuations exceeding this threshold: the higher the threshold the lower the number of false alarms per unit time but the higher the minimum level required of the target threshold signal. The instantaneous power, energy per unit time, in a signal is defined by $f^2(t)$ usually represented by current or voltage with units of mean square volts or mean square current. There are various statistics that express the different possible states.

Pd = probability that a target present is declared = (1 - Pm).

Pm = probability that a target present is not declared = (1- Pd).

Pfa = probability that in the absence of a target a target is declared.

An optimum receiver is defined in terms of the Neyman-Pearson criterion or a likelihood ratio which is much easier to implement. Both relate to the concept of a threshold with the probability that a return above an assigned level will be a target versus the probability that an equally high background return will be a false alarm. The probability of a correct target absent decision is (1 - Pfa). Receiver Operating Curves,(ROC), due to Peterson and Birdsall are available for a number of cases involving different degrees of knowledge about the signal in a Gaussian noise background that relate a detection index d, to the input signal-to-noise ratio, for an optimum receiver. Noise terms, No, are assumed to be

zero-mean Gaussian and independent of each other and the probability density function, Pn of the background defines its shape and magnitude. In modelling similar classes of active sonar the above conditions are assumed and the occurrence of other forms of unwanted signals are rarely addressed. Each independent sonar channel receives B independent range input samples per second and hence presents B independent decision opportunities per second.

Assume that the matched filter has bandwidth B Hz. then the time interval between decisions is 1/To secs.

For a constant FA. the B decisions per sec will result in an average of $Nfa = P_{fa}B$ false alarms per sec.

The average time-interval between false-alarms is:

$$T_{fa} = 1/Nfa = 1/P_{fa}B. \qquad 4.191$$

A fluctuation index is defined as the ratio of the mean square signal level plus noise to the variance of the noise at the input to the display, $[\sigma^2_{S+N}/\sigma^2_N]$. A representative model used for comparison of the two receivers would be that of an unknown signal in a Gaussian background for various values of detection index d as per the receiver operating curves, ROC.

$$d = Bt\left(\frac{S}{N}\right)^2$$

B = bandwidth.

N = noise power in bandwidth B.

S = signal power in bandwidth B.

t = observation time.

Solving S/N for a 1 Hz bandwidth noise, No.

$$S/No = SB/N = (d.B/t)^{1/2}$$

A RD Threshold is then defined by.

$$RD = 10 \log S/No = 5 \log d.B/t. \qquad 4.192$$

If To < t the pass-band of the filter exceeds the bandwidth of the signal and the added noise increases the optimum threshold level.

If To > t then the signal energy is reduced.

Combining the above conditions.

$$DT = 5 \log d.BW/t + | 5 \log To/t |$$

4.193

This usual expression for the Detection Threshold refers to the end of the processing change at the input to the display which here is termed RD. If a number of coherent signal pulses are integrated, as noise would be uncorrelated from scan-to-scan, the false alarm probability would be reduced. Experiment and experience have shown that for hull sonars with semi-alert operators a typical DT = RD value is between 9 and 15 dB. A RD of 12 dB equates to a detection index of 16 with a theoretically single target return of 50% and a false alarm probability of about 0.001%. Latter states have been used for comparing the two receivers with corrections for differences in the number

of decision cells. Assume a constant TS target strength with the monostatic receiver output decreasing at a constant 40 db range rate, for detection this would exceed the minimum RD level out to a range where RL = TS - RD. The transmission loss for bistatic target signals is:

$$R_s^2 R_g^2 \exp\alpha(R_s + R_g)$$

While that of the monostatic sonar is:

$$R^4 \exp 2\alpha r$$

As R_s increases, R_g decreases,

and vice versa. 4.194

The intercept footprint of the monostatic sonar is a simple beam arc increment range geometry while that for the bistatic receiver varies with both range, beam arc and bistatic angle, ref tables at 4.13.

At a receiver range $R_g = R_m$

The footprint of the bistatic is less than that of the monostatic, due to the smaller beamwidth of the line array.

When $R_g > R_m$ 4.195

the bistatic receiver intercepts part of the R_m area.

Target intercept is inversely proportional to $R_g^2 \exp\alpha R_g$

The overlap of the receiving beam with the propagation path of the transmission waveform allows for a greater variation in S/RL for both range and bearing.

At long distances it is common to assumed that the grazing angle approaches a lower limit of say 5 degrees or so, due to the velocity profiles and bottom roughness when Lambert's law no longer applies and the scattering strength is a constant; thus S/RL should decrease and the

number of false alarms increase with range due to the increasing size of the scattering area.The background level for the two receivers is proportional to the reverberation area and the false alarm to the variance which is multiplied by the number of decision cells Nfa. The total bistatic surveillance arc to monostatic arc ratios are 240 degrees to 270 degrees a ratio of 0.9. Two system measures of P(fa) are the average number of independent decisions for which N false-alarms would occur per range bearing scan and, a mean time between false-alarms. The rate of false-alarms will increase in proportion to the number of decision cells i.e,number of beams,range increments and Doppler channels. Cell dimensions per the tables of 4.13 have say a 3/1 less scattering area over much of the surveillance area with a 4.8 dB advantage.

$$\text{Fluctuation Index} = \left[\frac{\sigma^2_{S+N}}{\sigma^2_N}\right].$$

$$N = \sigma^2_n;\ S = \sigma^2_r.$$

The variance σ^2_N is reduced by 3.

The standard deviation of σ_N is reduced by $\sqrt{3}$.

The σ_N probability of a value being within

$$\pm 3 \text{ SD is } 99.73\ \%. \qquad 4.196$$

The upshot, depending on the effectiveness of the normalisation process, is that for the same signal level, the bistatic false alarms per arc cell should be reduced.The range R(R) determines the number of reverberation range increments and in general is less than R(m) so that an

equal number of range cells is a reasonable approximation. There are a more beams for the line array which increases the number of decision cells and for equal scan angles the number of spatial cells is increased on average by (7.5 /2.7) = 2.8 with dimensions equivalent to, $R_s.\theta.c.To$. When combined with the reduced false alarms per cell this monostatic/bistatic model suggests little difference in the total false alarm rates for the two receivers. Not included is a variation in both range and bearing of the S/RL level for the bistatic geometry as per the Ovals of Cassini, noting that with the chosen parameters the S/N contours approach that of the range sum ellipse. Also no account of a loss of target detection where the direct path and bistatic target returns overlap, A difference with the bistatic Doppler channels is the addition of the bistatic angle in the Doppler shifts so that the two platform contributions are functions of both the broadside range and scan angles. The platforms would be in a line-ahead formation and their near-equal Doppler components would sum so that the target component difference would be about the same as for a hull sonar. A maximum output for both receivers would be when the frequency shift matched the appropriate Doppler filter but inclusion of the bistatic angle means that the Doppler cells vary with range.

4.20 The values for P(fa) as estimated for reverberation need to be treated as model values only since the tails of the distributions for real conditions can show large inconsistencies. Consider a model where a coherent sinusoidal

signal S(t) is in a background of Gaussian noise, then the input to the detector v(t) may be expressed by:

$$v(t) = [(S(t)+x(t))\cos\omega t + y(t)\sin\omega t]$$

The detector output is the envelope of this function.

$$v(t) = \sqrt{[(S(t)+x(t)]^2 + y^2(t)}$$

for a linear detector and $v^2(t)$ for a square law detector.

Signal bandwidth B will be << than fo and

and with no signal the envelope

is described by a Rayleigh distribution. 4.201

S.O. Rice in his classic paper has obtained an expression for the probability density and the cumulative probability for the envelope v of signal plus noise.

$$p(v) = v \exp\left[-\frac{(v^2+2S/N)}{2}\right] I_0\left[\sqrt{2\frac{S}{N}}\, v\right]$$

and,

$$\int_0^v p(v)dv = \int_0^v v \exp\left[\frac{(-v^2-2S/N)}{2}\right] I_0\left[\sqrt{2\frac{S}{N}}\, v\right]dv \qquad 4.202$$

S/N = signal-to-noise power ratio, and the multiplier 2 is to convert rms signal power to peak signal power.

v = envelope of signal plus noise.

Io = hyperbolic Bessel function of zero order.

p(v) = probability density of v.

The probability of a voltage consisting of signal plus noise exceeding some threshold setting Et is:

$$P_s = 1 - \int_0^{\delta t} \exp\left[\frac{(-v^2-2S/N\}}{2}\right] I_0\left[\sqrt{2\frac{S}{N}}\, v\right]dv \qquad 4.203$$

In the case of no signal present, S/N = 0, when an output that exceeds the threshold is classified as a single cell false alarm.

$$p_{fa} = 1 - \int_0^{E_t} v \exp(-v^2/)dv = \int_{E_t}^{\infty} v.\exp(-v^2/2)dv. \text{ So,}$$

$$p_{fa} = \exp(-E_t^2/2) \qquad 4.204$$

Above shows that with matched filtering arranged to maximize the signal energy, P(d) depends only on the SNR and the P(fa).It also indicates that the effect of the threshold on the rate of false alarms is closely linked to the tails of the noise-like probability distributions. A notion of the sensitivity of the threshold setting on the false alarm probability is:

For a Pfa of 10^{-4} $E_t^2/2 = 9.2 = 9.64dB.$

This corresponds to 50% Pd.

For a Pfa of 10^{-5} $E_t^2/2 = 10.6$ dB

An increase in E_t of 1 dB

reduces by tenfold the Pfa.

Also for a Pfa = 10^{-6}

a 4dB increase in Signal power will increase Pd

from 10% to more than 70 %. 4.205

If the target signal is the sum of several scattering returns, and hence phase and amplitude additions, then this signal would also have an own distribution about a mean value. A considerable source of uncertainty in relating a model reverberation background to real conditions is the common assumption that the constituents of the geometric scattering area are uniformly spread and

of near equal size,i.e belong to the same group. If on the other hand the scattering components are ill-sorted with some larger than a wavelength, then the acoustic properties of a reverberation footprint, particularly in the tails of probability distributions, can be distorted by the geometrical shape and size of these individual scatterers. Even for conventional sonars, as already indicated, at-sea-measurements with reverberation limiting conditions are very sensitive to the form and structure of the environment with large variations in the observed returns. Within such reservations, and based on equivalent models, estimates of the overall P(d),P(fa) values for the two receivers were shown to be comparable having regard to the sensitivity of the assumptions of the input distributions.

Man-Machine Interface.

4.21 For acoustics, the display messages for active sonars are a description of the acoustic reflectivity over the scanned ocean area and the information rate is determined by the number of range/Doppler/bearing elements and just noticeable brightness levels on the display. The first relates to system parameters while the latter is associated with the observer responses. A search period may be a single transmission, a full day, or a month or more.The information contained in a set of M possible measures with a priori probability of Pi is defined as,

$$H = \sum_{i=1}^{M} p_i \log_2 p_i \text{ bits / message.} \qquad 4.211$$

H = the entropy of comunication theory.

p_i = the probability that a signal is in the range δv.

The simplest case is where all messages are equally likely, that is pi = 1/M for all i which represents the maximum information capacity per search.

$$H = \log_2 M \text{ bits /message.} \qquad 4.212$$

The term single scan search refers to the number of independent range and bearing elements in a single transmission, excluding Doppler cells which would be selected for a maximum output.

$$N_r = \frac{R}{\delta r}$$

R = range and δr = range increment .

Number of independent bearing elements is,

$$N_b = \phi/\theta$$

ϕ is the arc examined per transmission.

θ is the number of independent beams.

The total number of resolution elements is,

$$N_t = \left(\frac{R}{\delta r}\right)\left(\frac{\phi}{\theta}\right). \qquad 4.213$$

Each of the display cells may have any one of L possible intensity brightness levels, Just Noticeable Differences , JND = $\frac{\delta i}{I}$. depending on functions of phospher type, sweep speed, observation time and operator perception, when the

number of possible messages per cell is the number of different levels of L.

$$M = L^{(R/\delta r)(\phi/\theta)} \qquad 4.214$$

Again assume that all inputs level are equally likely,1/M , then an upper limit for the information presented to the operator per transmission would be,

$$H = \left(\frac{R}{\delta r}\right)\left(\frac{\phi}{\theta}\right)\log_2 L \text{ bits per search.}$$

$L \log_2$ is the number of Just Noticeable Differences. 4.215

Observed at-sea JND values are between 2 and 4 bits , an order lower than those measured with operators under laboratory conditions.Information density may be defined as,

N_a = bits per unit area.

$$N_a = \frac{N_r N_\theta \log_2 L}{A}.$$

N_r = range increments per look.

N_θ = bearing increments per look.

L = number of JND's

A is the actual area searched. 4.216

4.22 At the display, operator attention will be concentrated on changes in scan patterns so that there is a relationship between the density of false alarms and the amount of area observed by the operator. Lowering the threshold level not only increases the number of false alarms but also raises the number of bits per unit area to be examined. When the rate of change of information at the display exceeds the operator's input capacity the trend is

for him to limit the scan angle and range over which attention is given. It is often the case that limiting the information rate, i.e., raising the threshold level with an observer further away from the display, that target returns are detected outside the operator's area of perception.

The number of independent range elements is $\frac{\Delta R B}{c}$.

The number of independent space elements is $\frac{\phi}{\theta}$

ΔR = actual range examined per look.

$\frac{\phi}{\theta}$ = bearing increments per look.

The information density is,

$$\frac{\text{Information Capacity H}}{\text{Area}} \qquad 4.221$$

For a linear aperture the information rate is proportional to the number of channels and the information density per square meter is a function of the changing patterns formed by the background. The inherent information rate of the bistatic receiver is higher than that of a hull sonar which for the former is partially compensated by an expected improvement in signal to noise/reverberation ratio.It would be useful if an optimum search procedure could be set for each specific range/waveform combination but much depends on the acoustic environment and operational situation. Pulse compression type waveforms have a general advantage of range resolution over the CW type with least direct transmission overlap. A roof-top frequency sweep could assist in resolving the Doppler

anomaly. At a loss of information at the hull sonar,it is possible to shorten the transmission interval and increase the information flow at the bistatic receiver since propagation progresses in a forward direction from source to target to receiver. Where the surveillance areas overlap,the two receivers provide twice the target information opportunities and so should improve the input data flow to the Escort Ship.In the vulnerable ahead bearings where a slow moving target could lie in wait or close the range below the layer to lower the available discovery time, detection with the bistatic proposal is limited to an ahead port-starboard 60 degree scan angle. With the Variable Depth Sonar system, forward beams are formed without image rejection to cover these in front areas.

4.23 At the man-machine interface there is no one single rule that separates out the signal levels and background clues that decides the stage at which an operator choses a false alarm or to report a probable target.The higher the perceived threat the more immediate is the need for action at a lower level of surety reporting: procedures are sensitive to the consequences of missed targets and/or the interruption of patrol procedures that would allow gaps to be opened in surveillance routines. An attacking submarine making as much use as possible of below surface duct travel to minimize detection by hull sonars may afford few opportunities for in-duct detection at any range. Command decisions progress upwards, from an operator report of a first alert to an immediate assessment of the threat which

is continually updated as the flow of information progresses through to positive confirmation of a target, followed by location, identification, tracking and gaining weapon control inputs for positive countermeasures. In subsequent analyses of operator performance in naval exercises, it is a common experience to find that target returns, even when available, were present well above detection threshold levels some time before operator alert. One of the many problems with modern sonars is the difficulty in maintaining equal attention over all parts of a display. An Escort ship would have three operator positions for a 24 hour sonar watch, one for general sonar surveillance, one for conducting a closer examination of doubtful false alarm/target signals, and one for passive sonar returns. This number of operators is at no small cost in the provision of accommodation and supporting services and would be particularly so for small ships. This question of a minimum of number of operators for a small ship became prominent with the commercial VDS where there was, and still is, strong customer demand for a single operator, as would be the case for a bistatic ship.

4.24 The author at various times has experimented with alternate arrangements of single operator passive/active screen formats,including past history multiple beam recorders and different forms of data displays. Making good the advantages of the permanent recorded trace memory afforded to the single beam scan of the early sonars is yet to be achieved. The kernel of the difficulty is an operator's limited capacity, about 25 bits per second for

both sonar and radar, to assimilate changes in display patterns between the scan range intervals. Qualitative tests on colour displays showed about the same limit on operator information rate but with some gains on the occasions where a dominant colour drew attention to cells worthy of most attention, e.g, a likely cluster displayed in red. Sonar detection of real targets is a rare event and the information build-up is at a relatively low data rate compared with the occurrence of false targets so that operators spend a great deal of their time rejecting negative information. Above issues are intended to highlight that a minimum operator number for small ships is not a simple matter and forms part of the whole of the system-role requirements. What is being stressed is that this problem of the number of operators and the optimum division of their observation time still remains a matter of experience with no certainty that the best choice has been made because of the difficult in deciding and measuring relevant parameters. This field of analysis is what the author terms a" sink of iniquity, where gains expected in early parts of the system through improved technology are too often difficult to discern or lost in operator performance. Reducing the number of operators places even greater import to the need for operator assistance in the automatic sorting and classification of the incoming information: e.g pattern recognition and effective clustering techniques.The author also stresses the

requirement to provide for continuous training aboard ship using simulated targets while on "watch ", through to a whole system involvement.

References

Beckmann. P. and Spizzichino. A. Scattering of Electromagnetic Waves from Rough Surfaces. Pergamon Press. 1963.

Benjamin. R. Modulation,Resolution and Signal Processing in Radar, Sonar and Related Systems. Pergamon Press. 1966.

Blankenship. P.E and Hofstetter. E.M. Digital Pulse Compression via Fast Convolution. IEEE Trans on Acoustics,Speech and Signal Proceessing.Vol ASSP-23 No 2 Apr 1975.

Burdic. W.S. Underwater Acoustic System Analysis. Prentice-Hall. 1984.

Butterworth. W.J. The Grass Propagation Loss Model at A.U.W.E. Divisional Note 62678 October 1980. UK Unclassified.

Camp. L.W. Underwater Acoustics. J.Wiley. 1970.

Casper. J.M. Bistatic and Multistatic Radar. Radar Handbook. Sholnik.M.J.ed. Chap 36. McGraw-Hill Book Co. 1970.

Cook. C.E and Bernfield. M. Radar Signals. Academic Press.1967.

Etter. P.C. Underwater Acoustic Modelling: Principles, Techniques and Applications. Elsevier 1991.

Grimley. W.K. Status of Applied Underwater Acoustics. M.Sc Thesis. Univ of Bath. 1972.

Hanle.E. Survey of Bistatic and Multistatic Radar. Proc.IEE.Vol 133. pt F pp-587-595 Dec 1986.

Hovanessian.S.A. Radar System Design and Analysis. Artec House.1984.

Jackson. M.C. The Geometry of Bistatic Systems. IEE Proc. Vol 133. pt F. pp 604-612. Dec 1986.

Knight. W.C., Pridham. R.G., and Kay.S.M. Digital Signal Processing for Sonar. Proc IEEE, Vol 69, No.11 Nov 1981

Moyer. L.R., Morgan. C.J, Rugger. D.A. An Exact Expression for Resolution Cell Area in Special Case of Bistatic Radar Systems. IEEE Trans.Vol 25. No 4 July 1989.

Peterson. W.W, and Birdsall. T.G. The Theory of Signal Detectability. Univ. Mich. Eng.Res.Inst.Rep. 13. 1953.

Schwartz. M. Information, Transmission, Modulation and Noise.McGraw-Hill. 1980.

Skolnik. M.I. An Analysis of Bistatic Radar. IRE Trans.Vol.ANE-8 pp19-27. March 1961.

Strasberg.M. Hydrodynamic Flow Noise in Hydrophones. Adaptive Methods in Underwater Acoustics, 125-143. Ed Urban.H.1985.

University of Birmingham. Presentations on Underwater Acoustics. Portland. April 1985. (Background Papers.)

Urick.R.J. Ambient Noise in the Sea. Undersea Warfare Technolgy Office, Naval Sea Systems Command, Department of the Navy. Washington,D.C.20362. 1984.

WENZ.G.M. Acoustic Ambient Noise in the Ocean:Spectra and Sources. Jour of Acoustic Soc of Am.34 1936-56. 1962.

Westerfield. F.C ,Prager.R.H. and Stewart. J.L. Processing Gains Against Reverberation (Clutter) Using Matched Filters. IRE Trans on Information Theory.June 1960.

Woodward. P.M. Probability and Information Theory with Aplications to Radar. McGraw-Hill .1953.

Section 5

Contents.

Section 5.

Variable Depth Sonar.

Section 5.

Variable Depth Sonar.

Variable Depth Sonars.

5.1 The goal of the BAe company funded research and development programme ATAS, Active Towed Array Sonar,was to produce an essentially low cost variable depth active sonar that could be installed in a wide range of small ships, down to 250 to 500 tonnes displacement, with a range detection performance comparable with or better than that attained by a medium size Escort ship hull sonar. The few VDS systems in service, of which the RN type 199 is typical, are based on a towed body containing a high frequency scaled-down version of the hull type transmit/receive transducers. Experience has been that the system is expensive in terms of perfomance gains and the wet-end components in particular are bulky, difficult to handle and control at Fleet speeds. There are also problems of ship radiated and self noise that combined with the higher frequency make the below layer range detection, in all but a few ocean environments, not sufficient to merit the additional sonar operators needed. A helicopter-borne dipping sonar such as the RN type 195 [1] has a similar advantage of placing the source and receiver at a better depth for below layer targets but with even more constraints on space and payload that limit the size of the transducers to an optimum frequency of around 10 kHz. An advantage of the helicopter fit is that it can

---

1 A listing of the above military sonar systems is in the 1985 and subsequent editions of " Jane's Weapon Systems".

partially compensate for a shorter detection range with a more rapid approach to progressive surveillance zones, followed by a stationary hover which, with suitable precautions, can be a low self noise environment with good Doppler discrimination and an attack capability with an air-borne torpedo. Time-on-station for continuous surveillance is however a limiting operational feature, so that the overall Fleet cost in terms of the number of platforms and manpower needed is expensive. Later developments in this sonar have centred on lower source frequencies with umbrella type folding receiving arrays. A different approach to the bottom bounce mode has been explored by the French navy for those conditions where, because of the particular thermal structure, a Reliable Acoustic Path is present. One such region is the Mediterranean where, unlike most oceans, the depth of a source for a Reliable Acoustic Path, is relatively shallow, less than 3000m: the path is similar to the upward halve of the convergence zone path. To explore the possibilities for this propagation mode, the French constructed a large experimental towed sonar, order of several tons, with a specially adapted ship operating at a very low tow speed with the active sonar at the RAP depth. Cost and operational problems ruled out this approach as a practical system.

Active Sonar Towed Array Project.

5.2 The BAe development goal was to produce an ATAS demonstration system which would include most of the basic features for a family of similar type sonars that could be tailored to meet the needs of different customer

operational requirements.In particular alongside installation was a feature. Customer research indicated that the widest interest was for ship speeds up to about 15 knots. The design of the sonar sub systems was to be of modular form with the capacity to change or add functions as the programme progressed. The major programme sections many of which were progressed in parallel, were as listed below .

(i) Directive Towed Line Array with 360 degree cover.

(ii) Omnidirectional Towed Source , 3kHz .

(iii) Deck Handling Equipment.

(iv) Cables and Towed Body.

(v) Power Supplies.

(vi) Beamforming.

(vii) Signal and Data Processing .

(viii) Detection Formats.

(ix) Displays.

(x) System Control.

(xi) Computer Hardware .

(xii) Software Functions.

(xiii) Performance Analysis .

(xiv) Trials of In-Water Sub Systems .

(xv) Action Information Interfaces.

(xvi) Cabinets and Peripherals.

(xvii) System Integration.

(xviii) Test Equipment.

(xix) System Performance Trials and Analysis.

(xx) Quality Control.

(xxi) Cost Control .

(xxii) Documentation and Handbooks.

(xxiii) Continuing Market Research.

(xxiv) Operational Trials of Demonstrator System.

Demonstrating operational cost value was a necessary end point of the programme so that price effectiveness studies were an essential ingredient at all stages.

5.3 As presented in the thesis, a key feature of the Bistatic System was the practical realisation of the wet-end assemble, the combination of the directive line array with cable twist compensation and deck handling equipment suitable for a small ship. At an early stage of the bistatic system research the opportunity was taken by the author, using the acoustic facilities at Bath University, to test the validity of the formulations and errors of the key components of a Directive Line Array with cable twist compensation. The results had demonstrated that the proposed concept was a practical proposal. Tests to obtain the order of flow noise were not successful. Previous experience with the development of the RN Towed Decoy had highlighted grey areas where cable size and structure were closely related to a minimum reel diameter which, together with cable vibration and a very variable loading, had at first resulted in a short cable life. Considerable effort on the part of the cable manufacturer succeeded in producing a structure that eventually met the towing requirements with an acceptable tow life. The previous manufactures of the cable and deck handling equipment of the Towed Decoy were consulted and furnished some tentative wet-end data that was applicable to the Bistatic application. Using the towing tank of the Hydrodynamic

Department at Bath University it was possible to verify that the whole of the wet-end proposal for small ships was also a viable scheme.During the course of the Bistatic System Research the question of the telemetry bandwidth of the suggested towed cable arose, it being anticipated that a fibre optic link would be available. However the cable manufacturers advised that there would be problems with a fibre optic core in obtaining an acceptable cable life unless considerable protection was arranged against the effects of the variable strain loads and cable vibration coupled with the imposed small bending radius of the reels: all of these modifications required a substantial increased in the cable diameter. Author experience in towing bodies from ships had shown that maximum vibrational amplitudes with steel encased cables could be between one and twice the cable diameter which is known to increase the drag coefficient C and decrease cable life. Various types of fairings were tried at that time and compared with an estimated Cd of 1.2 for bare cable. Streamer fairings and trailing rubber types, Cd from 0.3 to 0.4 gave little noticeable improvement.The more sophisticated types with a good streamline profile, Cd from 0.2 to .01, sustained damage during passage over sheaves on recovery and in stowage on the drum due to the constrained bending dimensions: there was no easy mechanical solution for this approach and it was not pursued.

5.4 A major shortfall at the start of the programme was the provision of a suitable low frequency source. The Flextensional Class IV form of transducer was assessed to be the

most promising configuration,ref Brigham and Glass 1980, but there were considerable uncertainties about meeting the requirements of ATAS in the form of a practical and reliable product. J.Oswin et Al supported by the engineering expertise of BAe produced a design for a 3kHz source which met the ATAS requirement within a compact size and to an operating depth down to 200m. A proposed scheme for the bistatic sonar using amplitude modulation that met the cable bandwidth constraint for the bistatic sonar had been analysed, Section 3, and while technically satisfactory, it was not very flexible in the application of signal processing techniques. A more technically advanced telemetry system was devised by the BAe engineers using digital technology where signals are sampled at 12 kHz in groups of eight controlled by a system clock using Walsh function encoding to form a serial stream of 6.912 M bits/s. Other channels for housekeeping data and status commands, power supplies to the receiver module and to the transmitter are also included in the tow cable. The price to pay for this was a reduction of two to one in the number of array elements. Thirty two cardioid modules spaced at 0.21m formed the receiving array sensors contained in a polyurethane tube 88mm diameter, 20m long, with a Kevlar strain member; the cardioid elements occupy the central 7m of the hose. Disposition of the processing units in end hose spaces are apportioned to make the whole neutrally buoyant when filled with transformer oil. The cardioid network allows for twenty eight full beams to be formed simultaneously on the port and starboard sides with -3 dB cross-over points to give 360 degree reception: fig

3.191 Section 3 provided by BAe. Beam steer angles are from +- 2.1 degrees at broad side to +- 75 degrees with beamwidths from 4.2 degrees increasing to 22 degrees at end-fire. Measured values of port-starboard discrimination were better than 15 dB from broadside to +- 45 degrees and more than 6 dB for angles within +- 6o degrees decreasing as expected to nil as the end-fire position is approached. After amplification and automatic gain control for active sonar signals and variable gain for passive signals the output is fed to cardioid port starboard filters and then digitized and multiplexed for serial transmission through a single coaxial line up the tow cable to the shipboard electronics. A consequence of the limited bandwidth with serial sampling was that it was not possible to sample at a sufficient high rate to " sample and hold". This meant that the element output samples would not have coherent time delay intervals in the summing process for steering beams to a specific directions for maximum response. Methods of interpolation for combining sampling with different degrees of interpolation,linear,quadratic and cubic were simulated and tested for effectiveness,ref Butler and Hill also Knight et al. Chebychev weighting of the linear interpolation coefficients provide measured side lobe reductions of - 20dB. The Directivity Index for the array is 14 dB plus 4 dB for the cardioids. Linear beam interpolation of the ratios of the signal amplitudes in adjoining beams is arranged to give an eight fold improvement in the angular resolution, 0.5 degrees broadside, depending on the target signal to noise ratio which was a big improvement on the original spatial

discrimination of the longer array. Port and starboard signals from the same range cell are also compared and the lesser return suppressed which improves the image discrimination factor over a wider reception arc. Normalisation in range is performed independently for each beam by scaling the data points by the geometric mean value in a window surrounding that point. Window size is variable but is of the order of 39 range cells. A detection threshold of 9dB is then applied which for Rayleigh distributed noise and a Swerling 1 target signal gives a PD of 10^{-4}. In practice, as discussed in the sonar system research sections, the false alarm rate will depend on the statistics and pattern of the acoustic background as well as the just noticeable differences in the target returns and operator response, so allowance was made to vary threshold parameters in the light of accumulated trials data. The passive sonar capability at 3kHz [2] was intended to be better than that obtained by the ship hull sonars but inferior to that available with the tactical very low frequency passive towed arrays.

5.5 As anticipated, and also believed would be the case for a bistatic system, there was strong customer preference for a single operator display console. BAe experimented and made sea trials with various formats having a combination of tracker-ball and a limited number of programmable keys. Switching between the passive and active sonar modes is

---

2 The author was influence in the choice of 3kHz as a possible fall-back bistatic system application should the flextensional source developement fail to meet the commercial VDS requirement.

under operator control with inputs preserved within the intercept periods. Ranges scales of 0-10km, 0-16km, 0-32km and 0-64km are provided for the active sonar mode with a zoom facility of the order of 30 range cells updated on each transmission. After thresholding, the sonar data can be displayed either as a range vs bearing, or PPI plot, with amplitude as intensity. Use of colour is made in identifying new data and for annotation and overlays with features for maintaining track on 25 targets and a tote on ten. Consideration was to be given at a later date for including automatic cluster alert and automatic tracking. Processed passive data is presented to the operator using a waterfall format with inputs from 56 beams, squared and summed over the period of a variable integration time from 1s to 30s; short time period is for fast incoming noisy targets. To avoid long term targets being lost, the data is normalised by computing the mean value of samples over N samples up to 1000 and scaling and comparing with the mean value of an equivalent beam on the opposite side.The waterfall format stores up to 300 integration periods equivalent to 2.5 hours of observation time. With only one screen, provision is made for multiple pages of information on system status, data displays and access to points in the processing chain for parameter evaluation during trials. An audio output is included for the operator as well as recording of processed data and subsequent replay for eventual off-line analysis.

Sea Trials.

5.6 At-sea trials were conducted for a variety of reasons.

(1) To obtain acoustic environmental data for parameter formulation.

(2) To test the performance of the in-water components of the system.

(3) Trials of modular sections of the system.

(4) Demonstrations of whole system to naval customers. Early trials related to the line array from single hydrophones in a tube for noise levels through to a performance evaluation of the complete array. Handling trials followed to measure the hydrodynamic stability of the transmitter towed body and later of the completed assembly with the array and deck handling equipment. The system was tested both for modular performance and as a whole in different acoustic environments in both the active, CW -FM, and passive modes and operational data gathered for analysis to evaluate performance with a variety of acoustic backgrounds and sea states. Where possible recording were made which were added to the data bank to optimise and enhance the processing modules and for inputs to test different display formats. Not least of the objects of these trials was installation analysis for ease of fitting and on-deck handling of the wet-end over a range of ship conditions. An assortment of small trial ships were hired, varying from 16 tonnes to 800 tonnes, and Noise Ranging was part of the pre-trial measurement programme. For the purposes of hydrodynamic measurements the transmitter towed body,TTB , was fitted with an

instrumentation package: the line array included depth,temperature and heading sensors with a three-axes magnetometer. Array bearing accuracy and resolution were investigated for a mixture of helm and speed tow ship manoeuvres. Where oceanographic conditions showed that an operational advantage could be gained from operating at more than one depth, measurements were repeated at different depths. Targets were calibrated transponders and, for the demonstrator system, submarines provided by the customer. Maximum range was identified for both opening and closing targets or by variation of the transponder signal level.In conditions of high seabed returns,the ability to detect and track a slowly moving target using CW and FM waveforms was tested and the recording used for possible track history display formats. What is not known is the means of providing target fire control imformation after correcting for the separation distance of source and receiver from the tow platform although this should be a relatively straightforward computer computation.

5.7 Some of major points of the trials which refer back to the bistatic sonar system research are listed below.

(1) The port/starboard discrimination of the array with switching for cable twist met the performance estimates. The beamwidth was shown to be within the design accuracy with a 15 dB port/starboard discrimination within 45 degrees of broadside.

(2) On a steady course depth there was no evidence of any observable beam forming degradation with small helm changes. Variations of the array depth was within 1.5 m of

normal and following a 360 degree ship turn a 4 minute delay restored conditions to steady ahead operations.

(3) Self noise measurements up to 14 knots were less than sea state 2 and there was no evidence of contributions from flow noise. Addition of Vibration Isolation Modules in the tow cable produced no obvious effects on either the active or passive performance at the 3kHz frequency.

(4) The theoretical line array gain is 14dB plus 4dB for the cardioid elements. Measured values in the tow noise field were - 20 dB which represents the gain due to side-lobe rejection of the more directive noise field.

(6) The beam former generally had an accuracy of plus and minus 2 degrees with sidelobes of 26 dB and occasional lower values of 15 to 20 dB. With regard to the latter, as is common in most sonar measurements, it was difficult to differentiate between spurious side lobes, random noise peaks and unwanted sources.

(7) The normalisation processing with Automatic Gain Control appeared to operate as expected over a range of noise and reverberation limiting conditions.

(8) Multipath propagation was less of a problem than had been anticipated; when present it appeared as a "ghost echo" with a small path length offset.

A bonus with the lower active frequency operation was that as the background decreased to low sea state levels the radiated noise of some of the targets became evident in the tracking beam and this aided classification.

(9) Trials of the demonstrator VDS system over many hundreds of hours were made in European and N American

waters that encompassed measurements under controlled conditions using calibrated responders to free-play exercises with submarines.

The advantages of the variable depth capability was demonstrated and ranges were comparable with those expected of a medium power Escort sonar.

(10) At all times the availability and reliability of the system was of a very high order.

Not tested was the role of a bistatic operation, consequentially the following remain unresolved.

(A) An assessment of the operational value of a bistatic capability to Escort ships in a defence of shipping role. Role sequences in surveillance tasking etc.

(B) The co-ordination of the two platforms in a bistatic geometry and information exchange.

(B) The errors in the data inputs for functional outputs.

(C) The effects of the bistatic geometry on resolution cells and signal to noise ratio.

(D) Flow noise values for Fleet tow speed of 18 plus knots.

(E) Tow body stability for Fleet speeds of 18 plus knots.

(F) Effect of the interference of direct transmissions on near target detection.

(G) Integration into the weapon capability of the Fleet.

In addition to being a valuable contribution to the family

of sonars,the ATAS system offers the opportunity for a comprehensive series of trials to evaluate the Bistatic concept.

Comment.

6.8 Credit must go to the BAe engineers of the many disciplines who devised the means of converting the VDS concept with many challenging problems into hardware that meet the original goals. Considerable importance was given at all times to aspects of reliability, availability and maintainability as well safety all of which were a prominent needs for small ship installations. As is the case with all innovative sonar systems, there was a continuous interchange between operational capabilities and the need to satisfy a multitude of other requirements. The world wide marketing strategy for many navies meant that provision for a broad spectrum of possible operational scenarios had to be within the capabilities of the ATAS demonstrator system and kept under constant review. Obtaining a balance is made particularly difficult in sonar systems due to the interactive nature between the wide range of unspecified acoustic environments, platform characteristics in different seas, numerous operational situations with diverse targets and tactics together with the relative slow information rate and amount of false target returns as well as the constrains in ship installations and costs.The developed system has now been supplied to several small navies.

Section 6

Contents.

Section 6.

Conclusions of Sonar System Research.

Section 6.

Conclusions of Sonar System Research.

6.1 Sonar Systems Research as is demonstrated in this thesis for two specific naval requirements, is a multi-discipline task since the operational needs define the requirement and the acoustic environment the medium. The platform characteristics determine many of the sonar system parameters, and the basic problem area is the ability by an attacker to utilize a three dimensional space compared with the two dimensional space of the defender. Defence roles and aspects of the capabilities of the platforms that includes the operators, are an integral part of the analysis. Over recent years advances in submarine speed/depth/endurance technology has provided ever greater freedom to the aggressor to exploit the below-sea temperature-pressure-depth features of the ocean to his enhanced advantage.The surveillance counter-action has been to lower sonar operating frequencies and increase the power to improve detection ranges and the volume search of Escort ship sonars to negate the tactics of an attacker who attempts to exploit environmental features, but at a cost which shows diminishing returns.

6.2 The NATO request was for a wide ranging investigation for a way-ahead, particularly for active detection systems, that was to include the prospects of alternative sources of energy other than sonar. A criterion was that proposals for improvements were to be within the budgets of small navies. Making use of some basic physics to estimate the various source energy propagation losses in sea-water, it

is shown that underwater acoustics remains the prominent source energy for anti-submarine defence. It is then shown that the additional propagation paths,bottom reflected and convergence zone as provided by raising the power and lowering the frequency of Escort ship sonars impact on role detection probabilities, even in favourable environments and in particular on surface duct detections. The addition of these extra propagation paths is at a price of less surveillance time in the surface duct mode so that any detection range gains here may be negated. Among the possible alternative approaches considered was the addition of a variable depth sonar to access below-layer sonar paths simultaneously with the above-layer paths, but the conventional form of this type of sonar is not cost effective for most oceans. To make it worthwhile, a lower frequency at more power was needed and the existing arrangement of a smaller version of a hull sonar in a towed body had major limitations on the size and weight of the source as well as on the dimensions of the receiving array aperture. A possible future technology for the source was the use of flextensional forms but considerable problems were recorded in processing the experimental transducers to a product of suitable size, weight and cost for a Variable Depth Sonar role at the frequencies and operating depth required. In view of this uncertainty of an adequate small dimensional source being available, the author renewed his interest in making a more effective use of the source of the powerful Escort sonars through the

Bistatic concept of a distance receiver in a relatively low cost ship. Such a system had some years previously been discarded at an early stage as no suitable large aperture receiver for a small ship hull fit could be devised.[1] The later development of the low frequency passive towed array fitted to Escort Ships and Submarines appeared to be a more promising format to overcome the receiver aperture constraints. A serious active sonar shortfall with the then existing technology was that there was no discrimination between port and starboard signals.

6.3 The material aspects of the bistatic system formulation may be separated into two parts, a so-called wet-end that includes all the components associated with the line receiving array through to the deck handling equipment aboard the tow ship and a second part which encompasses the remainder of the system in-board of the tow ship.It is demonstrated that the tow forces, cable structure and the cable handling arrangements impact on the array format consequence of dimensions of the array hose, cable twisting and constraints on the telemetry bandwidth. In its turn, the radiated noise of the tow ship determines the length of the array astern sufficient to reduce the background tow ship noise to an acceptable level at the array sensors. Also the weight/speed /length drag characteristics of the array and the cable, control the depth at which stable towing conditions are required. A means of compensating for cable twist and parameters for a

---

1 The rationale for the bistatic system is given in Section 1, para 1.6.

cable that will allow suitable deckhandling equipment to be provided for a small ship fit are proposed, subsequent of personal discussions with the cable and winch manufactures. This was later confirmed with the BAe Active Towed Array Sonar (ATAS) development.

6.4 Various techniques were investigated to overcome the lack of the port-starboard discrimination of target signals that is characteristic of the usual form of towed line arrays, and the replacement of single elements by a cardioid network was deemed to be the most promising solution. Starting from the basic format for a line array, a formulation is derived with image rejection and an overall detection perfomance that meets the requirement of parity with a representative in-service hull form of the source sonar.The original idea was that, except for the inclusion of improved digital technology, the signal processes would be not too dissimilar from that for the hull sonar. However, as the research progressed it became manifest that the two-platform geometry of a bistatic system introduced significant differences.To compute the range to the target requires data on the source position, time of transmission and waveform type together with the receiver look-angle. In computations for the additional sonar surveillance area, the two ship-separation distance, the sum-range and the bistatic angle are prominent parameters. A dedicated acoustic link between the two ships is therefore intended for data exchange on transmission start time, ship course and speed, separation distance, waveform types and other bistatic information.

The target range cannot be measured directly but must be computed from the bistatic geometry and for optimum replica correlation, the corrections needed for the two-ship Doppler and the expansion or compression of the waveforms are dissimilar. Unlike the monostatic situation, Doppler correction for a fixed course is no longer constant with range since the source,target and receiver angles are changing.These shifts are greatest at close ranges and also as the source-to-target angles decrease, i.e as the source-to-receiver separation distance increases. The Doppler shift with range is least at long ranges, the monostatic sonar condition. Depending on the configuration and wave forms, not allowing for these bistatic Doppler shifts could result in matched filter losses of several dB. Contours of constant signal-to-noise are now described by Cassinian Ovals and Doppler shifts from target motion are components orthogonal to the bistatic range-sum ellipsoidal surfaces.

6.5 With a monostatic sonar the reverberation cell area, footprint, may be described in relatively simple terms of bandwidth (range) and the beam spatial dimensions at the transmission/receiver intercept boundaries. In the case of the bistatic geometry a two-dimensional approximation assumes that the area within the footprint is a parallelogram with isorange contours as straight lines.For small range sums the cell shape is trapezoidal or triangular while for large bistatic angles it is rhomboidal or hexagonal. Based on this bistatic radar approximation the parameters intended for the sonar receiver array

beamwidths and common bandwidths have an advantage over their hull sonar equivalents. Although the bistatic footprint is less, the intercept angles of the transmission path and receiving angles complicate the insonification path within the receiving beam.It is possible for the transmission energy within the receiver beam to be either beam limited or pulse limited with consequences for the signal processing chain.The omni-directional transmitter while beneficial for solving the bistatic geometry, has the disadvantage of being a masking background for near range bistatic target signals. This means that FM time-compressed waveforms would have prominence in a bistatic operations.

6.6 A monostatic sonar model was applied for comparison of recognition differentials,RD, with a fixed point target in an ideal acoustic environment free from distortion, multi-paths or direct path overlap with target returns.These conditions also presumed that a single steady state target signal is present in stationary Gaussian noise. Since the wave shape is known, the optimum processor is a correlator in which the transmitted signal with the required Doppler corrections is correlated against the input signal plus noise. On this basis, it is shown that the false alarm rate for the monostatic and bistatic sonars are comparable. Attention is drawn to the sensitivity of the threshold values to relative small shifts in the tails of the assumed signal plus noise distributions. At the end of the detection chain is the operator whose responses have a strong influence on system performance but cannot at

present be described analytically.This is particularly so for a small ship installation where manpower and space are at a premium. One solution is outlined in section 5.On completion of the formulation of the directive line array the opportunity was taken to test by model experiments the validity of the parameters and allowed errors of the key components with cable twist compensation using the acoustic facilities at Bath University. Other model experiments using the towing tank in the Hydrodynamic Department provided data on the towing parameters. Attempts to establish the order of the array flow noise level using the wind tunnel were not possible due to the high level of the background noise. Further validation of the formulations was obtained during the at-sea trials of the commercial VDS which was developed with the background of the bistatic system research.

6.7 The outcome of the performance analysis for the bistatic system based on the parameters presented in the thesis is that there are cost and operational advantages, as listed in Section 1, in gaining additional worthwhile active sonar volume cover using low value platforms as compared with another high cost escort ship. However, once a low cost small dimensional source became available, the high profile accorded to a bistatic system on the grounds of an improved use of an expensive source facility became less prominent although most of the operational advantages of an extra range passive receiver not broadcasting its presence remain. What the new VDS format offers is another approach for increasing the defence of shipping at a

relatively low cost that small navies could afford. Such a sonar allows for separate sonar surveillance for targets located below surface sound duct channels, leaving the major escort ships to concentrate on detection opportunities in the vulnerable above-layer regions and to exploit their superior flexibility in manoeuvres and overall use of integrated weapon systems. A VDS capability on its own is of course not a universal answer for providing complete surveillance against the different tactics that an attacker could use. Thus setting the depth for below-layer detection is at a loss of the surface duct mode. With the present ATAS operating frequencies of 3 kHz a bistatic role is possible but if acting as a separate sonar in a close support formation, then with the limited bandwidth available there would be a advantages in raising the operating frequency to the 4kHz band, i.e, between the bands of the high power and medium power sonars. A significant cost advantage is that the whole system could be installed with the ship alongside requiring only small hull modifications.

6.8 Another proposal is to add the VDS capability to the sonar suite of the Escort Ships where the addition of an extra operator would be cost effective for reasons already given about lost-time in serially searching the three propagation modes. At the higher patrol ship speeds needed there remains some unresolved grey areas such as the stability of the towed transmitter body where my own experience is that this becomes more difficult to achieve without the addition of active control units. Also the

level of flow noise at these higher speeds is still to be determined. On the plus side is that the problem of ship self noise reduction measures are less severe since receiver and platform are separated by the tow line distance. An additional feature partially investigated was the inclusion of a broadband higher frequency intercept facility for the detection of torpedoes and high speed intruder craft: but this has to wait for improvements in the tow cable telemetry bandwidth. It is possible that the larger ships needed for open ocean roles would allow an increase in the cable diameter and deckhandling equipment and hence allow for sufficient protection within the tow cable for a fibre optic core. As already realised by smaller navies who have purchased or expressed interest in the system is the scope for other independent surveillance operations.

6.9 So far as is known this research on a bistatic sonar system is the first complete investigation of all aspects, from role requirements through to the ship fit. Bistatic radar with distributed receivers using one or more transmitters in fixed positions already has applications for Radar surveillance. In a narrow sense,it consists of one transmitter and one separate receiver at a fixed site where the detection volume is the intersection of fixed single beams in a bistatic configuration. The scheme, as for the sonar application, is sensitive in the beam cross-over region whose extent affects the size of the

resolution cells.It is however less complex than its sonar counterpart in having a constant environmental space, fixed stations and good communication links between sites.

6.10 In total, apart from the investigations into the feasibility of new concepts, what the thesis is intended to demonstrate is the part played by this form of System's Research. The latter is required not only to be innovative in the concept, but also familiar with and manipulate a very wide spectrum of technology in order to plan both the proposed approach and assess its implications on performance, ship needs,integration with other defence needs, costs and time scales. Of major importance are the system formulation stages where failure to define clear objectives for the defence roles and a realistic assessment for solving crucial grey areas with fall-back positions has seen the demise of many large projects across many areas of defence. The development of ATAS also emphasises the point made in Section 1, that the task of System Research is to establish the connection between the operational need and the feasibility of a concept to match the requirement. While taking cognizance of the advancing technology, choice of techniques is not an integral part of the task.The latter is the role of the specialists in the particular fields. Finally repeating a previous observation, although the immediate threat by a major naval power has now diminished, the sonar system research as described in this thesis has highlighted the difficulties of obtaining cost effect solutions in

continuing the past processes of increasing the power of hull type sonars and the possibilities for fresh alternative approaches.

Recommendations.

6.11 It is recommended that the concept of the new form of variable depth sonar is worthy of further research into the feasibility of extending the operational use of the concept. In particular for the defence of shipping by increasing the operational speed to 18 knots and more would appear to offer more cost-effective overall gains than a policy of lowering the frequency and increasing the power of the present Escort Ship hull type sonars. Research is needed to establish values for flow noise in the band from around 2 to 5kHz along with a model for optimising the parameters for a towed line array.It is also observed that the bandwidth of the tow cable sets a limit on exploiting the prospects for including such functions as torpedo detection particularly if added to an Escort's existing sonar installation. A systems study on the merits of increasing the dimensions of the deck handling gear and so raising the tow cable diameter to accept a fibre optic core versus the drag forces and towing characteristics would aid in cost effective studies of choice for a way-ahead.The minimum size of a VDS only ship as an addition to the defence of shipping in open oceans might set one of the upper limits to dimensions, and weight. The author also considers that the variable depth capability of a small dimensional source with a directive line array having a more rigid structure also

has possible applications for mine-hunting sonars. It is further suggested that the effectiveness of using helicopter sonars in a bistatic mode, with and without the addition of the new line array, is worthy of attention. Here one of the platforms is stationary and the use of synchronise clocks for the Escort ship transmissions to obtain a start time might be acceptable for short period operations with a predetermined bistatic geometry.It is also observed that the line array as formulated for this study is a basic arrangement and allows for greater sophistication with modern technology.